Final Report

Title

Efficiency of physical water treatments in controlling calcium scale accumulation in recirculating open cooling water system

ASHRAE Research Project 1155-TRP

Submitted to

ASHRAE, Inc.
1791 Tullie Circle, NE
(Technical Committee 3.6)

Professor Young I. Cho
Department of Mechanical Eng. & Mechanics
Drexel University
Philadelphia, PA 19104
Phone: 215-895-2425
Fax: 215-895-1478
e-mail: choyi@drexel.edu

May 29, 2002

Executive Summary

This report describes the work done at Drexel University under ASHRAE Research Project No. 1155-TRP entitled "Efficiency of physical water treatments in controlling calcium scale accumulation in recirculating open cooling water system" during the period between September 1, 2000 and March 31, 2002.

The physical water treatment (PWT) device is defined as a non-chemical method of water treatment utilized for the purpose of scale prevention or mitigation. The present research is limited to recirculating open cooling water system, where the circulating water is repeatedly exposed to the PWT device.

Three different PWT devices, including permanent magnets, solenoid coil device, and high-voltage electrode, were used under various operating conditions,. Although there are other PWT devices marketed for the purpose of scale control such as ultrasound device, device using a sudden pressure drop, vortex device, etc. these are not included in the present research.

Due to huge volume of data, the test results for each device are described separately in a separate chapter to avoid confusion. A paper summarizing the present research project is under preparation and will be presented at the ASHRAE Chicago Meeting, January, 2003 and will be published in ASHRAE Transaction.

Codes used for the identification of PWT devices:

PMDU: a small permanent-magnet unit. This is similar in design to the one used earlier by Busch's group at Baylor University in 1980s.

PMSM-1: an in-line, flow-through, three round bar permanent magnets producing multiple alternating magnetic fields, encompassed within a steel shield.

SCED: a solenoid coil unit using a pulsating square-wave current to induce electric field using Faraday's law

ESPH-1: Electrostatic precipitator having a high-voltage electrode at the center of a pipe

Disclaimer

GE Betz has provided water analysis as a service to the project and the ASHRAE technical committee TC3.6, and neither challenges nor endorses the findings of this study.

TABLE OF CONTENTS

Chapter 1

Introduction: Fouling and Physical Water Treatment (PWT) Devices

For every solute and solvent combination, there is a characteristic amount of solute that will dissolve under a given condition such as temperature, pressure, and pH. The solubility of a substance is the amount that will dissolve in a given solvent to produce a saturated solution [Moeller 1989]. Two forms of solubility are possible: normal and inverse. Some salts have greater solubility as the temperature is raised; these salts are called normal solubility salts, and examples include NaCl and $NaNO_3$. Other salts show less solubility as the temperature is raised, usually termed inverse solubility salts such as $CaCO_3$, $CaSO_4$, and $MgSiO_3$ [1]. Due to the heating (or cooling) process in thermal equipment, the temperature-dependent solubility leads to a supersaturated state (or an undersaturated state).

Calcite and Aragonite

Calcium carbonate is one of the most common scale types. The two structures of calcium carbonate crystal commonly found in nature are calcite and aragonite in morphology. They have the same chemical component, $CaCO_3$, but differ in many aspects. Calcite is formed at room temperature (i.e., below 30^oC), easily removable with weak hydrochloric acid, less adherent than aragonite, and has a hexagonal crystal shape, with a specific gravity of 2.71 [2].

Aragonite is formed at high temperature (i.e., above 30^oC) and is difficult to remove, having an orthorhombic crystal shape and a specific gravity of 2.94 [2]. Aragonite is a more

troublesome form of calcium carbonate than calcite because it forms a harder and denser deposit than calcite in boilers and other heat transfer equipment [2].

It has been of interest to see whether calcium carbonate scales produced in water treated by a PWT device is Calcite or Aragonite. The present study investigates this issue by analyzing scale samples using an X-ray diffraction method.

Fouling in Untreated Water: Crystallization Fouling

Circulating cooling tower water contains excess amount of mineral ions such as calcium and magnesium due to the evaporation of water, thus making the water hard. When the hard water is heated inside heat transfer equipment, the calcium and bicarbonate ions precipitate due to the changes in solubility, forming hard scale on heat-transfer surfaces, and clogging heat exchanger pipes and manifolds. When any undesirable material deposits on a heat exchanger surface, it is called fouling [3-9]. It is of note that calcium bicarbonate is used to represent a group of mineral salts that deposit as foulants on the surface of a heat exchanger.

When the circulating water is not treated, one often has a hardened scale deposit on the heat transfer surface, see Fig. 1. The costs of fouling in several developed countries are shown in Table 1. This is due to a crystal formation on the heat-transfer surface, often known as a crystallization fouling. Factors affecting nucleation and subsequent crystal formation are the concentration of fouling materials (foulants), temperature, pH, pressure, time, flow velocity, mechanical motions, radiation, and impurities. Mechanical motions include shaking, mixing, and friction, which can be characterized as turbulence.

The initial crystals formed by a precipitation reaction may not be the most stable solids (i.e., thermodynamically stable phase) for reaction conditions. Over a period of time the crystal

structure changes to that of a stable phase. This change may be accompanied by an additional precipitation from solution. A phenomenon, called ripening, may also take place whereby the crystal size of the precipitate increases [10]. Such a hardened scale is common in heat transfer equipment using untreated water as a cooling medium. It is well known that such a hardened scale cannot be removed by brush punching. An acid cleaning is often required to remove the hardened scale, which may cause premature equipment replacement and producing chemical wastes for disposal. It is of note that the present study examined scale specimen obtained at the end of 250-hr heat transfer tests using scanning electron microscopy and X-ray diffraction methods. Hence, the final state of the scale crystals, not the initial crystal status, could be examined from the SEM and X-ray diffraction measurements.

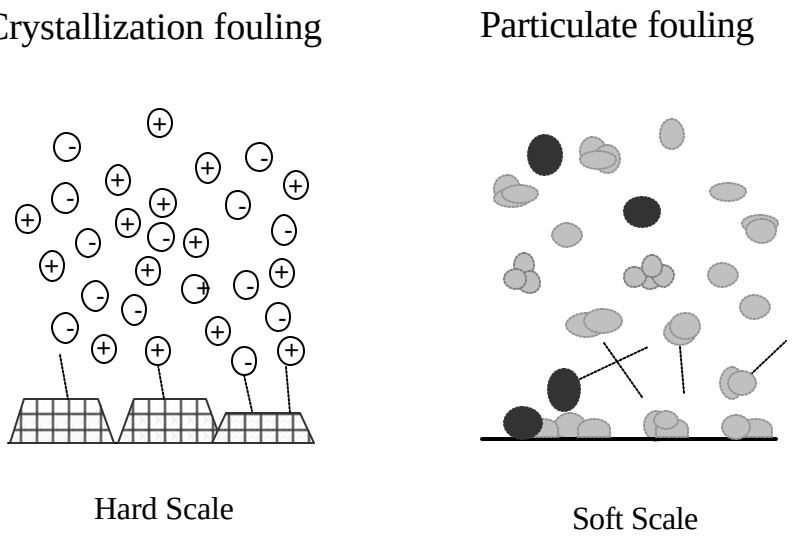

Fig. 1 Sketches of crystallization and particulate foulings

Table 1: Total Fouling Costs for Several Countries

Country	Fouling in costs (million $)	1992 GNP (billions $)	Fouling as % of GNP
United States	14,175	5,670	0.25
Japan	10,000	4,000	0.25
Germany	4,875	1,950	0.25
United Kingdom	2,500	1,000	0.25
Australia	463	309	0.15
New Zealand	64	43	0.15

(Source: Data from www.cpe.surrey.ac.uk/dptri/hms/fouling.htm)

Particulate Fouling

Particulate fouling is a deposition process of particles carried by a flowing fluid as well as by matters generated in a solution. When compared with the scales produced in crystallization fouling, the scales produced in particulate fouling are much softer, as illustrated in Fig. 1. The term "particle" is general and may refer to particulate matter, bacteria, corrosion products and so on. The term "particle" also refers to particles that may be generated at the surface, such as the products of chemical reaction or crystallization [1]. The arrival of particles at a surface can take place by two mechanisms, i.e., gravitational settling and particle transport.

Beal [11] categorized the particulate fouling into three major processes: transport of the particles from the bulk fluid to the surface, the attachment of the particles to the surface, and re-entrainment of previously deposited particles from the surface back into the bulk fluid.

Bott [1] divided particle deposition into transport mechanism and agglomeration. First the particle has to be transported to the surface by one or a combination of mechanisms including Brownian motion, turbulent diffusion, or by virtue of the momentum possessed by the particle. Other factors that must be borne in mind in a consideration of the particle deposition, although difficult to incorporate in any mathematical model, include the agglomeration of particles in the bulk or at or near the surface, and the complex interactions of the forces near the wall.

Proposed Mechanism of the PWT Devices for the Mitigation of Mineral Fouling

It is known that the magnetic and electric fields affect the characteristics for the nucleation of mineral ions and other electrically charged sub-micron particles [12]. The influence that an externally applied electro-magnetic field may exert on nucleation and particle behavior is studied from the point of view of fouling mitigation. One of the most reasonable mechanisms in fouling mitigation by external fields is a generation of nucleation in a bulk solution. Based on Russian scientists' research, Al-Qahtani [13] reported that the magnetic treatment processes accelerated the coagulation-flocculation of solid particles suspended in water and increased the crystal formation on the bulk solution instead of deposition on heat-transfer surfaces.

Thus, it is hypothesized that the water treated by the PWT devices tends to produce particles of $CaCO_3$ and other mineral salts in bulk water, resulting in particulate fouling. In other words, the PWT devices produce soft sludge coatings on the heat transfer surface. Subsequently,

when the shear force generated by the flow velocity in heat transfer equipment is sufficiently large to remove the soft sludge coating, then the PWT device can prevent new scale deposit or significantly mitigate the scale.

Hypothesis of PWT Technology

External magnetic or electric fields precipitate mineral ions and form clusters (i.e., colloidal particles of submicron size [32] in solution. The clusters grow in size as the solubility of the mineral ions drops due to increased temperature of the solution inside heat transfer equipment, resulting in the mitigation of fouling at heat-transfer surfaces.

Devices for the Physical Water Treatment

In order to prevent or mitigate fouling problem, various physical water treatment (PWT) methods have been applied, using one of the following means: magnetic fields, electric fields, alteration of surface charges, mechanical disturbance such as ultrasound, and sudden pressure changes.

Especially, magnetic devices have a long and controversial history in their efficiency [14]. Numerous researchers investigated the feasibility of using a permanent magnet in reducing mineral fouling [14-27]. Some of them reported that the physical water treatment (PWT) changed water properties and/or produced nucleation sites in a bulk solution, whereas others reported that the PWT did not work. After reviewing the literature, it is rather clear that the effect of the PWT (with permanent magnets) on scale prevention was not consistent because the

effectiveness of the PWT critically depended on the test conditions, particularly, the flow velocity through permanent magnetic fields [14-25].

Accordingly, one can ask whether there is an optimum flow velocity, which makes the PWT device very effective. Furthermore, it is interesting to find whether the efficiency of the PWT device substantially decreases when the flow velocity is smaller or larger than this velocity. A number of researchers [14, 24-27] reported that there are other factors, affecting the effectiveness of the PWT, which were a supersaturated state and a circulating flow loop (i.e., continuous treatment). The present study investigates the effect of flow velocity and concentration on the effectiveness of the permanent magnets on reducing mineral fouling in circulating cooling-tower water. Furthermore, the present study also examined the factors affecting the performance of a solenoid-coil device such as the frequency and strength of the current signal.

Next, we briefly introduce the basic operating principle and general specification of three PWT devices tested in the present study.

Permanent Magnets

Figure 2 shows a classification of permanent magnets [14, 18]. -As water passes through magnetic fields in Classes I and IV, the water molecules face magnetic fields fixed in a certain direction, whereas in Classes II, III, V, and VI, water experiences magnetic fields whose directions change along the flow direction. It is of note that actual permanent magnets tested in the present study (see Chapters 2,3, 4, and 5) may not be exactly identified as one of the classes. (modified after CS' s comments) Table 2 shows the strength of permanent magnets for various applications.

When charged molecules or ions pass through a region under magnetic fields, electric fields are induced, which can be expressed as [28]:

$$\mathbf{E} = \mathbf{V} \times \mathbf{B} \qquad (1)$$

where **E** is an induced electric field in permanent magnet, **V** is a flow velocity vector, and **B** is a magnetic field strength vector created by a permanent magnet.

It is hypothesized that the permanent magnet modifies solution properties, that is, the precipitation of mineral ions in a bulk solution and the alteration of water properties, when mineral ions and molecules are exposed to the induced electric fields produced by alternating magnetic fields observed from moving water molecules, see Fig. 3. Previous Investigators [21, 25, and 28] reported that magnetically treated water produced different types of scale formation due to the modification of solution properties. Kronenberg [21] reported that the calcium carbonate from magnetically treated water formed a soft sludge instead of hard lime scale clinging to surface. Donaldson and Grimes [29] speculated that magnetic fields acted at the surface of crystallites, modifying the nature of the charges at the surface. Parsons [25] reported that the physical water treatment led to the formation of irregularly shaped crystal forms.

The effectiveness of the permanent magnet appears to be strongly related to a flow velocity passing through magnetic fields. Grutsch [18] reported through a full-scale field test that scaling was completely prevented at a flow velocity through magnets of 6 m/s using a magnetic device (1,700 gauss), where the cooling-tower water moved between the magnets at the center and pipe wall. Szostak [19] reported that he could operate a cooling tower at 3,000-ppm hardness without scale buildup by using a magnetic fluid conditioning system. He designed the internal structure of the magnetic device such that the cross-sectional area was reduced to

increase the flow velocity to 6 m/s through the magnetic treatment device. In addition, Busch and Busch reported that the induced voltage by permanent magnets was linearly increasing with flow velocity [22]. When the flow velocity at the upstream pipe was 4.5 ft/s, they could obtain the maximum induced voltage. Note that the cross sectional area at the upstream pipe was four times bigger than the cross sectional area of the pipe with permanent magnets so that the actual flow velocity through the permanent magnets were 18 ft/s (5.5 m/s).

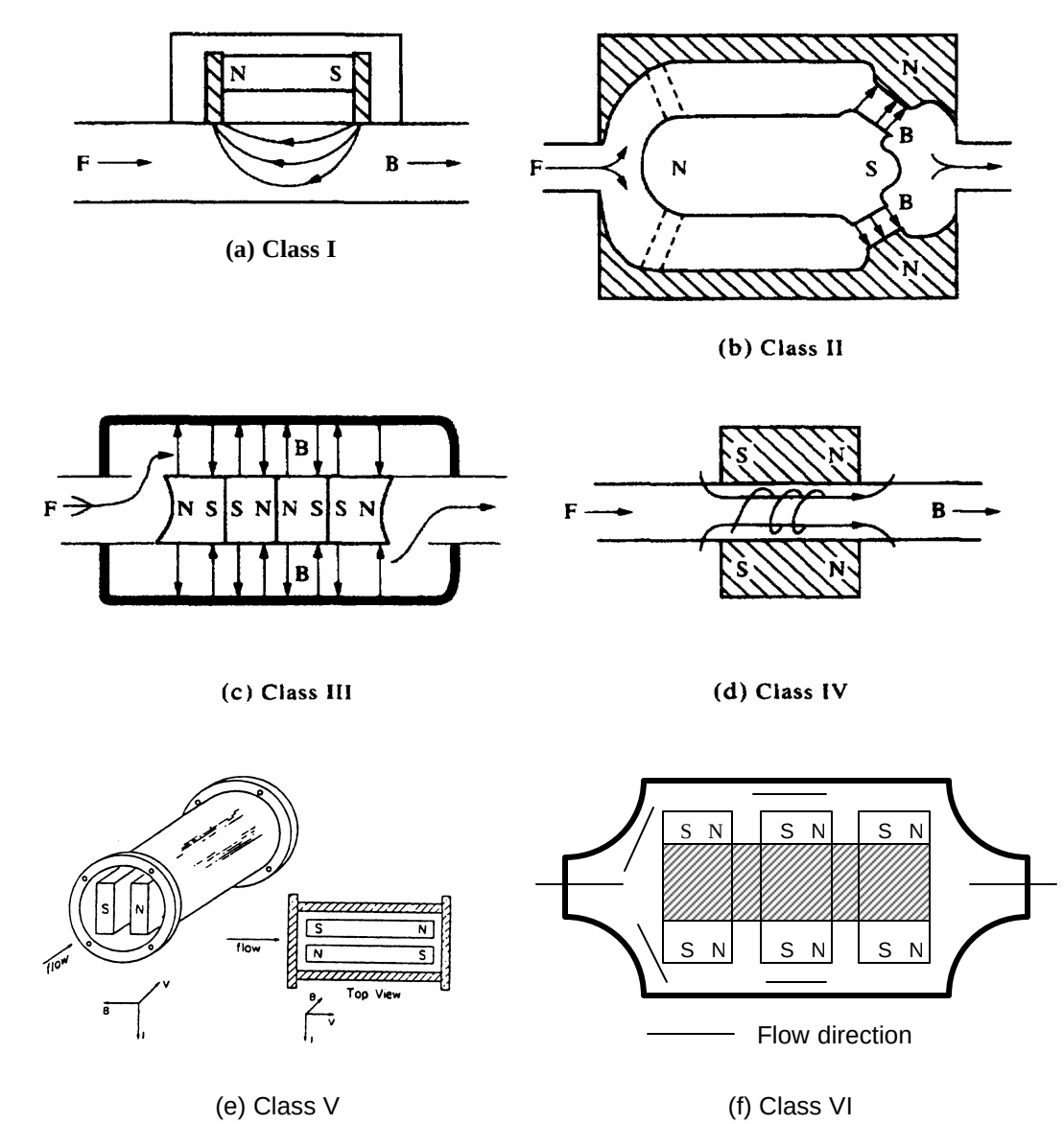

(a) Class I : clamp-on magnetic device
(b) Class II : radial magnetic flow transverse near poles
(c) Class III : radial flow, alternating magnetic field direction
(d) Class IV : parallel magnetic field, collinear solenoid, spiral metal element in field
(e) Class V : perpendicular magnetic field
(f) Class VI : separated magnetic device

Fig. 2 Classification of permanent magnet devices [13, 17, 18, 21, 24, 30-32]

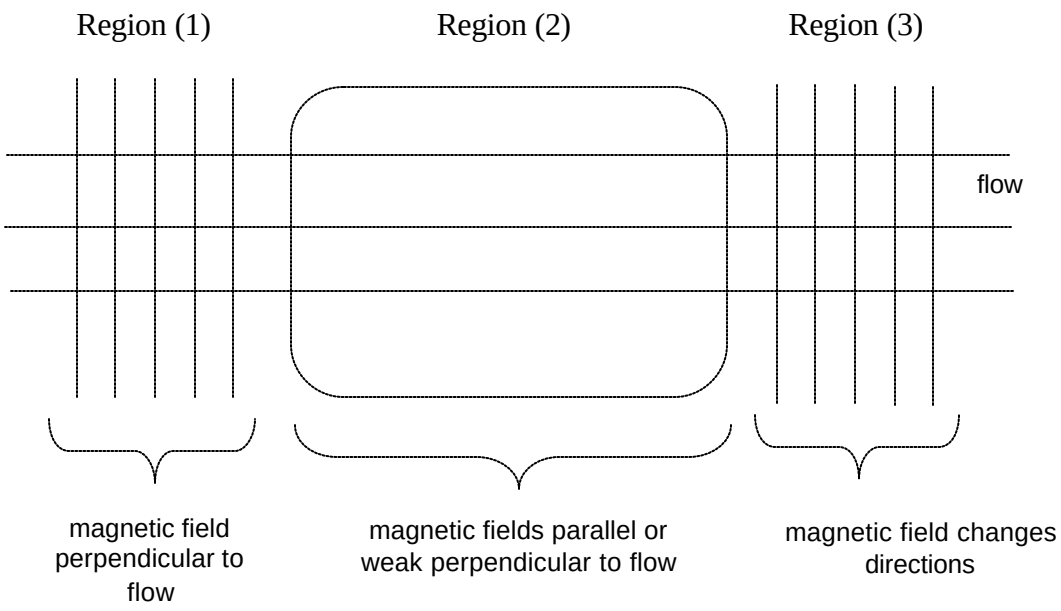

(a)

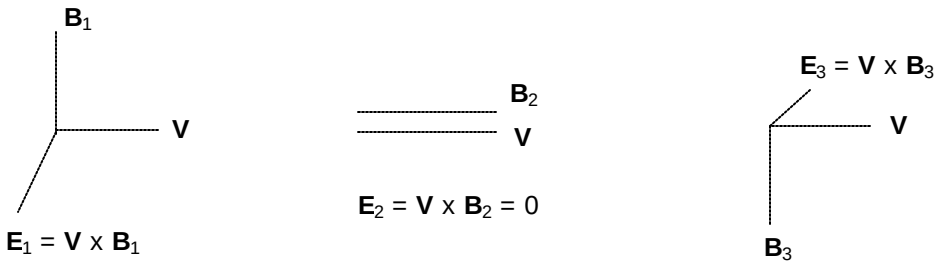

(b)

Fig. 3 (a) Sketch of directions of magnetic fields and flow in permanent magnetic devices, and (b) vectors for flow velocity, magnetic field, and induced electric field. Note that E_1 and E_3 are in opposite directions. The magnitude of induced electric field by permanent magnets at a velocity of 6.0 m/s was (6 m/s) x (1,600 Wb/m^2) = 0.96 mV/m.

Table 2 Comparison of Strength of Various Magnets

Refrigerator magnets that hold notes ---100 Gauss

Bar magnet ----------100 - 1,000 Gauss

Magnets for scale control ---------- 1,200 - 6,000 Gauss

Large scientific magnets ---------- 20,000 - 40,000 Gauss

Superconducting magnets -------- 5,000,000 - 10,000,000 Gauss

Solenoid-Coil Induction Devices

Figure 4 shows a sketch of a solenoid coil device (SCED), and a method to measure the induced electric field inside a tube. As shown in Fig. 4(a), a solenoid coil was wrapped over a plastic tube which was used just for forming of solenoid coil and also plastic material doesn't affect to the electromagnetic field due to non-ferrous material. Two ends of the solenoid coil were connected to an electronic control unit. The copper tube was located at the off-centered position relative to the solenoid coil since the strength of the induced electric field had a maximum value at the surface of the coil and a minimum value at the center of the coil. Figure 4(b) shows a schematic diagram of a test set-up with a circular-pickup-wire probe to measure the induced electric field inside a copper tube.

Figure 5 shows the peak-to-peak voltage generated by a time-varying electric current at three different axial locations inside the copper tube. The SCED control unit was adjusted to produce a pulsing current at approximately 650 Hz. Subsequently, an induced pulsating electric field was generated inside the pipe by Faraday's law [28]:

$$\int \mathbf{E} \cdot d\mathbf{s} = -\frac{\partial}{\partial t} \int \mathbf{B} \cdot d\mathbf{A} \qquad (2)$$

where **E** [V] is an induced electric field vector, **s** is a line vector along the circumferential direction, **B** [Wb/m^2] is a magnetic field strength vector, and **A** is the cross sectional area of the solenoid coil. Figure 5 shows a typical output of the induced electric field measured at the axial center of the solenoid coil.

Figure 6 shows a cutaway view of a pipe, where magnetic and induced electric fields are produced by a pulsating current through the solenoid coil. As illustrated in Fig. 6, counterclockwise and clockwise induced electric fields, $\mathbf{E}_1$ and $\mathbf{E}_2$, were generated consecutively and repeatedly.

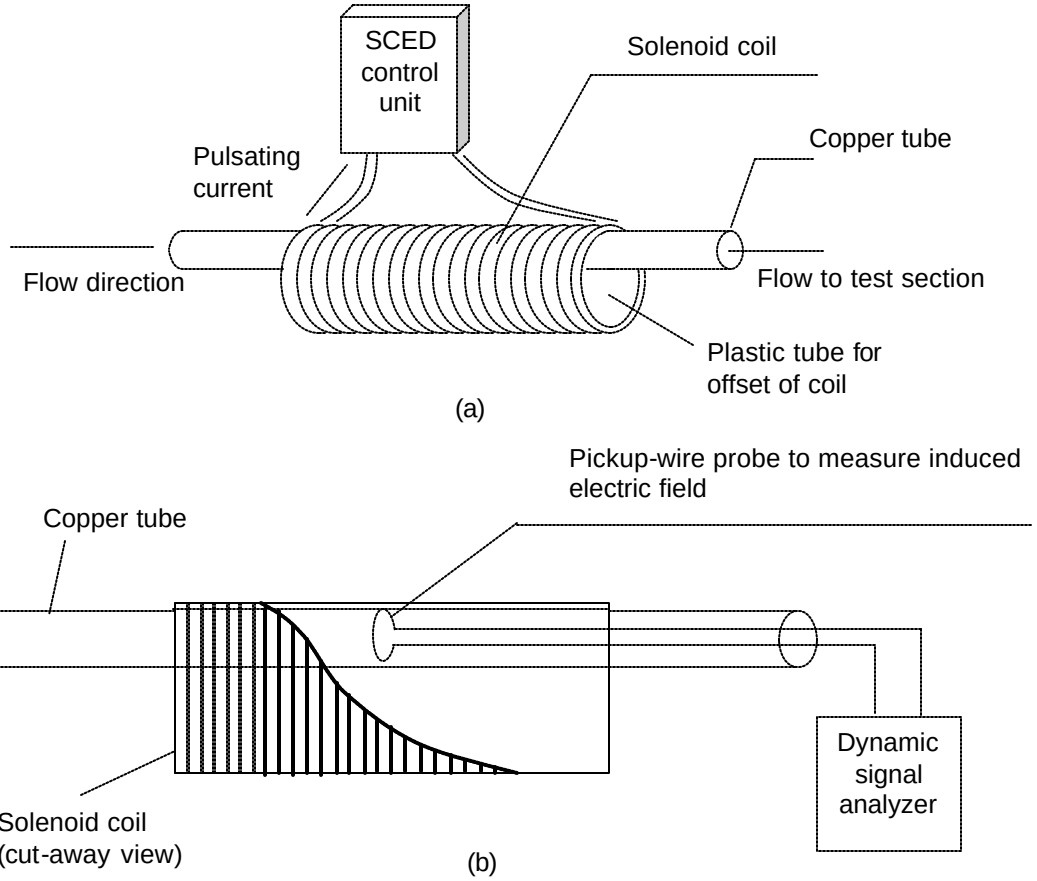

Fig. 4 (a) Installation of an EAF unit and a solenoid coil; (b) Measurement of an induced electric field inside a copper tube

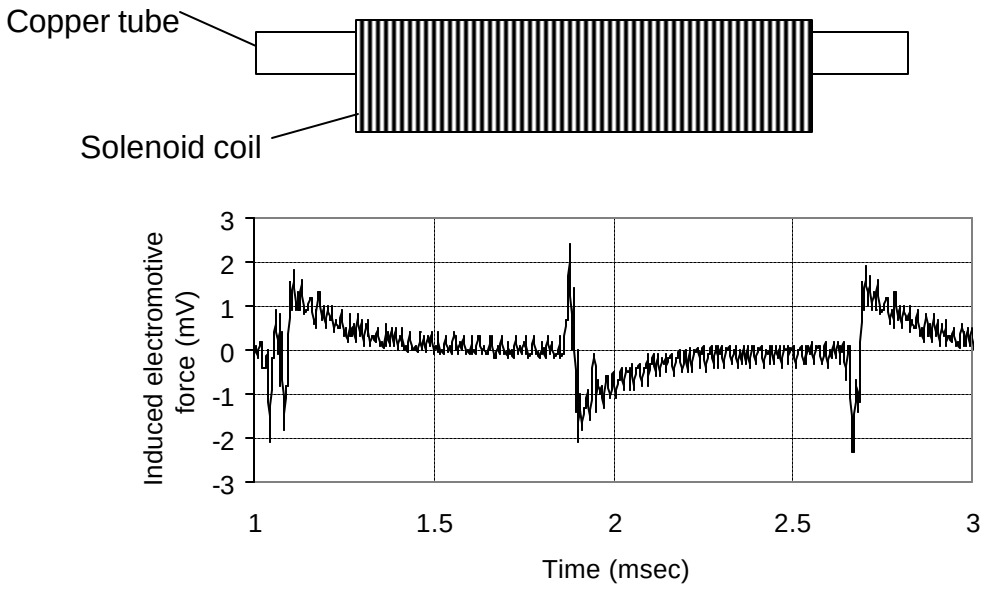

Fig. 5 Induced electromotive forces generated by a time-varying electric current at three different axial locations inside copper tube

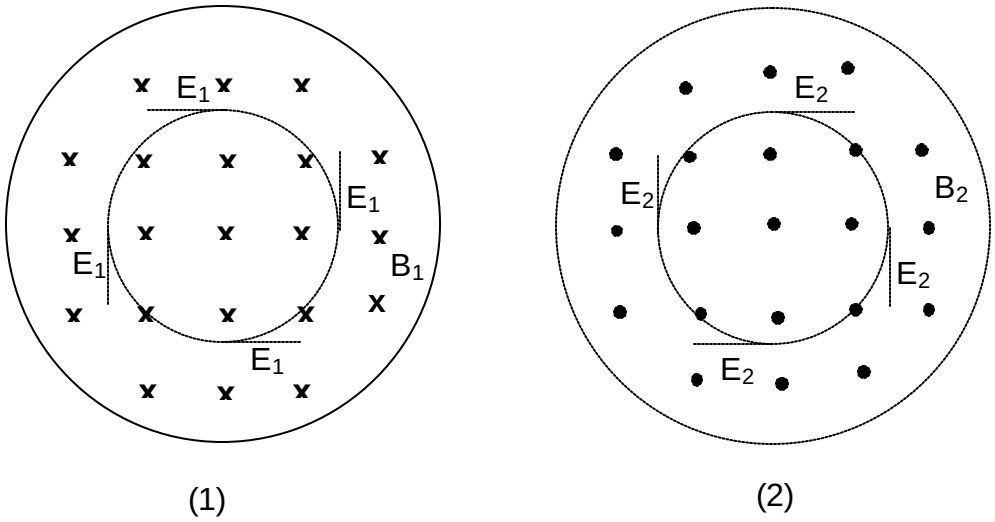

Fig. 6 Cut-away view of a pipe indicating directions of current, and electric (E) and magnetic (B) fields at different times inside a copper tube. A symbol, **x**, indicates that magnetic field goes into paper, whereas a symbol, •, indicates the magnetic field comes out of paper.

High-Voltage Electrode Devices

This type of PWT device uses a high-voltage electrode positioned at the center of a pipe filled with water, see Fig. 7. The device works by transmitting an electric signal that changes the electrical and physical properties of the scale-forming calcium molecules. The technology introduces additional electrons into the water solution using the electrode in water. The benefit of adding electrons to the water solution is the reduction of hydrogen bonding between H_2O molecules, a statement which has to be validated yet. This action is sometimes referred to as the reduction in "surface tension". In short, the manufacturer claims that the device provides electrons to the water solution. This enables electrochemical changes to occur that: (1) inhibit scale and corrosion formation; (2) dissolve existing scale and corrosion; (3) increase the cleaning power of water; (4) break down and leach away excessive salts from soils. The present study tested this device and the results are given in Chapter 7.

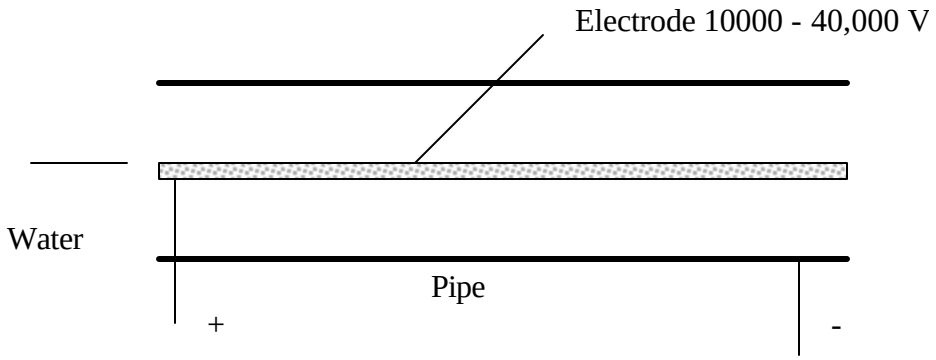

Fig.7 Sketch of a high-voltage electrode device. The electrode is coated with dielectric materials for electrical insulation.

Principle of Physical Water Treatment

When a particle with charge q moves in electric (**E**) and magnetic fields (**B**),

the particle experiences the Lorentz Force.

$$\mathbf{F} = q\mathbf{E} + q(\mathbf{V} \times \mathbf{B})$$

where **F** = Lorentz force vector [N], and **V** is the particle velocity vector [m/s].

The Lorentz force consists of the electric force (i.e., the first term in the right hand side)

and the magnetic force (i.e., the second term).

Physical Water Treatment Methods

Permanent magnet device

Solenoid-coil induction device

High-voltage electrode device

They all produce time-varying electric fields, which cause the precipitation of mineral ions,

producing particulates in bulk water.

Subsequently, particulate fouling takes place on a heat transfer surface,

and the soft sludge coating is removed by flow.

The rest of the chapters describe the test results obtained to validate various issues involved in the use of physical water treatment (PWT) devices. The tests are limited to cooling-tower water applications, where water is repeatedly treated by the PWT device. All tests were conducted with a biocide, glutaraldehyde (Union Carbide), to eliminate the effect of biofouling on the present mineral fouling study.

References

1. Bott T.R., The Fouling of Heat Exchangers, Elsevier Science, New York (1995)
2. Cowan J.C., and Weintritt D.J., "Water-Formed Scale Deposits," Gulf Publishing Company, Houston, TX (1976)
3. D. Hasson, M. Avriel, W. Resnick, T. Rozenman and S. Windreich, Mechanism of Calcium Carbonate Scale Deposition on Heat-transfer Surface, Ind. Eng. Chem. Fund., 7 (1968) 58-63
4. J. Taborek, T. Aoki, R. B. Ritter, and J. W. Palen, Fouling: The Major Unresolved Problem in Heat Transfer, Chemical Engineering Progress, 68, (1972) 59-67
5. A.P. Watkinson and O. Martinez, Scaling of Heat Exchanger Tubes by Calcium Carbonate, Transaction of the ASME, 97 (Nov. 1975) 504-508
6. R.W. Morse and J.G. Knudsen, Effect of alkalinity on the scaling of simulated cooling tower water, Canadian Journal of Chemical Engineering, 55 (1997) 272-278
7. W.G. Characklis, A Rational Approach to Problems of Fouling Deposition, Proceedings of the Engineering Foundation Conference, White Haven, Pennsylvania (1982) 1-31
8. E.F. Somerscales, Fouling of Heat Transfer Surfaces: An Historical Review, Heat Transfer Engineering, 11 (1990) 19-36
9. H. Muller-Steinhagen, Cooling Water Fouling in Heat Exchangers, Advances in Heat Transfer , Academic Press, New York, 33 (1999) 415-496
10. Snoeyink V.L. and Jenkins D., Water Chemisry,Wiley, New York (1982)
11. Beal S.K., Deposition of particles in turbulent flow on channel or pipe walls, Nuclear Science and Engineering, 40 (1970) 1-11
12. Kashchiev D., Nucelation: basic theory with applications, 1st edition, Butterworth-Heinemann, Boston (2000)
13. Al-Qahtani H., Effect of magnetic treatment on Gulf seawater, Desalination, 107 (1996) 75-81
14. J.S. Baker and S.J. Judd, Magnetic amelioration of scale formation, Wat. Res., 30, 2 (1996) 247-260
15. V.I. Klassen, Magnetic water: between Scylla and charybdis, Khimiya I Zhizn, Russian, No 9 (1969) 24-27
16. R.M.E. Diamant, Magnetic treatment of water, Hospital Engineering (1970)
17. A.V. Sandulyak and V.V. Krivtsov, Heat and hydrodynamic conditions of magnetic treatment of water against scale formation, Soviet Power Engineering, 5 (1982) 362-367
18. J.F. Grutsch and J.W. McClintock, Corrosion and deposit control in alkaline cooling water using physical water treatment at AMOCO' s largest refinery, Corrosion 84, 330 (1984) 1-26
19. R.J. Szostak, Magnetic fluid conditioning system allows 3000 ppm hardness without cooling tower scale buildup, Chemical Processing (1985) 44-45
20. D.H. Parker, An investigation of the role of physical water treatment devices in calcium carbonate scale formation, MS thesis, Baylor University, Texas (1985)
21. K.J. Kronenberg, Physical water treatment de-mystified, Magnets (1986) 6-15
22. K.W. Busch and M.A. Busch, Laboratory studies on physical water treatment and their relationship to a possible mechanism for scale reduction, Desalination, 109 (1997) 131-148, also Proceedings of the 45th International Water Conference, Pittsburgh, PA, October 23, 1984. (added)

23. J.S. Baker, S.J. Judd and S.A. Parsons, Antiscale magnetic pretreatment of reverse osmosis feedwater, Desalination, 110 (1997) 151-166
24. K. W. Busch, M. A. Busch, D. H. Parker, An investigation of the role of physical water treatment devices in calcium carbonate scale formation, Baylor University, Waco, TX 1985. also, Laboratory studies involving physical water treatment devices, Corrosion 85, Paper no. 251, 1985., also, Corrion-NACE, Vol.42, (1986) 211-221
25. S.A. Parsons, S.J. Judd, T. Stephenson, S. Udol and B-L. Wang, Magnetically augmented water treatment, Institution of Chemical Engineers, 75, B2 (1997) 98-104
26. R. E. Herzog, Q. Shi, J. N. Patil and J. L. Katz, Magnetic water treatment: The effect of iron on calcium carbonate nucleation and growth, Langmuir, Vol.5, no.3, (1989) 861-867
27. J.D. Bernardin and S.H. Chan, Magnetic effects on simulated brine properties pertaining to magnetic water treatment, 28th National Heat Transfer Conference, HTD, 164 (1991) 109-117
28. R.A. Serway, Physics for Scientists and Engineers (3rd Ed). Saunders College Publishing, Philadelphia, PA (1990) 874-891
29. J. D. Donaldson and S. Grimes, Lifting the scales from our pipes, The City University, London, UK, Newscientist, 1990. also, Tube International, (1988) 111-118
30. Lipus L., Krope J. and Garbai L., Magnetic water treatment for scale prevention, Hungarian Journal of Industrial Chemistry, 22 (1994) 239-242
31. Kronenberg K.J., Experimental evidence for effects of magnetic fields on moving water, IEEE Transactions on magnetics, MAG-21 (1985) 2059-2061
32. Hiemenz P.C., 2nd edition, Principles of Colloid and Surface Chemistry, Marcel Dekker, Inc., New York (1986)

Chapter 2

Flow Velocity Effect of Permanent Magnets (PMDU) on the Mitigation of Mineral Fouling (Rectangular Heat Transfer Test Section)

Abstract

The purpose of the present study was to investigate the effect of flow velocity on the effectiveness of permanent magnets of circulating cooling-tower water in reducing mineral fouling. Flow velocities through the permanent magnets (a physical water treatment, PWT, device) varied from 2.0 to 8.5 m/s, and the fouling resistance was measured as a function of time at each velocity. A high flow velocity of approximately 6 m/s through the PWT device was most effective in generating a maximum performance of the PWT in mineral scale prevention. As the flow velocity departs from this optimum value, the performance of the PWT significantly decreased. SEM photographs of scales were taken at the end of tests. According to the SEM photographs, the PWT changed the nature of crystal formation forming an irregular growing surface and sludge-like crystal formation indicative of a particulate fouling, whereas the case without the PWT showed a regular pattern of the scale crystal morphology, indicative of a crystallization fouling.

Introduction

One of the critical factors affecting the performance of magnetic water treatment is flow velocity around the permanent magnets. After reviewing the literature, it is rather clear that the effect of the PWT on scale prevention was not consistent because the effectiveness of the magnetic water treatment critically depended on the test conditions, particularly, the flow velocity through the permanent magnet.

Accordingly, one can ask whether there is an optimum flow velocity, which makes the PWT using permanent magnets very effective. Furthermore, it is interesting to find whether the efficiency of the PWT device substantially decreases when the flow velocity is smaller or larger than this velocity. The purpose of the present study is to investigate the effect of flow velocity on the effectiveness of the PWT of circulating cooling-tower water in reducing miner fouling at approximately 5-6 cycles of concentration.

Experimental Methods

Figure 1 shows a schematic diagram of the test facility, which consists of a water-circulating loop, a cooling tower, a side-stream flow loop, a permanent magnet device, a pump, a deposit-accumulation-test system, a conductivity meter, a floating-ball valve for automatic feeding of make-up water, and an automatic blowdown system controlled by a solenoid valve. The deposit-accumulation-test system consisted of a copper plate as a heat-transfer surface, an observation window, a cooling-water channel, and a hot-water channel.

The cooling water and hot water flowed in opposite directions, thus forming a counter-flow heat exchanger. The dimension of the cooling-water channel was 1.6 mm x 6.4 mm x 254 mm (height x width x length), whereas the dimension of the hot-water channel was 13.7 mm x

6.4 mm x 254 mm (height x width x length). Flow rates of both the cooling water and hot water were measured by rotameters (Omega Engineering), which were calibrated using a precision weighing balance. The flow velocity of circulating-cooling water in the cooling-water channel was fixed to be 1.2 m/s for all runs in the study, and the corresponding Reynolds number was 3,350, based on the hydraulic diameter of the rectangular cooling-water channel.

T-type thermocouples were used to measure the inlet and outlet temperatures of both the cooling water and hot water. The inlet temperature of the circulating water prior to the heat-transfer test section was maintained at 21^{o}C by means of the evaporative cooling tower, whereas the inlet temperature of the hot water was maintained at 89 to 92^{o}C throughout the entire experiments. Table 1 shows the test conditions used by the previous researchers who conducted fouling experiments in laboratories. In the present study, a heat flux between heating and cooling sides of the copper plate was 380 kW/m^2.

Fouling resistance was estimated by the following equation [1]:

$$R_f = \frac{1}{U_{fouled}} - \frac{1}{U_{ini}} \qquad (1)$$

where U_{ini} and U_{fouled} are the overall heat transfer coefficients at the initial time and at $t \geq 0$, respectively.

In order to calculate a surface temperature, Chiranjivi and Rao's convective heat-transfer correlation in a bottom-wall-heated rectangular duct case [2] was used as follows:

$$h = 0.79 Re^{0.4} Pr^{0.52} \frac{k_w}{De} \qquad (2)$$

where h is the convective heat-transfer coefficient, k_w is the thermal conductivity of water, and De is the equivalent diameter for the cross-sectional area in the cooling flow channel. To

calculate the average surface temperature, Newton's law of cooling [3] was introduced as following:

$$Q = hA_s(T_s - T_m) \qquad (3)$$

where h is the convective heat-transfer coefficient, A_s is the heat-transfer surface area, T_s is the surface temperature, and T_m is the mean temperature of the fluid. The average surface temperature of the copper plate, T_S, was estimated to be 59 ± 2^oC using Eqs. (2) and (3). In the calculation of Langelier saturation index (LSI), the heat-transfer-surface temperature was applied.

The cooling-tower system had a sump tank, where fresh make-up water entered through a floating-ball valve, thereby maintaining a constant water volume in the cooling tower. Tap water provided by the City of Philadelphia was used as the make-up water. The amount and frequency of blowdown of the circulating cooling water was automatically controlled with a solenoid valve. When the electric conductivity of the cooling-tower water reached a pre-set upper limit, the conductivity meter sent a triggering signal to the solenoid valve such that the valve opened until the electric conductivity in the cooling tower water dropped to another pre-set lower limit.

Figure 2 shows four different arrangements of permanent magnets. Figure 3 shows the arrangement and cross-sectional dimensions of a permanent magnet device used in the present study, which ~~was~~ consisted of four permanent magnets. The one used in the present study is similar to the ones in Class I and Class IV (see Fig.2, Chapter 1). The strength of the magnetic field was measured to be 0.16 T (or 1,600 gauss) by using an AlphaLab DC Magnetometer. The cross-sectional dimension of the flow channel in the PWT device was 0.68 mm x 9.27 mm (height x width) (see Fig. 3).

Figure 4 shows test procedure and variations of electric conductivities vs. time for the case without the PWT and four cases with the PWT. The four different flow velocities were used at the PWT device in the side-stream flow loop, which were 2.0, 4.0, 6.3, and 8.5 m/s while the flow velocity at the heat-transfer test section was fixed at 1.2 m/s. The corresponding Reynolds numbers were 5600, 11000, 17000, 24000, respectively, based on the hydraulic diameter of the flow channel in the PWT device. At the end of one run, the cooling-tower water was circulated for 1 day without the heat transfer with PWT device at the next flow-velocity condition. At the end of 1-day pretreatment of the water, the fouling test began with a brand new copper plate in the heat transfer test section.

All runs were performed while maintaining the same level of conductivity in a cooling tower. The cycles of concentration (COC) is defined as the ratio of the concentration of dissolved ions in circulating water to the dissolved ions in the make-up water [4]. The COC estimated using the electric conductivity of water was used for convenience to operate the automatic blowdown system in the study. Since the conductivity of the make-up water was about 500 μS/cm and a set point of conductivity was 2,500 μS/cm, we had approximately 5 COC based on the conductivity. Based on a mass balance, the correct number of COC was found to be 6.17 on average. The COC calculated from the conductivity values was underestimated because the method did not consider the precipitation of dissolved mineral ions in water.

Table 2 shows water quality data provided by the City of Philadelphia (Bureau of Laboratory Service) in 1999. Since the water quality varied with season, the minimum, maximum and average values are given in Table 2. Table 3 shows the water analysis data for both the make-up and circulating cooling-tower water measured in each test. The water qualities for each run were almost the same. The Langelier saturation index (LSI) was calculated to see

how much precipitation tendency the circulating water possessed. The values of the LSI were in the range of 2.1 to 2.3, indicating that the circulating water had a condition to cause severe mineral fouling.

To estimate the uncertainty in experimental results, a method presented by Kline and McClintock [5] was used. The uncertainty analysis was carried out based on the uncertainties for dimensions, flow rate and temperature. The basic uncertainties of a surface area, a temperature, and the flow rate of cold water were found to be ±0.8%, ±0.35%, and ±0.3%, respectively. The uncertainty for the fouling resistance was estimated to be 10 %.

Results and Discussion

Figure 5 shows fouling-resistance curves vs. time for five different runs, each of which was conducted for 160 hrs. The trend of the fouling resistance without the PWT was different from the trends with the PWT. The fouling-resistance curve obtained without the PWT, indicated by a cross symbol, increased very slowly for the first 20 hrs and began increasing gradually for the next 20 hrs. From t = 40 hrs, the fouling resistance continued to rapidly increase until the end of the run. The fouling resistances in the cases with the PWT consistently increased linearly for the first 70 hrs, and then the fouling resistances began to increase at different rates. For the case of 6.3 m/s, the rate of increase in the fouling resistance was the smallest, thus resulting in the smallest fouling resistance at the end of 160-hr test. As the flow velocity was further increased from 6.3 to 8.5 m/s, a very different fouling curve was obtained. From the beginning, the fouling resistance began increasing almost linearly till the end of 160-hr test.

Based on the values of the fouling resistance obtained without the PWT, the percentage reductions of the fouling resistance in the cases with the PWT were calculated. When the flow velocity through the PWT device was 2.0 m/s, the fouling resistance was reduced by 37% at the end of the run. As the velocity passing through the PWT device increased, the effectiveness of the PWT device was enhanced. The fouling resistance decreased by 43% at 4.0 m/s and by 57% at 6.3 m/s. However, when the flow velocity was further increased to 8.5 m/s, the effectiveness of the magnetic device significantly dropped. The fouling resistance decreased only by 26% in this case.

Figure 6 shows the percentage reduction of the fouling resistance vs. the flow velocity through the PWT device, i.e., the effectiveness of the PWT device at different flow velocities. The optimum flow velocity at the PWT device for the maximum effectiveness appears to be between 5 and 7 m/s.

Figure 7 shows the photographs of fouled surfaces taken after the surfaces were completely dried. Run #4 with a flow velocity of 6.3 m/s gave the least amount of scale deposit (see Fig. 7(c)). No treatment case (Run #1) resulted in the most severe fouling according to photographs; see Fig. 7(a). When the circulating water passed through the PWT device at a velocity greater than the optimum velocity, i.e., at 8.5 m/s, the PWT was not effective, as manifested by the photograph shown in Fig. 7(d).

Figure 8 shows scanning electron microscope (SEM) photographs of scale samples obtained at the end of 160-hr tests with a magnification of 1000x. In the SEM photographs, only the top surfaces of the scale layer are seen. Figure 8(a) shows a SEM photograph for Run #1 after 160-hr test. The crystals are close to rhombic shape with round edges. The growing surface of each crystal (i.e., the interface between solution and solid phase) appears to be very

smooth, indicating that the crystals grew through crystallization reaction assisted by ion diffusion. In other words, the scale layer without the PWT formed due to a mechanism of crystallization fouling on the surface.

Figure 8(b) shows a SEM photograph for Run #2 after 160-hr test with the PWT. Compared to the pattern in Fig. 8(a), the crystals are completely different in their morphology. The growing surface of scale is rough and irregular, suggesting that the mechanism of scale formation in a magnetically treated solution is quite different from the crystallization reaction. A similar pattern of the scale was observed in Run #3 with the PWT when the flow velocity through the PWT device was 4.0 m/s (see Fig. 8(c)). The top surface of each mineral scale in both Run #2 and Run #3 appears to be flat as shown in Figs. 8(b) and 8(c), whereas Run #4 and Run #5 treated at higher flow velocities of 6.3 and 8.5 m/s, respectively, resulted in a very rough surface of scale layer (see Figs. 8(d) and 8(e)). It is speculated that the different patterns of scale seen from the top surface resulted from different mechanisms of scale growth. In Run #4 and Run #5, it is clear that the scale layer appears to be formed by the accumulation of numerous small-sized crystallites suspended in the circulating. In short, the PWT changed the nature of crystal formation, forming an irregular growing surface and sludge-like crystal formation, whereas the case without the PWT showed regular patterns of crystal growth through crystallization reaction assisted by ion-diffusion process on the heat-transfer surface.

Conclusion

The present study demonstrated that a high flow velocity of approximately 6 m/s through the PWT device was effective in generating a maximum performance of the PWT in mineral scale prevention. At this optimum operating condition, the PWT could substantially reduce

mineral fouling in a heat exchanger using cooling-tower water even at 5-6 COC. However, away from the optimum operating condition, the benefit of the PWT was significantly reduced. According to the SEM photographs, the PWT changed a nature of crystal formation forming an irregular growing surface and sludge-like crystal formation, whereas the case without the PWT showed a normal pattern of the scale crystal morphology.

References

1. B. Bansal and H. Muller-Steinhagen, Crystallization Fouling in Plate Exchangers, J. Heat Transfer, 115 (1993) 584-591

2. M.A. Ebadian and Z.F. Dong, Handbook of Heat Transfer, 3rd edition, McGraw-Hill, New York (1998) 5.106-5.107

3. F.P. Incropera and D.P. Dewitt, Fundamentals of Heat Transfer, John Wiley & Sons, New York (1981)

4. BETZ Handbook of Industrial Water Conditioning, 9th edition, BETZ, 1991

5.S. J. Kline and F. A. McClintock, Describing Uncertainties in Single-sample Experiments, Mechanical Engineering (1953) 3

6.D. Hasson, M. Avriel, W. Resnick, T. Rozenman and S. Windreich, Mechanism of calcium carbonate scale deposition on heat-transfer surfaces, I&EC Fundamentals, 7, 1 (1968) 59-65

7.N.H. Kim and R.L. Webb, Particulate fouling of water in tubes having a two-dimensional roughness geometry, 34, 11 (1991) 2727-2738

8. E.F.C. Somerscales, A.F. Ponteduro, and A.E. Bergles, Particulate of heat transfer tubes enhanced on their inner surface, ASME, HTD-Vol. 164, Fouling and Enhancement Interactions (1991)

9. S. Nasrazadani and T. J. Chao, Laboratory evaluations of ozone as a scale inhibitor for use in open recirculating cooling systems, ASHRAE Research Project 765-RP, Final Report (1994)

10. R. Sheikholeslami and A.P. Watkinson, Scaling of plain and externally finned heat exchanger tubes, Journal of Heat Transfer, 108 (1986) 147-152

11. R.W. Morse and J.G. Knudsen, Effect of alkalinity on the scaling of simulated cooling tower water, Canadian Journal of Chemical Engineering, 55 (1997) 272-278

12. A. Helalizadeh, H. Muller-Steinhagen and M. Jamialahmadi, Mixed salt crystallization fouling, Chemical Engineering and Processing, 39 (2000) 29-43

Table 1. Test conditions used by previous researchers who conducted fouling experiments

References	Heat flux (kW/m^2)	Flow velocity (m/s)	Concentration (ppm)	Foulant
Hasson [6]	1.6	0.25 - 0.82	110 - 575	Calcium
Kim & Webb [7]	13	0.8 - 1.82	1500	Aluminum Oxide / Ferric Oxide
Somerscales [8]	28 - 52	0.9 - 1.0 1.4 - 1.5	2500	MgO
Nasrazadani [9]	137	1 - 1.98	300 - 450	Calcium
Sheikholeslami & Watkinson [10]	120 - 220	0.3 – 0.8	603 - 700	Calcium
Morse & Knudsen [11]	276	1.0	490 - 650	TDS
Helalizadeh & Muller-Steinhagen [12]	100 - 400	0.5 - 2.0	1.0 - 2.5 / 0.25 - 1.0	Calcium Sulphate / Calcium Carbonate
Present study	380	1.2	800	Total hardness

Table 2. Water quality data provided by the City of Philadelphia

	Minimum	Average	Maximum
Conductivity (μS/cm)	389	520	652
PH	7.3	7.5	7.6
Total hardness (mg/L)	150	190	247
Total Alkalinity (mg/L)	54	74	93
Chloride (mg/L)	56	75	149
Phosphate (mg/L)	0.2	0.25	0.3
Silica (mg/L)	3	5.8	7.8
Sulfate (mg/L)	37	61	89

Table 3. Water analysis data for both the make-up and circulating cooling-tower water

	Make-up water	Run 1	Run 2	Run 3	Run 4	Run 5
Conductivity (μS/cm)	492	2460	2410	2460	2450	2480
PH	7.2	8.3	8.15	8.2	8.35	8.2
Total hardness (mg/L)	227	786	790	782	760	788
Calcium hardness (mg/L)	174	538	526	532	528	542
Magnesium hardness (mg/L)	53	248	264	250	232	246
Total Alkalinity (mg/L)	81	202	210	206	218	216
Chloride (mg/L)	76	420	426	430	428	432
Langelier Saturation Index (at $60^{o}C$)	0.48	2.28	2.14	2.18	2.35	2.21

List of Figures

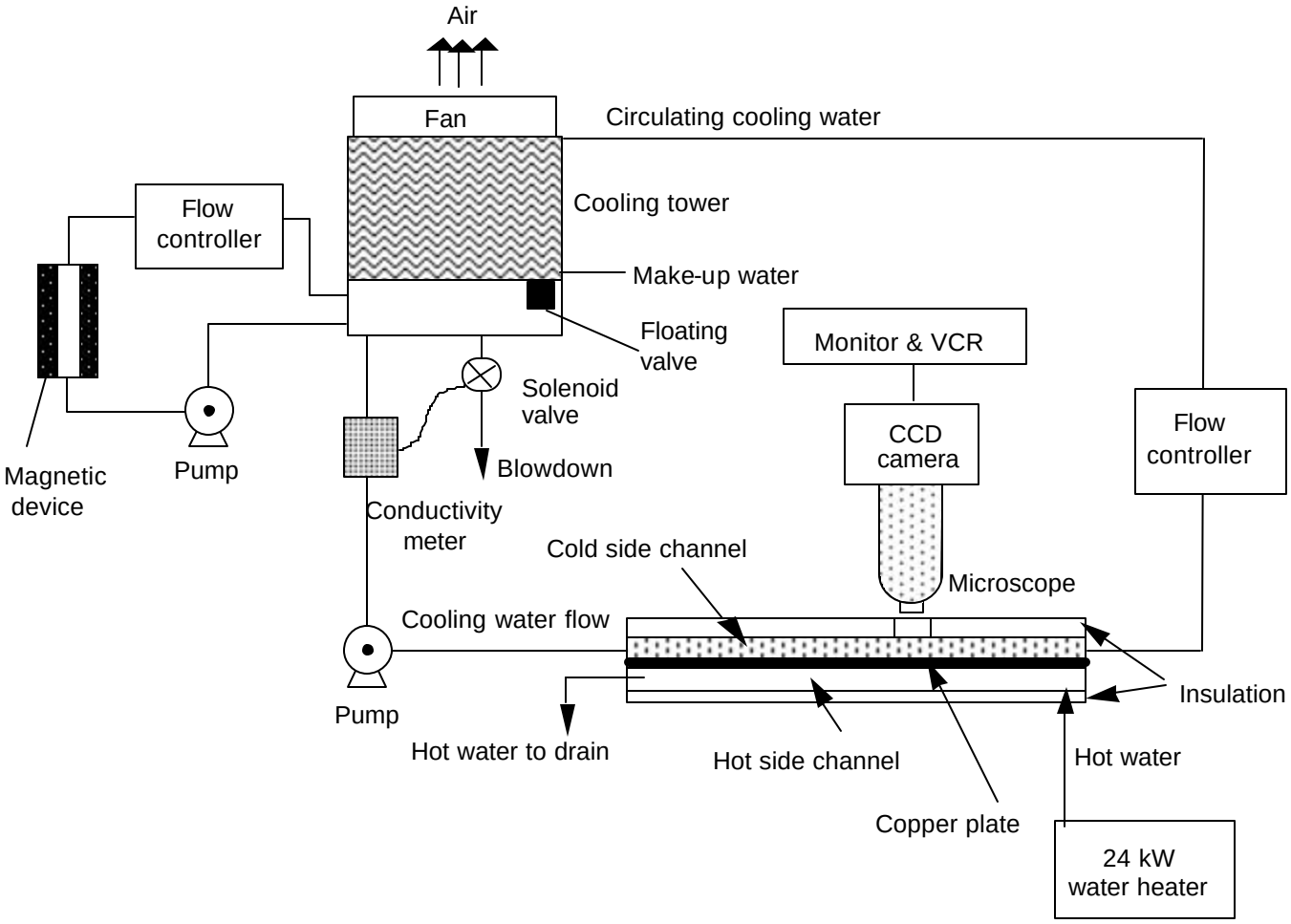
Air
Fan
Circulating cooling water
Cooling tower
Flow controller
Make-up water
Floating valve
Monitor & VCR
Solenoid valve
CCD camera
Flow controller
Magnetic device
Pump
Blowdown
Conductivity meter
Cold side channel
Microscope
Cooling water flow
Insulation
Pump
Hot water to drain
Hot side channel
Hot water
Copper plate
24 kW water heater

Figure 1

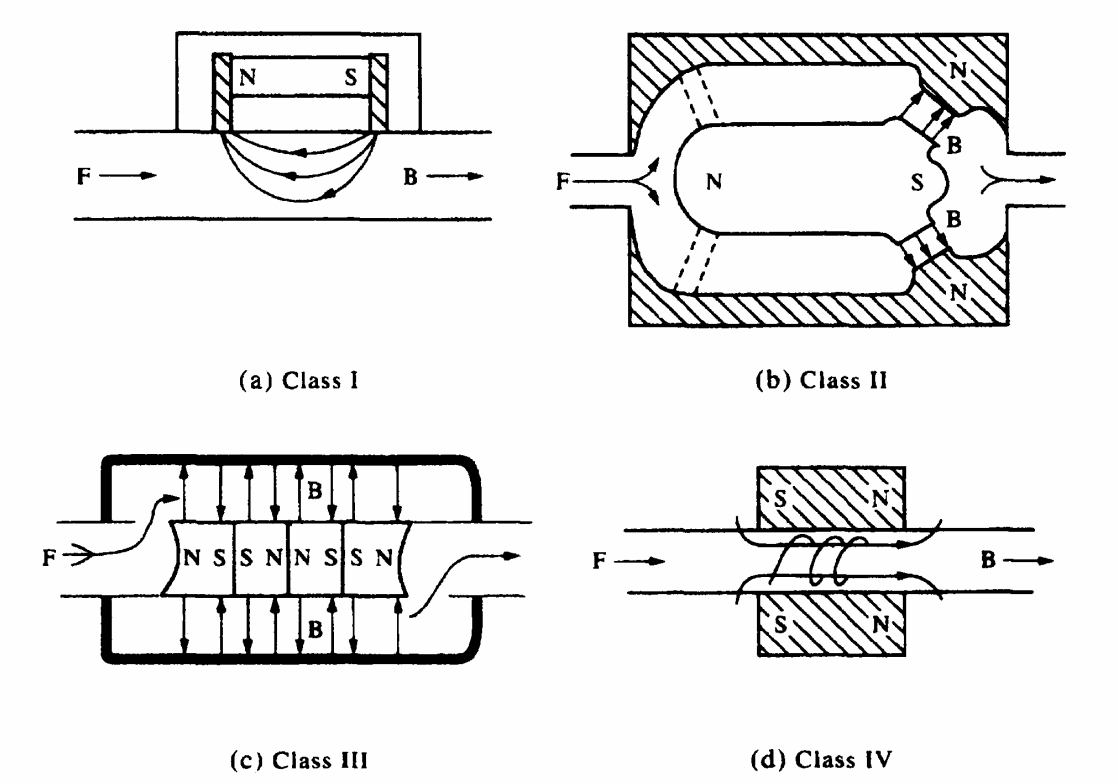

(a) Class I : clamp-on magnetic device

(b) Class II : radial magnetic flow transverse near poles

(c) Class III : radial flow, alternating magnetic filed direction

(d) Class IV : parallel magnetic field, collinear solenoid, spiral metal element in field

Figure 2

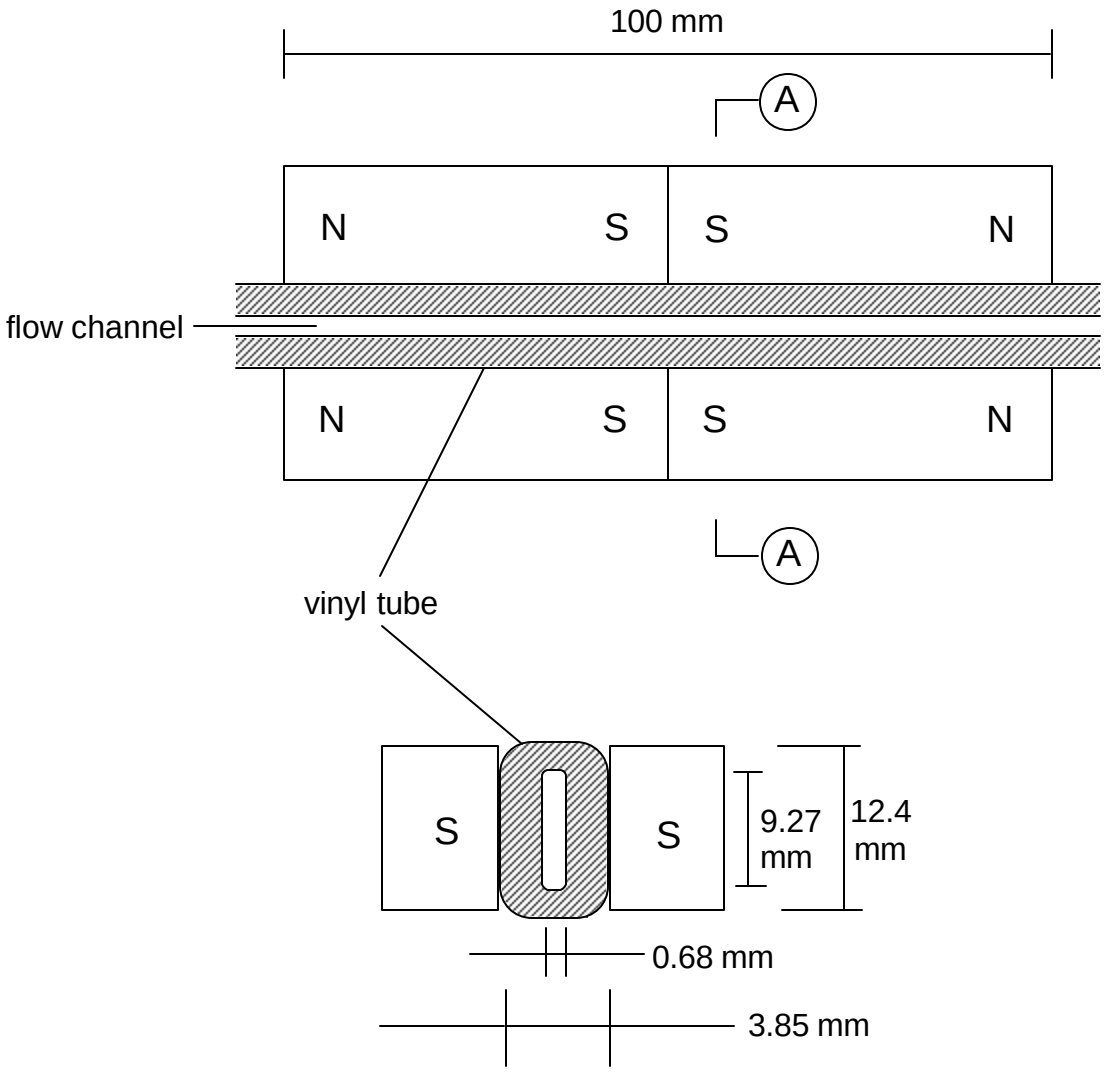

Section view <A-A>

Figure 3

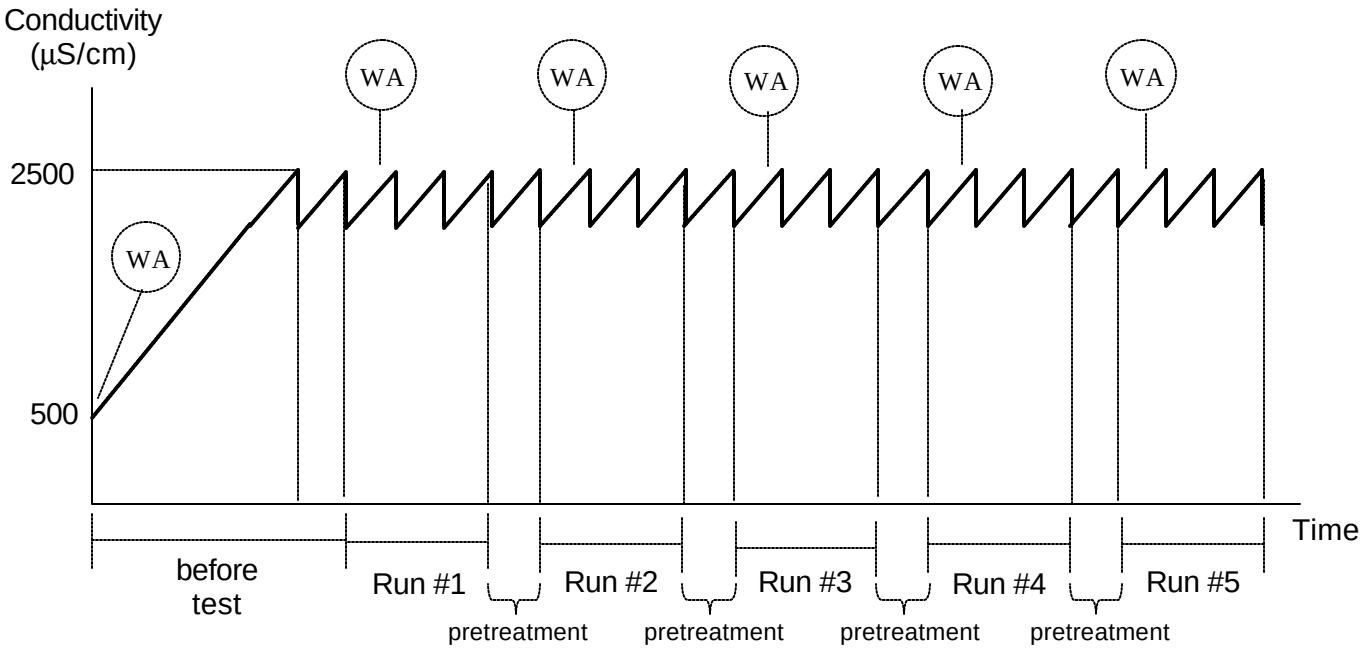

Run #1 : no physical water treatment

Run #2 : with PWT (2.0 m/s)

Run #3 : with PWT (4.0 m/s)

Run #4 : with PWT (6.3 m/s)

Run #5 : with PWT (8.5 m/s)

Figure 4

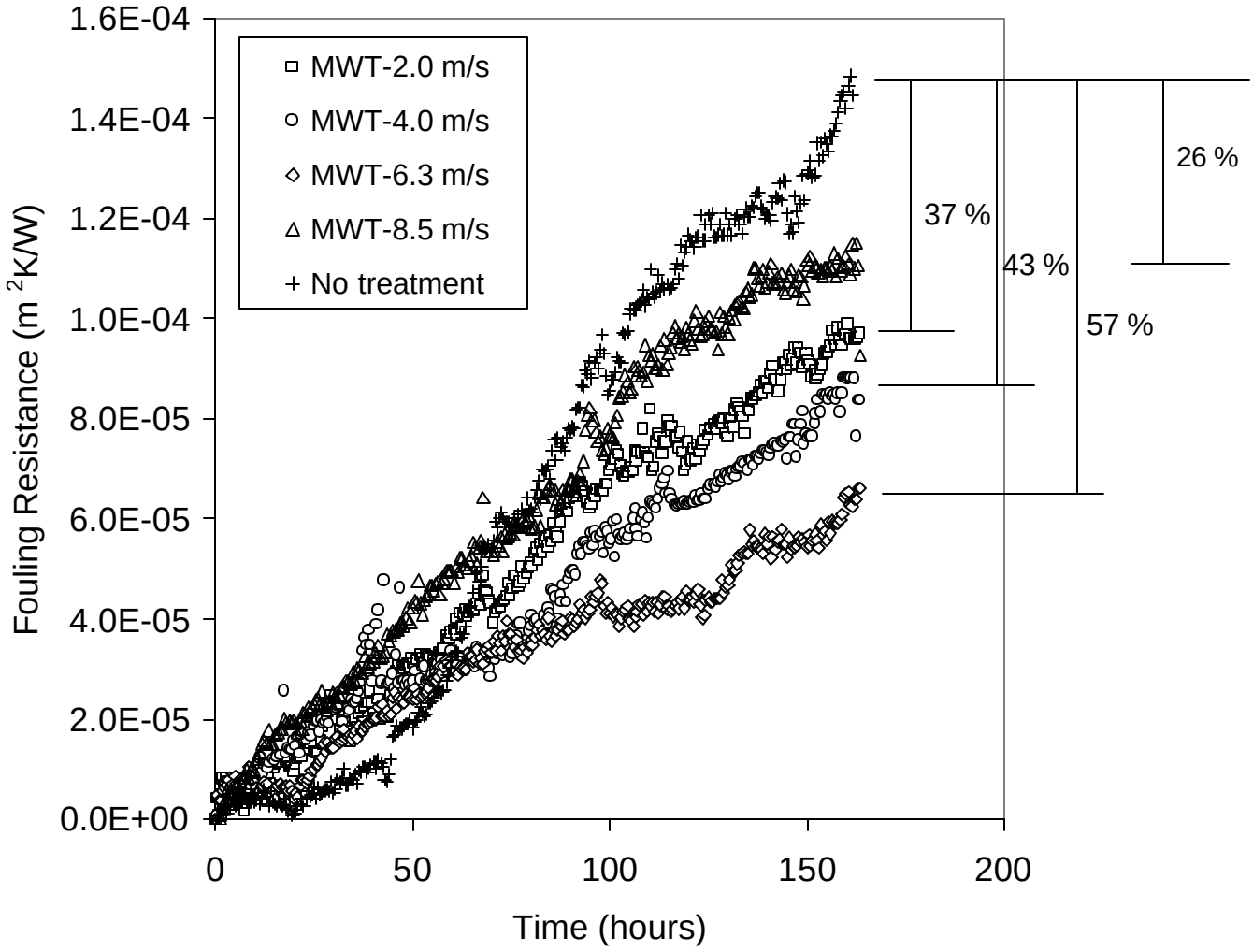

Figure 5 MWT = magnetic water treatment

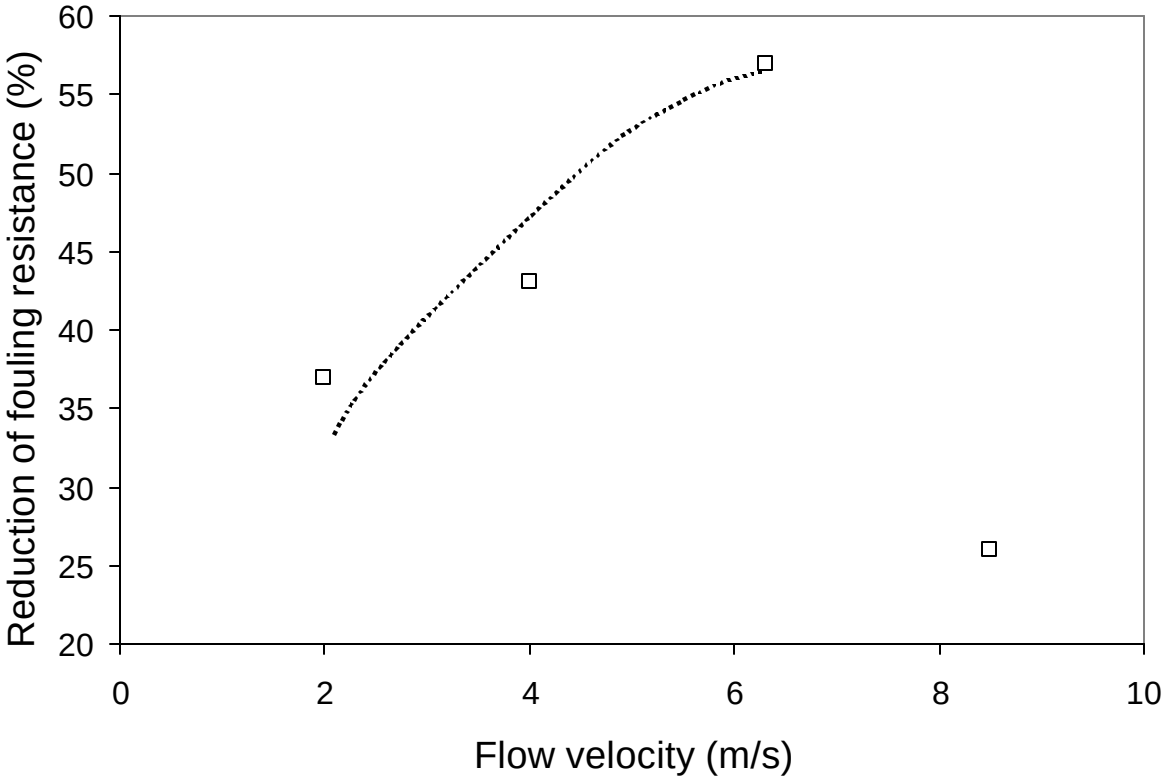
Reduction of fouling resistance (%)
60
55
50
45
40
35
30
25
20
0
2
4
6
8
10
Flow velocity (m/s)

Figure 6

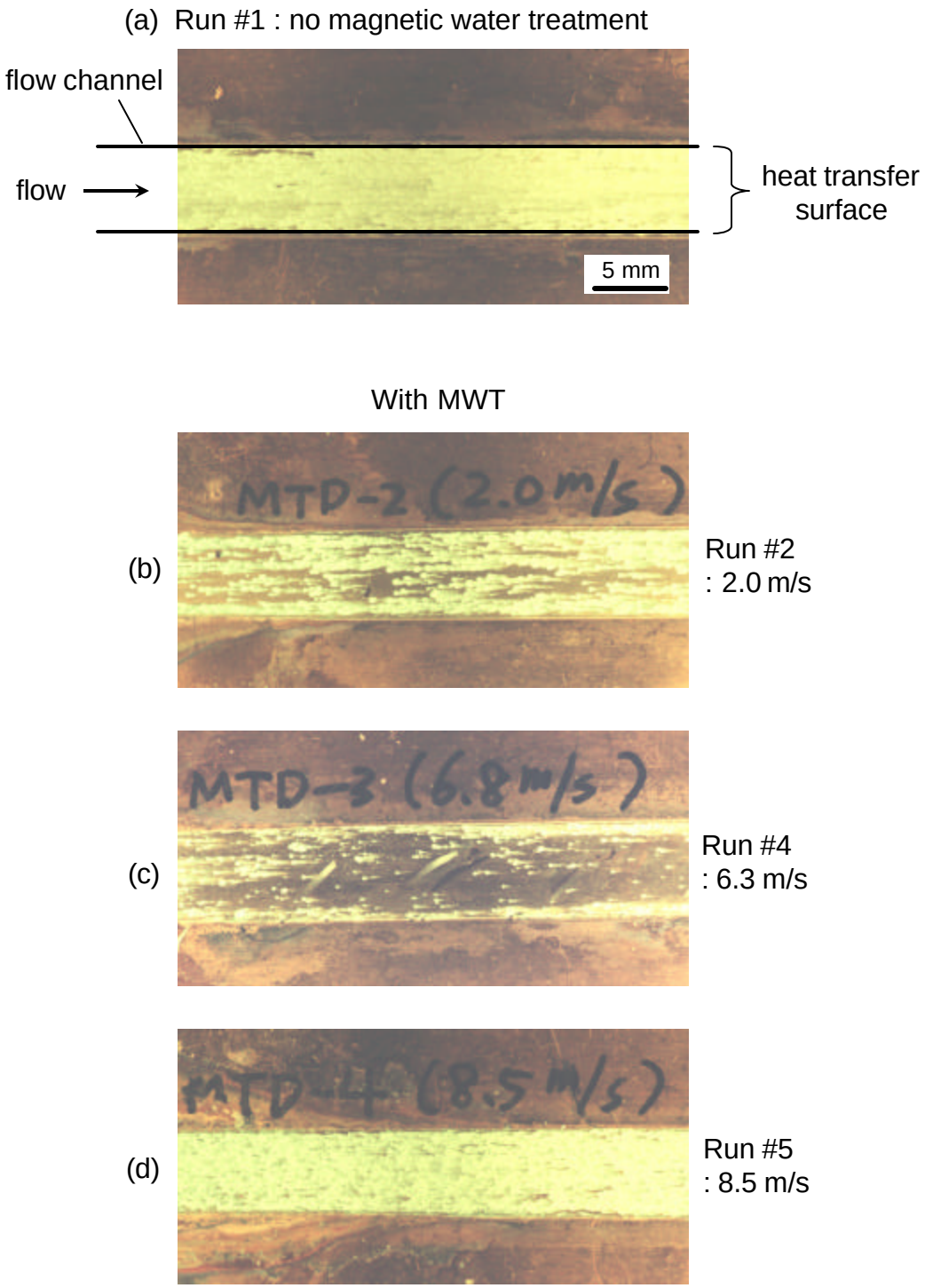
(a) Run #1 : no magnetic water treatment
flow channel
flow
heat transfer surface
5 mm
With MWT
(b)
MTD-2 (2.0 m/s)
Run #2
: 2.0 m/s
(c)
MTD-3 (6.8 m/s)
Run #4
: 6.3 m/s
(d)
MTD-4 (8.5 m/s)
Run #5
: 8.5 m/s

Figure 7

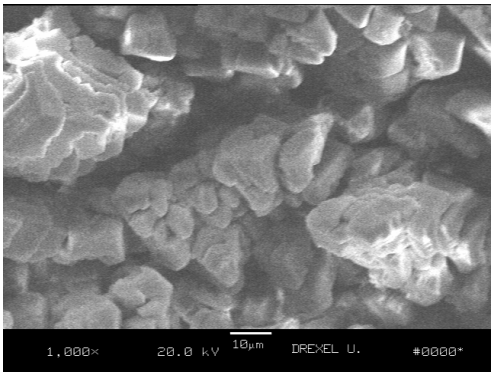

(a) no MWT – Run #1

10 µm

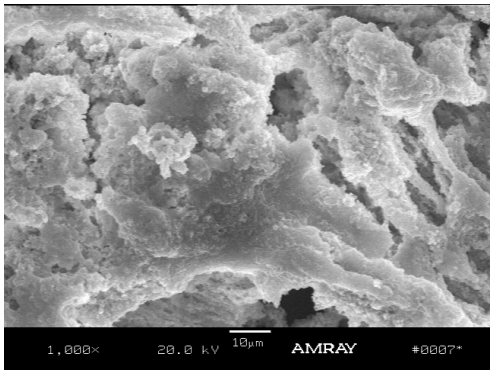

(b) w/ MWT – Run #2 (2 m/s)

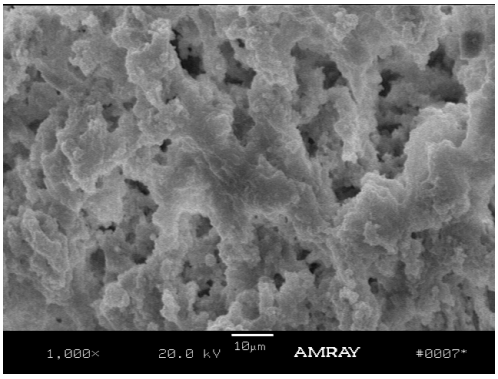

(c) w/ MWT – Run #3 (4 m/s)

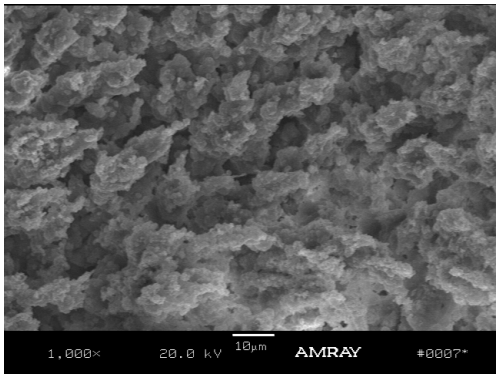

(d) w/ MWT – Run #4 (6.3 m/s)

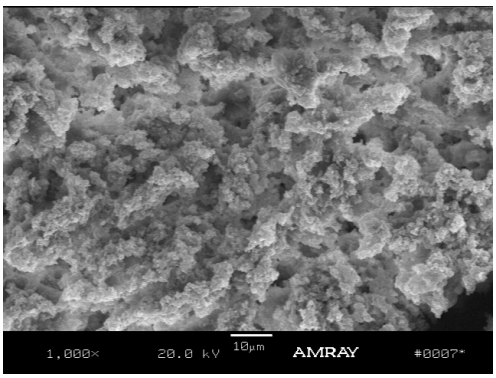

(e) w/ MWT – Run #5 (8.5 m/s)

Figure 8

Chapter 3

Flow Velocity Effect of Permanent Magnets (PMSM-1) on the Mitigation of Mineral Fouling (Rectangular Heat Transfer Test Section)

Abstract

The purpose of the present study was to investigate the effect of flow velocity through permanent magnets on the performance of the physical water treatment (PWT) for the mitigation of mineral fouling in a heat exchanger in an open cooling-tower system. The present study demonstrated that a high flow velocity of approximately 2.3 m/s through the permanent magnets was necessary to obtain the maximum performance of the PWT for the mitigation of mineral fouling. At this optimum operating condition which can be obtained by correctly sizing the PWT based on the flow rate (G.P.M.), the permanent magnets could substantially reduce mineral fouling in the heat exchanger using cooling-tower water. However, away from the optimum operating condition, the benefit of the permanent magnets was significantly reduced.

INTRODUCTION

One of the critical factors affecting the performance of magnetic water treatment is flow velocity around permanent magnets. After reviewing the literature, it is rather clear that the effect of the physical water treatment (PWT) using permanent magnets on

scale mitigation was not consistent because the effectiveness of the magnetic water treatment critically depended on the test conditions, particularly, the flow velocity through the permanent magnets.

Accordingly, one can ask whether there is an optimum flow velocity, which makes the PWT very effective. Furthermore, it is interesting to find whether the efficiency of the PWT device substantially decreases when the flow velocity is smaller or larger than this velocity. The purpose of the present study is to investigate the effect of flow velocity on the effectiveness of the PWT of circulating cooling-tower water in reducing mineral fouling at approximately 5-6 cycles of concentration.

EXPERIMENTAL METHODS

The flow velocity of circulating-cooling water in a cooling-water channel was fixed to be 1.5 m/s for all runs in the study, and the corresponding Reynolds number was 4,470, based on the hydraulic diameter. Four different flow velocities were used at the PMSM-1 device installed in a side-stream flow loop, which were 1.1, 1.7, 2.3, and 3.0 m/s while the flow velocity at the heat transfer test section was maintained constant at 1.5 m/s.

The inlet temperature of the circulating water prior to the heat-transfer test section was maintained at $20 \pm 1°C$ by means of the evaporative cooling tower, whereas the inlet temperature of the hot water was maintained at 89 to 92°C throughout the entire experiments. Heat flux between heating and cooling sides of the copper plate was 485.2 kW/m^2 which is extremely high and not normally found in field use.

RESULTS AND DISCUSSION

Table 1 shows the water analysis data for the make-up and circulating cooling-tower water for both the no-treatment and PWT treatment cases without filtration. There was no big difference in water qualities between the no-treatment case and the case with the PWT using PMSM-1. The Langelier saturation index (LSI) was calculated to examine the precipitation tendency of the circulating water. The values of the LSI were in the range of 2.48 to 2.51, indicating that the circulating water had a condition to cause severe mineral fouling. Table 2 shows the water analysis data for the same sample waters, which was illustrated in Table 1 with filtration with a 0.2 μm-filter (NALGENE). The result was almost the same to that of without filtration in Table 1. Table 3 and 4 shows the results of water analysis, which was performed by Commercial Water Treater with the same sample water. The maximum difference between table 3 and 4 was 3%. This difference seems to be caused by the measuring method (i.e., Drexel – titration method, Commercial Water Treater – light scattering method).

Figure 1 represents fouling resistance values vs. time for five different cases. The characteristics of fouling resistance for the no treatment case was that the increasing rate of scale deposition was not steep in the first 200 hours and then suddenly increased very rapidly and reached the asymptotic value. This phenomenon represents that a relatively long induction period existed due to the low water concentration (i.e., 2,000 μS/cm). When the flow velocity through the PWT was 2.3 m/s, the asymptotic value of the fouling resistance for the PWT case decreased by 80% from the value of the no-treatment case. For the cases of the flow velocity of 1.1 and 1.7 m/s, the fouling resistance

decreased by 25 and 42%, respectively. The asymptotic final fouling resistance for the flow velocity 3.0 m/s was only reduced 32% comparing to the no treatment case.

It is not clear why the performance of the magnetic treatment using PMSM-1 shows the optimum behavior at a specific velocity of 2.3 m/s (i.e., 80% drop in the fouling resistance compared to the no treatment case). One may speculate as follows: For the no treatment case, the scale deposition is mainly due to the diffusion of dissolved mineral ions, which results in crystallization fouling and tenacious hardened scale. When the cooling water was treated by the PWT at the optimum velocity through the magnet (i.e., 2.3 m/s for this case), the mineral ions that dissolved in the cooling water precipitated in the bulk water, and therefore, these precipitated particles were deposited on the heat exchanger surface in the form of a particulate fouling Particles deposited on the heat transfer surface as a soft sludge coating, which are easily removed by shear force unlike the hardened scale deposit produced by the diffusion of ions. However, this significant reduction of fouling could only be obtained when the flow velocity was reached at a certain optimized point such as 2.3 m/s.

When the flow velocity through the magnets was different from this optimum velocity, it is not clear why the performance of the magnetic treatment significantly decreased. When the flow velocity was greater than the optimum value, one can consider that the contact residence time was too short to be affected by the magnetic field. When the flow velocity was much smaller than the optimum value, the agitating force via Lorentz force may not be sufficient to cause bulk precipitation. The exact mechanism of the existence of the optimum condition in the magnetic treatment needs to be further investigated in the future.

Figures 2a and 2b show the percentage reduction of the fouling resistance vs. flow velocity for the PMSM-1 and PMDU cases. As can be seen in Fig.2, each permanent magnet device has its own optimum flow velocity range. The difference in the optimum flow velocity between the two devices may come from the specific arrangement and spacing of the alternating poles in the permanent magnets since the strengths of magnetic field were almost identical 1,200 – 1,400 gauss for both devices.

Figure 3 shows photographs of fouled surfaces taken after the fouled heat-transfer surfaces were completely dried. No-treatment cases resulted in much more severe fouling than PWT cases, regardless of flow velocity. However, in the PWT cases, the amount of fouling deposit decreased with increasing flow velocity until V=2.3 m/s. When the flow velocity was greater than 2.3 m/s such as 3.0 m/s, the amount of scale deposition was increased again. This observation was consistent with the trends in fouling resistances given in the Figure 1.

Figure 4 shows the scanning electron microscopic (SEM) photographs of scale layer for all cases (i.e., no treatment, PWT-1.1, 1.7, 2.3, and 3.0 m/s). It could be seen easily something different in morphology of scale layer and could be found no treatment, PWT-1.1 m/s, and 3.0 m/s case has similar surface pattern.

Figure 5 shows enlarged SEM photographs of scale layer for only three cases (no treatment, PWT-1.7 m/s, and PWT-2.3 m/s) to investigate the effect of flow velocity through the PWT device. Three cases have very different morphology. For the no-treatment case, numerous tiny crystals were agglomerated. However, in the case of PWT-1.7 m/s, the average crystal size was much bigger than that of no treatment case. In the PWT-2.3 m/s case, it was too difficult to determine the each crystal grain boundary,

so it looked like a one big irregular crystal. Hence, it can be concluded that the PWT produced $CaCO_3$ particles in water, which grew in size and eventually deposited on the heat-transfer surface as an amorphous colloidal form. The big difference in the morphology of scale layer between the untreated and PWT cases may explain the mechanism of the PWT (i.e., particulate fouling).

In Fig. 6, the difference of surface morphology between no treatment case and PWT-2.3 m/s case can be seen more clearly. Plenty of rhombic shape tiny crystals could be found in no treatment scale. The average size of each crystal was estimated as 0.5 μm. On the contrary, in the case of PWT-2.3 m/s, it looked like ~~a~~ one huge particle but this scale was composed of multi-layer of scale even the size could not be measured. This phenomenon could be explained that the colloidal particles which were made by PWT device

The structure of the calcium carbonate was investigated by several researchers [1-4] because the characteristics of the structure of the calcium carbonate scale have been used to explain the mechanism of the PWT method. Some researchers stated that a calcite structure was dominant for no-treatment cases, while when a PWT was applied, aragonite was formed instead of the calcite. Others stated that aragonite scale with a needle-shaped structure deposited on a heat exchanger surface for the untreated case, which was very hard to remove. On the contrary, calcite with a round-shaped structure is easier to remove it than aragonite-type scale.

In the present study, an X-ray diffraction method was used to investigate the structure of scale crystals that were sampled from the heat-transfer test section. As one can see in Figure 7, all six sampled crystals had the same structure of calcium carbonate

scale, which was calcite. From this result, it can be concluded that the PWT using permanent magnets produced calcite form of calcium carbonate, and there is no difference in the structure of the scale crystals removed from the heat transfer test section between the untreated and PWT cases.

Some previous researchers [5-7] reported that the crystal phase of scale deposits was aragonite when they applied physical water treatment (PWT). Appendix B at the end of this chapter reports detailed results of the measurements with X-ray diffraction methods, which were repeated following the procedure reported by the previous researchers [5-7].

The present study given in Appendix B found that the crystal phase of the scale sample changed with time, from an aragonite form initially to a calcite form in three days. Note that the first measurement was performed within two hours of scale formation, and the second measurement was conducted with the same scale sample three days later. For both 2,000- and 4,000-μS/cm cases, crystals changed from aragonite in the first measurement to calcite in the second measurement (i.e., aragonite:calcite = 10%:90%). This explains why the X-ray diffraction results from the scale samples collected from the heat transfer test section indicated a calcite form of $CaCO_3$. See Appendix B for more detail discussions.

CONCLUSIONS

The present study demonstrated that a high flow velocity of approximately 2.3 m/s through a PWT was necessary to obtain the maximum performance of the PWT in mineral scale prevention. At this optimum operating condition, the PWT could

substantially reduce mineral fouling in a heat exchanger using cooling-tower water. However, away from the optimum operating condition, the benefit of the PWT was significantly reduced. Hence, if the correct PWT could be sized or configured for a piping system with a known flow velocity, the PWT can effectively control hard water scale.

In the case of no-treatment, the crystallization fouling, which creates tenacious hardened scale deposits, seemed to be dominant. On the other hand, the PWT cases produced $CaCO_3$ particles (i.e., bulk precipitation) and, which grew inside the heat exchanger, eventually depositing on the heat-transfer surface in the form of particulate fouling. However, the particulate fouling creates a soft sludge coating on the heat transfer surface, which is easily flushed away and settles at a low point in the system, or in a less turbulent area where it can be easily drained or flushed out of the system. SEM photographs were obtained to render further support on the hypothesis of the particulate fouling.

REFERENCES

[1] Higashitani et al., Effects of a Magnetic Field on the formation of CaCO3 particles, J. of Colloid & Interface Science, 156, (1993) 90-95

[2] Grimes M.S., Magnetic field effect on crystals, Tube International, (1988)

[3] Barrett A.R. and Parsons S.S., The influence of Magnetic fields on calcium carbonate precipitation, Water Research., 32, 3 (1998) 609-612

[4] Cho Y.I. and Choi B.G., Validation of an Electronic Anti-fouling Technology in a Single-Tube Heat Exchanger, Int. J. Heat and Mass Transfer, 42, 8 (1999) 1491-1499

[5] Donaldson J.D. and Grimes S., Lifting the scales from our pipes, The City University, London, UK, Newscientist, 1990. also, Tube International, (1988) 111-118

[6] Higashitani K., et al., Effects of a magnetic field on the formation of CaCO3 particles, Journal of Colloid and interface science, 156 (1993) 90-95

[7] Kobe S., Drazic G., McGuiness P.J., Strazisar J., The influence of the magnetic field on the crystallization form of calcium carbonate and the testing of a magnetic water-treatment device, J. Magnetism and Magnetic Materials, 236 (2001) 71-76

	Make-up Water	Circulating water (without filtration)				
		No treatment	PMSM-1 V=1.1m/s	PMSM-1 V=1.7m/s	PMSM-1 V=2.3m/s	PMSM-1 V=3.0m/s
Conductivity (μS/cm)	510	1960 (3.8)	1980 (3.9)	1980 (3.9)	1980 (3.9)	1995 (3.9)
pH	7.4	8.3	8.3	8.4	8.4	8.4
Total hardness (mg/L)	176	860 (4.9)	844 (4.8)	844 (4.8)	850 (4.8)	840 (4.8)
Ca^{+} hardness (mg/L)	131	540 (4.1)	530 (4.0)	548 (4.2)	540 (4.1)	556 (4.2)
Total alkalinity (mg/L)	68	228 (3.4)	236 (3.4)	232 (3.4)	230 (3.4)	228 (3.4)
Chloride (mg/L)	93	390 (4.2)	406 (4.4)	386 (4.2)	390 (4.3)	386 (4.2)
LSI**	-0.01	2.48	2.48	2.49	2.49	2.51
R_f (m^2K/W)***		$4.7x10^{-5}$	$3.5x10^{-5}$	$2.7x10^{-5}$	$0.8x10^{-4}$	$3.0x10^{-4}$

* ( ) represents the ratio of each treatment to the make-up water
** LSI = Langelier Saturation Index
*** R_f = Fouling resistance at the end of 200-hour test

Table 1. Water quality data measured for make-up and circulating water

	Make-up Water	Circulating water (with filtration)				
		No treatment	PMSM-1 V=1.1m/s	PMSM-1 V=1.7m/s	PMSM-1 V=2.3m/s	PMSM-1 V=3.0m/s
Conductivity (μS/cm)	510	1956 (3.8)	1980 (3.9)	1980 (3.9)	1976 (3.9)	1990 (3.9)
pH	7.4	8.3	8.3	8.4	8.4	8.4
Total hardness (mg/L)	176	860 (4.9)	844 (4.8)	844 (4.8)	840 (4.8)	840 (4.8)
Ca^{+} hardness (mg/L)	131	540 (4.1)	530 (4.0)	548 (4.2)	532 (4.0)	556 (4.2)
Total alkalinity (mg/L)	68	228 (3.4)	236 (3.4)	232 (3.4)	230 (3.4)	228 (3.4)
Chloride (mg/L)	93	390 (4.2)	406 (4.4)	386 (4.2)	390 (4.3)	386 (4.2)
LSI**	-0.01	2.48	2.48	2.49	2.49	2.51
R_f (m^2K/W)***		$4.7x10^{-5}$	$3.5x10^{-5}$	$2.7x10^{-5}$	$0.8x10^{-4}$	$3.0x10^{-4}$

* ( ) represents the ratio of each treatment to the make-up water
** LSI = Langelier Saturation Index
*** R_f = Fouling resistance at the end of 200-hour test

Table 2. Water quality data measured for make-up and circulating water

ASHRAE RP1155 – Water Analyses Performed by Commercial Water Treater

Before filtration	Make up	PMSM V=1.1 m/s	PMSM V=1.7 m/s	PMSM V=2.3 m/s	PMSM V=3.0 m/s
pH	7.7	8.3	8.4	8.3	8.4
Sp Cond @ 25C, µmhos	525	1990	2010	2030	1970
Alk, "P" as CaCO3, ppm	0	0	3.6	8.3	0
Alk, "M" as CaCO3, ppm	70	228	189	229	194
Sulfur, as SO4, ppm	54	195	314	184	231
Chloride, as Cl, ppm	81	385	356	410	369
Hardness, Total, as CaCO3, ppm	185	824	845	853	757
Calcium, Total, as CaCO3, ppm	126	565	560	581	508
Magnesium, Total, as CaCO3, ppm	58	258	284	271	248
Copper, Total, as Cu, ppm	<0.05	0.28	0.24	0.26	0.33
Iron, Total, as Fe, ppm	<0.05	<0.05	<0.05	<0.05	<0.05
Sodium, as Na, ppm	39	129	126	134	122
PO4, Total Inorg, as PO4, ppm	1.1				
PO4, Ortho, as PO4	1.2	0.6	0.9	0.9	0.6
Silica, Total, as SiO2, ppm	5.7	15.1	20	13.9	23

Observations:

(1) - Based on sulfur, chloride, magnesium, and sodium, it appears that the tower was cycled about 5.3 times when sampled. No evidence of gross precipitation is seen.

Table 3. Water quality data measured for make-up and circulating water

ASHRAE RP1155 – Water Analyses Performed by Commercial Water Treater

After filtration	Make up	PMSM V=1.1 m/s	PMSM V=1.7 m/s	PMSM V=2.3 m/s	PMSM V=3.0 m/s
pH	7.7	8.5	7.9	8.6	7.4
Sp Cond @ 25C, µmhos	525	2000	2000	2030	1970
Alk, "P" as CaCO3, ppm	0	8.2	0	18.8	0
Alk, "M" as CaCO3, ppm	70	221	187	228	222
Sulfur, as SO4, ppm	54	189	308	184	228
Chloride, as Cl, ppm	81	396	358	418	372
Hardness, Total, as CaCO3, ppm	185	834	846	853	735
Calcium, Total, as CaCO3, ppm	126	571	561	580	492
Magnesium, Total, as CaCO3, ppm	58	262	283	273	242
Copper, Total, as Cu, ppm	<0.05	0.26	0.24	0.25	0.33
Iron, Total, as Fe, ppm	<0.05	<0.05	<0.05	<0.05	<0.05
Sodium, as Na, ppm	39	131	123	133	122
PO4, Total Inorg, as PO4, ppm	1.1				
PO4, Ortho, as PO4	1.2	0.8	0.8	0.9	0.6
Silica, Total, as SiO2, ppm	5.7	15.4	20	14.0	23

Table 4. Water quality data measured for make-up and circulating water

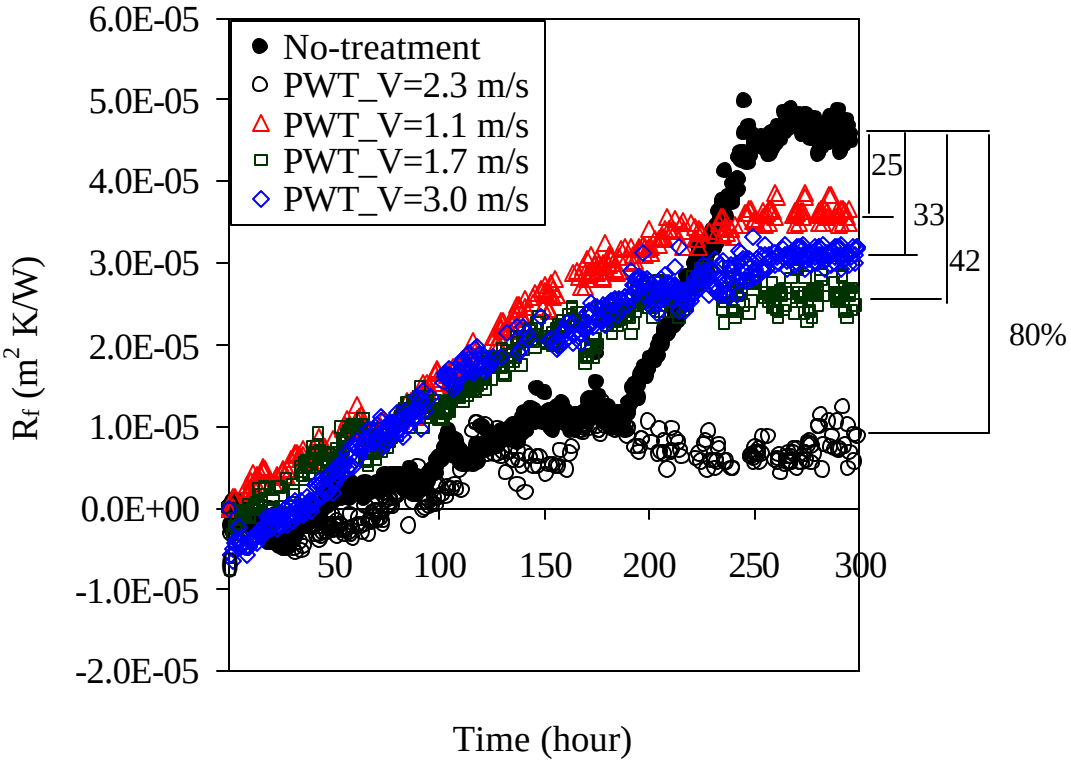

Fig. 1 Variations of fouling resistance vs. time for four different flow velocity cases through PMSM-1

Fig. 2a

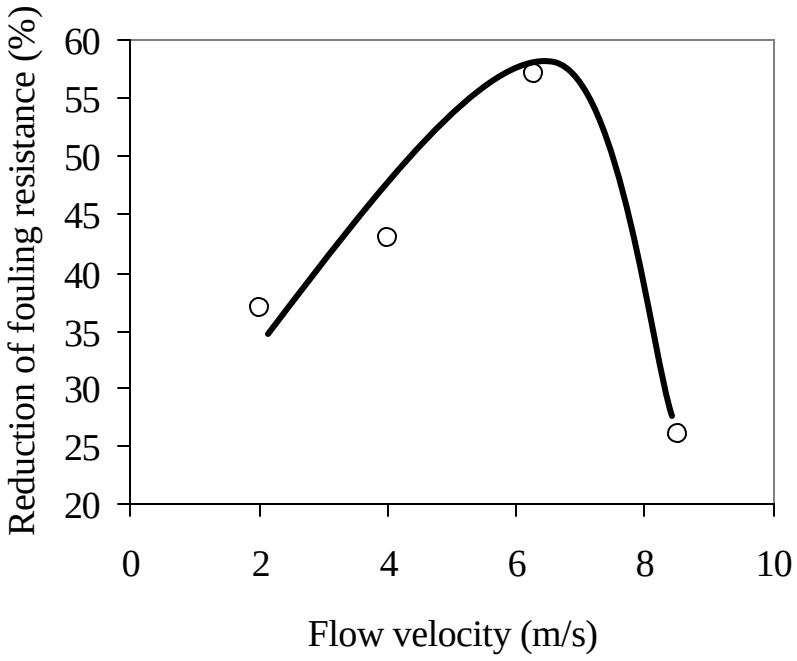

Fig. 2b

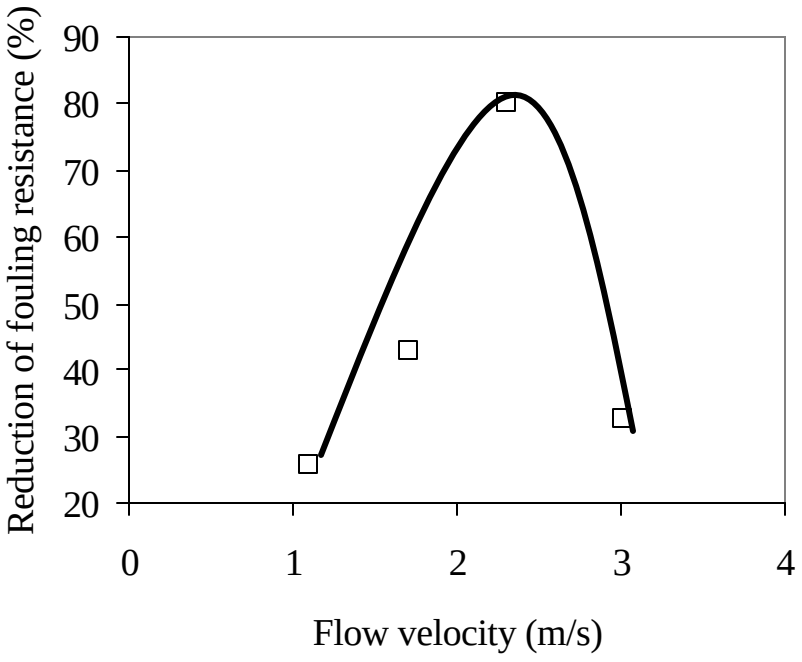

Figure 2 (a) Performance of PMDU over a range of flow velocity, and (b) Performance of PMSM-1 over a range of flow velocity

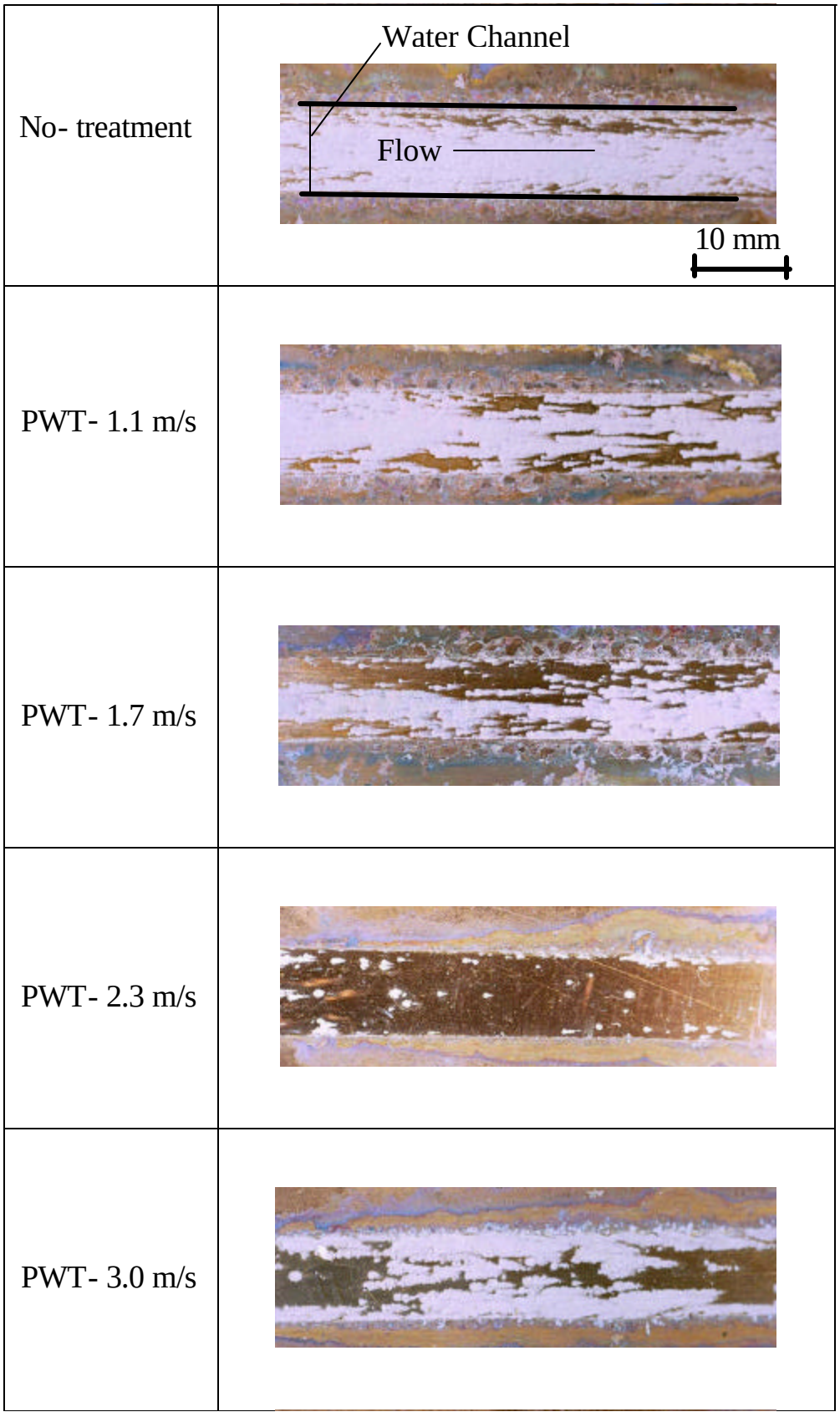

Fig. 3 Photographs of fouled surfaces taken after the fouled heat-transfer surfaces were completely dried

No-treatment 10μm	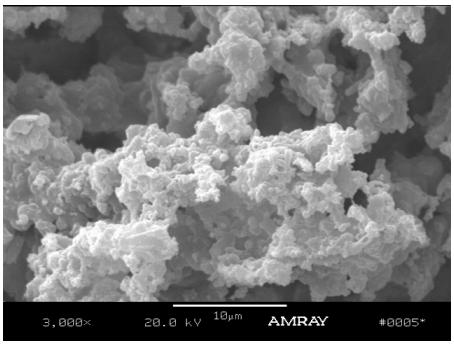
PWT- 1.1 m/s	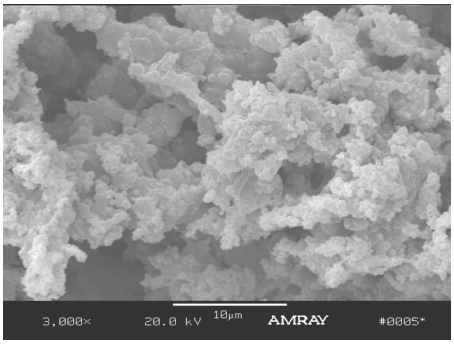
PWT- 1.7 m/s	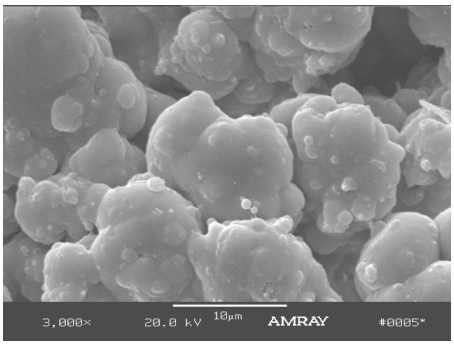
PWT- 2.3 m/s	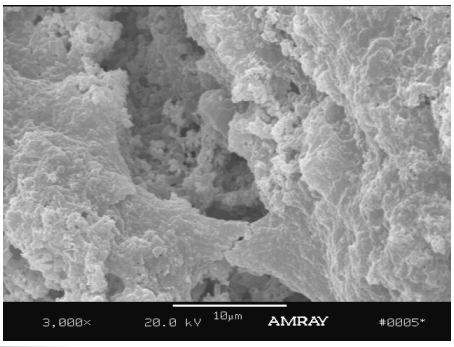
PWT- 3.0 m/s	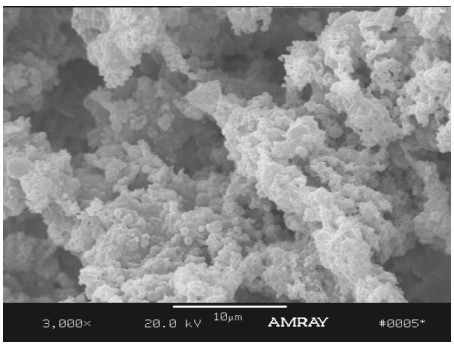

Fig. 4 SEM photographs for all cases, 3,000X

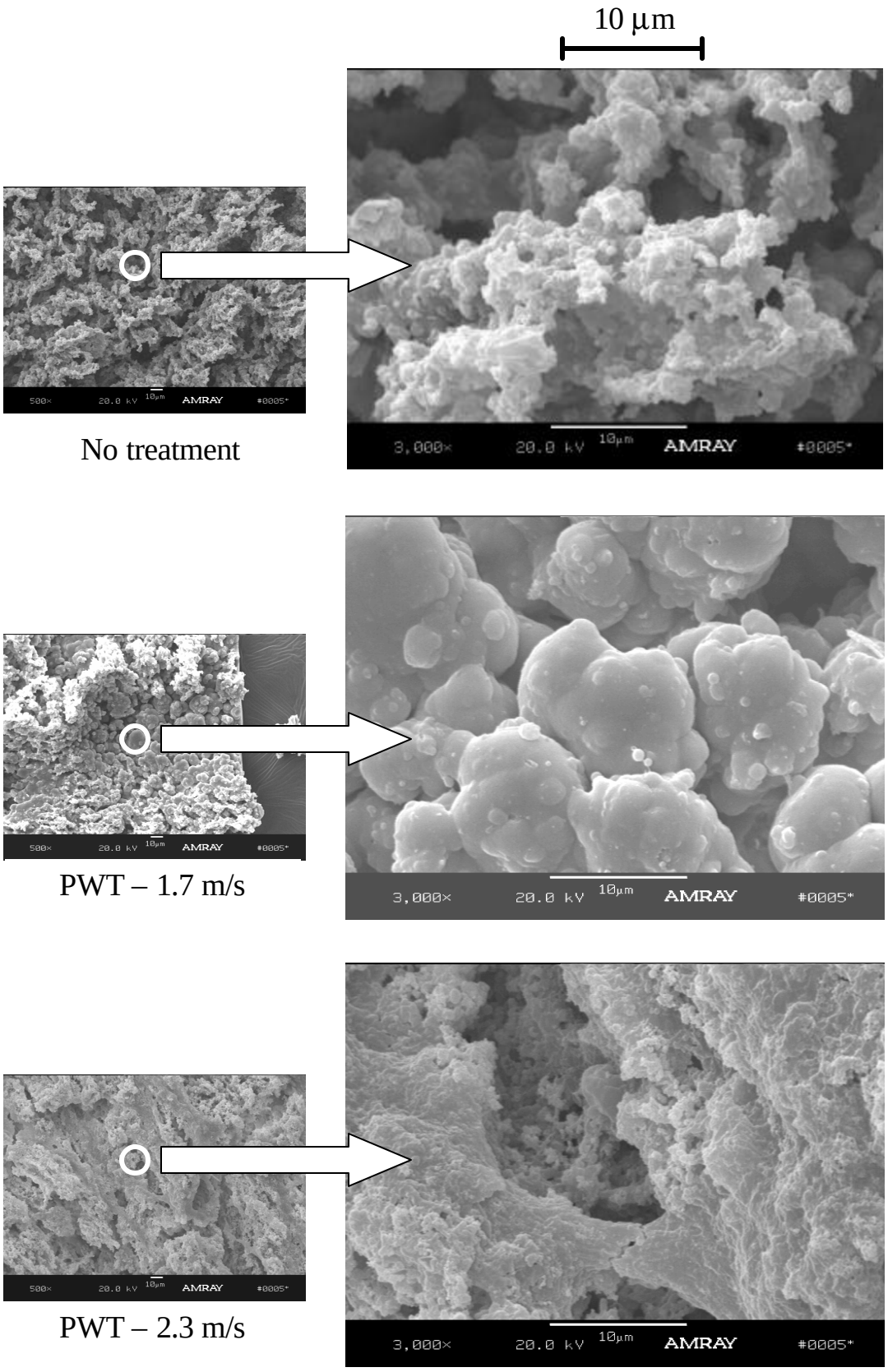

Fig. 5 SEM photographs for cases of no treatment, PWT-1.7 and 2.3 m/s, 3,000X

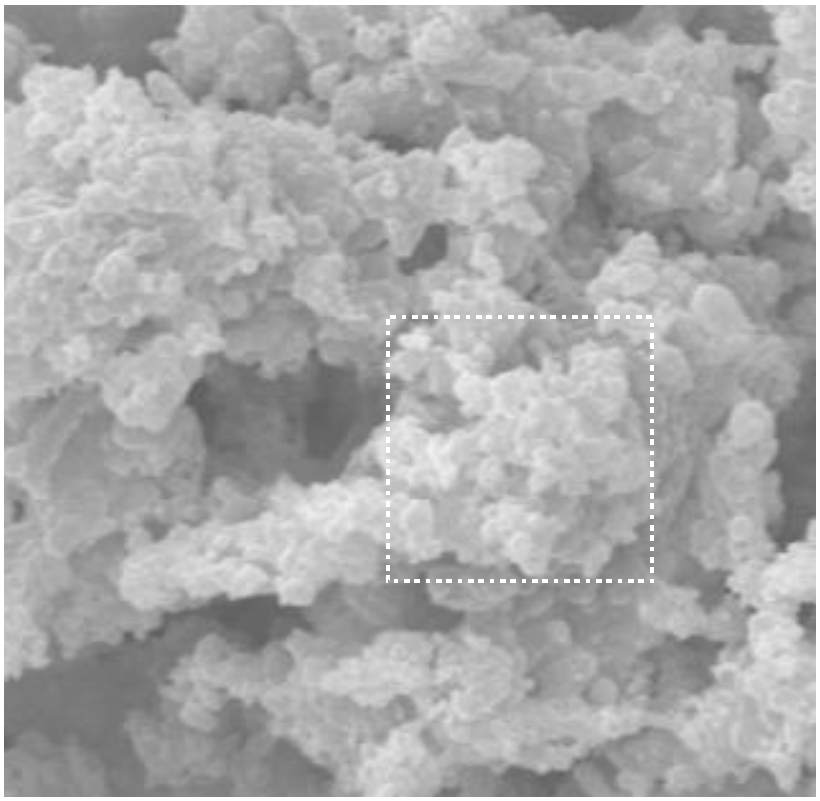

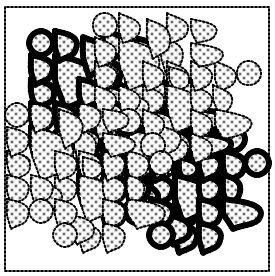

(a) No treatment

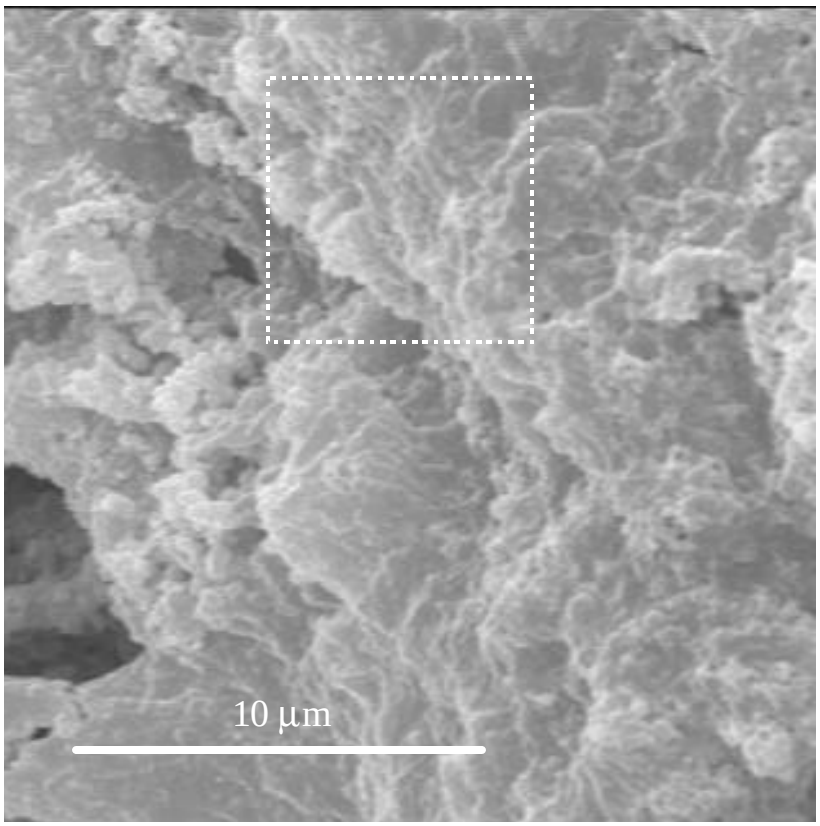

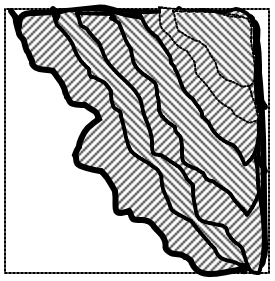

(b) PWT- 2.3m/s

Fig. 6 Enlarged SEM photographs for cases of no treatment and PWT-2.3 m/s, 3,000X

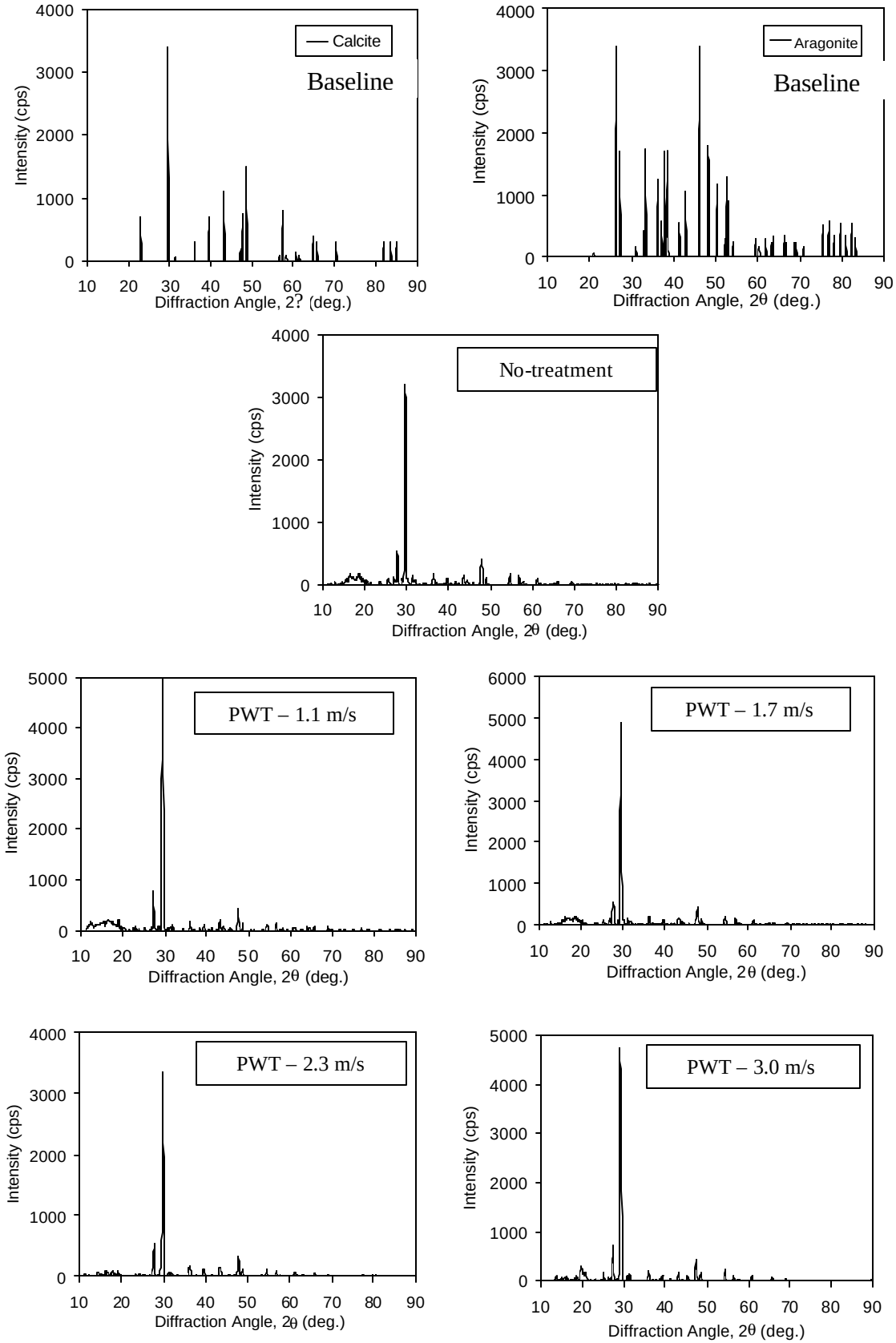

Fig. 7 Results of X-ray diffraction measurements of scale deposits

Appendix A: Comparison of water analyses between Commercial Water Treater and Drexel University

Figure 1 Variations of electric conductivity. Water sampled at a4 and a5 for analyses.

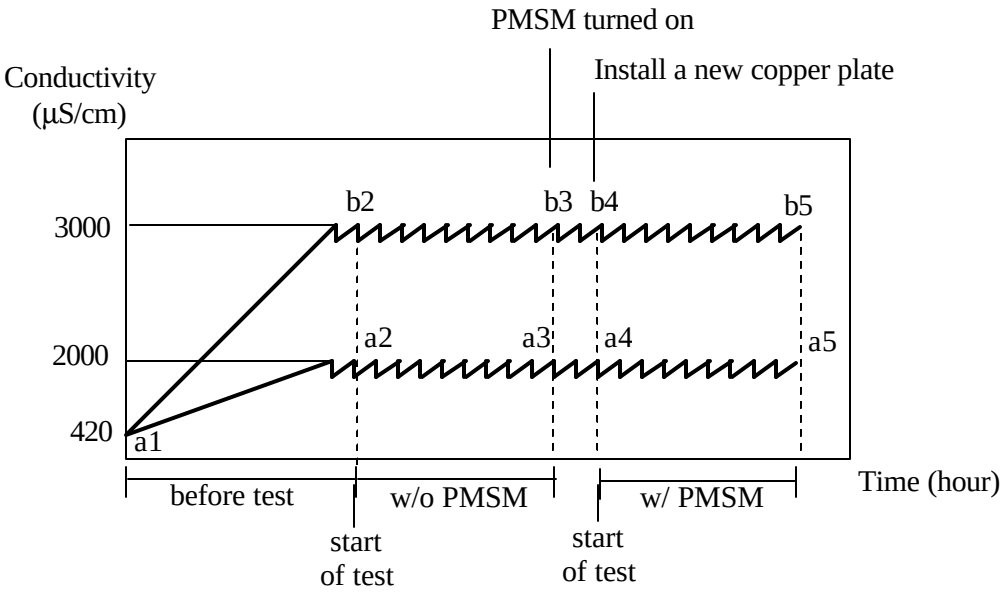

Table 1
Drexel – Water Analyses (a5, PMSM-1 treated case) (2,000 μS/cm case) 08/08/01

	Make-up	Unfiltered	COC	Filtered
Conductivity (μS/cm)	420	1970	4.7	1960
pH	7.3	8.0		8.0
Total hardness (mg/L)	149	780	5.2	780
Ca^{+} hardness (mg/L)	111	520	4.7	510
Total alkalinity (mg/L)	55	232	4.2	232
Chloride (mg/L)	80	432	5.4	432
L.S.I. (at T = 68°C)	0.34	2.16		2.16

Table 2
Drexel – Water Analyses (Untreated case) (2,000 μS/cm case)

	Make-up	Untreated case	
	a1	a2	a3
Conductivity (μS/cm)	410	1955	1910
pH	7.1	8.2	8.2
Total hardness (mg/L)	116	626	601
Ca^{+} hardness (mg/L)	84	448	427
Mg^{+} hardness (mg/L)	32	180	174
Total alkalinity (mg/L)	64	172	151
Chloride (mg/L)	80	436	363
L.S.I. (at T = 68°C)	0.08	2.17	2.09

Table 3 ASHRAE RP1155 –
Water Analyses (Commercial Water Treater) (a4, treated by PMSM-1) Sample Date 8/3/01

	Makeup	Unfiltered Tower	Calc' d Cycles per Unfilt' d Twr	Filtered Tower
pH	7.6	8.4		8.6
Sp Cond @ 25C, µmhos	434	2030	4.7	2030
Alk, "P" as CaCO3, ppm	0	8.3		18.8
Alk, "M" as CaCO3, ppm	56	229	4.1	228
Sulfur, as SO4, ppm	38	184	4.8	184
Chloride, as Cl, ppm	70	410	5.9	418
Hardness, Total, as CaCO3, ppm	147	853	5.8	853
Calcium, Total, as CaCO3, ppm	101	581	5.8	580
Magnesium, Total, as CaCO3, ppm	46	271	5.9	273
Copper, Total, as Cu, ppm	<0.05	0.26		0.25
Iron, Total, as Fe, ppm	<0.05	<0.05		<0.05
Sodium, as Na, ppm	30	134	4.5	133
PO4, Total Inorg, as PO4, ppm	1.2			
PO4, Ortho, as PO4	1.2	0.9		0.9
Silica, Total, as SiO2, ppm	2.5	13.9	5.6	14.0

Observations:

(1) - Based on sulfur, chloride, magnesium, and sodium, it appears that the tower was cycled about 5.3 times when sampled. No evidence of gross precipitation is seen.

Table 4 ASHRAE RP1155 –
Water Analyses (Commercial Water Treater) (a5, treated by PMSM-1) Sample Date 8/8/01

	Makeup	Unfiltered Tower	Calc' d Cycles per Unfilt' d Twr	Filtered Tower
pH	7.5	7.4		8.5
Sp Cond @ 25C, µmhos	443	1990	4.5	2000
Alk, "P" as CaCO3, ppm	0	0		8.2
Alk, "M" as CaCO3, ppm	57	228	4.0	221
Sulfur, as SO4, ppm	43	195	4.5	189
Chloride, as Cl, ppm	69	385	5.6	396
Hardness, Total, as CaCO3, ppm	152	824	5.4	834
Calcium, Total, as CaCO3, ppm	105	565	5.4	571
Magnesium, Total, as CaCO3, ppm	47	258	5.5	262
Copper, Total, as Cu, ppm	<0.05	0.28		0.26
Iron, Total, as Fe, ppm	<0.05	<0.05		<0.05
Sodium, as Na, ppm	30	129	4.3	131
PO4, Total Inorg, as PO4, ppm	1.2			
PO4, Ortho, as PO4	1.1	0.6		0.8
Silica, Total, as SiO2, ppm	3.5	15.1	4.3	15.4

Observations:

(1) - Based on sulfur, chloride, magnesium, and sodium, it appears that the tower was cycled about 5.0 times when sampled. No evidence of gross precipitation is seen. Something very strange regarding tower pH' s (note discrepancy between the filtered and unfiltered pH' s).

Appendix B X-ray Diffraction Measurement

In the present study, the crystal phase of deposited scale on a heat exchanger surface was investigated with an X-ray diffractor. All scale samples revealed the calcite form of $CaCO_3$ regardless of the PWT.

Some previous researchers [Donaldson and Grimes 1985, Higashitani et. al. 1993, Kobe et al. 2001] reported that the crystal phase of scale deposits was aragonite when they applied physical water treatment (PWT).

Note that these researchers produced scale crystals without heat. They used a simple flow loop with artificially hardened water, made of distilled water and chemicals such as calcium chloride and sodium bicarbonate. To obtain scale samples, treated or untreated water drop was placed on a glass slide and evaporated. They used the dried scale crystal on the slide for X-ray diffraction measurements. As soon as they obtained the crystal sample, they measured the X-ray diffraction.

In order to verify that previous work, the identical method was applied in the present study. First, tests were conducted with artificial hard water of calcium hardness of 500 ppm in a simple flow system as the previous researchers did. X-ray diffraction measurement was performed within two hours after getting scale samples. Figure d.1 shows the X-ray diffraction results of the first experiment. The resultant crystal phase was primarily aragonite rather than calcite (i.e., aragonite:calcite = 70%:30%). Second, tests were repeated with cooling-tower water treated with the PWT which had the same calcium hardness of 500 ppm and electric conductivity of 2,000 μS/cm. In this case, the portion of aragonite was reduced (i.e., aragonite:calcite = 60%:40%) compared to that obtained with the artificial hard water, as can be seen in Fig. d.2. In addition, another test

with a higher hardness cooling water treated with the PWT (i.e., calcium hardness = 1,280 ppm, electric conductivity = 4,000 μS/cm) was conducted. The results in Fig. d.3 for the case of 4,000 μS/cm were almost the same as these obtained with the 2,000 μS/cm case, with a slightly higher intensity.

The results in Figs. d.1 to d.3 indicate that water property could affect the crystal phase. In other words, other ions such as magnesium, silica, chloride, or sulfate in cooling tower water might affect the formation of calcium carbonate crystals.

During the tests, one new phenomenon was found in the formation of the crystal phase of $CaCO_3$. The crystal phase of the scale sample changed with time, from an aragonite form initially to a calcite form in three days. Note that the first measurement was performed within two hours, and the second measurement was conducted with the same scale sample three days later. For both 2,000- and 4,000-μS/cm cases, crystals changed from aragonite in the first measurement to calcite in the second measurement (i.e., aragonite:calcite = 10%:90%). Figures d.4 and d.5 present the results obtained from the test conducted three days later, for the cases of 2,000- and 4,000-μS/cm, respectively, confirming that scales became calcite form of CaCO3 after three days.

In the present heat exchanger experiments, it took approximately three hundred hours (about 12 days) to finish one test, and after finishing the test, typically seven days were required to completely dry the scale layer before the X-ray diffraction measurements were conducted. In other words, there was enough time passed for the crystal phase to change to calcite, even if aragonite crystals had been made at the beginning. Results from Fig. d.4 and d.5 indicate that the scale from cooling-tower water were initially aragonite, which changed to calcite after 3 days.

More studies are needed in the future to further understand, for example, the relationship between crystal phase and other factors such as temperature, surface conditions of material, and water properties.

References

Donaldson J.D. and Grimes S., Lifting the scales from our pipes, The City University, London, UK, Newscientist, 1990. also, Tube International, (1988) 111-118

Higashitani K., et al., Effects of a magnetic field on the formation of CaCO3 particles, Journal of Colloid and interface science, 156 (1993) 90-95

Kobe S., Drazic G., McGuiness P.J., Strazisar J., The influence of the magnetic field on the crystallization form of calcium carbonate and the testing of a magnetic water-treatment device, J. Magnetism and Magnetic Materials, 236 (2001) 71-76

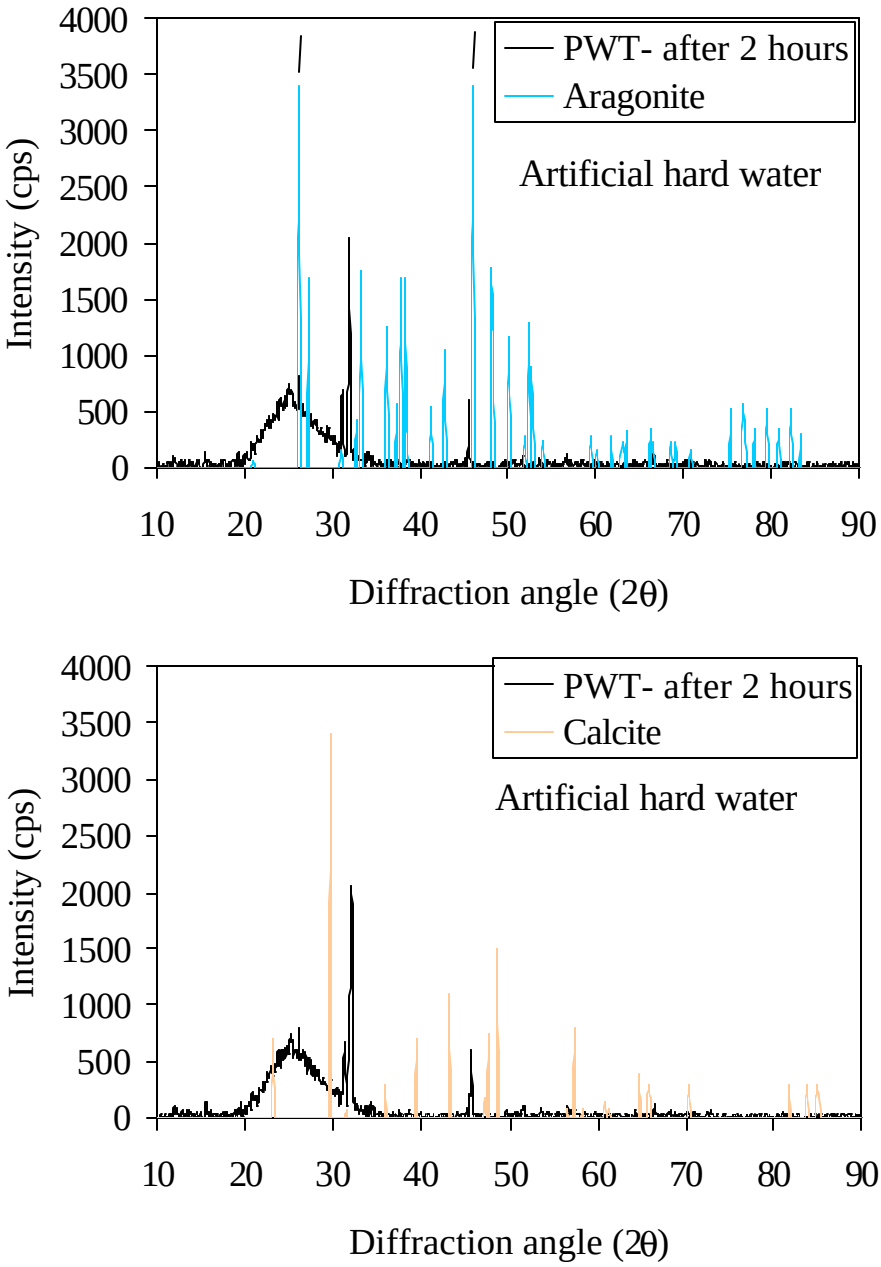

Fig. d.1 X-ray diffraction result of artificial hard water case

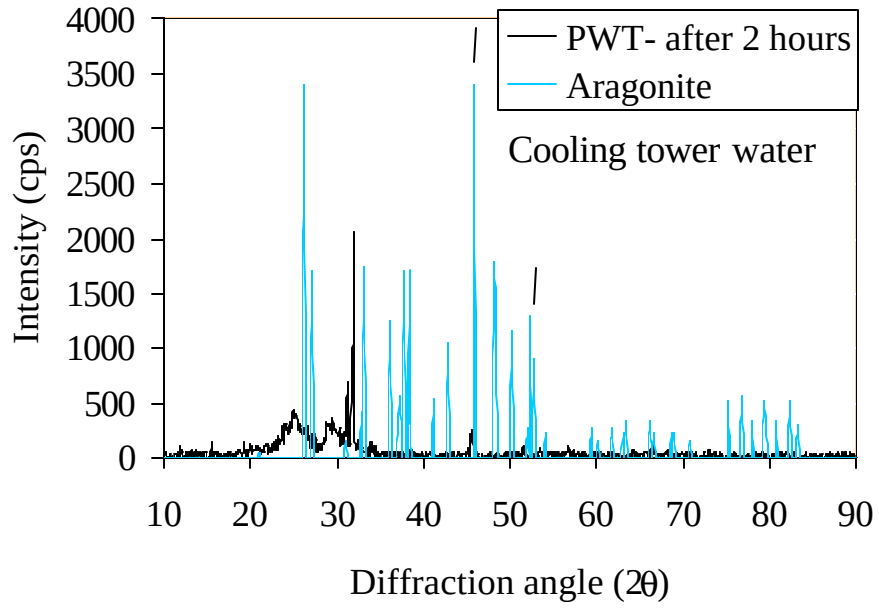

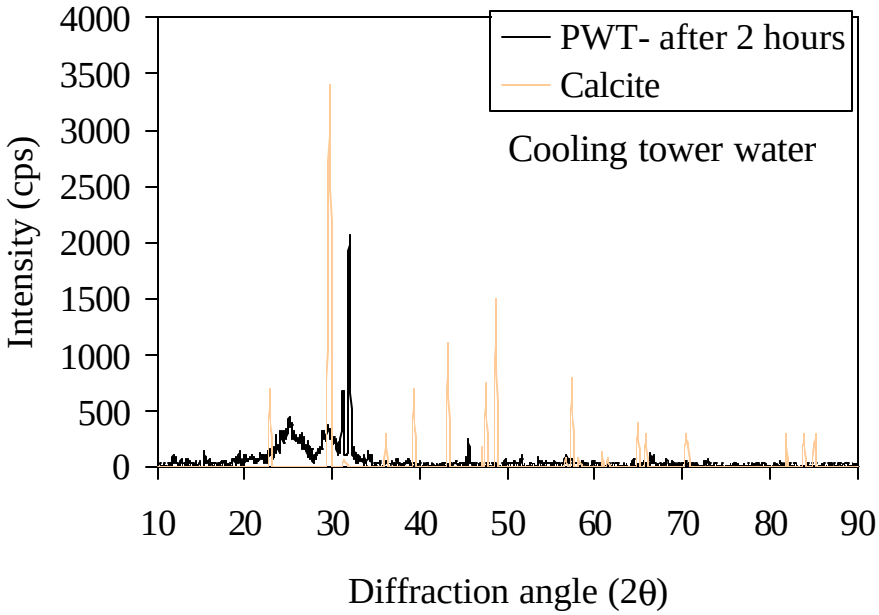

Fig. d.2 X-ray diffraction result of cooling tower water case, 2,000 μS/cm

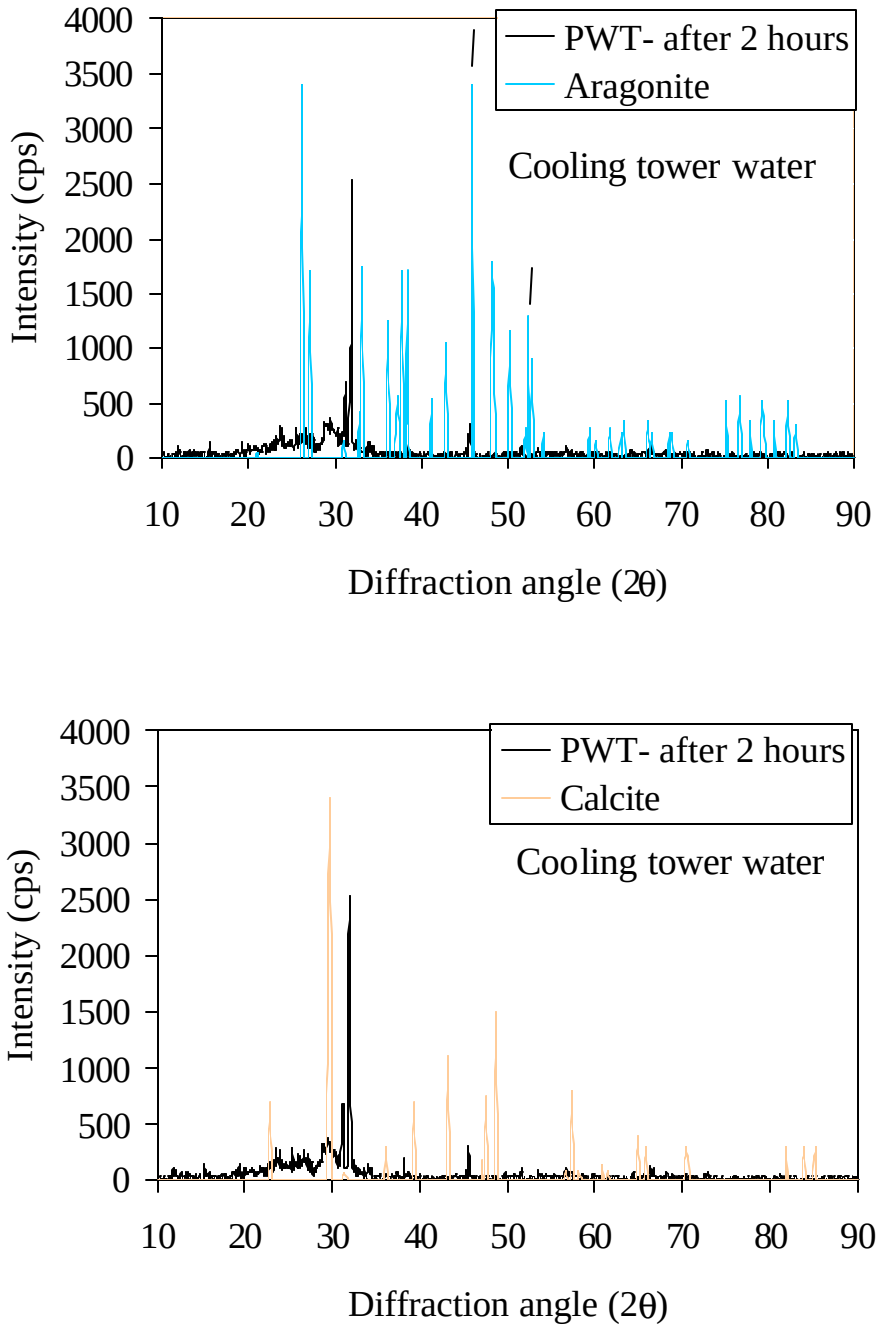

Fig. d.3 X-ray diffraction result of cooling tower water case, 4,000 μS/cm

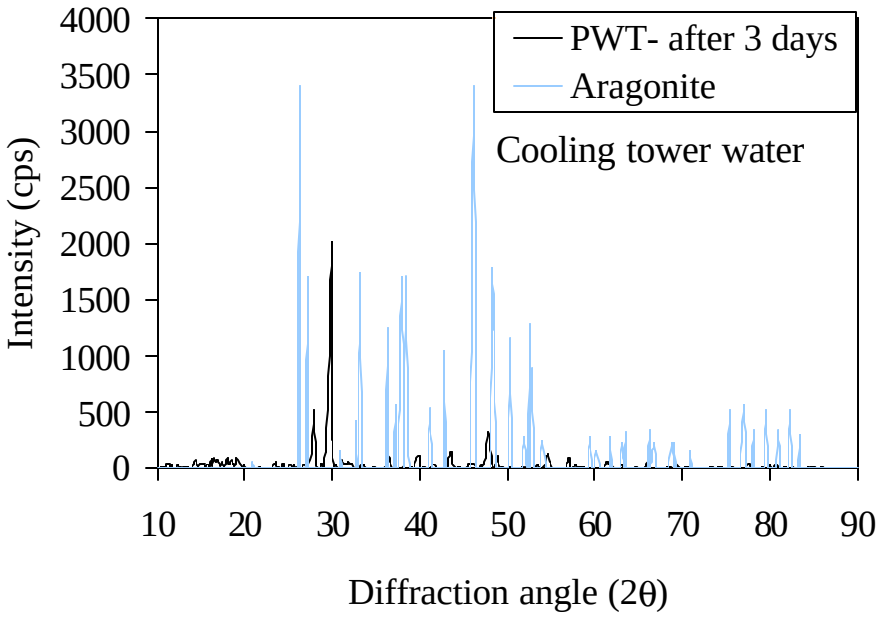

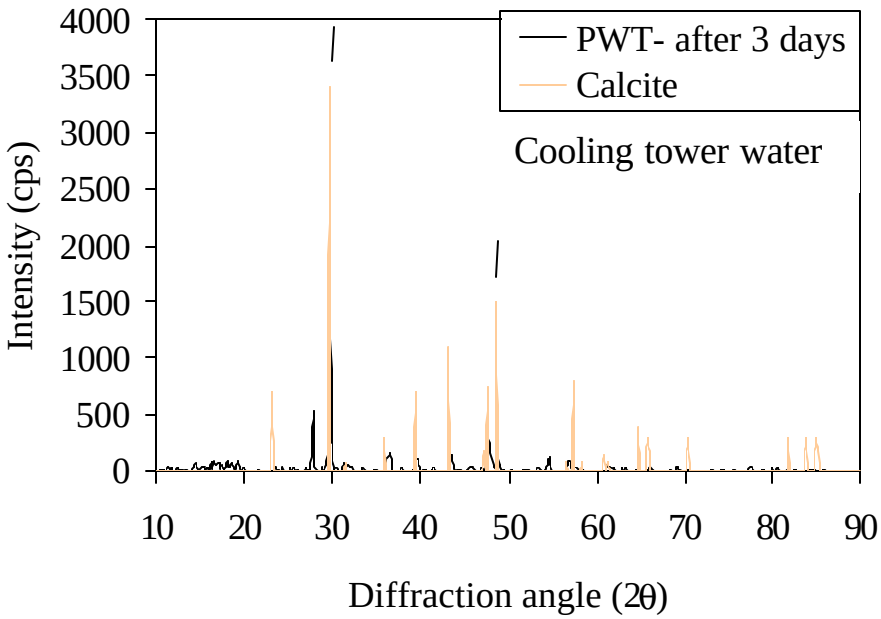

Fig. d.4 X-ray diffraction result of cooling tower water case, 2,000 μS/cm

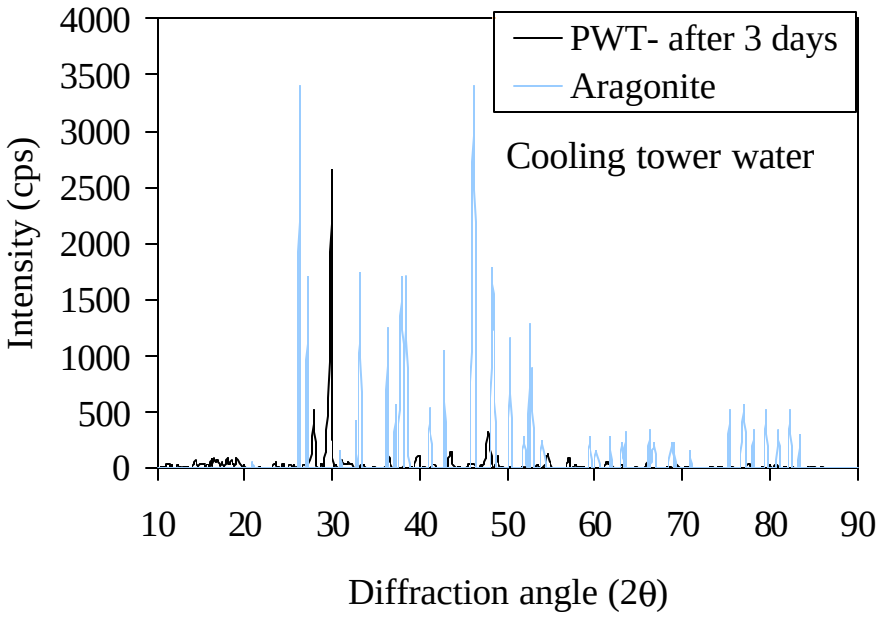

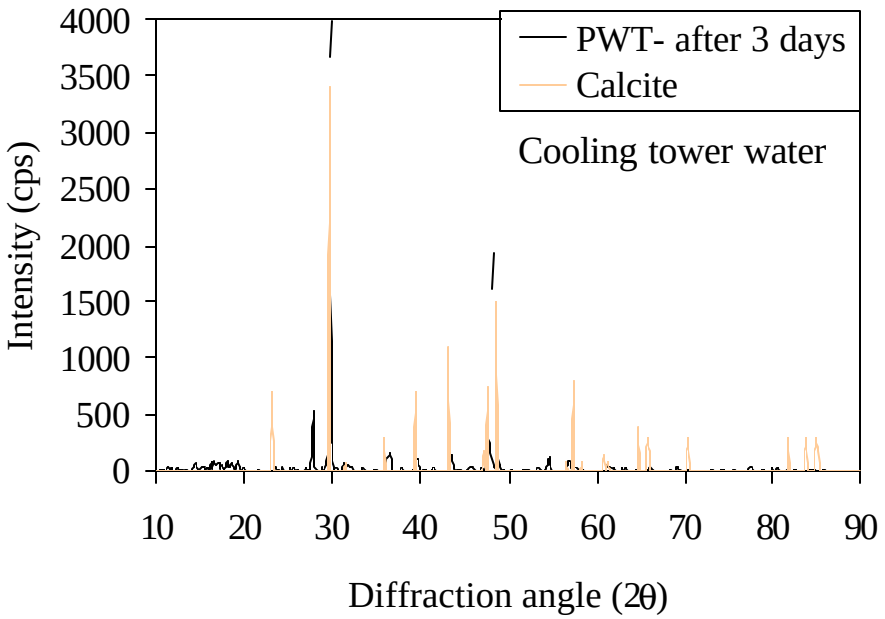

Fig. d.5 X-ray diffraction result of cooling tower water case, 4,000 μS/cm

Appendix C Sketch of magnetic fields (from C.J Quinn, T.C. Molden, C.W. Sanderson, Nonchemical approach to hard water scale, corrosion and white rust control, Proceedings AISE 1996 Annual Convention, Sept. 30, 1996, Chicago, IL.)

The permanent magnet used in the present study consists of three magnets along the center line as shown in the bottom illustration (e). The three magnets were fitted inside a single bar, loosely fit, inside an outer steel shell. Three ¼" copper rods were used around the single bar to center the three magnets in the steel shell, helping create a more laminar flow path for the water, a phenomenon which is also important for best results. Both ends were concentrically rounded to help reduce the turbulence in applications. The pole spacing between the three magnets can be adjusted to accommodate the flow rate of a system controlling the time needed in each magnetic field for proper treatment.

The arrangement shown in illustration (e) shows the optimum layout of three magnets. By containing the bar magnet in the center of the steel shield, the magnetic lines starting North Pole are attracted to the outer shield and then travel down to the steel pipe seeking the nearest South Pole. The magnetic lines then are pulled to the South Pole from the steel pipe shield. This causes the magnetic lines to make 90 degree right angle turns instead of an oval shaped path.

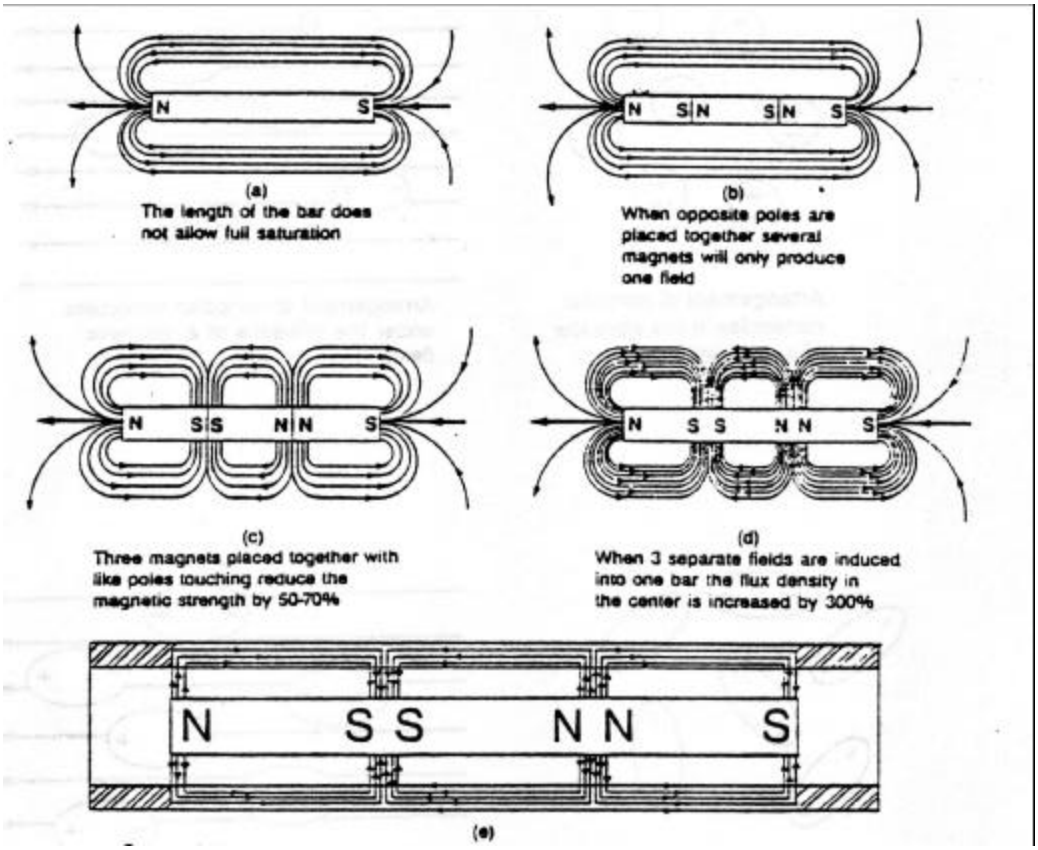
N
S
(a)
The length of the bar does not allow full saturation
N S N S N S
(b)
When opposite poles are placed together several magnets will only produce one field
N S S N N S
(c)
Three magnets placed together with like poles touching reduce the magnetic strength by 50-70%
N S S N N S
(d)
When 3 separate fields are induced into one bar the flux density in the center is increased by 300%
N S S N N S
(e)

Chapter 4

Concentration Effect of Permanent Magnets (PMDU) on the Mitigation of Mineral Fouling (Rectangular Heat Transfer Test section)

ABSTRACT

The purpose of the present study was to investigate the effect of a physical water treatment (PWT) using permanent magnets (PMDU) on the mitigation of mineral fouling in a heat exchanger with cooling-tower water. Fouling tests were conducted in a rectangular channel heat exchanger by varying the electric conductivity of the cooling-tower water from 2,000 to 4,000 μS/cm. Flow velocities at the heat exchanger and the PMDU were fixed 1.5 m/s and 6.3 m/s, respectively. As the electric conductivity of the water increased, the efficiency of the PWT as measured by the reduction in the fouling resistance decreased from 84 to 40%. To analyze the characteristics of scales produced by the PWT, real-time photographs with a microscopic imaging system, scanning electron microscopic (SEM) photographs, and X-ray diffraction data were obtained and analyzed and the results are discussed in the paper.

INTRODUCTION

The effectiveness of the PWT, in general, may depend on the test conditions, including the flow velocity through permanent magnets, water hardness (i.e., levels of supersaturation), and recirculation whether the PWT is used in a recirculation mode or once-through system. In a cooling-tower-water application, the concentration of dissolved mineral ions continues to increase due to the evaporation of water. In order to

maintain a consistent level of concentration of mineral ions, a portion of water has to be discharged, and the same amount of water has to be added in the form of make-up water. The consumption of fresh water, coupled with maintaining the maximum efficiency of the cooling system, is one of the major issues related to cooling water treatment. In other words, if one can use highly concentrated hard water without a serious fouling problem, it can be very helpful not only economically but also environmentally.

The purpose of the present study was to investigate whether the physical water treatment (PWT) using permanent magnets can be used to increase the cycles of concentration in an open-cooling-tower system while controlling mineral fouling in a heat exchanger at an acceptable level. The present study conducted fouling tests and characterized scale crystals using a light microscope, scanning electron microscopy (SEM), and X-ray diffraction technique.

EXPERIMENTAL METHODS

Figure 1 shows a schematic diagram of the test facility, which consists of a water-circulating loop, a cooling tower, a side-stream flow loop, permanent magnets, a pump, a heat transfer test section, a conductivity meter, a floating-ball valve for automatic feeding of make-up water, and an automatic blowdown system controlled by a solenoid valve. In order to change the flow velocity through permanent magnets, a side-stream flow loop was set up in a sump tank of the cooling tower.

In order to directly observe scale crystals on the heat-transfer surface as the fouling progressed, a fouling test facility with a microscopic-imaging system was developed. The microscopic-imaging system consisted of a microscope, an external illuminator, a Sony CCD (charged couple device)-IRIS camera, a 35-mm Nikon camera,

a video recorder, and a monitor. The images of $CaCO_3$ scale crystals on the cooling-water side were observed using the microscope and continuously recorded on VHS videotape via the CCD camera. Hard copies of the microscopic images of scale crystals were produced from the VHS tape using software called Snappy. A magnification of 40x was used for observation. In addition, still pictures were taken with the 35-mm Nikon-camera.

Figure 2 shows a cross-sectional view of the heat-transfer test section that consisted of a copper plate as the heat-transfer surface, a cooling-water channel (i.e., the upper part of the flow channel), and a hot-water channel (i.e., the lower part of the flow channel). Cooling water moved in the opposite direction of the hot water, thus forming a counter-flow heat exchanger. An acrylic plate was used as an observation window because of its excellent optical clarity.

Since the solubility of calcium-carbonate salt, $CaCO_3$, decreases with increasing temperature, scale deposited on the cooling-water side of the copper plate. At the end of a test, the fouled copper plate was removed for the further analysis of scale, and a new copper plate was installed for the next test. For the cooling-water channel, the two sidewalls were made of polypropylene plates, whereas the top wall was made of a transparent acrylic plate due to its thermal insulation properties. The hot-water channel was machined out of a Teflon block, which also had an excellent thermal insulation property. The dimension of the cooling-water channel was 1.6 mm $\times$ 6.4 mm $\times$ 254 mm (height $\times$ width $\times$ length), whereas the dimension of the hot-water channel was 13.7 mm $\times$ 6.4 mm $\times$ 254 mm (height $\times$ width $\times$ length).

Figure 3 shows an arrangement of permanent magnets and cross-sectional dimensions of a channel where water was treated by permanent magnets, a system Drexel University (PMDU) used in the present study. The strength of the magnetic field was 0.16 T (or 1,600 gauss) that was measured by an AlphaLab DC Magnetometer. The cross-sectional dimension of the flow channel in the PMDU was 0.68 mm × 9.27 mm × 100 mm (height × width × length).

The flow velocities of circulating-cooling water in the cooling-water channel and in the PMDU was fixed to be 1.5 m/s and 6.3 m/s, respectively, for all runs in the study, and the corresponding Reynolds numbers were 4,470, and 17,000, respectively, based on the respective hydraulic diameters. Figure 4 explains why the flow velocity at the PMDU was fixed at 6.3 m/s. To get the optimum flow velocity at the PMDU, tests were conducted with four different flow velocities (i.e., 2.0, 4.0, 6.3, and 8.5 m/s) in a separate study. As one can see in Fig. 4, the optimum flow velocity for the PMDU in the study was 6.3 m/s, a flow velocity that was chosen in the present study.

The inlet temperature of the circulating water prior to the heat transfer test section was maintained at 20 ± 1°C by means of the evaporative cooling tower, whereas the inlet temperature of the hot water was maintained at 89 to 92°C throughout the entire experiments. Heat flux between heating and cooling sides of the copper plate was 485.2 kW/m^2.

Table 1 shows, for comparison, the values of heat fluxes and flow velocities used in previous fouling studies reported in literature. As indicated in Table 1, previous researchers also used certain test conditions to accelerate fouling in their laboratory tests so that they could complete fouling tests in a reasonable time period.

After the cooling water passed the heat-transfer test section, it was sent to the cooling tower, where the water was cooled by evaporation. In order to maintain a constant volume of water in the system, the tap water was added as make-up water, a procedure that was controlled by an automatic floating-valve system. Table 2 shows water quality data of the tap water provided by the City of Philadelphia (Bureau of Laboratory Service) in 1999. Since the water quality varied with time, the minimum, maximum and average values are given.

Figure 5 shows the test procedure and variations of electric conductivities vs. time for a no-treatment case and the case with the PMDU at three different water concentrations conditions (i.e., 2,000, 3,000, and 4,000 μS/cm). The present study varied the electric conductivity because it was much more convenient to control the electric conductivity experimentally than the hardness of circulating water. Before starting each test, the water sample was prepared by circulating tap water through the cooling tower so that the desired electric conductivity was obtained (see Fig. 5). Once the circulating water reached the desired conductivity, the fouling test began with hot water in the hot water channel. At the end of the test for the no-treatment case, the cooling-tower water was continuously circulated while treated by the PMDU, but without heat transfer for one day (i.e., see the period between a3 and a4). After one-day pretreatment, a brand new copper plate was installed in the heat-transfer test section, and the fouling test began. Each fouling experiment was repeated for the reliability of test results at the same experimental condition. The error for the fouling resistance was within ± 5%.

The fouling resistance is often calculated using the following equation:

$$R_f = \frac{1}{U_f} - \frac{1}{U_i} \qquad (1)$$

where U_f is an overall heat transfer coefficient from a heat exchanger experiencing fouling, and U_i is the overall heat transfer coefficient from a clean heat exchanger. Both overall heat transfer coefficients were calculated from the following equation:

$$U = \frac{\dot{Q}}{A\Delta T_{lm}} \tag{2}$$

where ΔT_{lm} is a log-mean-temperature difference, which can be described as

$$\Delta T_{lm} = \frac{(T_{h,i} - T_{c,o}) - (T_{h,o} - T_{c,i})}{\ln\left[\frac{(T_{h,i} - T_{c,o})}{(T_{h,o} - T_{c,i})}\right]} \tag{3}$$

where subscripts *h* and *c* indicate hot and cold water sides, respectively, and subscripts *o* and *i* indicate outlet and inlet flows, respectively. The heat transfer rate, $\dot{Q}$, was estimated from both the heating and cooling channels as

$$\dot{Q} = [\dot{m}c_p(T_i - T_o)]_h = [\dot{m}c_p(T_o - T_i)]_c \tag{4}$$

where $\dot{m}$ is a mass flow rate ad c_p is the specific heat of water.

RESULTS AND DISCUSSION

Table 3 shows the water analysis data for the make-up, and circulating cooling-tower water for both the no-treatment case and the PWT treatment case. The property data of make-up water were in good agreement with the water analysis results by the City of Philadelphia given in Table 2. Water samples were taken from the circulating water were at times marked by a_i, b_i, c_i where i varies from 1 to 5 (see Figure 5). Large difference were not observed in concentrations of dissolved materials between no-treatment case and the case with the PWT. The Langelier saturation index (LSI) was calculated to examine the precipitation tendency of the circulating water. The values of

the LSI were in the range of 2.1 to 2.7, indicating that the circulating water had a condition to cause severe mineral fouling.

Figure 6 shows a series of photographs of fouling obtained using a microscopic imaging system for the no-treatment case and the case with the PWT. After 30 hours, numerous small particles deposited on a heat-exchanger surface in the case of the no-treatment, whereas several big particles were found for the PWT treatment. The number of the small particles for the no-treatment case increased with time and eventually covered the whole heat-exchanger surface at t = 150 hours. Hence, one can conclude that the crystallization fouling resulted from the mass diffusion of calcium ions was dominant in the no-treatment case.

But for the PWT case, the size of large particles was getting bigger, and these big particles developed tails, which were densely populated by scale crystals. This tail-shaped scale deposition can be attributed to a streamlined secondary flow behind a large particle, where flow velocity behind the particle is substantially smaller than that in the mainstream. When the cooling water was treated by the PWT, the mineral ions that dissolved in the cooling water precipitated in the bulk water, and therefore, these precipitated particles were deposited on the heat exchanger surface in the form of particulate fouling. Particles are more difficult to be deposited on the surface than dissolved ions, since large particles can be much more easily removed by shear force than small ions. Therefore, the number of the crystals in the no-treatment case is greater than that in the PWT case, while the size of the crystals in the no-treatment case is much smaller due to the crystallization fouling than that in the PWT case. The present result is consistent to what Higashitani et al. reported earlier [1-Ch.3]. They reported that a

magnetic treatment of water suppressed the nucleation frequency of $CaCO_3$ particles but accelerated the growth of the particles.

Figure 7 shows photographs of fouled surfaces taken after the fouled heat-transfer surfaces were completely dried. No-treatment cases resulted in much more severe fouling than PWT cases, regardless of water hardness. But in the PWT cases, the amount of fouling deposit increased with increasing conductivity. This observation was consistent with the trends in fouling resistances given in the Figure 8.

Figure 8 represents fouling resistance values vs. time for three different conductivity cases. When the electric conductivity of the cooling-tower water was 2,000 μS/cm, the asymptotic value of the fouling resistance for the PWT case decreased by 84% from the value of the no-treatment case. For the case of the electric conductivity of 4,000 μS/cm, the fouling resistance decreased by 40%. This result could be explained as follows: For the untreated 2,000 μS/cm case, the scale deposition is mainly due to the diffusion of dissolved mineral ions, i.e., crystallization fouling. Since the PWT can reduce the dissolved ions in water, the reduction in the fouling resistance was great, i.e., 84%. However, for the untreated 4,000-μS/cm case, the scale deposition is due to both the diffusion of the dissolved ions (i.e., crystallization fouling) and the deposition of large precipitated particles (i.e., particulate fouling) (also see Fig. 9a and 9c). Since the PWT only affects the crystallization fouling by reducing the number of dissolved ions in water, the reduction in the fouling resistance (i.e., 40%) was much smaller than that in the 2,000-μS/cm case.

Figure 9 shows scanning electron microscopic photographs of scale layer for the cases of 2,000, 3,000, and 4,000 μS/cm. For the no-treatment cases, numerous tiny

crystals were agglomerated regardless of water hardness. Although some crystals were as large as 5 μm, there were a lot of crystals less than 1 μm in the no-treatment cases. In the PWT cases, there was no distinctive crystal boundary. It looked like one big crystal for the PWT cases. Hence, it can be concluded that the PWT produced $CaCO_3$ particles in water, which grew in size and eventually deposited on the heat-transfer surface as an amorphous colloidal form. The big difference in the morphology of scale layer between the untreated and PWT cases may explain the mechanism of the PWT (i.e., particulate fouling).

Figure 10 shows the chemical composition of a scale layer that was obtained from the energy dispersive spectrum (EDS) method. In this figure, calcium and oxygen are the dominant chemical components except for gold and sodium. Copper and zinc came from the copper plate used in the study. As an initial process of the EDS measurement, a gold coating is applied on the scale layer because the scale layer was non-conductive. Therefore, the gold component can be discarded. Hence, when the natural hard water using tap water as the make-up water was circulated in a cooling-tower, one can conclude that calcium carbonate fouling is dominant in a heat exchanger, a well-known phenomenon.

The characteristics of the structure of the calcium carbonate scale have been investigated to explain the mechanism of the PWT method [19-22]. Some researchers stated that a calcite structure was dominant for no-treatment cases, while when a PWT was applied, aragonite was formed instead of the calcite. Others stated that aragonite scale with a needle-shaped structure deposited on a heat exchanger surface for the

untreated case, which was very hard to remove [23]. On the contrary, calcite with a round-shaped structure is easier to remove it than aragonite-type scale [23].

In the present study, an X-ray diffraction method was used to investigate the structure of scale crystals that were sampled from the heat-transfer test section. As one can see in Figure 11, all six sampled crystals had the same structure of calcium carbonate scale, which was calcite. From this result, it can be concluded that the PWT using permanent magnets produced calcite form of calcium carbonate, and there is no difference in the structure of the scale crystals between the untreated and PWT cases.

CONCLUSIONS

The present study investigated the feasibility of using the PWT using permanent magnets to increase the cycle of concentration in circulating cooling-tower water application while controlling mineral fouling. As the electric conductivity of the circulating water increased from 2,000 to 4,000 μS/cm, the efficiency of the PWT as measured by the percentage drop in the fouling resistance decreased from 84 to 40%. It is concluded that by using the PWT using permanent magnets one can substantially reduce mineral fouling in chillers and heat exchangers in a cooling-tower application with substantial energy and water savings.

In the case of no-treatment, the crystallization fouling seemed to be dominant. On the other hand, the PWT cases produced $CaCO_3$ particles (i.e., bulk precipitation), which grew inside the heat exchanger, eventually depositing on the heat-transfer surface in the form of particulate fouling. Real-time microscopic photographs and SEM photographs were obtained to render further support on the hypothesis of the particulate fouling.

From the results of X-ray diffraction measurement, the structure of calcium carbonate crystal was determined to be calcite for both the untreated and PWT cases.

REFERENCES

[1] J. Taborek, T. Aoki, R. B. Ritter, J. W. Palen and I. G. Knudsen, Predictive Methods for Fouling Behavior, Chemical Engineering Progress, 68, 69-78 (1972)

[2] D. Hasson, M. Avriel, W. Resnick, T. Rozenman and S. Windreich, Mechanism of Calcium Carbonate Scale Deposition on Heat-transfer Surface, Ind. Eng. Chem. Fund., 7, 58-63 (1968)

[3] Klassen V.I., Magnetic water: between Scylla and charybdis, Khimiya I Zhizn, Russian, No 9 (1969)

[4] Diamant R.M.E., Magnetic treatment of water, Hospital Engineering (1970)

[5] Sandulyak A.V. and Krivtsov V.V., Heat and hydrodynamic conditions of magnetic treatment of water against scale formation, Soviet Power Engineering, 5 (1982) 362-367

[6] Grutsch J.F. and McClintock J.W., Corrosion and deposit contro in alkaline cooling watr using magnetic water treatment at AMOCO' s largest refinery, Corrosion 84, 330 (1984) 1-26

[7] Szostak R.J., Magnetic fluid conditioning system allows 3000 ppm hardness without cooling tower scale buildup, Chemical Processing (1985) 44-45

[8] Parker D.H., An investigationof the role of magnetic water treatment devices in calcium carbonate scale formation, MS thesis, Baylor University, Texas (1985)

[9] Kronenberg K.J., Experimental evidence for effects of magnetic fields on moving water, IEEE Transactions on Magnetics, MAG-21 (1985) 2059-2061

[10] Busch K.W. and Busch M.A., Laboratory studies on magnetic water treatment and their relationship to a possible mechanism for scale reduction, Desalination, 109 (1997) 131-148

[11] Herzog R.E., Shi Q., Patil J.N. and Katz J.L., Magnetic water treatment: The effect of iron on calcium carbonate nucleation and growth, Langmuir, 5 (1989) 861-867

[12] Bernardin J.D. and Chan S.H., Magnetic effects on simulated brine properties pertaining to magnetic water treatment, 28th National Heat Transfer Conference, HTD, 164 (1991) 109-117

[13] Baker J.S. and Judd S.J., Magnetic amelioration of scale formation, Wat. Res., 30, 2 (1996) 247-260

[14] Baker J.S., Judd S.J. and Parsons S.A., Antiscale magnetic pretreatment of reverse osmosis feedwater, Desalination, 110 (1997) 151-166

[15] Parsons S.S., Judd S.J., Stephenson T., Udol S. and Wang B-L., Magnetically augmented water treatment, Institution of Chemical Engineers, 75, B2 (1997) 98-104

[16] Hasson, D., and Bramson, D., Effectiveness of Magnetic Water Treatment in Suppressing Calcium carbonate, Ind Eng Chem Proc Des Dev, 24, (1985) 588-592

[17] Sohnel, Otakar, M. J., Some Comments on the Influence of a Magnetic Field on Crystalline Scale Formation, Chemistry and Industry, June (1988), 356-358

[18] Alleman, J. E., Quantitative Assessment of the Effectiveness of Permanent Magnetic Water Conditioning Devices, Purdue Univ. Civil Eng. Res. Report, Contract 0651-57-1284, (1985)
[19] Higashitani et al., Effects of a Magnetic Field on the formation of CaCO3 particles, J. of Colloid & Interface Science, 156, (1993) 90-95
[20] Grimes M.S., Magnetic field effect on crystals, Tube International, (1988)
[21] Barrett A.R. and Parsons S.S., The influence of Magnetic fields on calcium carbonate precipitation, Water Research., 32, 3 (1998) 609-612
[22] Cho Y.I. and Choi B.G., Validation of an Electronic Anti-fouling Technology in a Single-Tube Heat Exchanger, Int. J. Heat and Mass Transfer, 42, 8 (1999) 1491-1499
[23] Cowan J.C., and Weintritt D.J., "Water-Formed Scale Deposits," Gulf Publishing Company, Houston, TX (1976)

References	Heat flux (kW/m^2)	Flow velocity (m/s)	Concentration (ppm)	Foulant
Hasson [2]	1.6	0.25-0.82	110-575	Calcium
Kim & Webb [14]	13	0.8-1.82	1500	Aluminum oxide, (or Ferric oxide)
Somerscales [17]	28-52	0.9-1.0 1.4-1.5	2500	MgO
Nasrazadani [20]	137	1-1.98	300-450	Calcium
Sheikholeslami & Watkinson [12]	120-220	0.3 – 0.8	603-700	Calcium
Morse & Knudsen [13]	276	1.0	490-650	TDS
Helalizadeh et al. [21]	100-400	0.5-2.0	1.0-2.5 / 0.25-1.0	Calcium sulphate / Calcium carbonate
Present study	485	1.5	448, 648, 1020	Calcium carbonate

Table 1. Data for heat flux used in laboratory fouling experiments

Philadelphia tap water			
	Minimum	Average	Maximum
Conductivity (μS/cm)	389	520	652
pH	7.3	7.5	7.6
Total hardness (mg/L)	150	190	247
Alkalinity (mg/L)	54	74	93
Chloride (mg/L)	56	75	149
Sulfate (mg/L)	37	61	89
Silica (mg/L)	3	5.8	7.8
Phosphate (mg/L)	0.2	0.25	0.3

Table 2. Water quality data of make-up water provided by the City of Philadelphia

	Make-up	w/o PWT		w/ PWT	
	a1	a2	a3	a4	a5
Conductivity (μS/cm)	410	1955	1910	1950	1900
pH	7.1	8.2	8.2	8.2	8.4
Total hardness (mg/L)	116	626	601	624	608
Ca^{+} hardness (mg/L)	84	448	427	444	436
Mg^{+} hardness (mg/L)	32	180	174	180	172
Total alkalinity (mg/L)	64	172	151	168	164
Chloride (mg/L)	80	436	363	432	360
L.S.I. (at T = 68°C)	0.08	2.17	2.09	2.15	2.34

(a) Conductivity = 2000 μS/cm

	Make-up	w/o PWT		w/ PWT	
	b1	b2	b3	b4	b5
Conductivity (μS/cm)	410	2950	2850	2950	2900
pH	7.1	8.2	8.0	8.2	8.3
Total hardness (mg/L)	116	982	880	980	972
Ca^{+} hardness (mg/L)	84	648	624	644	636
Mg^{+} hardness (mg/L)	32	334	256	336	336
Total alkalinity (mg/L)	64	232	220	232	228
Chloride (mg/L)	80	668	640	664	656
L.S.I. (at T = 68°C)	0.08	2.40	2.17	2.40	2.49

(b) Conductivity = 3000 μS/cm

	Make-up	w/o PWT		w/ PWT	
	c1	c2	c3	c4	c5
Conductivity (μS/cm)	420	3950	3780	3950	3800
pH	7.4	8.2	8.2	8.2	8.2
Total hardness (mg/L)	137	1496	1360	1488	1424
Ca^{+} hardness (mg/L)	114	1020	792	1012	820
Mg^{+} hardness (mg/L)	23	476	568	476	604
Total alkalinity (mg/L)	70	322	296	318	260
Chloride (mg/L)	73	864	860	864	872
L.S.I. (at T = 68°C)	0.55	2.70	2.56	2.69	2.52

(c) Conductivity = 4000 μS/cm

Table 3. Water quality data measured for make-up and circulating water

List of Figures

Figure 1. Schematic diagram of present experimental system

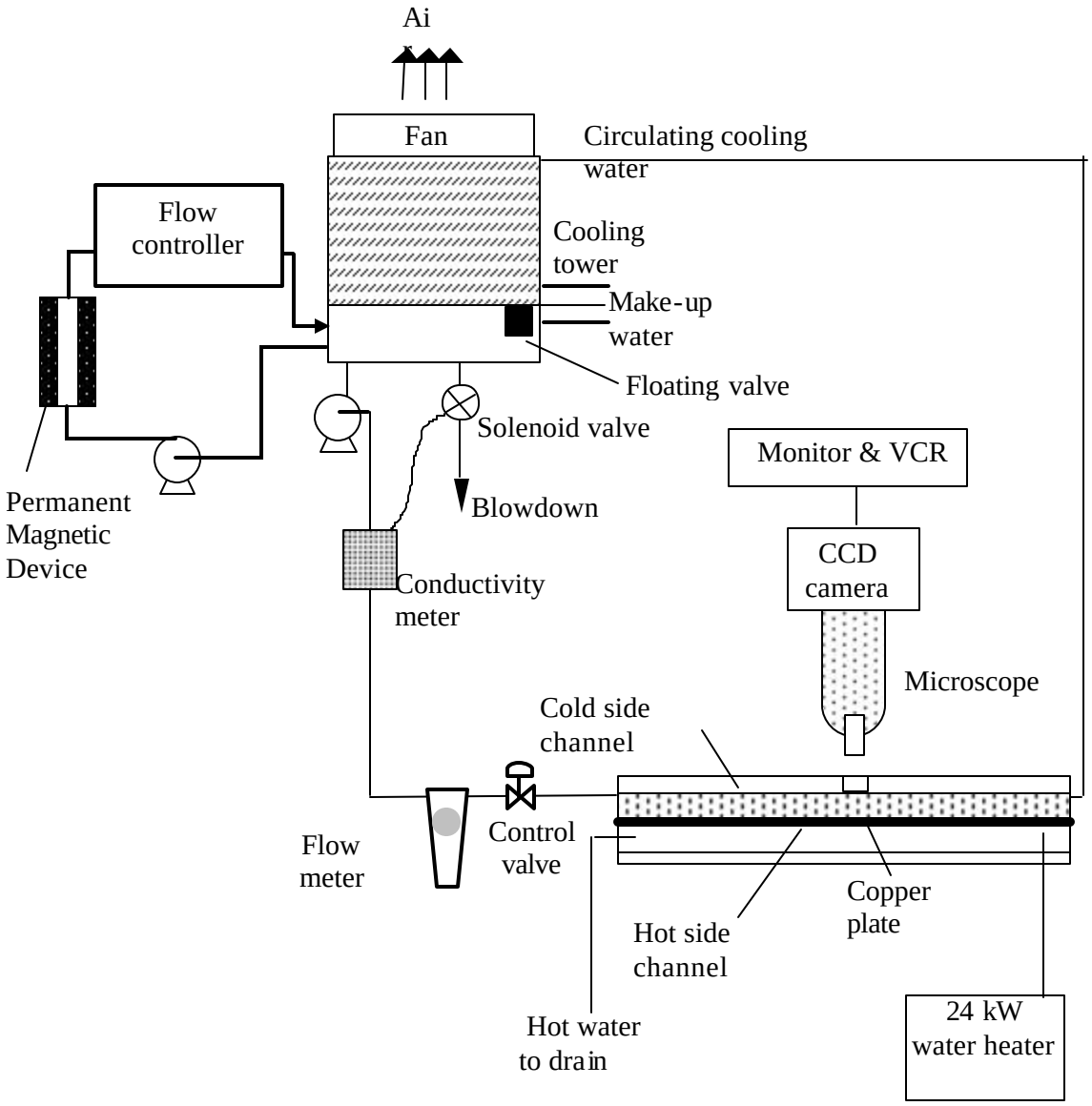

Figure 2. Cut-away view of a mini-channel heat exchanger

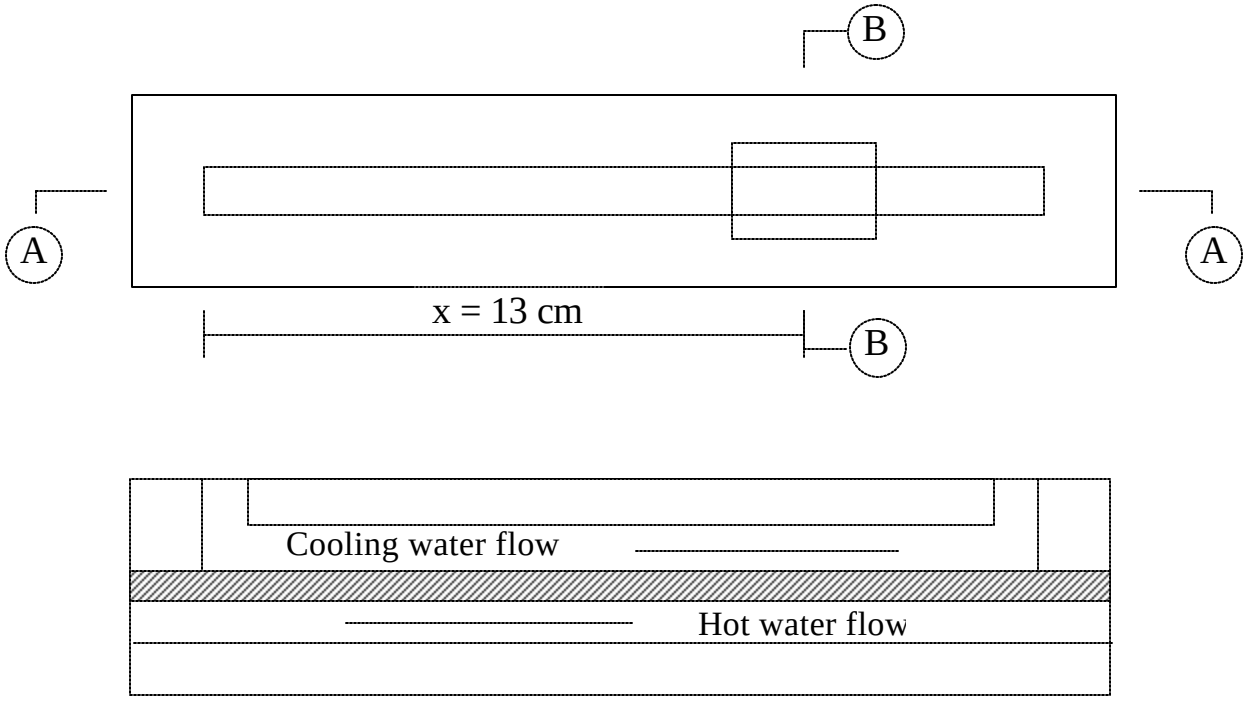

Section View (A-A)

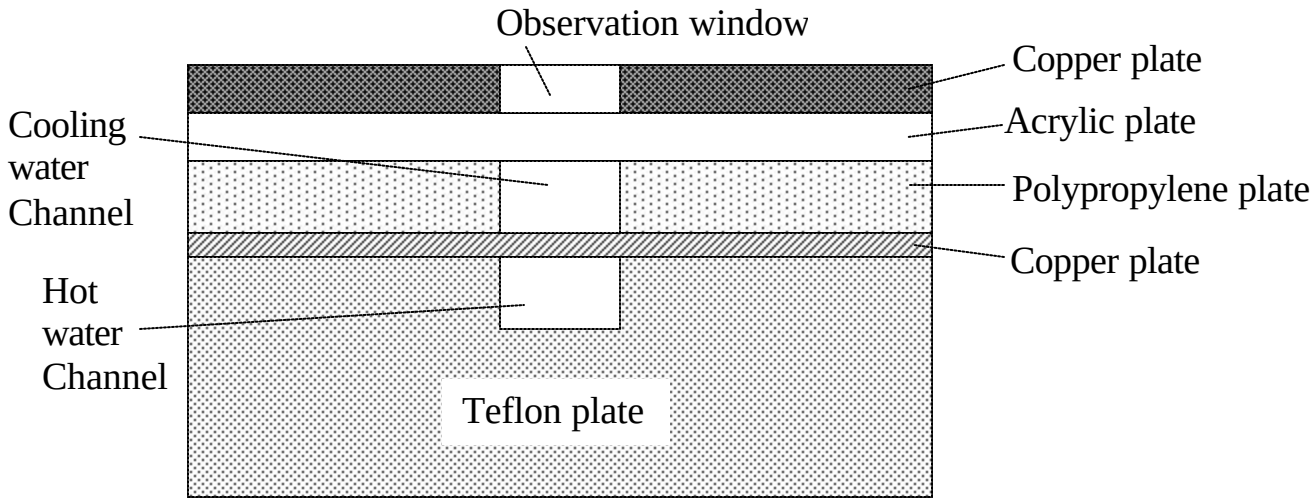

Section View (B-B)

Figure 3. Arrangement of permanent magnets and cross-sectional dimensions

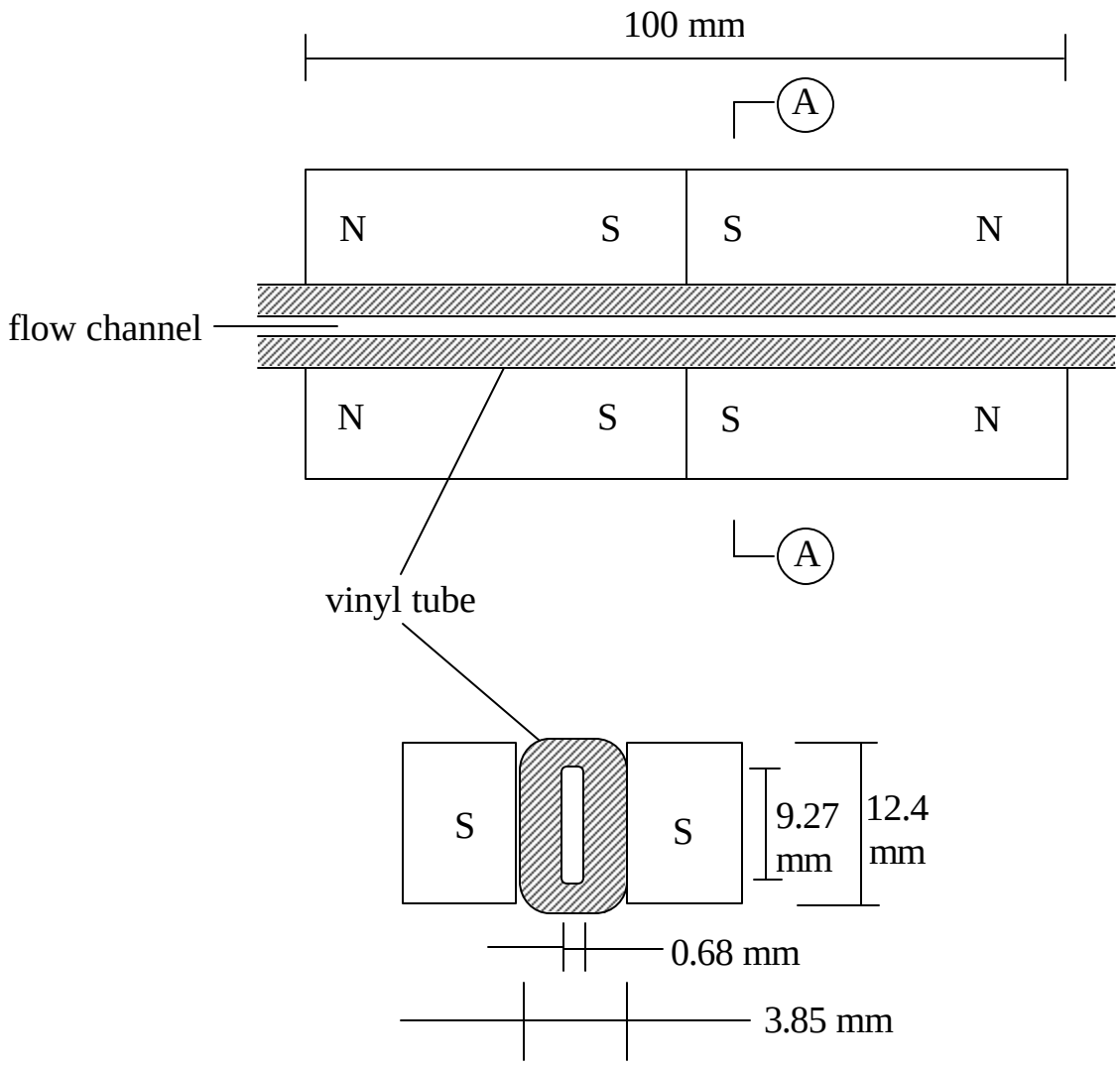

Section view <A-A>

Figure 4. Percentage reduction of fouling vs. flow velocity through PMDU device

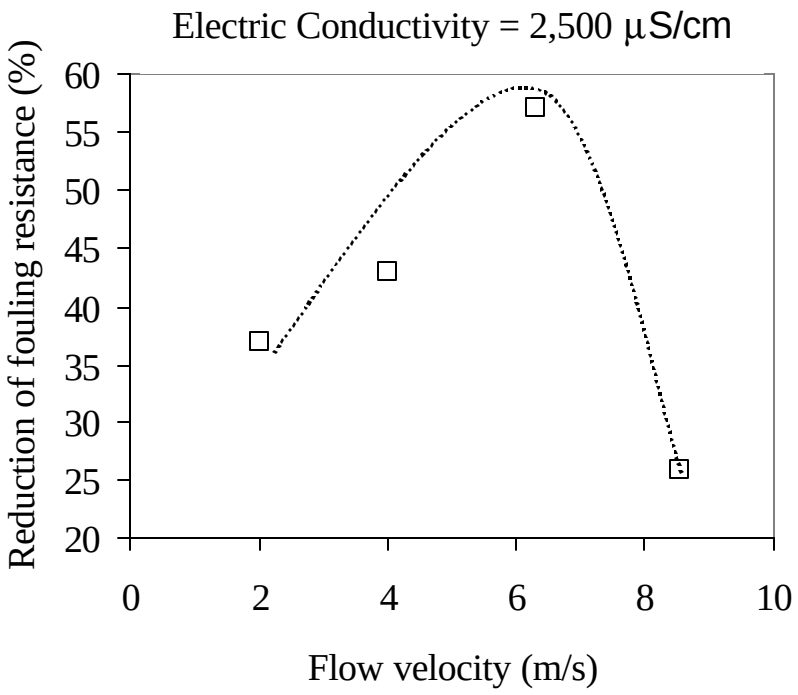

Figure 5. Test procedure and variations of electric conductivity vs. time

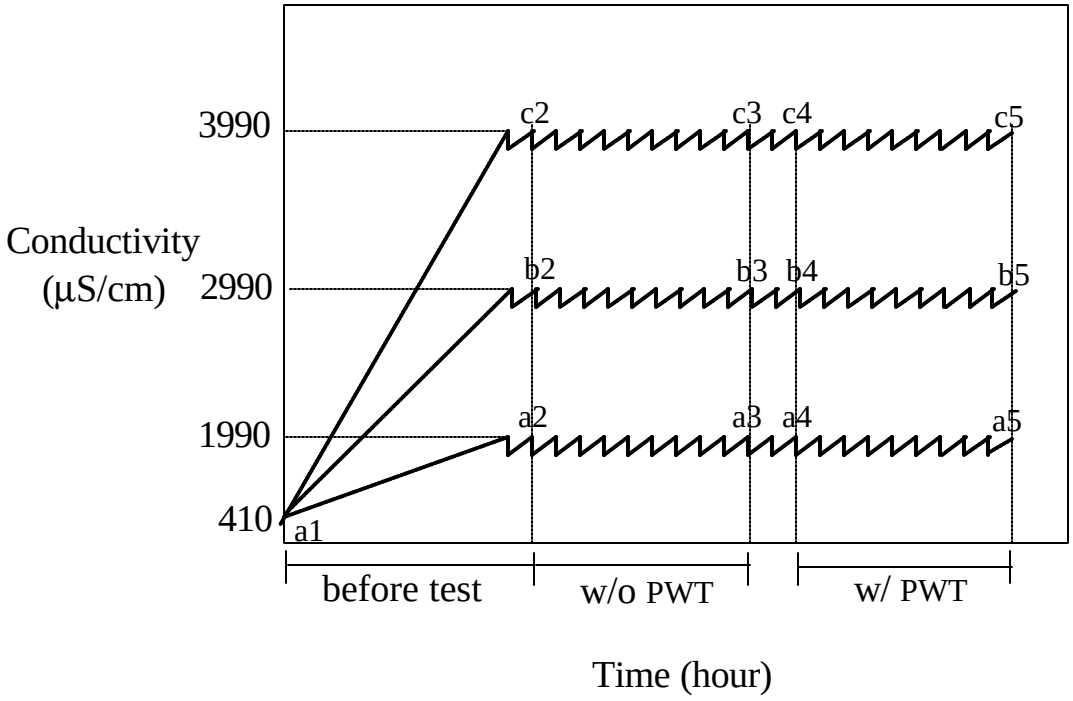

Figure 6. Photographs of fouled surfaces obtained using a microscopic imaging system

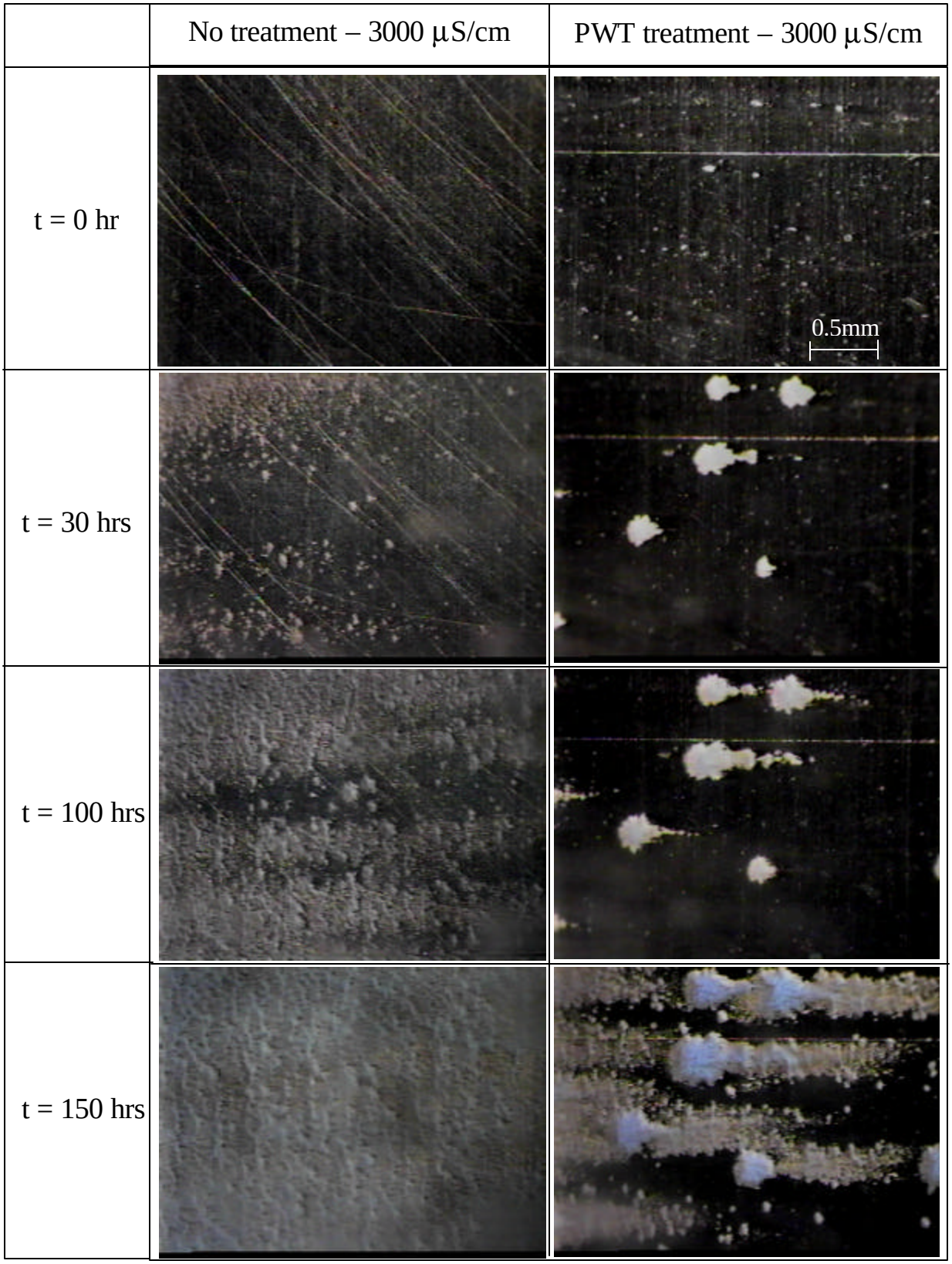

Figure 7. Photographs of fouled surfaces taken after fouled heat-transfer surfaces were completely dried

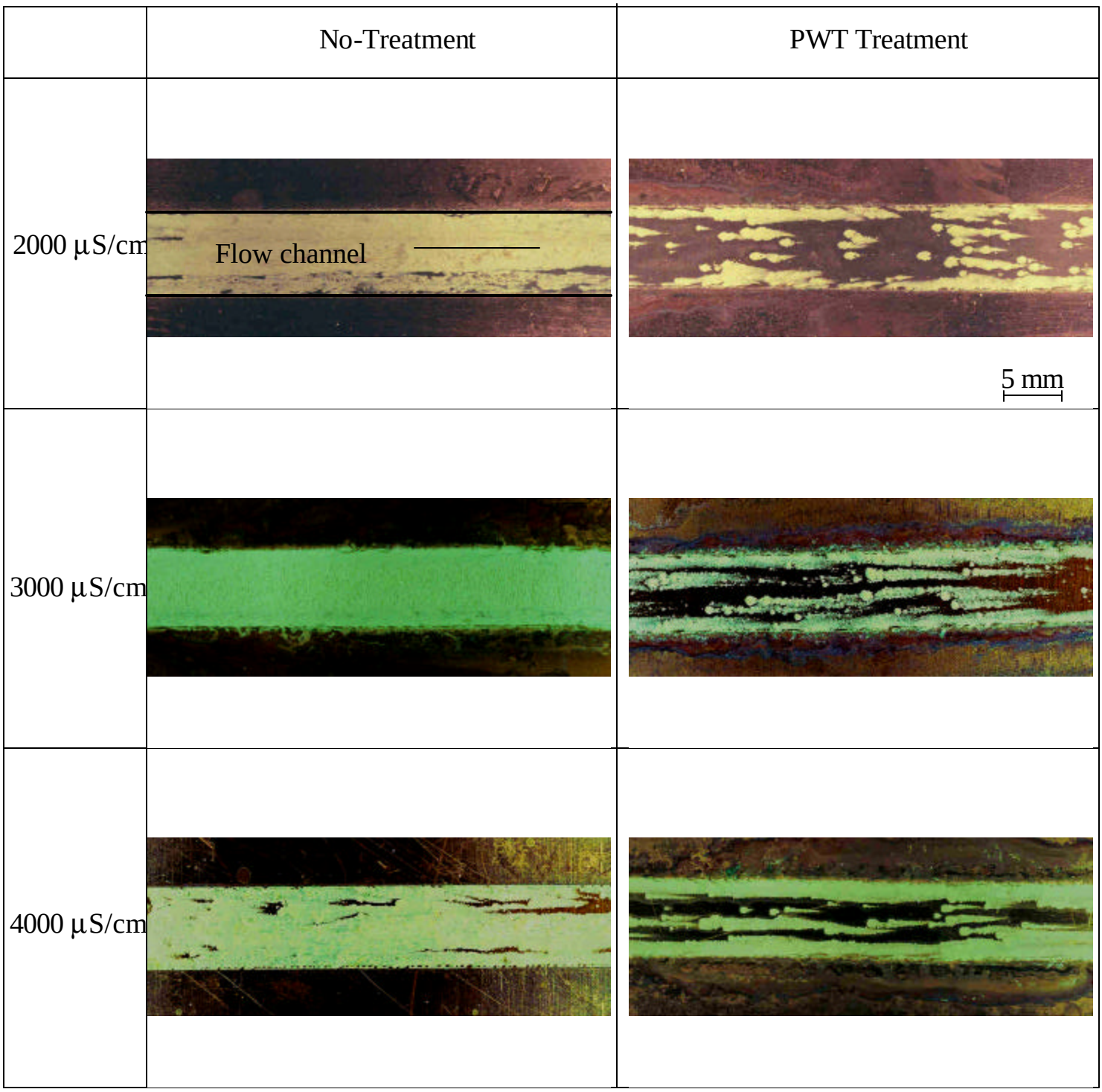

Figure 8. Fouling resistance values vs. time for three different conductivity cases

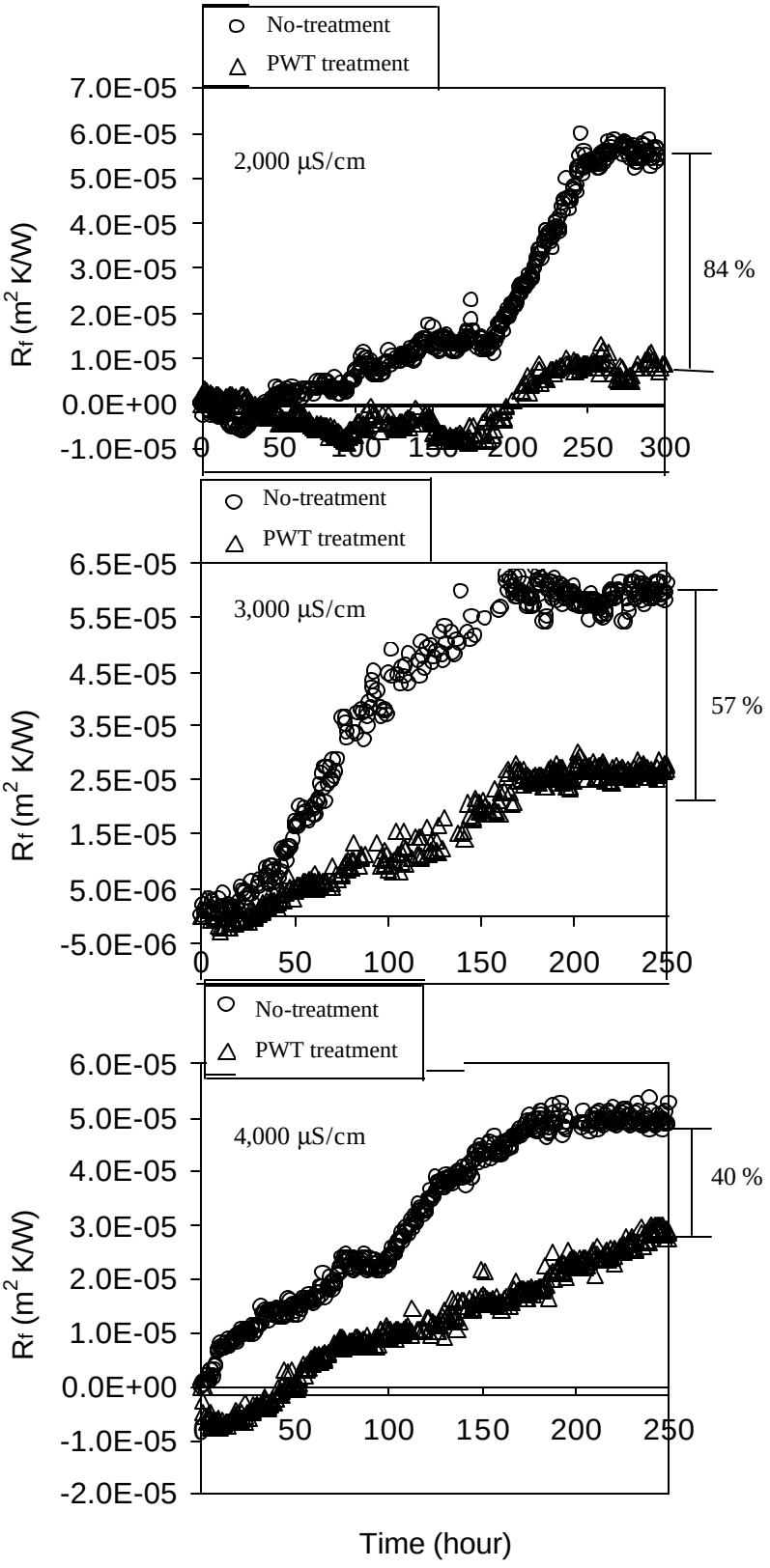

Figure 9. SEM photographs of scale layer for cases of 2,000, 3,000, and 4,000 μS/cm

	No-treatment	PWT treatment
2,000 μS/cm	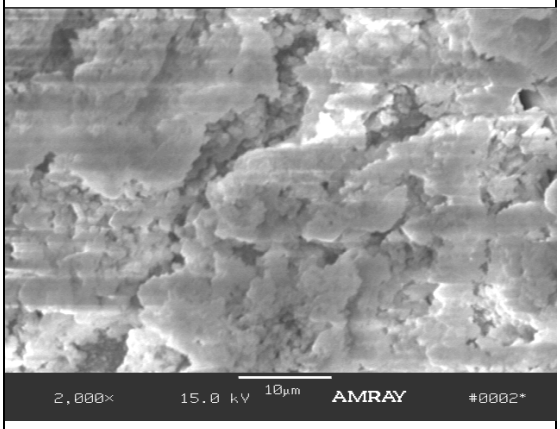	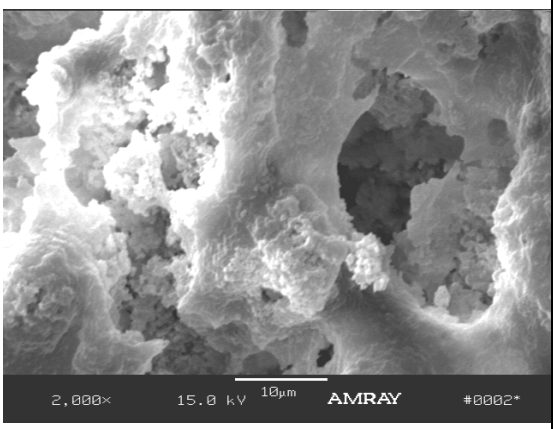
3,000 μS/cm	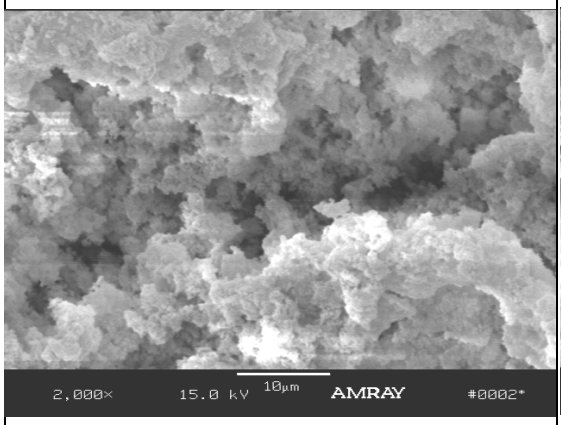	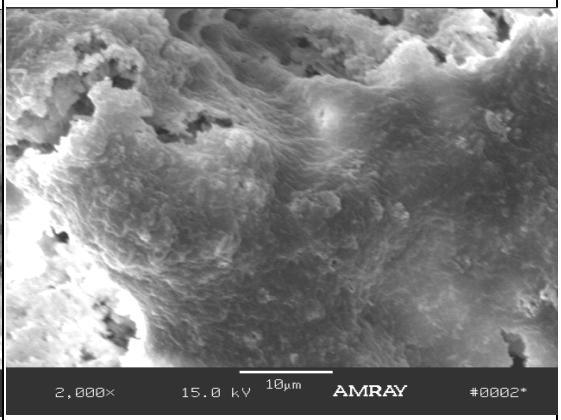
4,000 μS/cm	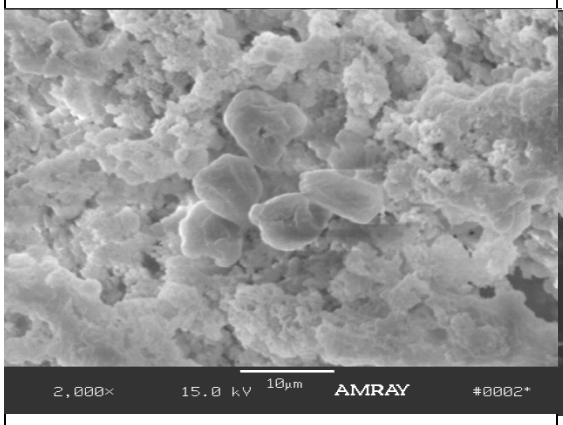	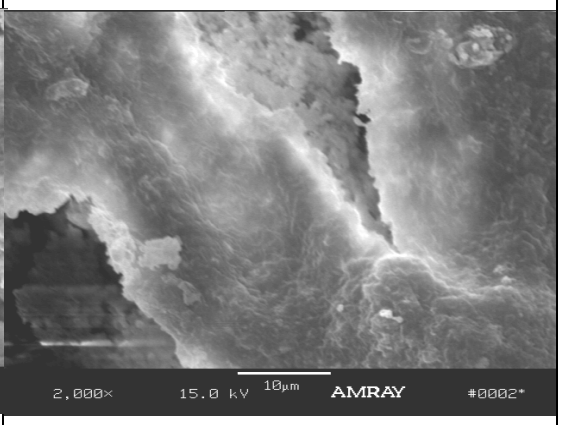

Figure 10. Result of the chemical composition of a deposited scale layer that was obtained from energy dispersive spectrum (EDS) method

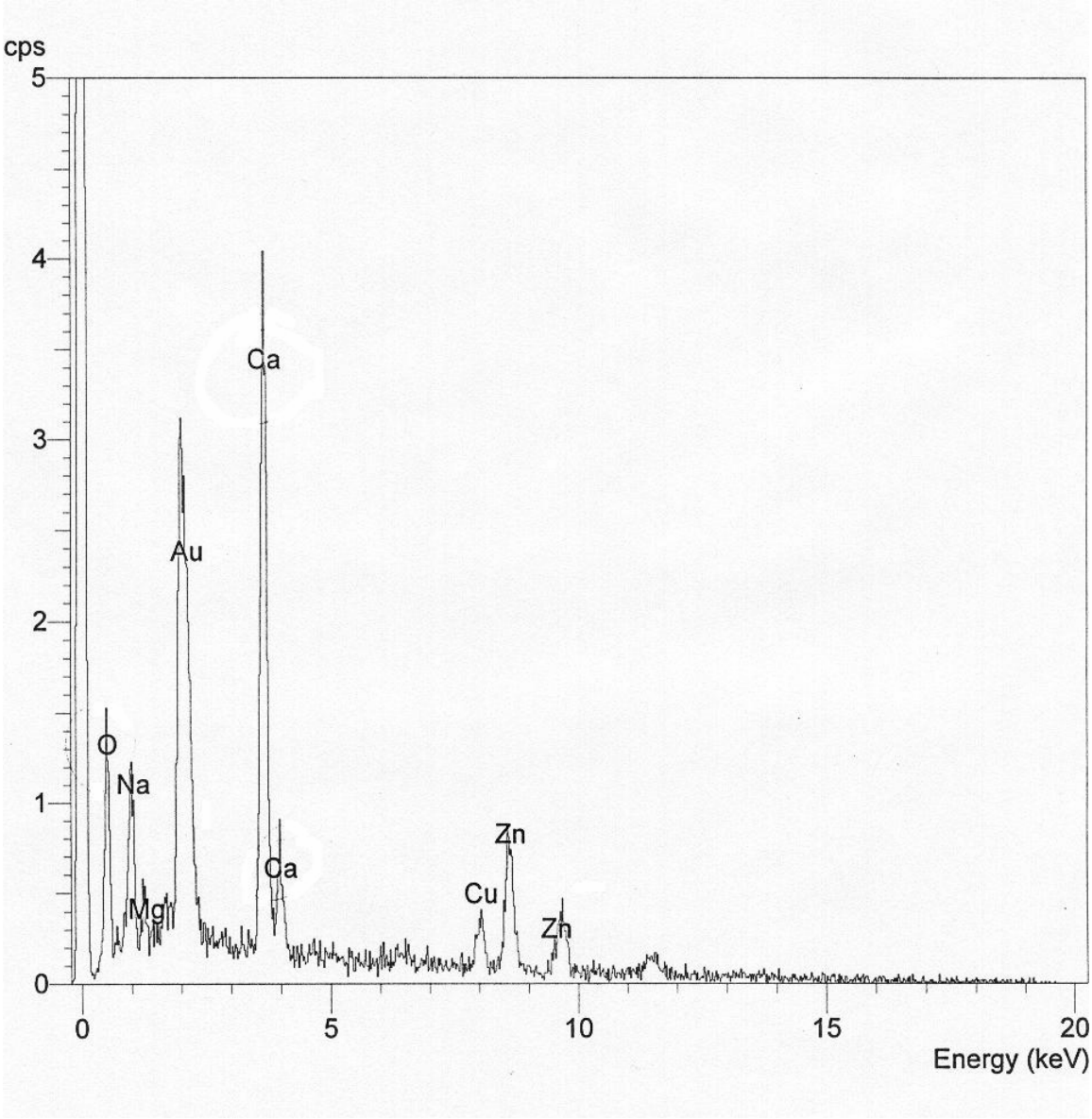

Figure 11. Result of X-ray diffraction for fouled crystal structure of all cases

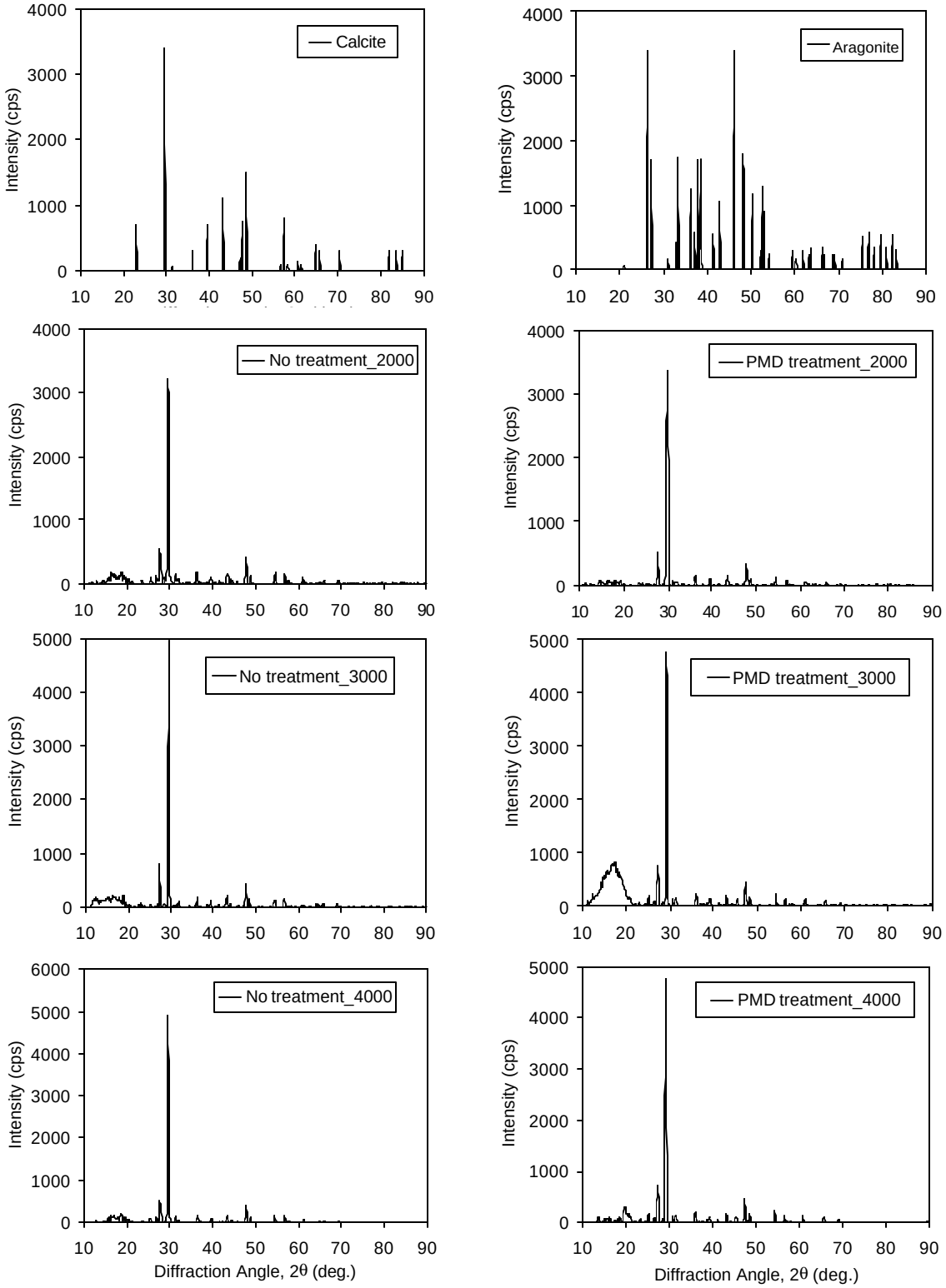

Appendix A: Calculation of the number of cycle based on mass consumption

A. For the case of 3000 μS/cm for no treatment

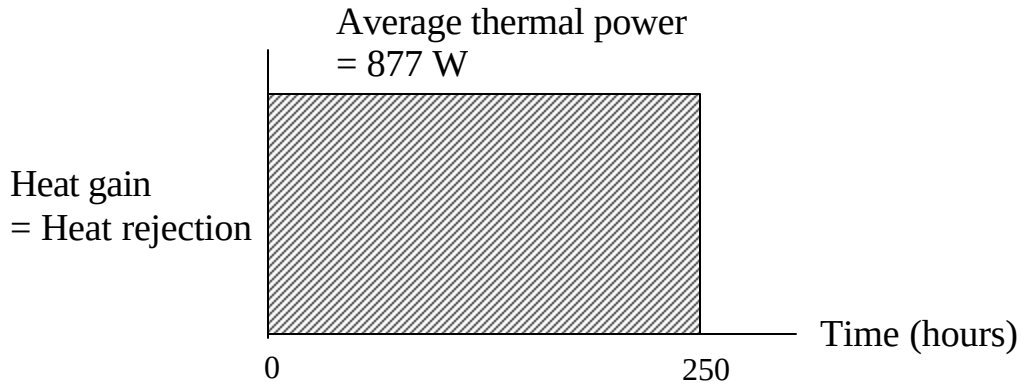

Total heat gain = 250 hrs × 0.877 kW × (3413 Btu/kW·hr)
= 748,300 Btu

Total evaporation mass = (748,300 Btu) / (970 Btu/lb)
= 771.4 lb

Total evaporation water volume (E) = (771.4 lb) × (0.016 ft^3/lb) × (7.48 gal/ft^3)
= 92.3 gallons

Total make-up water volume supplied (M) = 105 gallons

Total blowdown (B) = (0.7 gal/blowdown) × (6 blowdowns)
= 4.2 gallons

Total drift losses (D) = M – E – B = 105 – 92.3 – 4.2 = 8.5 gallons

Therefore, $COC = \frac{M}{B + D} = \frac{105}{4.2 + 8.5} = 8.2$

Appendix A: Calculation of the number of cycles based on mass consumption

B. For the case of 3000 μS/cm with PMDU-1

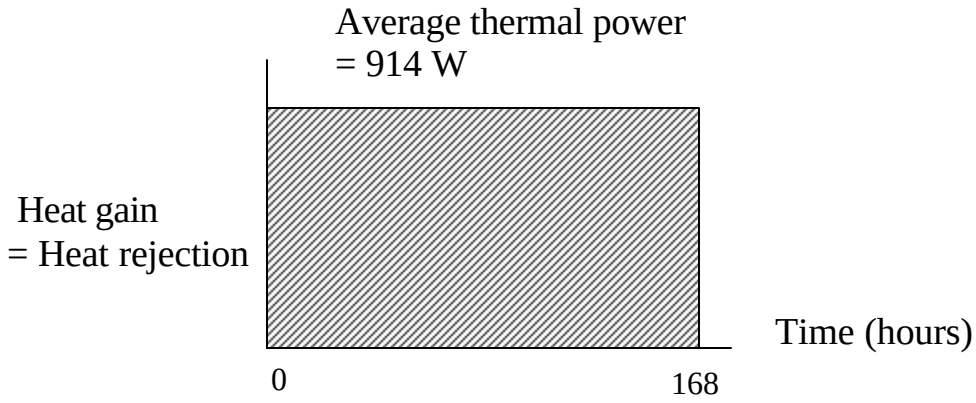

Total heat gain = 168 hrs × 0.914 kW × (3413 Btu/kW·hr)
= 524,072 Btu

Total evaporation mass = (524,072 Btu) / (970 Btu/lb)
= 540.3 lb

Total evaporation water volume (E) = (540.3 lb) × (0.016 ft^3/lb) × (7.48 gal/ft^3)
= 64.6 gallons

Total make-up water volume supplied (M) = 71 gallons

Total blowdown (B) = (0.7 gal/blowdown) × (3 blowdowns)
= 2.1 gallons

Total drift losses (D) = M – E – B = 71 – 64.6 – 2.1 = 4.3 gallons

Therefore, $COC = \frac{M}{B+D} = \frac{71}{2.1+4.3} = 11.1$

Appendix 2 Comparison of water analyses between Commercial Water Treater and Drexel University

Table 1
ASHRAE RP1155 – Water Analyses by Commercial Water Treater
(Untreated case) Sample Date 6/25/01

	Makeup	Unfiltered Tower	Calc' d Cycles per Unfilt' d Twr	Filtered Tower
pH	7.8	7.6		8.0
Sp Cond @ 25C, umhos	518	2950	5.7 (2)	2930
Alk, "P" as CaCO3, ppm	0	0		0
Alk, "M" as CaCO3, ppm	71	263	3.7 (2)	254 (3)
Sulfur, as SO4, ppm	54	344	6.4 (1)	349
Chloride, as Cl, ppm	78	616	7.9 (1)	620
Hardness, Total, as CaCO3, ppm	193	1110	5.8	1130
Calcium, Total, as CaCO3, ppm	134	704	5.3 (2)	713 (3)
Magnesium, Total, as CaCO3, ppm	59	409	6.9 (1)	415
Copper, Total, as Cu, ppm	<0.05	0.40		0.37
Iron, Total, as Fe, ppm	<0.05	<0.05		<0.05
Sodium, as Na, ppm	30	208	6.9 (1)	212
PO4, Total Inorg, as PO4, ppm	1.2			
PO4, Ortho, as PO4	1.2	2.5		1.7
Silica, Total, as SiO2, ppm	6.2	36	5.8 (2)	36 (3)

Observations:
(1) - Based on sulfur, chloride, magnesium, and sodium, it appears that the tower was cycled about 7.0 times when sampled.
(2) - Precipitation was occurring as suggested by reduced calcium, M alkalinity, specific conductance, and silica cycles.
(3) - Note that filtration through a 0.22 micron filter did not reduce calcium, M alkalinity, or silica. This suggests that precipitates were dropping out somewhere, as opposed to remaining suspended in the recirculating water.

Table 2
ASHRAE RP1155 – Water Analyses by Commercial Water Treater
(PMDU-1 treated case) Sample Date 7/2/01

	Makeup	Unfiltered Tower	Calc'd Cycles per Unfilt'd Twr	Filtered Tower
pH	7.6	7.6		8.4
Sp Cond @ 25C, umhos	365	3070	8.4 (2)	3030
Alk, "P" as CaCO3, ppm	0	0		7.5
Alk, "M" as CaCO3, ppm	51	252	4.9 (2)	241
Sulfur, as SO4, ppm	28	329	11.8 (1)	327
Chloride, as Cl, ppm	59	666	11.3 (1)	676
Hardness, Total, as CaCO3, ppm	135	1140	8.4	1140
Calcium, Total, as CaCO3, ppm	101	729	7.2 (2)	727 (3)
Magnesium, Total, as CaCO3, ppm	34	411	12.1 (1)	410
Copper, Total, as Cu, ppm	<0.05	0.41		.39
Iron, Total, as Fe, ppm	<0.05	<0.05		<0.05
Sodium, as Na, ppm	19.8	218	11.0 (1)	217
PO4, Total Inorg, as PO4, ppm	1.3			
PO4, Ortho, as PO4	1.2	1.6		1.9
Silica, Total, as SiO2, ppm	5.1	37	7.3 (2)	37 (3)

Observations:
(1) - Based on sulfur, chloride, magnesium, and sodium, it appears that the tower was cycled about 11.6 times when sampled.
(2) - Precipitation was occurring as suggested by reduced calcium, M alkalinity, specific conductance, and silica cycles.
(3) - Note that filtration through a 0.22 micron filter did not significantly reduce calcium or silica. This suggests that precipitates were dropping out somewhere, as opposed to remaining suspended in the recirculating water.

Table 3
Drexel – Water Analyses (Untreated case) Sample Date 6/25/01

	Make-up	Unfiltered	COC	Filtered
Conductivity (µS/cm)	490	2700	5.5	2780
pH	7.4	7.8		7.8
Total hardness (mg/L)	181	996	5.5	996
Ca^+ hardness (mg/L)	119	636	5.3	636
Total alkalinity (mg/L)	82	236	2.9	236
Chloride (mg/L)	85	580	6.8	580
L.S.I. (at T = 68°C)	0.63	2.01		2.01

Note from the review committee: Low COC for alkalinity implies that the sum of the two, $HCO_3^- + CO_3^{--}$, are decreased. Passably CO_2 is generated and lost to atmosphere or C is incorporated in compounds not yet determined. Conductivity is a composite of the sum of all the activity coefficients times the concentration of various ions. The sum of chloride and presumably other soluble ions, Na, would have the COC greater than the conductivity cycles, and the alkalinity would be less. It could be coincidence that the conductivity and hardness numbers are the same. It's probably beyond the scope of the study, but someone knowledgeable in the area of bicarbonate-carbonate-ionic solubilities could make some contributions.

Table 4
Drexel – Water Analyses (PMDU-1 treated case) Sample Date 7/02/01

	Make-up	Unfiltered	COC	Filtered
Conductivity (µS/cm)	340	2800	8.2	2760
pH	7.4	8.0		8.0
Total hardness (mg/L)	125	1060	8.5	1010
Ca^+ hardness (mg/L)	94	640	6.8	610
Total alkalinity (mg/L)	59	240	4.1	240
Chloride (mg/L)	64	640	10	640
L.S.I. (at T = 68°C)	0.41	2.22		2.20

Chapter 5

Effect of the Arrangement of Permanent Magnets on the Mitigation of Mineral Fouling (Rectangular Heat Transfer Test Section)

ABSTRACT

The present study investigated the effect of the PWT using different arrangements of permanent magnets on the mitigation of mineral fouling with circulating water of an electric conductivity of 2,0000 μS/cm. When the magnetic fields change their directions along the flow direction (i.e., alternating magnetic fields) (see Figures 4 and 6), the asymptotic values of the fouling resistance decreased by 80% from the values for the no-treatment case. On the contrary, for the cases of non-alternating magnetic fields, the fouling resistance increased at the level of no-treatment case. It is concluded by using the PWT using alternating magnetic fields one can substantially reduce mineral fouling in heat transfer equipment in a cooling-tower application with substantial energy and water savings.

INTRODUCTION

There are a number of different types and designs of permanent magnets that are used for the purpose of water treatment. Due to vastly different designs, some permanent magnets work very well, while others do not work at all. The former represents a group of products which have been perfected through the years of trial-and-error and continuous improvement.

From the scientific point of view, it is essential to understand what the critical condition is for the proper operation of the permanent magnets used for the purpose of the mitigation of mineral fouling. Thus, the present study investigated the effect of different arrangements of permanent magnets on the mitigation of fouling. More specifically, the present study focuses on finding whether one needs to have alternating magnetic fields for the effective water treatment or not.

EXPERIMENTAL METHODS

Figure 1 shows the various arrangements of permanent magnets used in present study and the corresponding cross-sectional views of flow channel where water was treated by the permanent magnets. The strength of the magnetic field of each type was similar to each other as 0.10–0.12 T (or 1,000–1,200 gauss) which was measured by an AlphaLab DC Magnetometer. Except for Type I, other four cases (i.e., Type II-A, B, and Type III-A, B) used the same size of a vinyl tube (4.32 mm–I.D., 6.35 mm - O.D.) where permanent magnets were installed.

Type I represents the optimum geometric arrangement of permanent magnets, a unit which was composed of three cylindrical magnets in the center of the device

jacket. Magnetic poles are arranged as NS-SN-NS along the flow direction as shown in Fig. 1. Cooling water was treated by passing through the narrow gap made by the permanent magnets and housing jacket. The cross-sectional dimension of the flow channel in the Type I was 15.7 mm, 12.7 mm (I.D., O.D.) so that flow accelerated as it passed the permanent magnets.

Type II-A was a ring-type magnet installed around a vinyl tube filled with water as shown in Fig. 1(b). In Type II-B, two ring magnets were used, with different magnetic poles facing each other (i.e., NS-NS) as shown in Fig. 1(d).

Type III-A was composed of two rectangular magnets, each positioned at the top and bottom, respectively, of a vinyl tube filled with water. The two rectangular magnets had different poles as shown in Fig. 1(c). In Type III-B, two more sets of rectangular magnets were installed in a manner that magnetic fields alternate along the flow direction as shown in Fig. 1(e).

The flow velocity of water was 1.5 m/s in the heat transfer test section, whereas the flow velocity at the permanent magnets was 2.5 m/s for all runs. The inlet temperature of the circulating water prior to the heat transfer test section was maintained at $20 \pm 1°C$ by means of an evaporative cooling tower, whereas the inlet temperature of the hot water was maintained at 89 to 92°C throughout the entire experiments. Heat flux between heating and cooling sides of the copper plate was 485.2 kW/m^2.

Figure 2 shows test procedure and variations of electric conductivities vs. time for all cases of the present experiment. The present study controlled the electric conductivity at a set-point of 2,000 μS/cm because it was much more convenient to

control the electric conductivity experimentally than the hardness of circulating water. Before starting each test, the water sample was prepared by circulating tap water through the cooling tower so that the desired electric conductivity was obtained (see Fig. 2). Once the circulating water reached the desired conductivity, the fouling test began with hot water in the hot water channel. At the end of the test for the no-treatment case, the cooling-tower water was continuously circulated while treated by one of the PWT devices, but without heat transfer for one day (i.e., see the period between a3 and a4, for example). After one-day pretreatment, a brand new copper plate was installed in the heat-transfer test section, and the fouling test began and continued for approximately 300 hrs.

RESULTS AND DISCUSSION

Table 1 shows the water analysis data for the make-up, and circulating cooling-tower water for both the no-treatment case and the PWT treatment case without filtration. The moments when water samples were taken from the circulating water were marked by a_i, where i varies from 1 to 13 (see Figure 2). There was no big difference in water qualities between no-treatment case and the case with the PWT.

The Langelier saturation index (LSI) was calculated to examine the precipitation tendency of the circulating water. The values of the LSI were in the range of 1.6 to 1.9, indicating that the circulating water had a condition to cause severe mineral fouling. In order to see if filtration removes any particulates from water, water analysis was conducted after filtration with 0.2-μm filter and the results

are shown in Table 2. The results obtained with and without filtration were almost identical to each other.

Figure 3 represents fouling resistances vs. time for a no-treatment case and three other cases with different arrangements of permanent magnets (i.e., Type I, II-A, and III-A). With a Type I device, the fouling resistance decreased by 80% from the value of the no-treatment case at the end of the test. On the contrary, the fouling resistance for the case of Type II-A increased almost at the level of no-treatment case (with negligible 5% reduction). For the case of Type III-A, the fouling resistance only reduced by 14% comparing to that from no-treatment case.

Clearly, the performance of permanent magnets critically depends on the arrangement of the permanent magnets. For the no-treatment case, the scale deposition is mainly due to the diffusion and crystallization of dissolved mineral ions at the heat transfer surface, i.e., crystallization fouling. When the cooling water was treated by the PWT device of Type I, the mineral ions that dissolved in the cooling water precipitated in the bulk water, and, the precipitated particles grew in size inside the heat transfer test section and deposited on the surface in the form of a particulate fouling. It is not easy for large particles to adhere to the heat transfer surface, because the large particles tend to be removed by shear force created by flow.

Based on the fouling resistance results, one can conclude that the PWT device of Type I was effective in precipitating dissolved ions into colloidal particles in water. Hence, the reduction in the fouling resistance was great, i.e., 80%. On the other hand, the arrangement shown in the Type II and III-A cases was not very effective in in precipitating dissolved ions into colloidal particles.

Since both Type II-A and III-A did not have alternating magnetic fields along the flow direction and the Type I had them, we speculated that the alternating magnetic fields may be necessary for the effective treatment of water. It is of note that the magnetic field and velocity vector are perpendicular in Type II and III, which should produce a strong induced electric field, whereas they are not perpendicular in the Type-I arrangement. Thus, we hypothesized that the performance of the Type II and III arrangements can be significantly improved if alternating magnetic fields can be provided.

To prove this hypothesis, Type II-B device was created as shown in Fig. 1(d), which provided the alternating magnetic fields. Figure 4 shows the magnetic fields for the Type II-A and B arrangements in detail. Figure 5 shows the results of the fouling resistance vs. time for the Type II-A and B together with those of the no-treatment case for reference. The Type II-B case produced a significant reduction of 84% in the fouling resistance compared with those from the no-treatment, whereas the Type II-A did not show any reduction in the fouling resistance, indicating the significance of the alternating magnetic fields in the physical water treatment.

Figure 6 shows the modification made in Type-III device, where two pairs of rectangular magnets were added to provide alternating magnetic fields, as shown in Fig. 6 (Type III-B). Figure 7 shows the fouling resistance results, indicating that Type III-B arrangement had substantially smaller fouling resistance values than those obtained in the Type III-A case. The results given in Fig. 7 also support the need of the alternating magnetic fields for the effective treatment of water for the purpose of the mitigation of mineral fouling.

Figure 8 shows the scanning electron microscopic (SEM) photographs of the scale layers for all six cases (i.e., no treatment, Type I, Type II-A, Type II-B, Type III-A, and Type III-B). In general, the SEM photographs can be grouped into two broad categories from the surface morphology point of view: One includes the cases of no treatment, Type II-A and Type III-A and the other includes Type I, II-B, and III-B. The Type III-B case is almost in the middle of two groups but is grouped to the latter.

Figure 9 shows enlarged SEM photographs of the scale layers for Type II-A and Type II-B which represent two groups, respectively. For the Type II-A case, scale layer consisted of numerous tiny round shape crystals, which were agglomerated together. Each crystal size was estimated approximately as 1 μm (see the top sketch at the right hand side of Fig. 9). In the case of Type II-B, each crystal grain boundary was not clearly defined. The scale layer appeared to be a one huge irregular crystal, and this big piece of crystal was composed of several layers as shown in the bottom sketch at the right hand side of Fig. 9.

Based on the SEM photographs and the fouling resistance results given in Fig. 3, one can conclude that alternating magnetic fields produced the precipitation of mineral ions in water, and the seed crystals grew in size and eventually deposited on the heat-transfer surface in the form of huge scale crystals made of a number of layers. The exact mechanism of forming multiple layers is not clear at this point.

In the present study, an X-ray diffraction method was also used to investigate the composition and structure of scale crystals that were sampled from the heat-transfer test section. As shown in Figure 10, all six crystal samples had the similar

structures of calcium carbonate scale, which was essentially calcite. Thus, it can be concluded that the PWT using permanent magnets produced calcite form of calcium carbonate, and there is no difference in the composition and structure of the scale crystals between the untreated and PWT cases.

CONCLUSIONS

The present study investigated the effect of the PWT using different arrangements of permanent magnets on the mitigation of mineral fouling with circulating water of an electric conductivity of 2,0000 μS/cm. When the alternating magnetic fields (i.e., Type I, II-B, and III-B) were used, the asymptotic values of the fouling resistance decreased by approximately 80% from the values of the no-treatment case. On the contrary, for the cases without the alternating magnetic fields (i.e., Type II-A, and III-A), the fouling resistance did not show any reduction compared with those of the no-treatment case.

In the cases of the no-treatment and the cases without alternating magnetic fields, the crystallization fouling seemed to be dominant as depicted by SEM photographs. On the other hand, the PWT cases using alternating magnetic fields produced scale crystals made of multiple layers of $CaCO_3$, which are believed to be due to particulate fouling. Real-time microscopic photographs and SEM photographs were obtained to render further support on the hypothesis of the particulate fouling. From the results of X-ray diffraction measurement, the composition and structure of scale crystal was determined to be calcite for the all six cases.

	Make-up Water	Circulating cooling tower water (without filtration)					
		No treatment	Type I	Type II-A	Type II-B	Type III-A	Type III-B
Conductivity (μS/cm)	600	1990 (3.9)	1995 (3.9)	1992 (3.9)	1997 (3.9)	1995 (3.9)	1994 (3.9)
pH	7.2	8.0	8.2	8.2	8.1	8.3	8.0
Total hardness (mg/L)	206	660 (4.2)	668 (4.2)	664 (4.2)	662 (4.2)	658 (4.2)	666 (4.2)
Ca^{+} hardness (mg/L)	153	440 (3.4)	444 (3.4)	441 (3.4)	442 (3.4)	436 (3.4)	440 (3.4)
Total alkalinity (mg/L)	70	200 (3.4)	206 (3.4)	210 (3.4)	204 (3.4)	202 (3.4)	208 (3.4)
Chloride (mg/L)	100	420 (4.7)	424 (4.7)	416 (4.7)	428 (4.7)	432 (4.7)	420 (4.7)
LSI**	-0.01	1.62	1.84	1.84	1.73	1.92	1.64
R_f x10^{-5} (m^2K/W) ***		4.5	0.9	4.5	0.75	4.0	2.0

* ( ) represents the ratio of each treatment to the make-up water
** LSI = Langelian Saturation Index
*** R_f = Fouling resistance at the end of 200-hour test

Table 1. Water quality data measured for make-up and circulating water

	Make-up Water	Circulating cooling tower water (with filtration)					
		No treatment	Type I	Type II-A	Type II-B	Type III-A	Type III-B
Conductivity (μS/cm)	600	1990 (3.9)	1995 (3.9)	1992 (3.9)	1990 (3.9)	1995 (3.9)	1994 (3.9)
pH	7.2	8.0	8.2	8.2	8.1	8.3	8.0
Total hardness (mg/L)	206	660 (4.2)	668 (4.2)	664 (4.2)	658 (4.2)	658 (4.2)	660 (4.2)
Ca^{+} hardness (mg/L)	153	440 (3.4)	444 (3.4)	441 (3.4)	442 (3.4)	436 (3.4)	440 (3.4)
Total alkalinity (mg/L)	70	200 (3.4)	206 (3.4)	210 (3.4)	204 (3.4)	202 (3.4)	208 (3.4)
Chloride (mg/L)	100	420 (4.7)	424 (4.7)	416 (4.7)	428 (4.7)	432 (4.7)	420 (4.7)
LSI**	-0.01	1.62	1.84	1.84	1.73	1.92	1.64
R_f x10^{-5} (m^2K/W) ***		4.5	0.9	4.5	0.75	4.0	2.0

∗ ( ) represents the ratio of each treatment to the make-up water
** LSI = Langelian Saturation Index
*** R_f = Fouling resistance at the end of 200-hour test

Table 2. Water quality data measured for make-up and circulating water

	Makeup	No treat W/ Filter	No treat W/O Filter	Type I
pH	7.4	7.7	7.7	7.8
Sp Cond @ 25C, µmhos	599	2130	2130	2130
Alk, "P" as CaCO3, ppm	0	0	0	0
Alk, "M" as CaCO3, ppm	65	196	194	196
Sulfur, as SO4, ppm	59	172	172	172
Chloride, as Cl, ppm	92	428	423	427
Hardness, Total, as CaCO3, ppm	185	658	666	660
Calcium, Total, as CaCO3, ppm	126	426	432	428
Magnesium, Total, as CaCO3, ppm	59	231	234	231
Copper, Total, as Cu, ppm	0.1	0.35	0.36	0.36
Iron, Total, as Fe, ppm	<0.05	<0.05	<0.05	<0.05
Sodium, as Na, ppm	31	153	146	153
PO4, Total Inorg, as PO4, ppm				
PO4, Ortho, as PO4	1.1	2.1	2.0	2.1
Silica, Total, as SiO2, ppm	1.9	19.2	19.4	19.1

Table 3. Water quality data measured by Commercial Water Treater

	Type II-A W/O Filter	Type II-B W/O Filter	Type II-A W/ Filter	Type II-B W/ Filter
pH	7.8	7.7	7.8	7.8
Sp Cond @ 25C, µmhos	2120	2120	2120	2120
Alk, "P" as CaCO3, ppm	0	0	0	0
Alk, "M" as CaCO3, ppm	196	196	196	195
Sulfur, as SO4, ppm	171	173	173	171
Chloride, as Cl, ppm	419	420	422	421
Hardness, Total, as CaCO3, ppm	659	664	663	655
Calcium, Total, as CaCO3, ppm	429	431	430	425
Magnesium, Total, as CaCO3, ppm	230	232	232	229
Copper, Total, as Cu, ppm	0.36	0.36	0.36	0.35
Iron, Total, as Fe, ppm	<0.05	<0.05	<0.05	<0.05
Sodium, as Na, ppm	146	150	151	149
PO4, Total Inorg, as PO4, ppm				
PO4, Ortho, as PO4	2.0	2.0	2.0	2.0
Silica, Total, as SiO2, ppm	19.1	19.4	19.3	19.1

Table 4. Water quality data measured by Commercial Water Treater

	Type III-A W/O Filter	Type III-B W/O Filter	Type III-A W/ Filter	Type III-B W/ Filter
pH	7.7	7.6	7.7	7.8
Sp Cond @ 25C, µmhos	2130	2130	2130	2130
Alk, "P" as CaCO3, ppm	0	0	0	0
Alk, "M" as CaCO3, ppm	196	196	197	196
Sulfur, as SO4, ppm	172	172	173	172
Chloride, as Cl, ppm	418	420	418	421
Hardness, Total, as CaCO3, ppm	660	665	663	665
Calcium, Total, as CaCO3, ppm	428	431	430	431
Magnesium, Total, as CaCO3, ppm	230	234	232	233
Copper, Total, as Cu, ppm	0.36	0.36	0.35	0.35
Iron, Total, as Fe, ppm	<0.05	<0.05	<0.05	<0.05
Sodium, as Na, ppm	149	151	149	148
PO4, Total Inorg, as PO4, ppm				
PO4, Ortho, as PO4	2.1	2.0	2.2	2.0
Silica, Total, as SiO2, ppm	19.2	19.3	19.4	19.4

Table 5. Water quality data measured by Commercial Water Treater

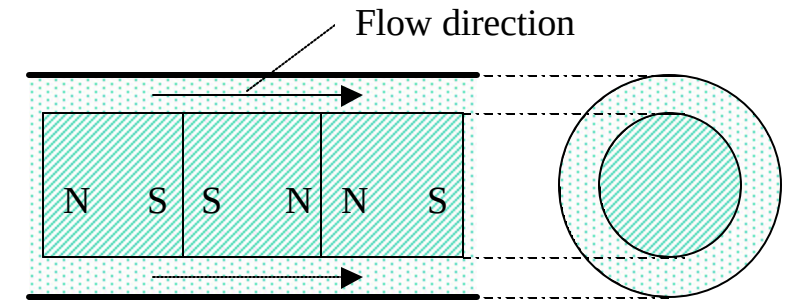

(a) Type I treatment

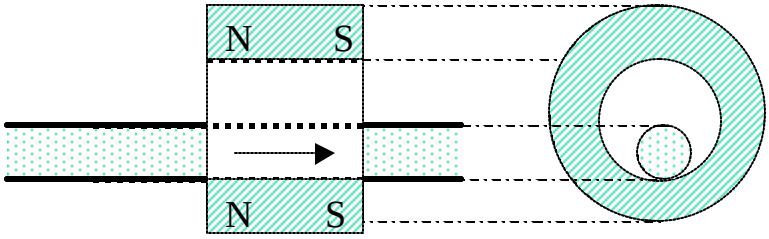

(b) Type II-A treatment

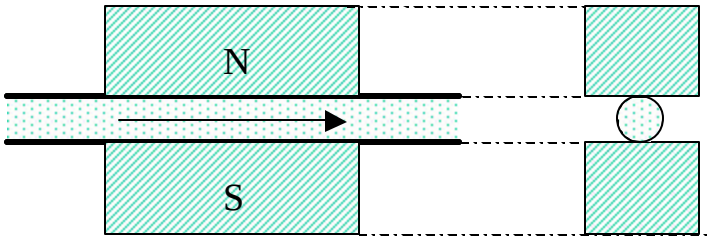

(c) Type III-A treatment

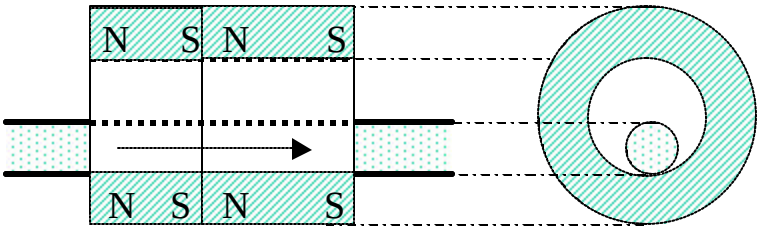

(d) Type II-B treatment

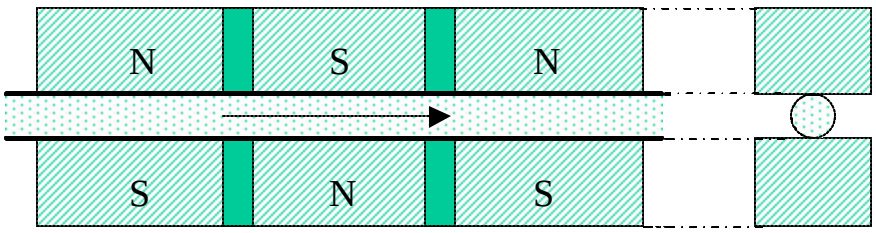

(e) Type III-B treatment

Figure 1. Arrangement of permanent magnet devices

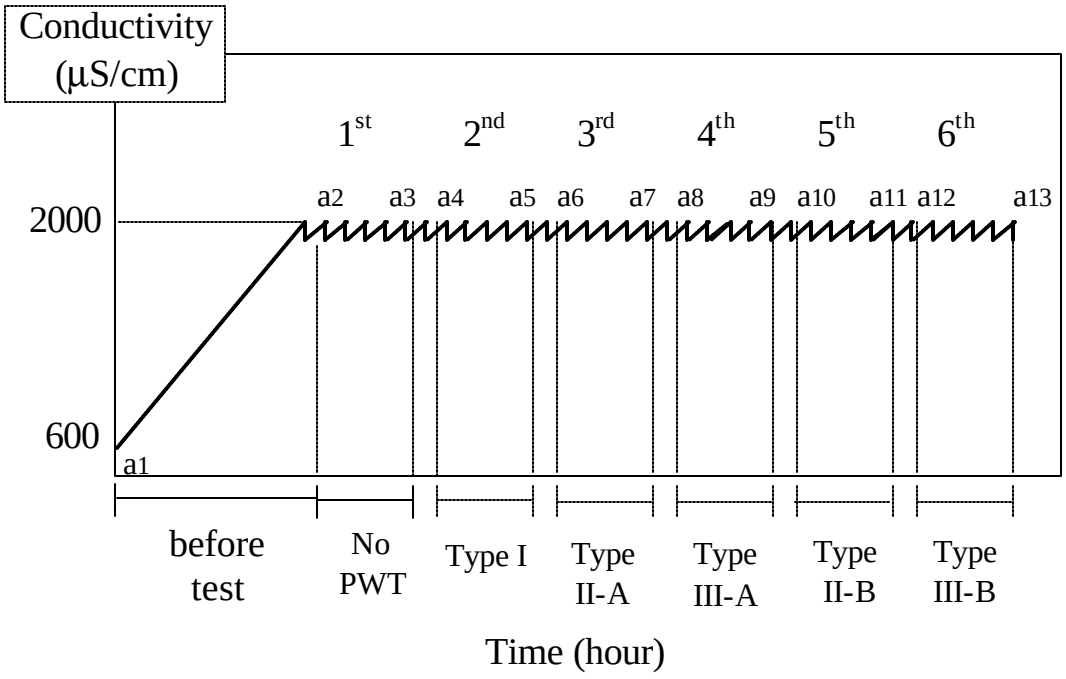

Figure 2. Test procedure and variations of electric conductivities vs. time

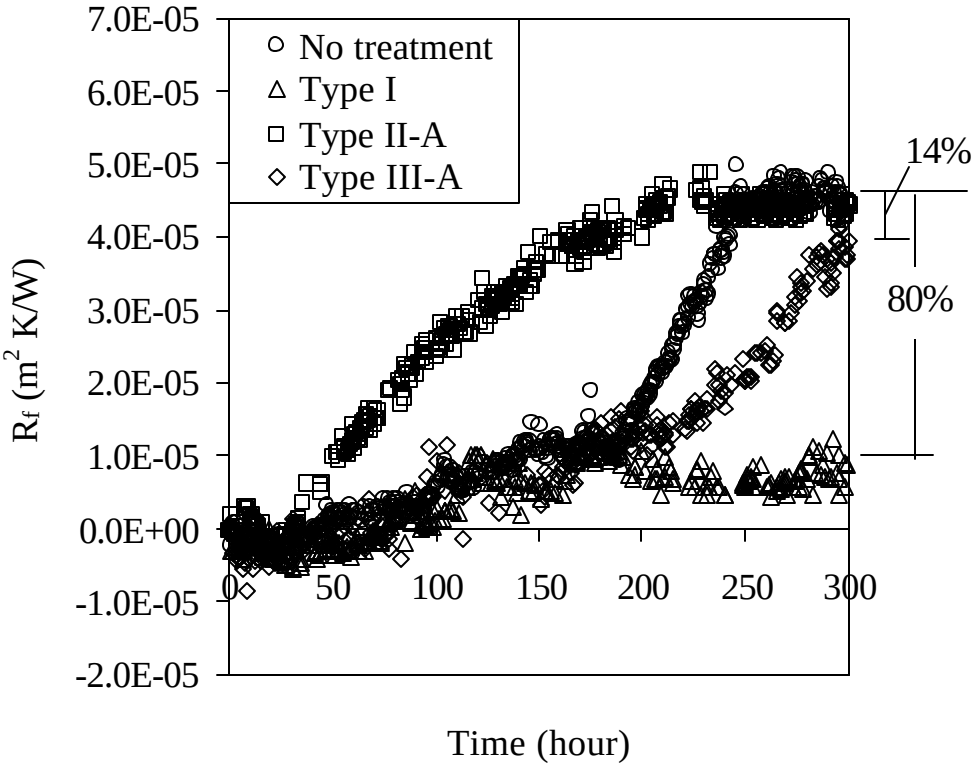

Figure 3. Fouling resistance values vs. time for the all cases

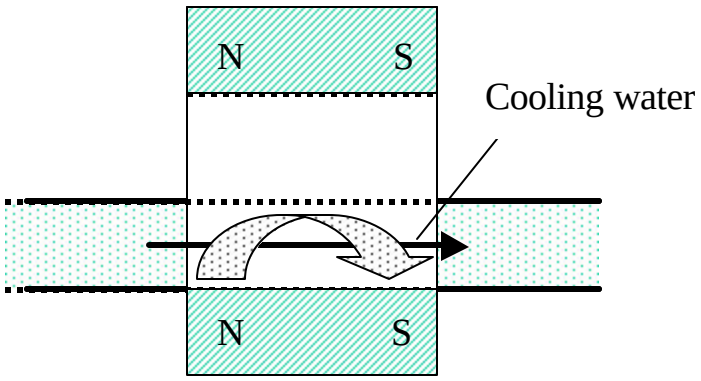

(a) Type II-A

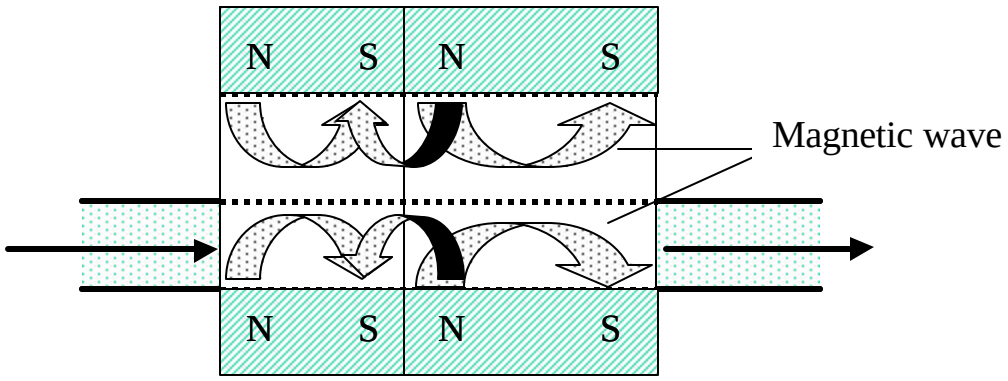

(b) Type II-B

Figure 4. Sketch of magnetic fields for Type II-A and Type II-B

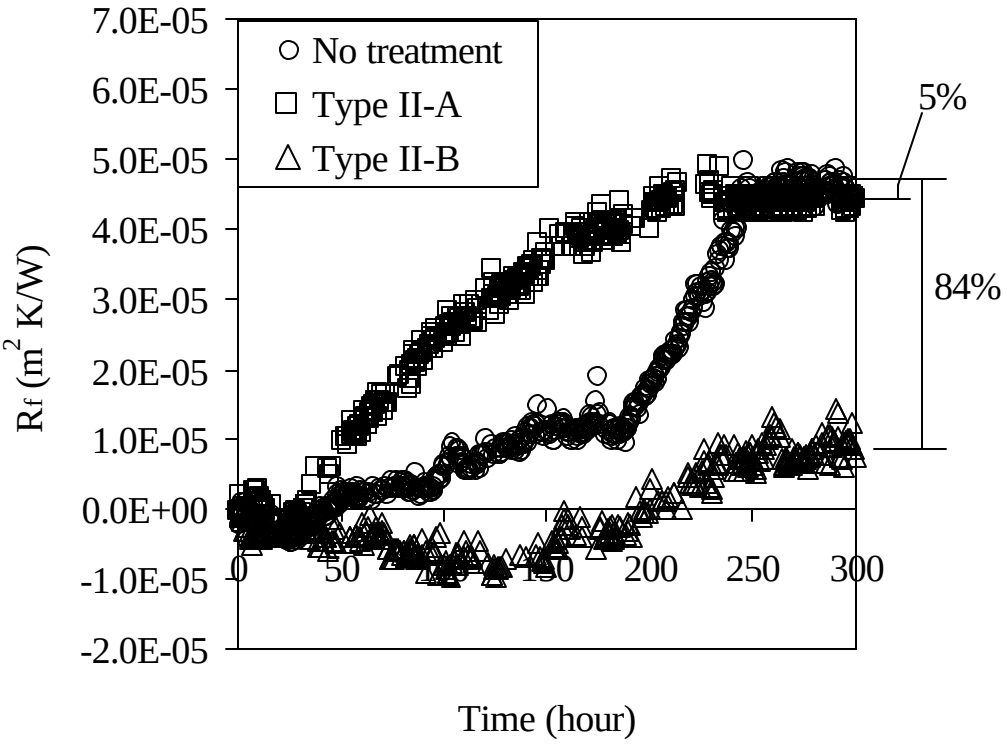

Figure 5. Fouling resistances vs. time for cases of Type II-A and B

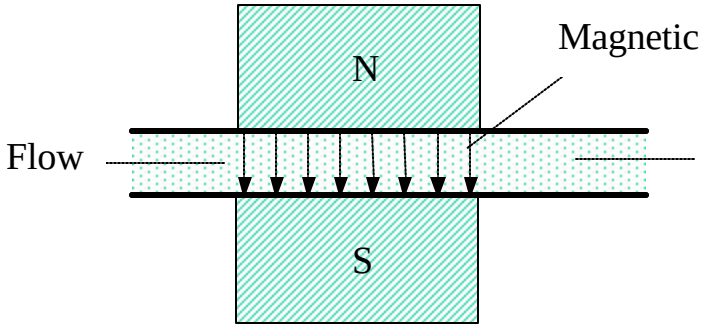

(a) Type III-A

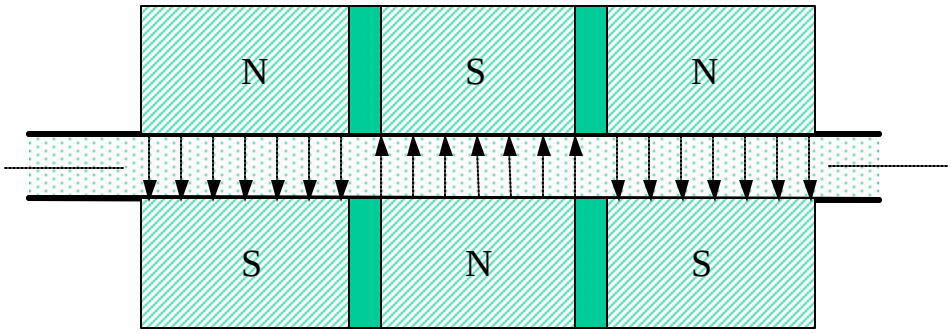

(b) Type III-B

Figure 6. Sketch of magnetic fields for Type III-A and Type III-B

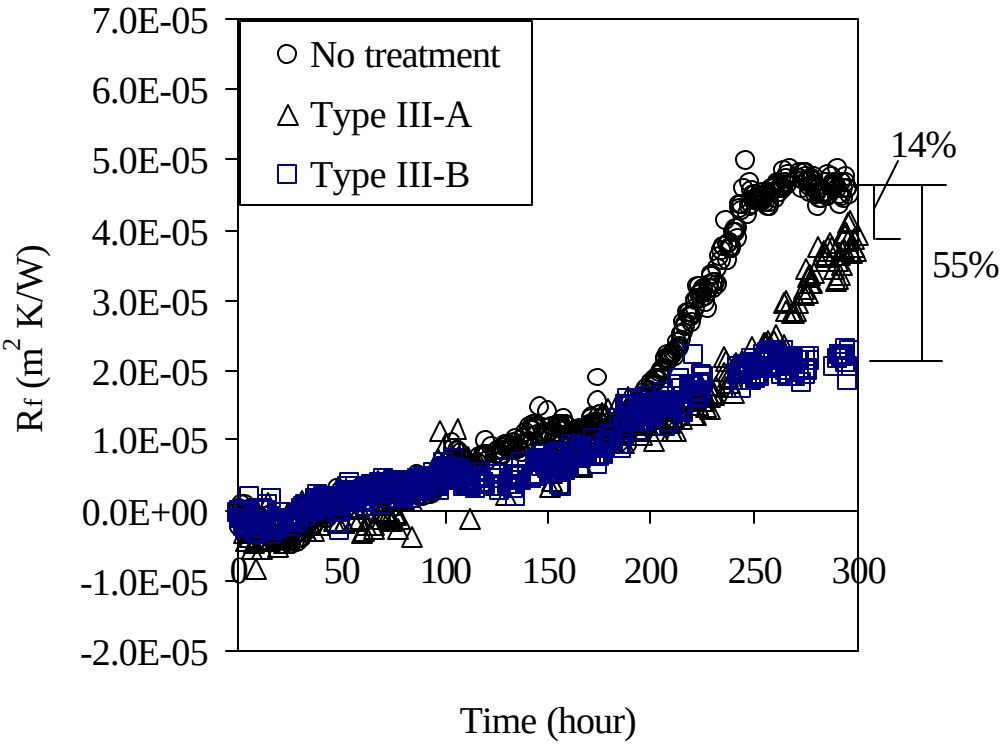

Figure 7. Fouling resistances vs. time for cases of Type III-A and B

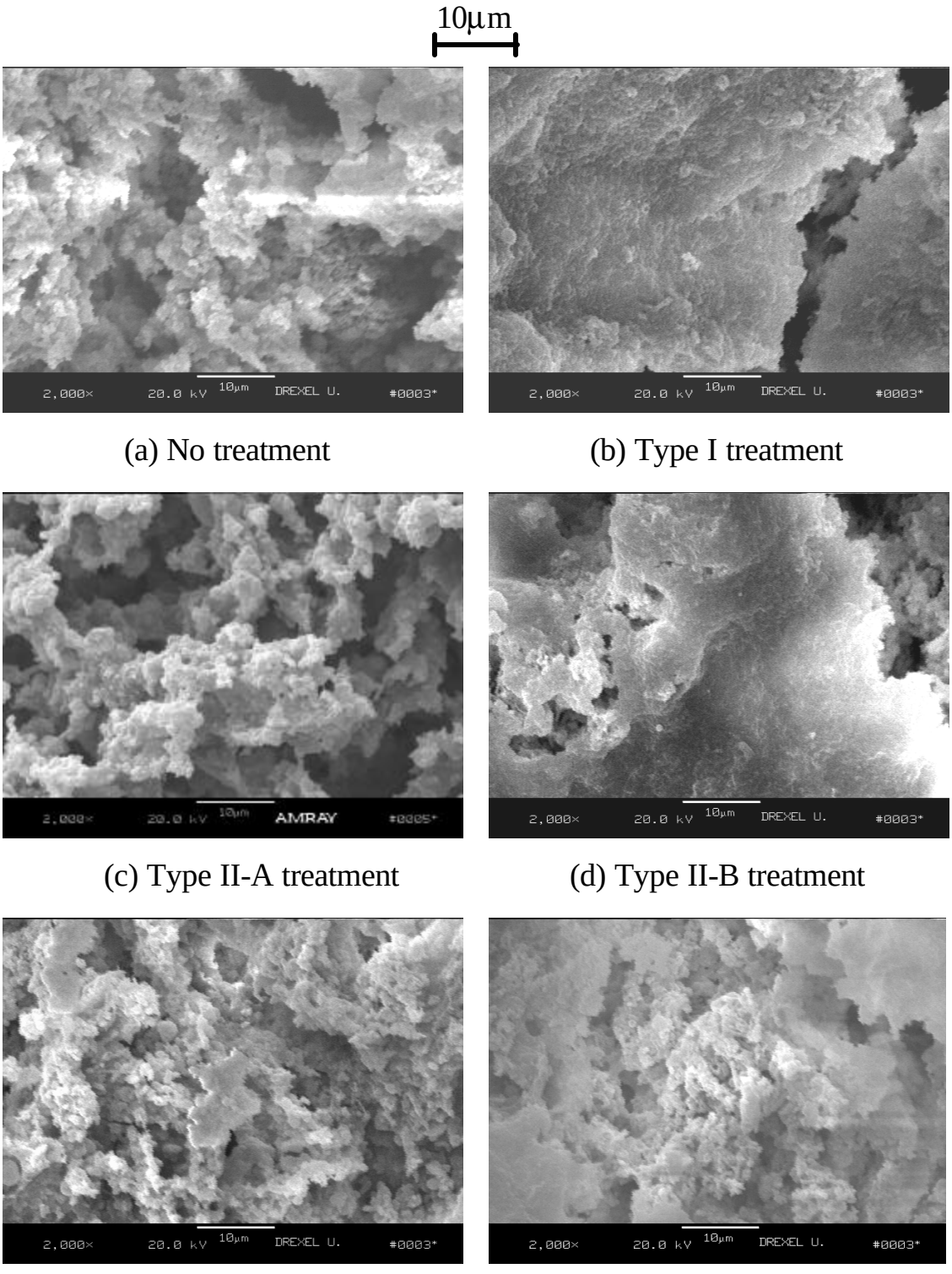

(a) No treatment (b) Type I treatment

(c) Type II-A treatment (d) Type II-B treatment

(e) Type III-A treatment (f) Type III-B treatment

Figure 8. SEM photographs of scale deposits, 2,000X

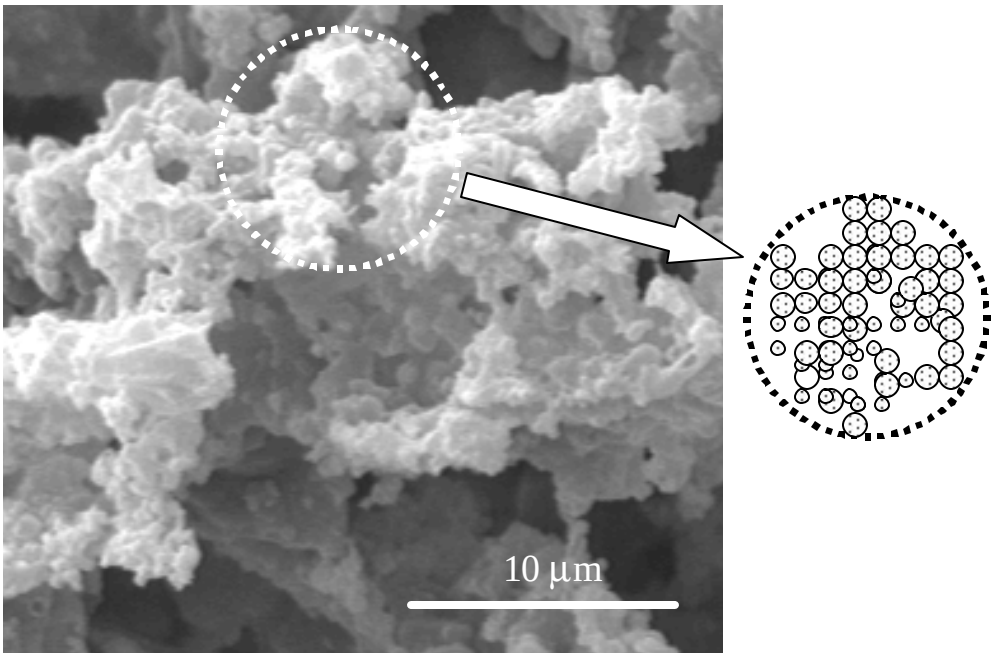

(a) Type II-A treatment

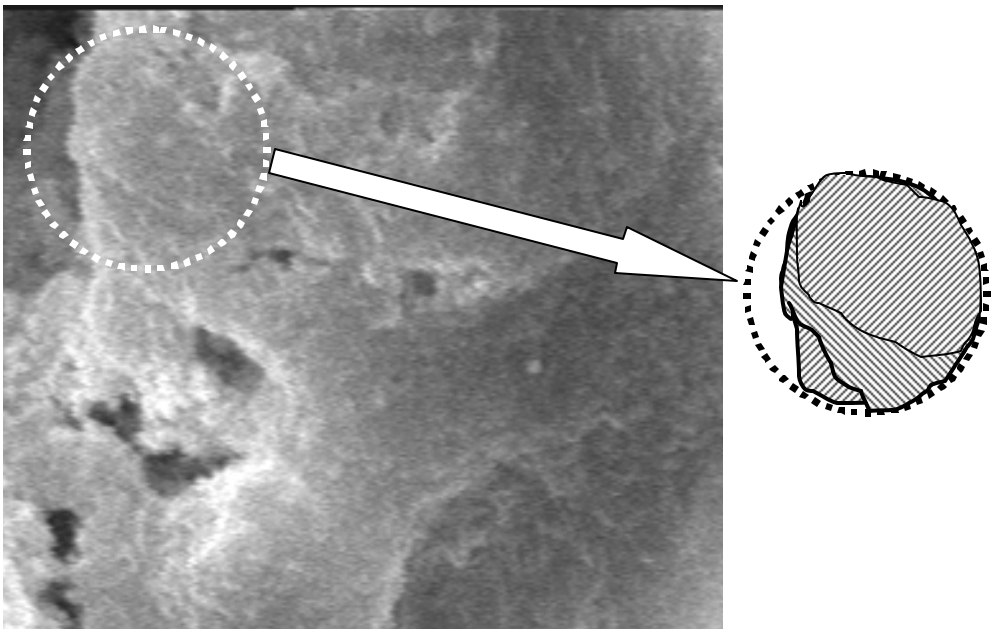

(b) Type II-B treatment

Figure 9. Enlarged SEM photographs for cases of Type II-A and B, 2,000X

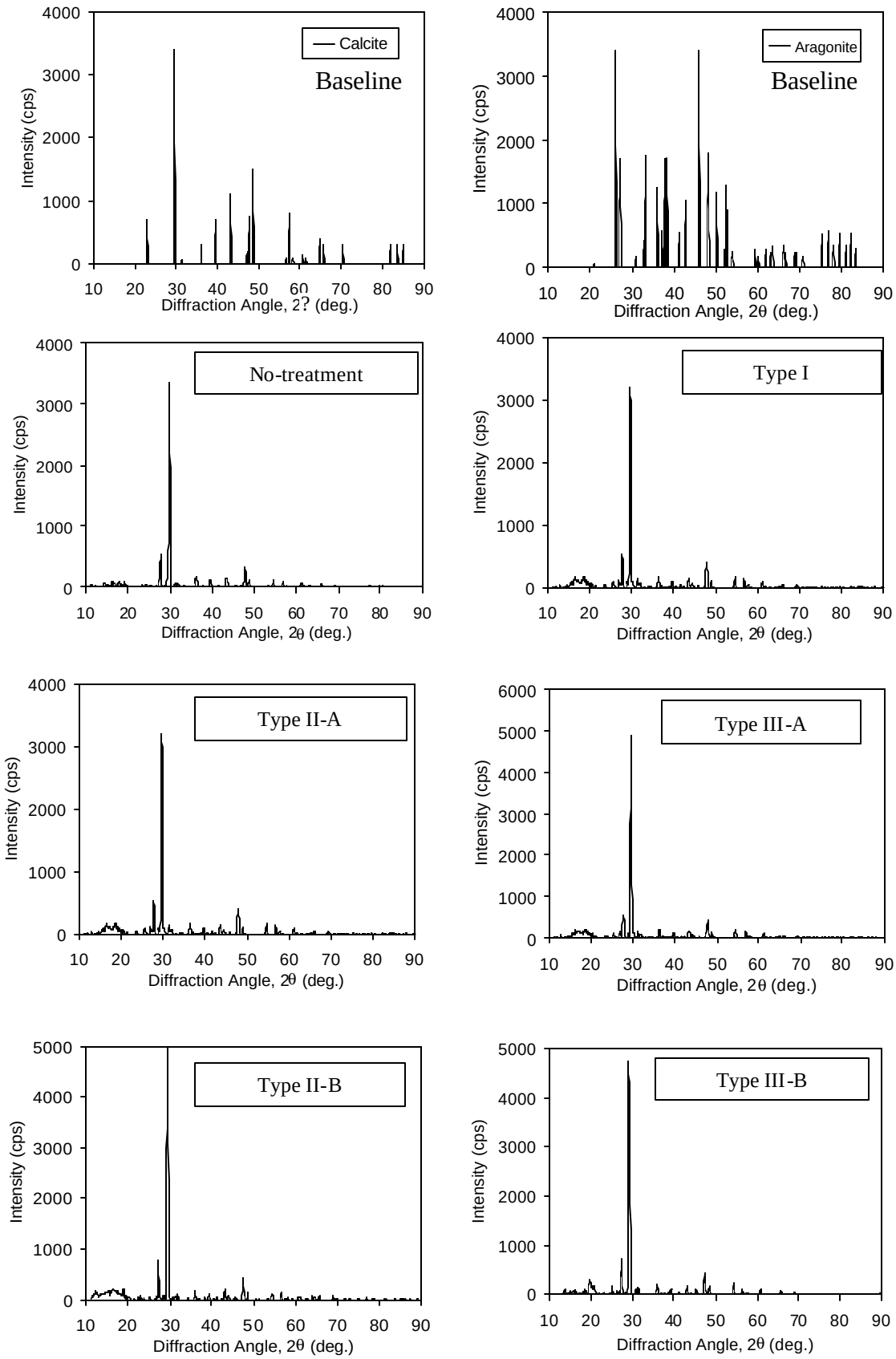

Figure 10. Results of X-ray diffraction measurements of scale deposits

Chapter 6

Effects of Frequency and Strength of a Current Signal of a Solenoid-Coil Device on the Mitigation of Mineral Fouling (Concentric Heat Transfer Test Section)

ABSTRACT

The purpose of the present study was to investigate the effect of physical water treatment (PWT), using a solenoid coil, on the mitigation of mineral fouling in a heat exchanger with cooling-tower water. Fouling tests were conducted in a concentric-tube heat exchanger by varying the strength and the frequency of a current signal used in a solenoid coil for a SCED device. The electric conductivity of the water was 3,000 μS/cm. As the current strength and frequency of the SCED signal increased from 0.7A, 0.5 kHz to 7.0A, 3.5 kHz, the fouling resistance decreased from the baseline data (i.e., no treatment case) by 20% and 53%, respectively, suggesting that a stronger current strength and a greater frequency improve the performance of the PWT using a solenoid coil. To support the experiment result obtained from the fouling test, water drop evaporation tests were conducted with three different water samples to see how the crystallization process of calcium ions was affected by the PWT. As increasing the frequency and strength of current signal, the size of crystal was increased but the number of crystal was reduced tremendously.

INTRODUCTION

Cho et al. studied the feasibility of the SCED to mitigate mineral fouling in various heat exchangers [1-9]. However, the effect of frequency and strength of current signal in the EAF technology on the performance of the technology was not investigated. The purpose of the present study was to investigate the performance of a physical water treatment (PWT) using a solenoid coil in the mitigation of mineral fouling in a heat exchanger in an open-cooling-tower system. In particular, the effect of the strength and frequency of the current signal used in the solenoid induction device on the overall performance of the solenoid coil induction device was investigated.

Therefore, the purpose of the present study was to investigate the effect of physical water treatment (PWT) using a solenoid coil on the mitigation of mineral fouling in a heat exchanger with cooling-tower water by changing the frequency and strength of current signal.

EXPERIMENTAL PROCEDURE

Figure 1 shows a schematic diagram of the present test facility, which consists of a water-circulating loop, an solenoid coil device (SCED), a cooling tower, a pump, a concentric-tube test section, a floating-ball valve for automatic feeding of make-up water.

The main heat-transfer test section was composed of two concentric tubes: the inner one was made of a smooth copper tube, and the outer one was made of an glass tube. The dimension of the inner tube was 6.35 mm × 4.06 mm × 441 mm (O.D. × I.D. × L), whereas the dimension of the outer tube was 25.4 mm × 16.3 mm × 20.3 mm (O.D. × I.D. × L). The two tubes were connected with compression fittings at both ends of the

inner and outer tubes. The cooling water moved inside of the inner tube, whereas hot water moved in the annulus gap between the two tubes (see Fig. 1 for details). The flow directions of the hot and cold water were opposite each other, thus forming a counter-flow heat exchanger.

The flow rate of the cooling water was 0.157×10^{-4} m^3/s (i.e., 0.25 gpm). The corresponding flow velocity in the cooling channel, where fouling occurred, was 1.0 m/s (i.e., 3.3 ft/s) and corresponding Reynolds number was 4,511. During the fouling test, the flow rate was maintained at 0.25 gpm within ± 5%. Since the solenoid coil was installed in a pipe prior to the heat-transfer section, the flow velocity at the SCED was also 1.0 m/s.

Hot water was produced by an electric water heater and circulated at a flow rate of 6.309×10^{-5} m^3/s (i.e., 1.0 gpm). The water heater had a heating element of 4.2 kW, and its temperature was controlled using a thermostat (Omega Engineering, Inc). The heat flux used in the study was about 10.1×10^4 W/m^2 (i.e., 32,041 $Btu/hr \cdot ft^2$). Note that the majority of water chillers manufactured today are designed to operate with a full-load condenser heat flux in the range of 1.89×10^4 to 3.15×10^4 W/m^2 (i.e., 6,000 to 10,000 $Btu/hr \cdot ft^2$). In the present study, a much higher heat flux of 10.1×10^4 W/m^2 was used to accelerate the fouling so that each test could be completed in two weeks.

To calculate the fouling resistance, temperatures were measured at four different positions: cooling-water inlet and outlet, and hot-water inlet and outlet, see Fig. 1. The cooling water entered the test section at $20 \pm 0.5°C$ and heated to $31 \pm 0.5°C$, whereas the hot water entered the test section at $91 \pm 0.5°C$ and cooled to $87 \pm 0.5°C$ initially but due to the fouling of heat exchanger surface the exit temperature of cooling water was

decreased 28.5± 0.5°C at the end of test which was dependent on each case. (see details at Appendix C)

After the cooling water flowed past the heat-transfer test section, it was sent to the cooling tower, where the water was cooled by evaporation. In order to maintain a constant volume of water in the system, the tap water was added as make-up water, a procedure that was controlled by an automatic floating-valve system. Table 1 shows water quality data of the tap water provided by the City of Philadelphia (Bureau of Laboratory Service). Since the water quality varied with time, the minimum, maximum and average values are given.

Figure 2 shows a sketch of an electronic anti-fouling system using a solenoid coil, and a method to measure the induced electric field inside a tube. As shown in Fig. 2(a), a solenoid coil was wrapped over a plastic tube with an outside diameter of 50.8 mm. 14-gage wire was wound with 80-turns. Two ends of the solenoid coil were connected with a control unit. The copper tube was located at the off-centered to a solenoid coil since the strength of the induced electric field had a maximum value at the surface of the coil and a minimum value at the center of the coil. Figure 2(a) also shows a schematic diagram of a test setup with a circular pickup-wire probe to measure the induced electric field inside a copper tube.

Figure 2(b) represents the four induced electric field signal waves that were made by a solenoid coil control unit. In the present study, two different frequency and strength of current signal (i.e., 0.7A-0.5kHz, 0.7A-3.5kHz, 7.0A-0.5kHz, and 7.0A-3.5kHz) of control unit were used. The control unit was adjusted to produce a variable pulsing current signal. Subsequently, an induced pulsating electric field was generated inside the

pipe by Faraday's law [10]. Excess mineral ions such as calcium and magnesium precipitate into mineral salts, which then become seed crystals and assist the mitigation of fouling in a heat exchanger. Details of the operating principle of the SCED can be found elsewhere [1-9].

Figure 3 shows test procedure and variations of electric conductivities vs. time for a no-treatment case and the cases with the PWT. Before starting each test, the water sample was prepared by circulating tap water through the cooling tower so that the desired electric conductivity (3,000 μS/cm) was obtained (see Fig. 3). Once the circulating water reached the desired conductivity, the fouling test began with hot water in the hot water channel. Sample water was taken from the reservoir tank which was placed beneath the cooling tower during the heat transfer experiment without stopping the test system. Each water analysis was performed at least twice to increase the accuracy and also measured at Commercial Water Treater Company. At the end of the test for the no-treatment case, the cooling-tower water was continuously circulated with the PWT but without heat transfer for one day (i.e., see the period between a3 and a4). After one-day pretreatment, a brand new copper tube was installed in the heat transfer test section, and the fouling test began. The no-treatment case was repeated twice for the accuracy of the overall test procedure. The error for the fouling resistance was within ± 5% for the case.

The second test (see the period marked by a4 and a5 in Fig. 2) was carried out by treating the cooling water with the SCED having a current signal of 0.7A and 0.5 kHz before the cooling water entered the test section.

The third test (see the period marked by a6 and a7 in Fig.2) was performed by treating the cooling water with the SCED, where the frequency of the current signal

increased from 0.5 to 3.5 kHz in the same electric current strength of 0.7A. In the forth test (see the period marked by a8 and a9 in Fig.2), the strength of current signal was increased from 0.7 to 7.0A, but the frequency maintained as 0.5 kHz. The fifth test (see the period marked by a10 and a11 in Fig.2) was performed with a current signal of 7.0A and 3.5 kHz. Each test was performed with a brand new smooth copper tube in the main heat-transfer test section.

During the fouling test with heat exchanger, water drop evaporation experiment was conducted to investigate the effect of induced electric field in the bulk water.

Figure 4 shows the schematic diagram of water drop evaporation experiment which composed of a microscope (Edmund Scientific Co.), a CCD camera (Sony-IRIS), a VCR (Panasonic), and a computer system with Snappy software. In each different case, water was sampled with micropipette and placed on precleaned glass slides in the mass of and allowed to evaporate. The development of the forming crystals of the mineral content of the water was observed microscopically through a microscope and a CCD camera. Whole solidification processes were recorded photographically with VCR and then each step of process was captured with Snappy software as figure file.

The fouling resistance is often calculated using the following equation:

$$R_f = \frac{1}{U_f} - \frac{1}{U_i} \tag{1}$$

where U_f is an overall heat transfer coefficient from a heat exchanger experiencing fouling, and U_i is the overall heat transfer coefficient from a clean heat exchanger. Both overall heat transfer coefficients were calculated from the following equation:

$$U = \frac{\dot{Q}}{A\Delta T_{lm}} \tag{2}$$

where ΔT_{lm} is a log-mean-temperature difference, which can be described as

$$\Delta T_{lm} = \frac{(T_{h,i} - T_{c,o}) - (T_{h,o} - T_{c,i})}{\ln\left[\frac{(T_{h,i} - T_{c,o})}{(T_{h,o} - T_{c,i})}\right]} \tag{3}$$

The heat transfer rate, $\dot{Q}$, was estimated from both the heating and cooling channels as

$$\dot{Q} = [\dot{m}c_p(T_i - T_o)]_h = [\dot{m}c_p(T_o - T_i)]_c \tag{4}$$

The heat transfer rate estimated from the hot-water side, $\dot{Q}_h$, was consistently bigger by 6% than that of the cooling-water side, $\dot{Q}_c$, a phenomenon which may be attributed to the heat loss to the surroundings via the acrylic tube. The heat transfer rate in the cooling-water side, $\dot{Q}_c$, was used to calculate the overall heat transfer coefficient in the study.

RESULTS AND DISCUSSION

Table 2 shows the water analysis data for the make-up and unfiltered circulating cooling-tower water for both the no-treatment and PWT treatment cases. The property data of the make-up water were in good agreement with the water analysis results provided by the City of Philadelphia given in Table 1. The moments when water samples were taken from the circulating water were marked by a_i, where i varies form 1 to 11 (see Figure 3). Note that water sample data indicated in Table 2 are the average value of start and end points for each case. The maximum difference between these two points was 2%, actually between 2950 to 3000 μS/cm. There was no big difference in water qualities between the no-treatment case and the case with PWT. The Langelier saturation index (LSI) was calculated to examine the precipitation tendency of the circulating water.

The values of the LSI were in the range of 2.70 to 2.80, indicating that the circulating water had a condition to cause severe mineral fouling.

The water chemistry results shown in Table 2 indicate that no scale is forming because the ratio of calcium ions between the circulating water and the make-up water is similar to those of conductivity, chlorine, etc.. Perhaps the reason that the bulk analysis does not shows a reduction in calcium is due to the present experimental setup. By having a very high heat flux and a very high temperature at the surface of the heat exchanger, the system is strongly driven to precipitate only at the heat exchanger surface. The rest of the system, though supersaturated, is not forming precipitation. The absolute quantity of the precipitate then is very small, not enough to show in the bulk analysis. Even the amount of precipitate on the heat exchanger surface might be relatively very small compared to the amount of total dissolved mineral ions in circulating water. Therefore, water analysis might not show the scale deposition. Another reason could be that the tower contains calcium precipitate on the fill. This precipitate acts as an additional source of calcium to compensate for what is lost.

Table 3 shows the water analysis data for the make-up and filtered circulating water with 0.2 μm filter. There was no big difference in the water analyses between Tables 2 and 3. These results could be explained as follows: for the no-treatment case, most mineral ions existed in the form of dissolved ions, therefore, filtration would not affect water analysis. On the other hand, for the PWT case, even though colloidal particles were made by the PWT in the bulk cooling water, these particles were still very small and could pass through the filter pores, resulting in almost identical results of the water analyses. Table 4 shows the result of water analysis which was performed by

Commercial Water Treater with same water samples. There was no big difference between Table 2,3 and 4 nothing but maximum 7%. This difference seems to be caused by the difference of measuring method (i.e., Drexel – titration method, Commercial Water Treater – light scattering method).

Figure 5 represents fouling resistance values vs. time for all five cases. In the case of the current strength of 7.0A and frequency of 3.5 kHz, the fouling resistance calculated at the end of 200-hr tests for the PWT case decreased by 53% from the value of the no-treatment case, whereas for the case of the current strength of 7.0A and frequency of 0.5 kHz, the fouling resistance decreased by 33%. Thus, one can summarize that as the frequency of the current signal increases in the SCED, the chance for mineral ions to collide in cooling-tower water also increases. In other words, the more mineral ions would precipitate in the bulk water for the higher frequency case. Furthermore, the effectiveness of the SCED increased by increasing ~~of~~ current strength from 0.7 to 7.0A because the current strength directly affects the strength of an induced electric field. Subsequently, the above-mentioned collisions among dissolved mineral ions increase, thus producing more seed crystals and making the PWT more effective.

Figure 6 shows the photographs of the result of water-drop-evaporation experiment with three different water samples of an electric conductivity of approximately 3,000 μS/cm (i.e., no-treatment, SCED-0.7A, 0.5kHz, and SCED-7.0A, 3.5kHz). The micrographs show a part of the perimeter of a drop because almost all the solidification of the minerals takes place at or close to the outer rim of the drops. This is caused by a vigorous radial convection inside the evaporating drop which transports the heavier minerals towards the drop perimeter [11]. For the no treatment case, no crystal

was found in the water drop for the first 30 minutes. At 45 minutes, plenty of tiny particles were found around the boundary of water drop. Until 55 minutes passed from t = 45 minutes, more crystals were made but the size of each crystal was not much changed. Otherwise, SCED cases had much less crystal at the same time duration but much bigger size and crystal growth could be seen clearly.

In the no-treatment case, as the drop evaporated the mineral concentration in solution became supersaturated to a point where homogeneous nucleation took place. This homogeneous nucleation resulted in the sudden appearance of a large number of small crystals. This explains why we did not have any crystals at t = 30 minutes and had suddenly a large number of crystals at t = 45 minutes for the untreated case. With the PWT, as heterogeneous precipitation occurred at a tower level of supersaturation, crystals appeared after only 30 minutes in the treated water. Since minerals were being crystallized, the liquid never becomes saturated enough to form homogeneous nucleation sites, and all growth occurs only on or near the original crystals as indicated by the photographs in Fig. 6.

In Fig. 7, two photographs at the final stage were illustrated for no-treatment and SCED-7.0A, 3.5kHz cases for water samples of an electric conductivity of approximately 3,000 μS/cm. Both cases have similar giant crystal band around perimeter of water drop. No treatment case shows lots of tiny crystal particles, the average size of each crystal is 10-15 μm, except this crystal band. Whereas in case of SCED-7.0A, 3.5kHz, one huge crystal was covered the whole surface of water drop. Several big air pockets were placed on this huge crystal.

This result could be explained as follows: no-treatment case diffusion of ions would be the dominant mechanism of crystallization. But those mineral ions in cooling water by passing through the induced electric field would be precipitated as the form of colloid particles. Therefore, the size of crystal which is treated by SCED is much bigger than that of no treatment case. With this phenomenon, the theory of bulk precipitation could be supported much clearly.

CONCLUSIONS

The purpose of the present study was to investigate the effect of physical water treatment (PWT) using a solenoid coil on the prevention of fouling in a heat exchanger with cooling-tower water. Fouling tests were conducted in a concentric-tube heat exchanger by varying the strength and frequency of a current signal used in a solenoid coil (SCED) system. Flow velocities at the heat exchanger and a solenoid coil were fixed at 1.0 m/s. The electric conductivity of the water was 3,000 μS/cm. As the strength and frequency of the current signal increased from 0.7A, 0.5 kHz to 7.0A, 3.5 kHz, the efficiency of the physical water treatment (as measured by the reduction in the fouling resistance relative to the no-treatment case) increased from 20 to 53%.

To support the fouling experiment result, water drop evaporation tests were conducted with three different water samples. As increasing the frequency and strength of current signal, the size of crystal was increased but the number of crystal was reduced tremendously.

References

[1] Y. I. Cho and R. Liu, Control of Fouling in a Spirally-Ribbed Water Chilled Tube with Electronic Anti-Fouling Technology, International Journal of Heat and Mass Transfer, Vol. 42, pp.3037-3046, 1999.

[2] Y.I. Cho, C. Fan and B.G. Choi, Theory of Electronic DescalingTechnology of Control Precipitation Fouling in Heat Exchangers, Int. Comm. Heat Mass Transfer, Vol.24, 747-756, 1997.

[3] C. Fan and Y.I. Cho, Microscopic observation of calcium carbonate crystallization induced by an electronic descaling technology, Int. Comm. Heat Mass Transfer, Vol.24, 757-770, 1997.

[4] Y. I. Cho, C. Fan and B.G. Choi, Use of Electronic Anti-Fouling Technology with Filtration to Prevent Fouling in a Heat Exchanger, Int. J. Heat Mass Transfer, Vol.41, pp.2961-2966, 1998.

[5] Y. I. Cho and B.G. Choi, Effect of Fouling on Temperature Measurement Error and a Solution, Journal of Heat Transfer, Vol.120, pp.525-528, 1998.

[6] Y. I. Cho and B.G. Choi, Validation of an Electronic Anti-Fouling Technology in a Single-Tube Heat Exchanger, International Journal of Heat and Mass Transfer, Vol.42, pp.1491-1499, 1999.

[7] C. Fan, A Study of Electronic Descaling Technology to Control Precipitation Fouling, Ph.D. Thesis, Drexel University, 1997

[8] B.G. Choi, A Study of Fouling Control in Heat Exchangers with Electronic Anti-Fouling Technology, Ph.D. Thesis, Drexel University, 1998

[9] R. Liu, Study of Scale Removal and Prevention in Heat Exchangers with Electronic Anti-Fouling Technology, Ph.D. Thesis, Drexel University, 1999

[10] R.A. Serway, Physics for Scientists and Engineers (3rd Edition). Saunders College Publishing, Philadelphia, PA (1990) 874-891

[11] Kronenberg K.J., Experimental evidence for effects of magnetic fields on moving water, IEEE Transactions on magnetics, MAG-21 (1985) 2059-2061

Philadelphia tap water			
	Minimum	Average	Maximum
Conductivity (μS/cm)	389	520	652
pH	7.3	7.5	7.6
Total hardness (mg/L)	150	190	247
Alkalinity (mg/L)	54	74	93
Chloride (mg/L)	56	75	149
Sulfate (mg/L)	37	61	89
Silica (mg/L)	3	5.8	7.8
Phosphate (mg/L)	0.2	0.25	0.3

Table 1. Water quality data of make-up water provided by the City of Philadelphia

	Make-up Water	Circulating water (Unfiltered)				
		No treatment	SCED 0.7A, 0.5kHz	SCED 0.7A 3.5kHz	SCED 7.0A 0.5kHz	SCED 7.0A 3.5kHz
Conductivity (μS/cm)	600	2990 (5.0)	2970 (5.0)	2980 (5.0)	2990 (5.0)	2990 (5.0)
pH	7.5	8.4	8.3	8.4	8.4	8.4
Total hardness (mg/L)	220	1190 (5.4)	1175 (5.4)	1184 (5.4)	1190 (5.4)	1184 (5.4)
Ca^{+} hardness (mg/L)	150	760 (5.1)	760 (5.1)	720 (5.1)	750 (5.1)	720 (5.1)
Total alkalinity (mg/L)	85	308 (3.7)	316 (3.7)	319 (3.7)	322 (3.7)	321 (3.7)
Chloride (mg/L)	97	636 (6.6)	644 (6.6)	641 (6.6)	635 (6.6)	640 (6.6)
LSI**	0.23	2.79	2.70	2.78	2.80	2.79
R_f (m^2K/W) ***		$4.5x10^{-4}$	$3.5x10^{-4}$	$3.0x10^{-4}$	$3.0x10^{-4}$	$2.2x10^{-4}$

* ( ) represents the ratio of each treatment to the make-up water
** LSI = Langelier Saturation Index (T = 38° C)
*** R_f = Fouling resistance at the end of 200-hour test

Table 2. Water quality data measured for make-up and circulating water

	Make-up Water	Circulating water (Filtered)				
		No treatment	SCED 0.7A, 0.5kHz	SCED 0.7A 3.5kHz	SCED 7.0A 0.5kHz	SCED 7.0A 3.5kHz
Conductivity (μS/cm)	600	2990 (5.0)	2970 (5.0)	2980 (5.0)	2980 (5.0)	2980 (5.0)
pH	7.5	8.4	8.3	8.4	8.4	8.4
Total hardness (mg/L)	220	1190 (5.4)	1175 (5.4)	1184 (5.4)	1188 (5.4)	1176 (5.4)
Ca^{+} hardness (mg/L)	150	760 (5.1)	760 (5.1)	720 (5.1)	740 (5.1)	712 (5.1)
Total alkalinity (mg/L)	85	308 (3.7)	316 (3.7)	319 (3.7)	322 (3.7)	321 (3.7)
Chloride (mg/L)	97	636 (6.6)	644 (6.6)	641 (6.6)	635 (6.6)	640 (6.6)
LSI**	0.23	2.79	2.70	2.78	2.80	2.79
R_f (m^2K/W) ***		$4.5x10^{-4}$	$3.5x10^{-4}$	$3.0x10^{-4}$	$3.0x10^{-4}$	$2.2x10^{-4}$

∗ ( ) represents the ratio of each treatment to the make-up water
** LSI = Langelier Saturation Index (T = 38°C)
*** R_f = Fouling resistance at the end of 200-hour test

Table 3. Water quality data measured for make-up and circulating water with filtration

	Makeup	Unfiltered Tower SCED 7.0A 3.5kHz	Calc' d Cycles per Unfilt' d Twr	Filtered Tower SCED 7.0A 3.5kHz
pH	7.5	8.2		8.5
Sp Cond @ 25C, µmhos	567	2880	4.5	2860
Alk, "P" as CaCO3, ppm	0	0		14.4
Alk, "M" as CaCO3, ppm	58	285	4.0	287
Sulfur, as SO4, ppm	46	361	4.5	356
Chloride, as Cl, ppm	73	569	5.6	569
Hardness, Total, as CaCO3, ppm	158	1080	5.4	1070
Calcium, Total, as CaCO3, ppm	108	684	5.4	675
Magnesium, Total, as CaCO3, ppm	49	397	5.5	392
Copper, Total, as Cu, ppm	<0.05	0.18		0.18
Iron, Total, as Fe, ppm	<0.05	<0.05		<0.05
Sodium, as Na, ppm	34	213	4.3	213
PO4, Total Inorg, as PO4, ppm	1.2			
PO4, Ortho, as PO4	1.2	2.1		2.0
Silica, Total, as SiO2, ppm	4.8	29	4.3	29

Table 4. Water quality data for make-up and tower water of SCED-7.0A, 3.5kHz

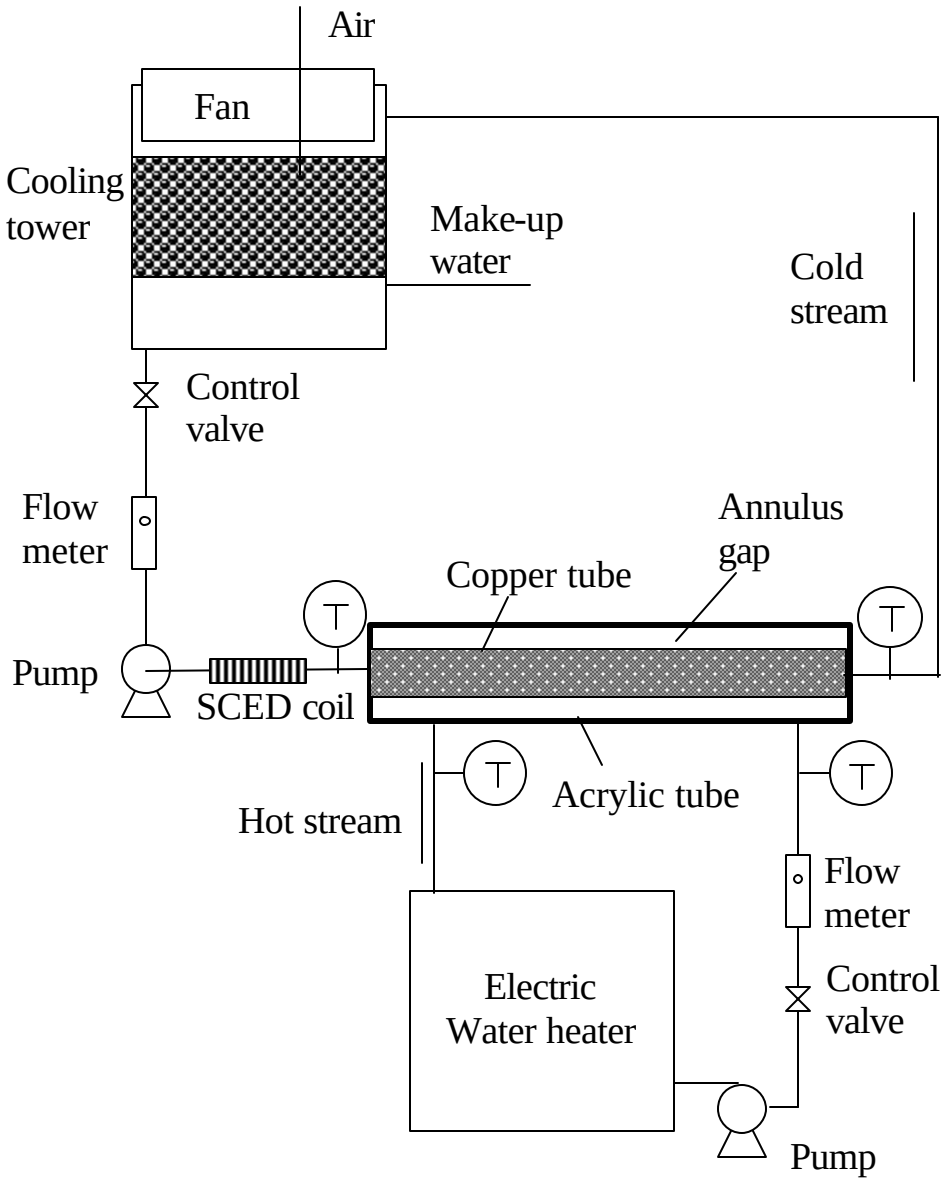

Fig. 1 Schematic diagram of the test facility and a view of counter-flow heat-transfer test section

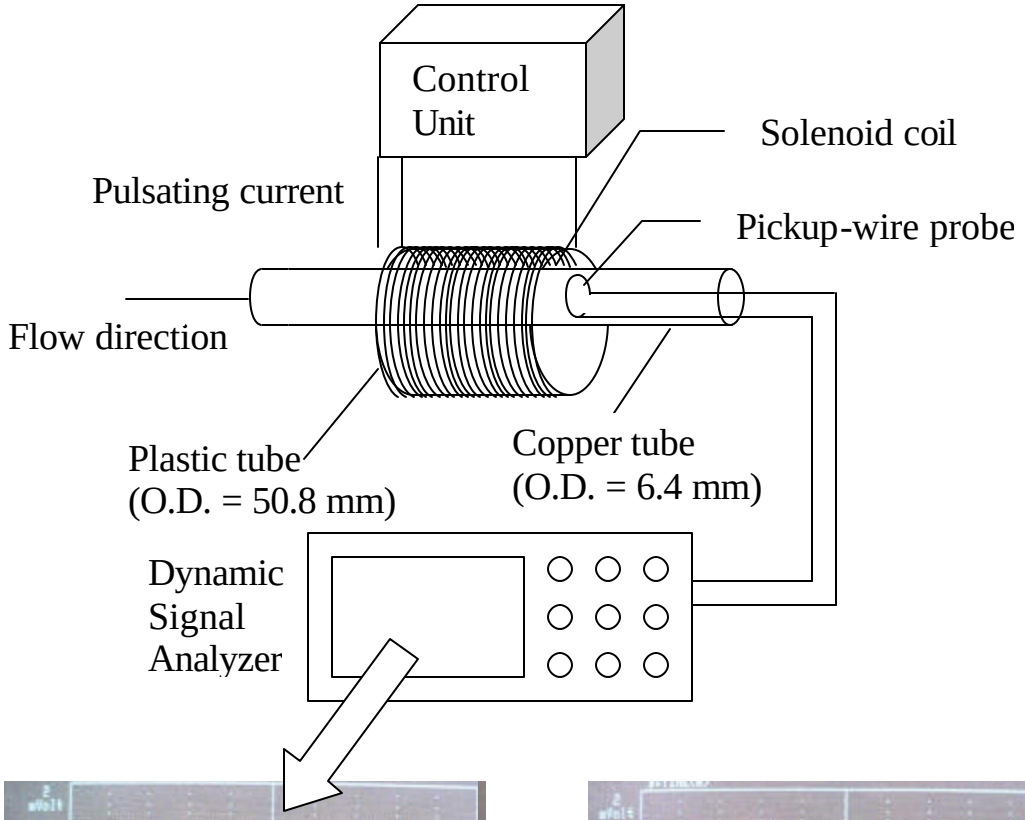

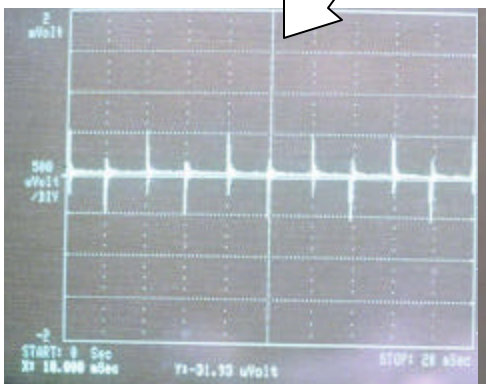

(a) SCED-0.7A, 0.5 kHz

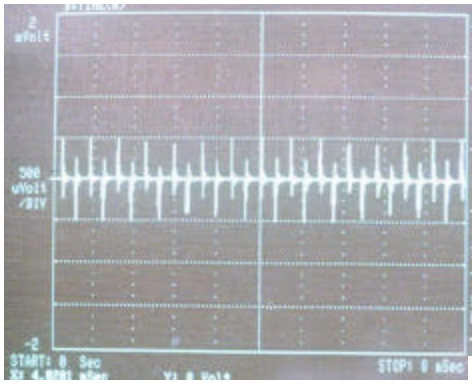

(b) SCED-0.7A, 3.5 kHz

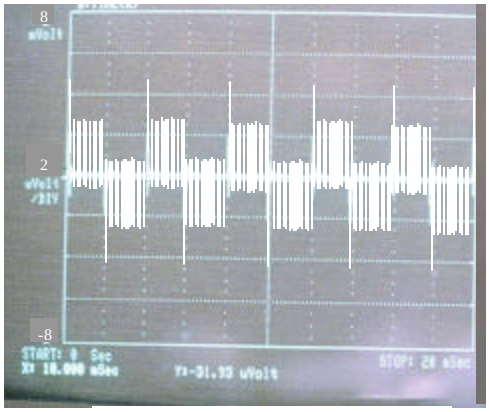

(c) SCED-7.0A, 0.5 kHz

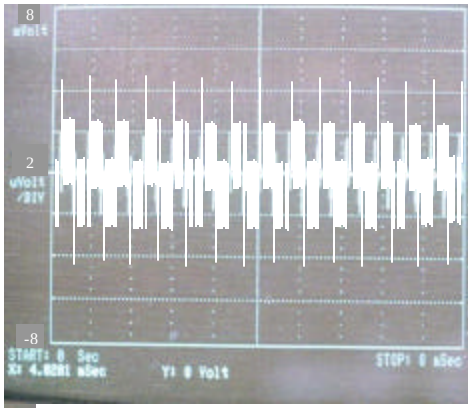

(d) SCED-7.0A, 3.5 kHz

Fig. 2 Composition of SCED system and results of induced electric field

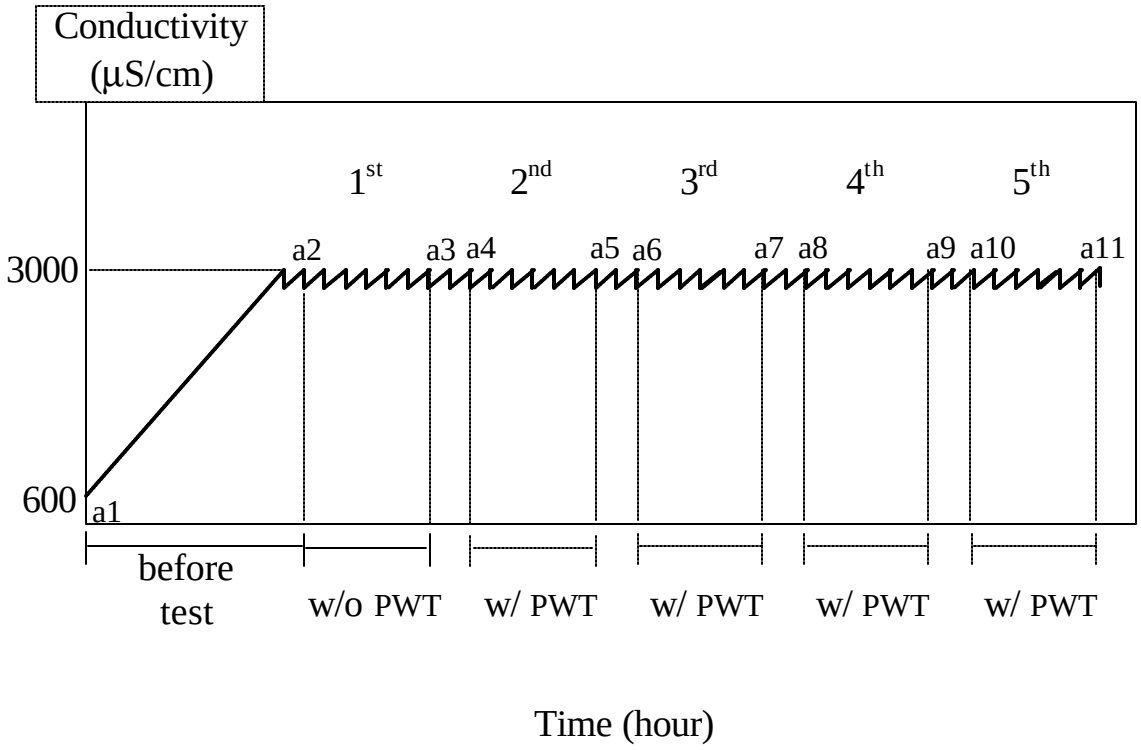

Fig. 3 Variations of the electric conductivity of circulating water

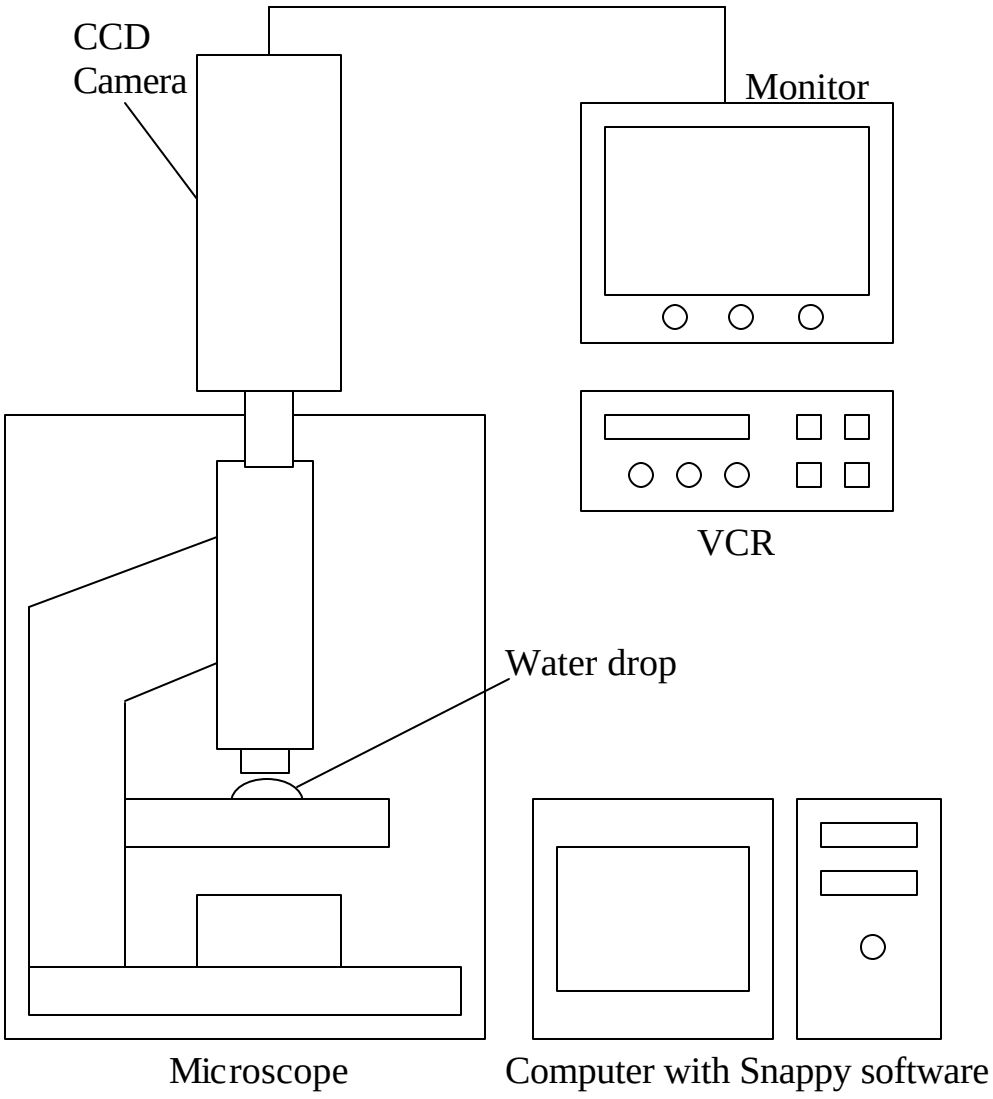

Fig. 4 Schematic diagram of water evaporation experiment system

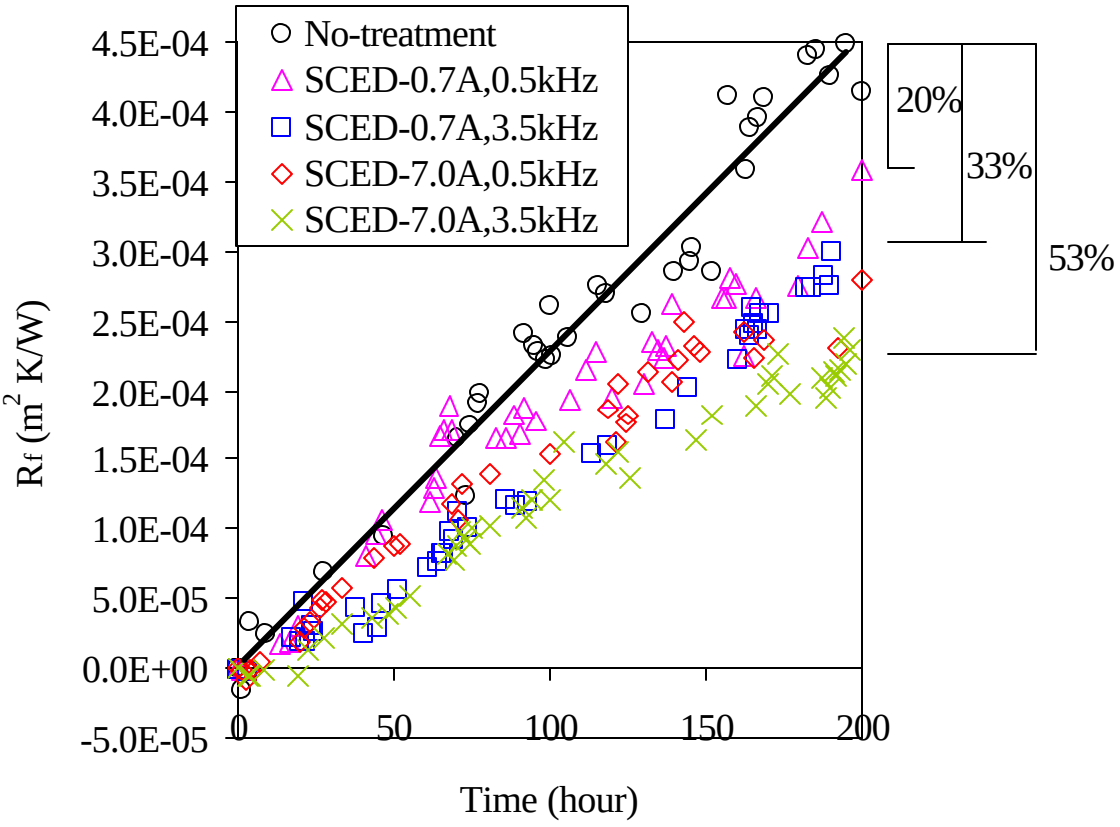

Fig. 5 Changes in fouling resistance vs. time

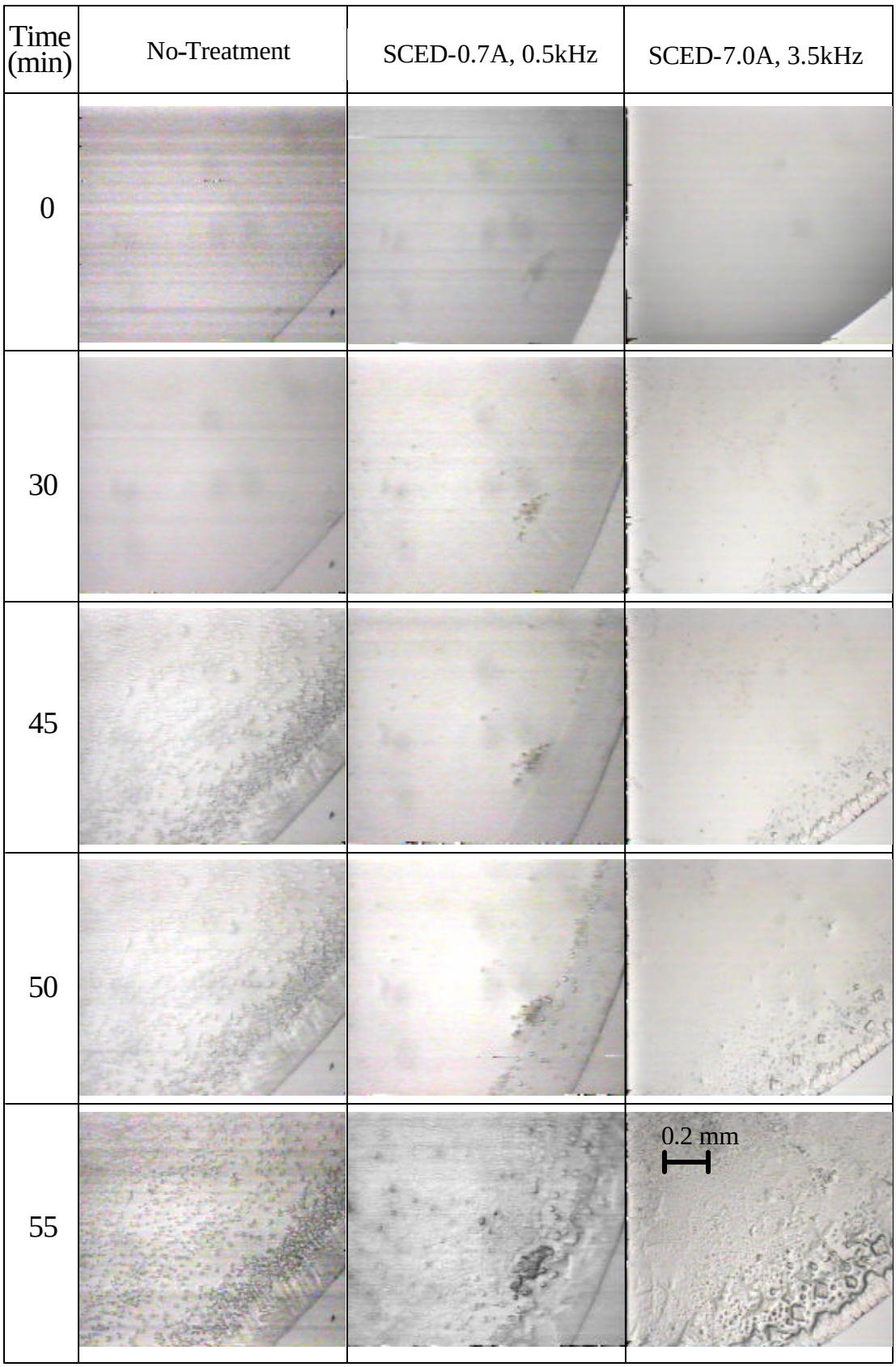

Fig. 6 Photographs of result of water drop evaporation experiment as time sequence

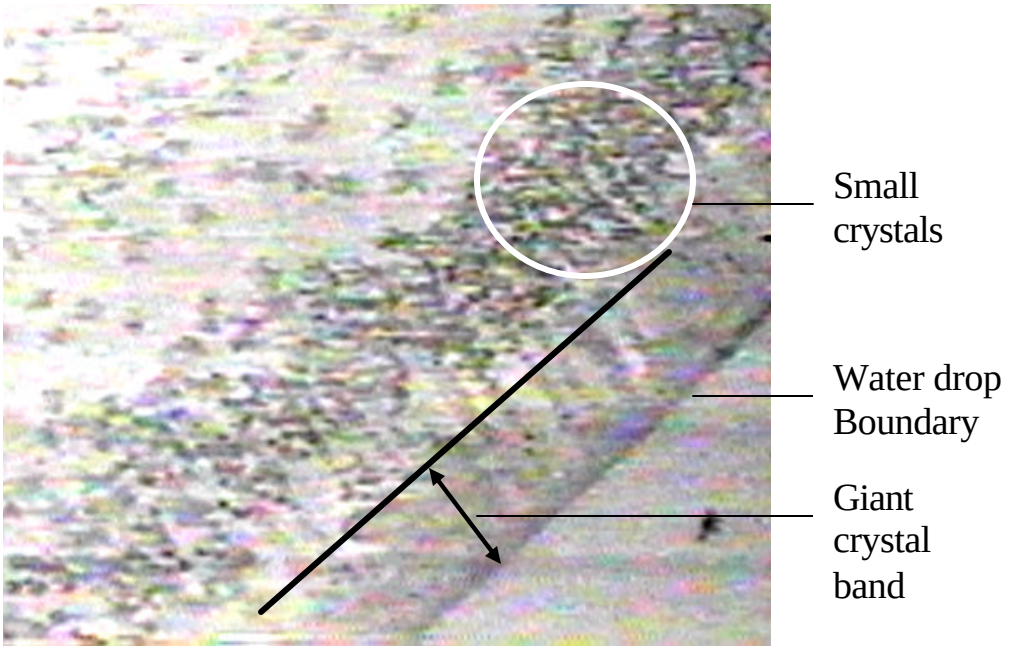

(a) No-treatment

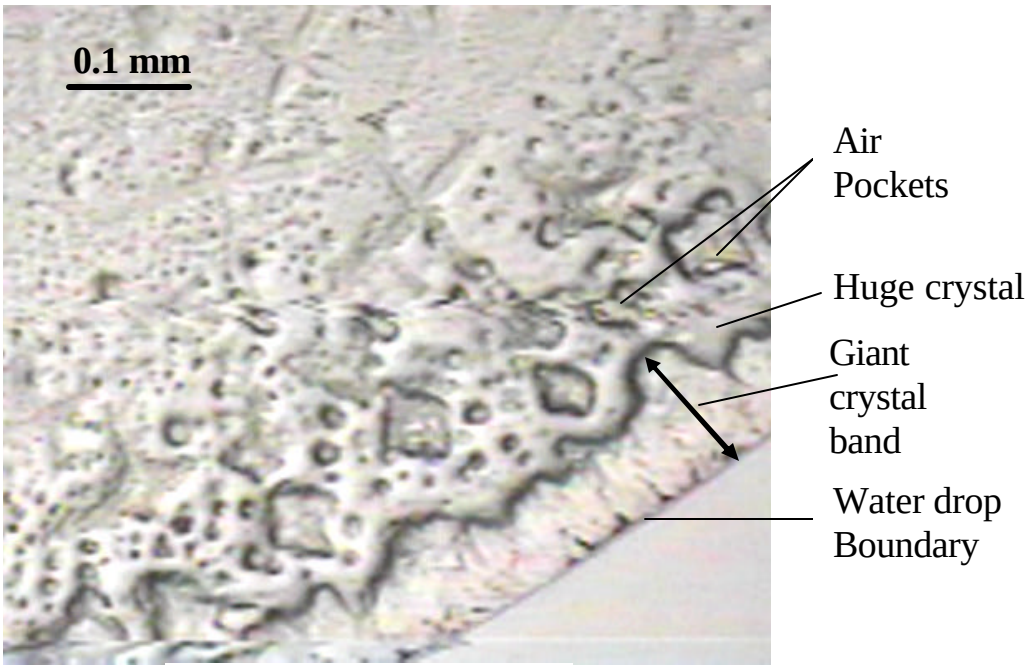

(b) SCED-7.0A, 3.5kHz

Fig. 7 Photographs of result of water drop evaporation experiment for cases of no-treatment and SCED-7.0A, 3.5kHz

Appendix A Calculation of Cycles of Concentration (COC)

Blowdown is defined as the amount of water discharged from the system to control the concentration of salts or other impurities in the circulating water [Cheremisinoff 1989]. In order to maintain an appropriate degree of concentration for a desired system operation, blowdown is needed. The COC is defined as the ratio of the dissolved solids in the cooling tower water to the dissolved solids in the makeup supply water. Automatic controls for operating cooling towers determine the cycle of concentration based on the conductivity of the circulating water but measure should be checked based on the mass balance between the make-up and discharged waters. A simple material balance can be expressed as:

$$M = E+D+B \qquad (c.1)$$

where M = total makeup water supplied into cooling tower

E = total evaporative water

D = total drift water loss

B = total blowdown water

To predict the amount of evaporated water, a latent heat due to evaporation is introduced. The evaporation of 1 lb of water requires 970 Btu. A total heat gained in a heat exchanger is equal to the amount of heat rejected to the atmosphere due to evaporation.

Note that the concentration of mineral ions in blowdown and loss equals that in the circulating water. The cycle of concentration (COC) is defined as:

$$COC = \frac{X_c}{X_m} \qquad \text{(c.2)}$$

where X_c is the mineral-ion concentration in the circulating water and X_m is the mineral-ion concentration in the makeup water.

Assuming that there is no loss of chemicals through precipitation, the ion balance is given by:

$$MX_m = BX_c + DX_c \qquad \text{(c.3)}$$

Thus, the COC is obtained in terms of mass balance as follows:

$$COC = \frac{M}{B + D} \qquad \text{(c.4)}$$

The following pages detail the calculation of COC, based on material balance, for the various experiments described in this thesis.

(1) The case without SCI treatment

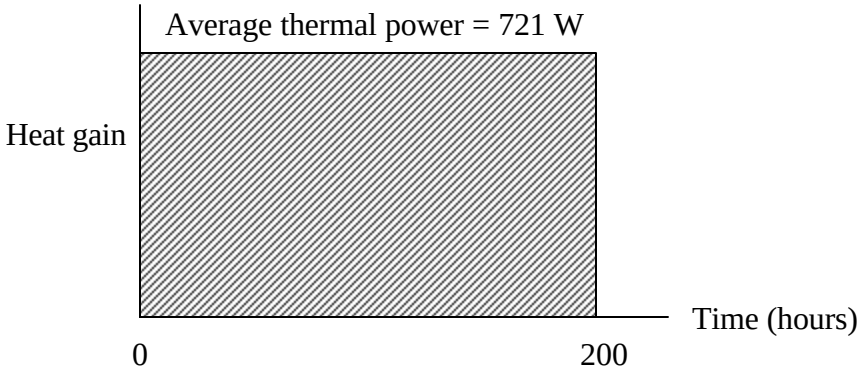

Total heat gain (Q) = (200 hrs) × (0.721 kW) × (3413 Btu/kW-hr) = 492154.6 Btu

Total evaporation mass (EM) = (492154.6 Btu) / (970 Btu/lb) = 507.4 lb

Total evaporation volume (E) = (507.4 lb) × (0.016 ft^3/lb) × (7.48 gal/ft^3) = 60.7 gallons

Total make-up water volume supplied (M) = 72 gallons

Total blowdown volume (B) = 7 gallons

Total drift losses (D) = M – E – B = 72 – 60.7 – 7 = 4.3 gallons

Therefore, the COC based on material balance is :

$$Cycles = \frac{M}{B + D} = \frac{72}{7 + 4.3} = 6.4$$

(2) The case with SCI treatment (0.7A, 0.5 kHz)

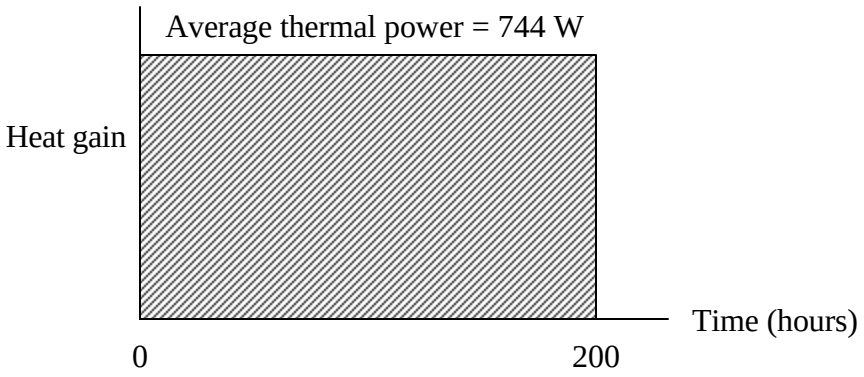

Total heat gain (Q) = (200 hrs) × (0.744 kW) × (3413 Btu/kW-hr) = 507854.4 Btu

Total evaporation mass (EM) = (507854.4 Btu) / (970 Btu/lb) = 523.6 lb

Total evaporation volume (E) = (523.6 lb) × (0.016 ft^3/lb) × (7.48 gal/ft^3) = 62.7 gallons

Total make-up water volume supplied (M) = 74 gallons

Total blowdown volume (B) = 8 gallons

Total drift losses (D) = M – E – B = 74 – 62.7 – 8 = 3.3 gallons

Therefore, the COC based on material balance is :

$$Cycles = \frac{M}{B + D} = \frac{74}{8 + 3.3} = 6.5$$

(3) The case with SCI treatment (0.7A, 3.5 kHz)

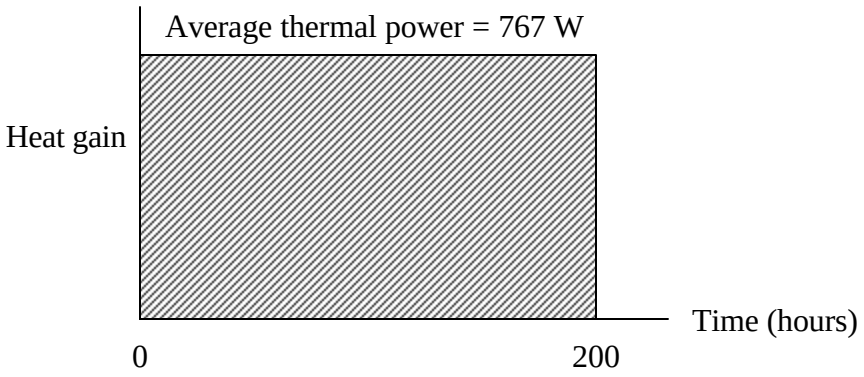

Total heat gain (Q) = (200 hrs) × (0.767 kW) × (3413 Btu/kW-hr) = 523554.2 Btu

Total evaporation mass (EM) = (523554.2 Btu) / (970 Btu/lb) = 539.7 lb

Total evaporation volume (E) = (539.7 lb) × (0.016 ft^3/lb) × (7.48 gal/ft^3) = 64.6 gallons

Total make-up water volume supplied (M) = 76 gallons

Total blowdown volume (B) = 9 gallons

Total drift losses (D) = M – E – B = 76 – 64.6 – 9 = 2.4 gallons

Therefore, the COC based on material balance is :

$$Cycles = \frac{M}{B + D} = \frac{76}{9 + 2.4} = 6.7$$

(4) The case with SCI treatment (7.0A, 0.5 kHz)

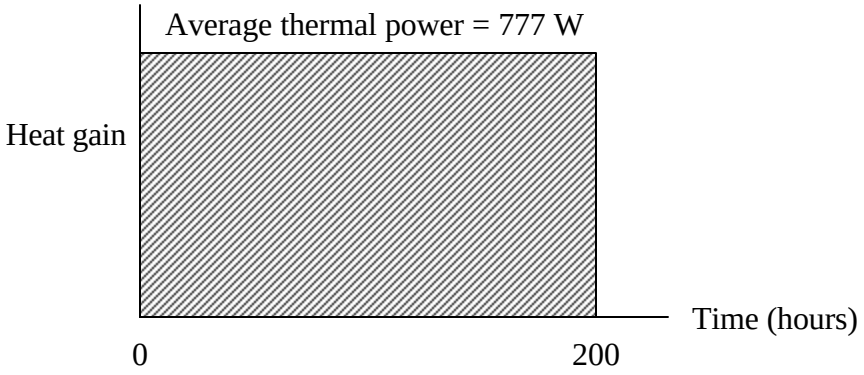

Total heat gain (Q) = (200 hrs) × (0.777 kW) × (3413 Btu/kW-hr) = 530380.2 Btu

Total evaporation mass (EM) = (530380.2Btu) / (970 Btu/lb) = 546.7 lb

Total evaporation volume (E) = (546.7 lb) × (0.016 ft^3/lb) × (7.48 gal/ft^3) = 65.4 gallons

Total make-up water volume supplied (M) = 77 gallons

Total blowdown volume (B) = 9 gallons

Total drift losses (D) = M – E – B = 77 – 65.4 – 9 = 2.6 gallons

Therefore, the COC based on material balance is :

$$Cycles = \frac{M}{B + D} = \frac{77}{9 + 2.6} = 6.6$$

(5) The case with SCI treatment (7.0A, 3.5 kHz)

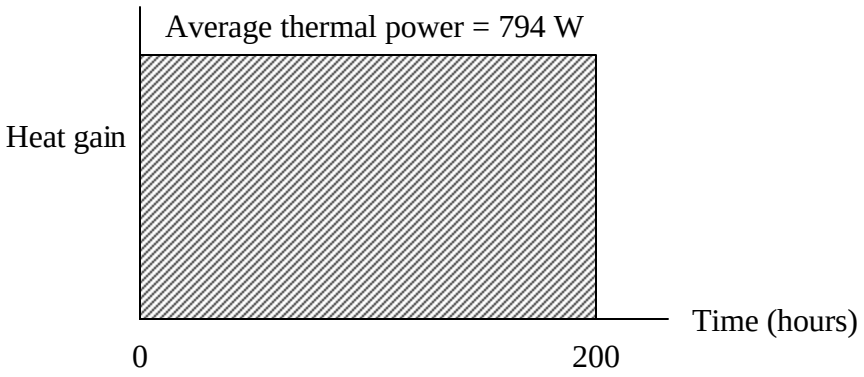

Total heat gain (Q) = (200 hrs) × (0.794 kW) × (3413 Btu/kW-hr) = 541984.4 Btu

Total evaporation mass (EM) = (541984.4 Btu) / (970 Btu/lb) = 558.7 lb

Total evaporation volume (E) = (558.7 lb) × (0.016 ft^3/lb) × (7.48 gal/ft^3) = 66.9 gallons

Total make-up water volume supplied (M) = 79 gallons

Total blowdown volume (B) = 10 gallons

Total drift losses (D) = M – E – B = 79 – 66.9 – 10 = 2.1 gallons

Therefore, the COC based on material balance is :

$$Cycles = \frac{M}{B + D} = \frac{79}{10 + 2.1} = 6.5$$

Appendix B Uncertainty Analysis

(1) For Concentric-tube Heat Transfer Experiment

The uncertainty analysis developed by Kline and McClintock [Kline,1953] was performed. The method is based on the uncertainties in various experimental measurements, which are dimension, flow rate, temperature, initial heat transfer coefficient. The estimation of the uncertainty in calculated results depends on the accuracy of the measurements. The result R is given as a function of independent variables x1, x2, ..., xn. Thus,

R = R(x1, x2...., xn)

Let w_r be the uncertainty in the result and w1, w2, ..., wn be the uncertainties in the independent variables. The calculated uncertainty is expressed as:

$$w_r = \left[\left(\frac{\partial R}{\partial x1} w1 \right)^2 + \left(\frac{\partial R}{\partial x2} w2 \right)^2 + ... + \left(\frac{\partial R}{\partial xn} wn \right)^2 \right]^{0.5}$$

At first, the uncertainty analyses were carried out for heat transfer rate and heat transfer surface area, and then using these results the uncertainty analyses were done for the overall heat transfer coefficient and fouling resistance under the following basic uncertainties and reference values:

heat exchanger length (m) L = 0.44 ± 0.0000127

tube inside diameter (m) $d_{t,i}$ = 0.00406 ± 0.00001

inlet temperature of cold water (°C) Tc,i = 19.5 ± 0.3

outlet temperature of cold water (°C) Tc,o = 32.8 ± 0.23

inlet temperature of hot water (°C) Th,i = 94.6 ± 0.12

outlet temperature of hot water (°C) Th,o = 90.6 ± 0.3

flow rate of cold water (gpm) Q = 0.25 ± 0.0006

overall heat transfer coefficient in clean state (W/m^2K) U_C = 1519

1. Heat Transfer Rate

Heat transfer rate was calculated based on the temperature increase of cold water because the inlet temperature of cold water was kept almost constant.

$$q = rC_pQ(T_{co} - T_{ci}) = 889 \text{ W}$$

The various terms required to calculate the uncertainty are as follows:

$$\frac{\partial q}{\partial Q} = rC_p(T_{co} - T_{ci}) = 3556 \qquad W_Q = 6.0\text{E-}4$$

$$\frac{\partial q}{\partial T_{ci}} = -rC_pQ = -66.8 \qquad W_{Tci} = 0.3$$

$$\frac{\partial q}{\partial T_{c,o}} = rC_pQ = 66.8 \qquad W_{Tco} = 0.23$$

Thus, the uncertainty of the heat transfer rate becomes

$$w_q = \left[\left(\frac{\partial q}{\partial Q} w_Q \right)^2 + \left(\frac{\partial q}{\partial T_{ci}} w_{Tci} \right)^2 + ... + \left(\frac{\partial q}{\partial T_{co}} w_{Tco} \right)^2 \right]^{0.5}$$

= 25.3 W or 2.8 % error

2. Surface Area

Using the same procedure, the uncertainty analysis for the heat transfer surface area was executed as shown below.

$A = p\, d_{t,i}\, L = 0.00561\ m^2$

$$\frac{\partial A}{\partial d_{t,i}} = pL = 1.38 \qquad W_{d_{t,i}} = 1E\text{-}5$$

$$\frac{\partial A}{\partial L} = p d_{t,i} = 0.0127 \qquad W_L = 1.27E\text{-}5$$

$$w_A = \left[\left(\frac{\partial A}{\partial w} w_W \right)^2 + \left(\frac{\partial A}{\partial L} w_L \right)^2 \right]^{0.5}$$

= 1.37E-5 or 0.2% error.

3. Overall Heat Transfer Coefficient

The uncertainty analysis for the overall heat transfer coefficient is given as:

$$U = \frac{q}{A}\frac{\ln\{(T_{ho}-T_{ci})/(T_{hi}-T_{co})\}}{(T_{ho}-T_{ci})-(T_{hi}-T_{co})} = 1519 \text{ W/m}^2\text{K}$$

$$\frac{\partial U}{\partial q} = \frac{\ln M}{AK} = 1.7 \qquad w_q = 25.3$$

$$\frac{\partial U}{\partial A} = \frac{-q\ln M}{A^2K} = -270766 \qquad w_A = 1.37\text{E-}5$$

$$\frac{\partial U}{\partial T_{ho}} = \frac{q}{A}\frac{(1-1/M)-\ln M}{K^2} = -17.1 \qquad w_{Th,o} = 0.3$$

$$\frac{\partial U}{\partial T_{ci}} = \frac{q}{A}\frac{(1/M-1)+\ln M}{K^2} = 17.1 \qquad w_{Tc,i} = 0.3$$

$$\frac{\partial U}{\partial T_{hi}} = \frac{q}{A}\frac{(1-M)+\ln M}{K^2} = -18.8 \qquad w_{Th,i} = 0.12$$

$$\frac{\partial U}{\partial T_{co}} = \frac{q}{A}\frac{(M-1)-\ln M}{K^2} = 18.8 \qquad w_{Tc,o} = 0.23$$

where $K = (T_{ho}-T_{ci})-(T_{hi}-T_{co}) = 9.3$

$$M = \frac{(T_{ho}-T_{ci})}{(T_{hi}-T_{co})} = 1.15$$

$$w_{Uc} = \left[\left(\frac{\partial U}{\partial q}w_q\right)^2 + \left(\frac{\partial U}{\partial A}w_A\right)^2 + \left(\frac{\partial U}{\partial T_{ci}}w_{Tci}\right)^2 + \left(\frac{\partial U}{\partial T_{co}}w_{Tco}\right)^2 + \left(\frac{\partial U}{\partial T_{ho}}w_{Tho}\right)^2 + \left(\frac{\partial U}{\partial T_{hi}}w_{Thi}\right)^2\right]^{0.5}$$

= 44 or 2.8% error

4. Fouling Resistance

$U_f = 911.4 \text{ W/m}^2\text{K}$

$$R_f = \frac{1}{U_f} - \frac{1}{U_c}$$

$$\frac{\partial R_f}{\partial U_f} = -\frac{1}{U_f^{\,2}} \qquad w_{Uf} = 41.8$$

$$\frac{\partial R_f}{\partial U_c} = \frac{1}{U_c^{\,2}} \qquad w_{Uc} = 44$$

$$w_r = \left[\left(\frac{\partial R_f}{\partial U_f} w_{Uf} \right)^2 + \left(\frac{\partial R_f}{\partial U_c} w_{Uc} \right)^2 \right]^{0.5}$$

= 4.47E-5 or 10% error

Appendix C Experimental Data

Time	Time (hours)
T_{ci}	Inlet temperature of cold water (^oC)
T_{co}	Outlet temperature of cold water (^oC)
T_{hi}	Inlet temperature of hot water (^oC)
T_{ho}	Outlet temperature of hot water (^oC)
T_{lm}	Log-mean temperature (^oC)
U_f	Overall heat-transfer coefficient (W/m^2K)
R_f	Fouling resistance (m^2K/W)

Effect of Frequency and Strength of Current of SCI (No treatment)

Time	T_{ci}	T_{co}	T_{hi}	T_{ho}	T_{lm}	U_f	R_f
0	19.1	32.6	94.6	90.4	66.54172	1519.239	0
10	19.5	32.5	94.8	90.8	66.69883	1459.525	2.7E-05
20	19.6	32.5	94.7	90.9	66.64649	1449.435	3.2E-05
30	19.7	32.1	94.8	90.8	66.81202	1389.804	6.1E-05
40	19.8	32	94.7	90.8	66.76404	1368.37	7.3E-05
50	19.6	31.6	94.8	90.9	67.16862	1337.831	8.9E-05
60	19.8	31.2	94.7	91	67.27658	1268.9	0.00013
70	19.5	30.8	94.7	91	67.62884	1251.217	0.00014
80	19.7	30.5	94.9	91.2	67.88813	1191.286	0.00018
90	19.8	30.4	94.8	91.3	67.88813	1169.226	0.0002
100	19.4	29.8	94.7	91.2	68.29191	1140.382	0.00022
120	19.7	29.7	94.6	91.3	68.19515	1098.077	0.00025
140	19.6	29.3	94.8	91.2	68.50474	1060.321	0.00028
160	19.7	29.1	94.9	91.5	68.75637	1023.767	0.00032
180	19.6	28.2	94.8	91.4	69.16743	931.0717	0.00042
200	19.8	28.2	94.7	91.4	69.0186	911.3799	0.00044

Effect of Frequency and Strength of Current of SCI (0.7A, 0.5 kHz)

Time	T_{ci}	T_{co}	T_{hi}	T_{ho}	T_{lm}	U_f	R_f
0	19.1	32.6	94.6	90.4	66.54172	1519.239	0
10	19.5	32.6	94.8	90.8	66.64649	1471.907	2.1E-05
20	19.6	32.5	94.7	90.9	66.64649	1449.435	3.2E-05
30	19.6	32.2	94.8	90.8	66.80777	1412.309	5E-05
40	19.8	31.9	94.7	90.8	66.81616	1356.095	7.9E-05
50	19.5	31.4	94.8	90.9	67.3208	1323.683	9.7E-05
60	19.8	31.2	94.8	91.1	67.37668	1267.014	0.00013
70	19.5	30.9	94.8	91	67.62884	1262.29	0.00013
80	19.6	30.7	94.9	91.2	67.83274	1225.378	0.00016
90	19.7	30.6	94.7	91.3	67.78086	1204.22	0.00017
100	19.6	30.4	94.7	91.2	67.8846	1191.349	0.00018
120	19.8	30.3	94.8	91.3	67.93991	1157.312	0.00021
140	19.7	29.8	94.8	91.2	68.19838	1109.005	0.00024
160	19.8	29.6	94.7	91.4	68.29846	1074.488	0.00027
180	19.7	29.3	94.8	91.4	68.55328	1048.647	0.0003
200	19.7	28.8	94.7	91.3	68.7106	991.754	0.00035

Effect of Frequency and Strength of Current of SCI (0.7A, 3.5 kHz)

Time	T_{ci}	T_{co}	T_{hi}	T_{ho}	T_{lm}	U_f	R_f
0	19.6	33.2	94.7	90.9	66.27929	1536.552	0
10	19.5	33	94.8	90.8	66.43684	1521.637	6.4E-06
20	19.7	32.8	94.8	90.9	66.49396	1475.283	2.7E-05
30	19.8	32.9	94.7	90.9	66.34139	1478.676	2.5E-05
40	19.6	32.3	94.8	90.7	66.70763	1425.655	5.1E-05
50	19.7	32.1	94.7	90.8	66.75984	1390.89	6.8E-05
60	19.6	32	94.8	91.1	67.05596	1384.747	7.1E-05
70	19.7	31.6	94.7	91.1	67.16455	1326.762	0.0001
80	19.8	31.5	94.8	91.3	67.31678	1301.514	0.00012
90	19.8	31.4	94.8	91.3	67.36886	1289.392	0.00012
100	19.6	31	94.8	91.4	67.72126	1260.567	0.00014
120	19.7	30.9	94.8	91.4	67.72516	1238.381	0.00016
140	19.6	30.4	94.9	91.5	68.13304	1187.004	0.00019
160	19.8	30.1	94.7	91.5	68.08831	1132.794	0.00023
180	19.7	29.7	94.7	91.5	68.34363	1095.691	0.00026
200	19.8	29.5	94.8	91.5	68.45014	1061.167	0.00029

Effect of Frequency and Strength of Current of SCI (7.0A, 0.5 kHz)

Time	T_{ci}	T_{co}	T_{hi}	T_{ho}	T_{lm}	U_f	R_f
0	19.5	33.2	94.6	90.9	66.27431	1547.967	0
10	19.6	33.1	94.7	90.8	66.28418	1525.142	9.7E-06
20	19.7	32.9	94.7	90.8	66.34139	1489.964	2.5E-05
30	19.6	32.7	94.6	90.9	66.48929	1475.387	3.2E-05
40	19.8	32.2	94.7	90.8	66.6597	1392.979	7.2E-05
50	19.7	32	94.8	90.9	66.91215	1376.532	8E-05
60	19.7	31.8	94.9	91.1	67.16455	1349.061	9.5E-05
70	19.8	31.6	94.8	91.1	67.16862	1315.533	0.00011
80	19.6	31.2	94.8	91.3	67.5691	1285.571	0.00013
90	19.8	31.4	94.8	91.3	67.36886	1289.392	0.00013
100	19.7	31	94.8	91.4	67.67317	1250.398	0.00015
120	19.8	30.7	94.7	91.3	67.68076	1206.001	0.00018
140	19.7	30.2	94.9	91.6	68.2367	1152.279	0.00022
160	19.7	30	94.8	91.5	68.24017	1130.273	0.00024
180	19.7	29.7	94.7	91.5	68.34363	1095.691	0.00027
200	19.8	29.7	94.8	91.6	68.39531	1083.915	0.00028

Effect of Frequency and Strength of Current of SCI (7.0A, 3.5 kHz)

Time	T_{ci}	T_{co}	T_{hi}	T_{ho}	T_{lm}	U_f	R_f
0	19.6	33.2	94.7	90.9	66.27929	1536.552	0
10	19.6	33.1	94.7	90.8	66.28418	1525.142	4.9E-06
20	19.7	33.2	94.8	90.8	66.23649	1526.24	4.4E-06
30	19.8	33	94.8	90.9	66.34139	1489.964	2E-05
40	19.7	32.8	94.7	91	66.48929	1475.387	2.7E-05
50	19.6	32.5	94.8	91.1	66.79444	1446.225	4.1E-05
60	19.6	32.4	94.7	91	66.74664	1436.041	4.6E-05
70	19.7	32	94.8	91.1	67.00805	1374.562	7.7E-05
80	19.6	31.7	94.7	91.2	67.20832	1348.182	9.1E-05
90	19.8	31.4	94.8	91.3	67.36886	1289.392	0.00012
100	19.7	31.4	94.7	91.3	67.3648	1300.586	0.00012
120	19.7	31.1	94.8	91.4	67.62115	1262.434	0.00014
140	19.6	30.8	94.7	91.4	67.77328	1237.502	0.00016
160	19.7	30.4	94.7	91.5	67.98106	1178.643	0.0002
180	19.7	30.3	94.8	91.5	68.08479	1165.848	0.00021
200	19.7	30.2	94.7	91.6	68.13304	1154.032	0.00022

Chapter 7

Performance of an Electrostatic Precipitator (ESPH-1) on the Mitigation of Mineral Fouling (Concentric Heat Transfer Test Section)

Abstract

The purpose of the present study was to investigate the validity of physical water treatment (PWT) using an electrostatic precipitator (ESPH-1) on the mitigation of mineral fouling in a heat exchanger in an open cooling-tower system. Experimental method and test conditions were the same as those in the PWT studies with permanent magnets and solenoid coils; thus they are not repeated here.

EXPERIMENTAL PROCEDURE

Figure 1 shows a schematic diagram of the present test facility, which consists of a water-circulating loop, a high-voltage electrode device (ESPH-1) in a side-stream loop, a cooling tower, a pump, a concentric-tube test section, a floating-ball valve for automatic feeding of make-up water.

The main heat-transfer test section was composed of two concentric tubes: the inner one was made of a smooth copper tube, and the outer one was made of a glass tube. The dimension of the inner tube was 6.35 mm × 4.06 mm × 441 mm (O.D. × I.D. × L), whereas the dimension of the outer tube was 25.4 mm × 16.3 mm × 20.3 mm (O.D. × I.D.

× L). The two tubes were connected with compression fittings at both ends of the inner and outer tubes. The cooling water moved inside of the inner tube, whereas hot water moved in the annulus gap between the two tubes. The flow directions of the hot and cold water were opposite each other, thus forming a counter-flow heat exchanger.

The flow rate of the cooling water was 0.157×10^{-4} m^3/s (i.e., 0.25 gpm). The corresponding flow velocity in the cooling channel, where fouling occurred, was 1.0 m/s (i.e., 3.3 ft/s) and corresponding Reynolds number was 4,511. During the fouling test, the flow rate was maintained at 0.25 gpm within ± 5%. The ESPH device was installed in a side-stream loop where the flow rate was maintained at 0.25 gpm, independent of the low rate at the main heat-transfer section.

Hot water was produced by an electric water heater and circulated at a flow rate of 6.309×10^{-5} m^3/s (i.e., 1.0 gpm). The water heater had a heating element of 4.2 kW, and its temperature was controlled using a thermostat (Omega Engineering, Inc). The heat flux used in the study was about 10.1×10^4 W/m^2 (i.e., 32,041 $Btu/hr \cdot ft^2$). Note that the majority of water chillers manufactured today are designed to operate with a full-load condenser heat flux in the range of 1.89×10^4 to 3.15×10^4 W/m^2 (i.e., 6,000 to 10,000 $Btu/hr \cdot ft^2$). In the present study, a much higher heat flux of 10.1×10^4 W/m^2 was used to accelerate the fouling so that each test could be completed in two weeks.

To calculate the fouling resistance, temperatures were measured at four different positions: cooling-water inlet and outlet, and hot-water inlet and outlet, see Fig. 1. The cooling water entered the test section at 20 ± 0.5°C and heated to 31± 0.5°C, whereas the hot water entered the test section at 91 ± 0.5°C and cooled to 87± 0.5°C during the test.

After the cooling water past the heat-transfer test section, it was sent to the cooling tower, where the water was cooled by evaporation. In order to maintain a constant volume of water in the system, the tap water was added as make-up water, a procedure that was controlled by an automatic floating-valve system.

RESULTS AND DISCUSSION

Table 1 shows the water analysis data for the make-up and circulating cooling-tower water for three different water qualities, respectively. There was no big difference in water qualities between the no-treatment case and the case with the PWT. The Langelier saturation index (LSI) was calculated to examine the precipitation tendency of the circulating water. The values of the LSI were in the range of 2.08 to 2.45, indicating that the circulating water had a condition to cause severe mineral fouling.

Figure 2 represents fouling resistance values vs. time for three different conductivity cases. No treatment cases were obtained for baseline data. As the water conductivity increased from 2,000 to 3,000 μS/cm, the fouling resistance significantly increased as expected. However, as the water conductivity was further increased from 3,000 to 4,000 μS/cm, the fouling resistance dropped noticeably, a phenomenon which was not intuitively acceptable. We had observed this peculiar behavior of the fouling resistance with respect to water conductivity or hardness in previous studies. A possible explanation could be as follows: As the water conductivity increases from 3,000 to 4,000 μS/cm, a large number of particulates are made in the bulk solution due to excessive amounts of dissolved mineral ions. Once the particles are formed, they grow in size as the water is heated inside a heat exchanger. Whether these particles are formed due to

excessive hardness in the circulating water or due to physical water treatment, once formed, they become the means to prevent scaling inside the heat exchanger. Furthermore, when these particles deposit on the heat transfer surface, the deposits form a soft sludge-type coating, which is readily removed by the shear force of moving water.

When circulating water was treated by ESPH-1, the fouling resistance at the end of the 200-hr tests was almost identical for all three water cases. In case of the 3,000-μS/cm case with ESPH-1 treatment, the fouling resistance dropped by 53% from the values of the no-treatment case. In the 4,000-μS/cm case, the fouling resistances were not reduced as much as the 3,000-μS/cm case because the baseline fouling data for the 4,000-μS/cm case was already small as discussed above. Note that the fouling resistance value for the no-treatment case kept increasing at the end of the test, whereas the fouling resistance value reached an asymptotic value and remained at the value for the rest of the test for the ESPH case. If the fouling test had continued, the difference in the fouling resistance between the two cases would have been bigger.

In the operation of the ESPH-1 device, there may be some operating conditions affecting the optimum performance of the device which include flow velocity, frequency and strength of the signal used in the control unit. These factors have not been studied in the present study and need to be further investigated in the future.

	Make-up	Unfiltered	COC	Filtered
Conductivity (μS/cm)	600	2000	3.3	2000
pH	7.2	8.4		8.4
Total hardness (mg/L)	206	700	3.4	700
Ca^{+} hardness (mg/L)	153	520	3.4	520
Total alkalinity (mg/L)	70	192	2.7	192
Chloride (mg/L)	100	372	3.7	372
L.S.I. (at T = 38°C)	0.04	2.08		2.08

Water Analysis Result – ESPH

Water Analysis Result – ESPH

	Make-up	Unfiltered	COC	Filtered
Conductivity (μS/cm)	600	3000	5	3000
pH	7.2	8.5		8.5
Total hardness (mg/L)	206	1140	5.5	1140
Ca^{+} hardness (mg/L)	153	696	4.5	696
Total alkalinity (mg/L)	70	296	4.3	296
Chloride (mg/L)	100	552	5.5	552
L.S.I. (at T = 38°C)	0.04	2.44		2.44

Water Analysis Result – ESPH (no-treatment)

	Make-up	Unfiltered	COC	Filtered
Conductivity (μS/cm)	600	3700	6.1	3700
pH	7.2	8.4		8.4
Total hardness (mg/L)	206	1280	6.2	1280
Ca^{+} hardness (mg/L)	153	940	6.1	940
Total alkalinity (mg/L)	70	300	4.3	300
Chloride (mg/L)	100	780	7.8	780
L.S.I. (at T = 38°C)	0.41	2.45		2.45

Table 1. Water quality data measured by Drexel

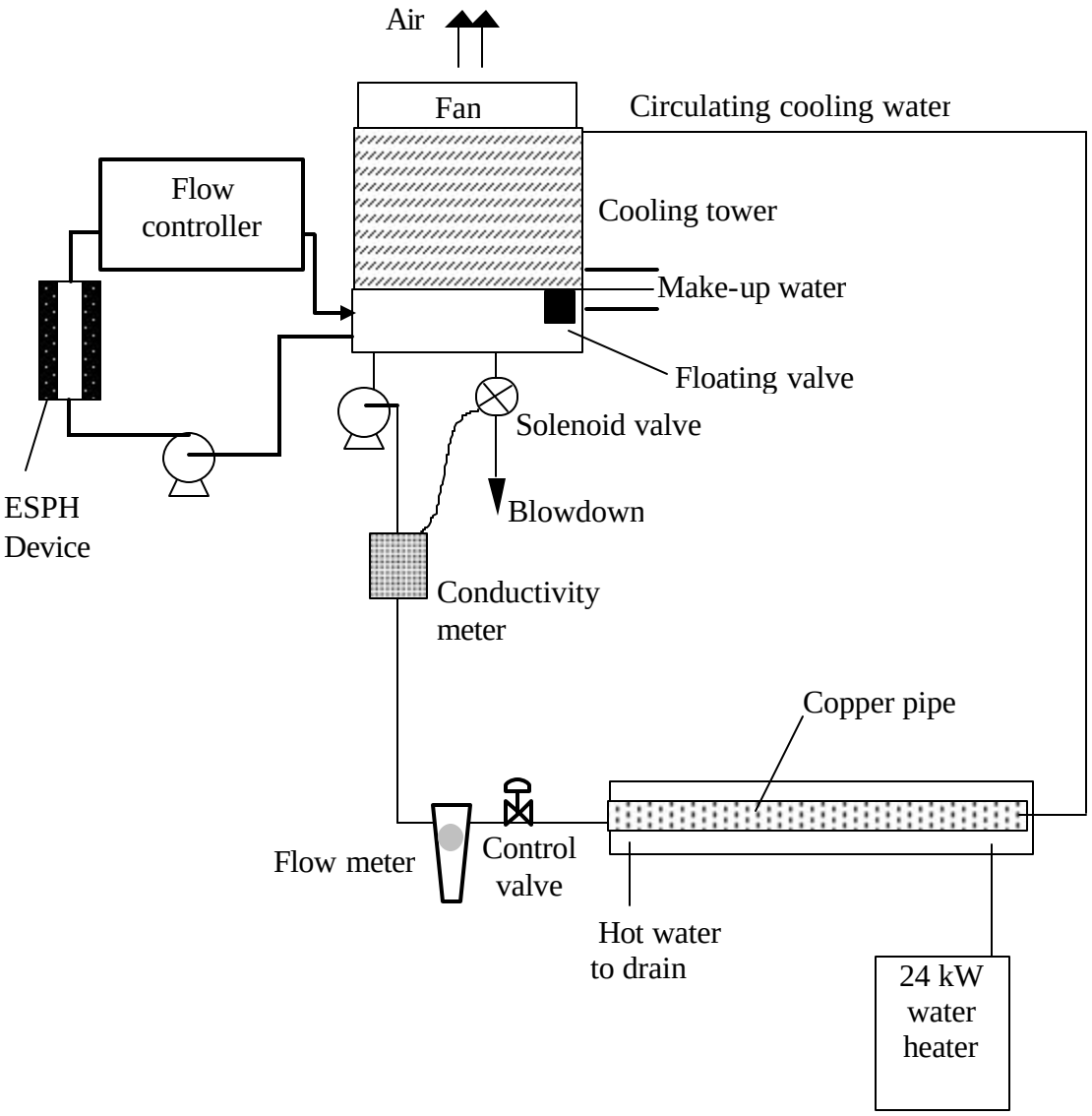

Fig. 1 Schematic diagram of flow loop where ESPH device is installed in a side-stream loop.

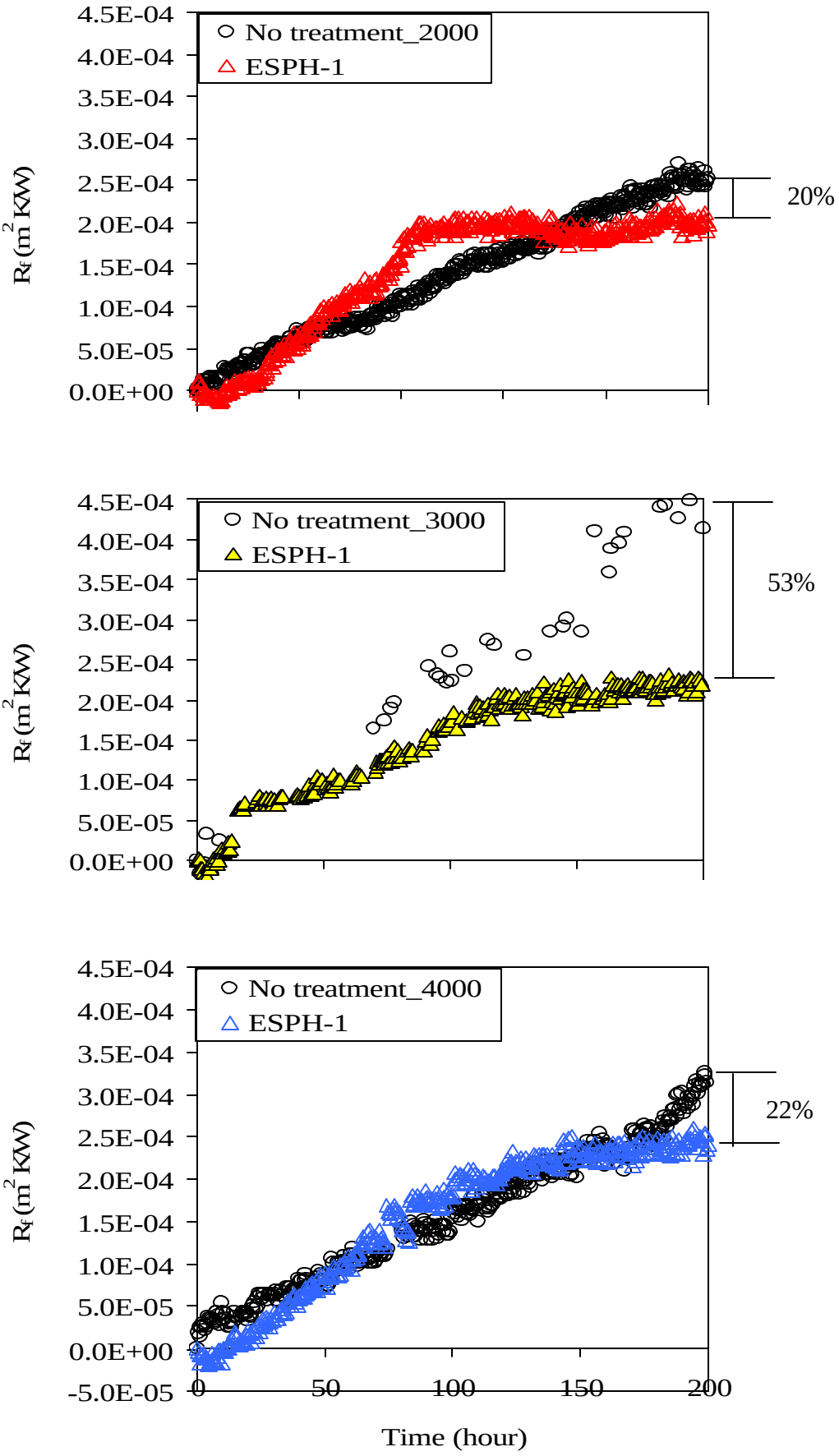

Figure 1. Fouling resistances vs. time for three different water hardness

Chapter 8

Effects of Physical Water Treatment with Permanent Magnets (PMDU) and a Solenoid-Coil Device (SCED) on the Surface Tension of Water

ABSTRACT

The purpose of the present study was to investigate whether or not a physical water treatment (PWT) changes the surface tension of hard water. Two different PWT devices were used: a permanent magnet device (PMDU) and a solenoid coil (SCED). The effects of the number of the PWT, water quality, flow velocity, and frequency on the surface tension were studied. Two separate experiments were conducted to measure the surface tension of the sample water: One is the measurement of surface tension, and the other is an observation of dye behavior in water samples. As the number of passes through the PWT increased, the surface tension of the sample water decreased, a phenomenon that is consistent with the dye behavior observed in the other experiment. When the flow velocity through the PMDU was 6.3 m/s, the sample hard water had the minimum surface tension. The maximum reduction of the surface tension was 8% compared to the value obtained for the no-treatment case. In the case of the SCED, the reduction of the surface tension was proportional to the increment of the frequency of a square-wave signal used. Changes in the surface tension are consistent with the variations in the fouling resistance results obtained from a heat exchanger.

Key words: surface tension, physical water treatment, and mineral fouling

NOMENCLATURE

A	cross sectional area, m^2
B	magnetic field strength vector, Wb/m^2
E	induced electric field vector, V
f	frequency, kHz
H	height, mm
I.D.	inner diameter of capillary tube, mm
O.D.	outer diameter of tube, mm
L	length of flow channel, mm
Lc	length of capillary tube, mm
R_f	fouling resistance, m^2K/W
SG	specific gravity
V	flow velocity, m/s
W	Width, mm

Greek symbols

?	specific weight, N/m^3
s	surface tension, N/m
θ	contact angle, deg.

INTRODUCTION

It is well known that the formation of solid deposits of scale in heat exchanger systems is a universal problem where liquids are in contact with pipes and walls of containment systems. The cost for the control of scale and corrosion is very large. Chemical treatment has been the principle method used to prevent and to remove scale. However, it requires handling and disposal of hazardous chemicals, raising environmental concerns. Hence, if there can be a physical water treatment method to effectively prevent or mitigate fouling, such a method will be beneficial not only to the industry but also to the environment.

Among the various physical water treatment (PWT) methods, a permanent magnetic and a solenoid coil are two most popular systems. A number of tests were conducted to verify the effect of these PWT devices on the mitigation of fouling [1-7]. The theory of the PWT device is as follows: when the hard water passes through the device, an electric field forces the motion of dissolved mineral ions into a certain plane such that the collision between positive and negative ions increase, resulting in the formation of seed crystals in the bulk solution. These crystals grow inside a heat exchanger, thus mitigating mineral fouling at the surface of the heat exchanger.

The fouling resistance value is often used to evaluate the efficiency of the PWT device. However, it takes approximately two weeks to obtain a fouling resistance value, and fouling tests often require rather sophisticated instrumentation and facility.

Some researchers tried to investigate the PWT with several different methods such as crystal morphology, crystal phase, solubility change, and water property change

[8-11]. The surface tension of water was mentioned by a former soviet scientist [Klassen 1969] but there is no specific experimental data reported in the literature.

Therefore, the purpose of the present study was to investigate whether or not the PWT (i.e., permanent magnet (PMDU) and a solenoid coil (SCED)) can reduce the surface tension of treated water. Furthermore, the study conducted a visualization study on the behavior of dye in water and related the dye behavior to the changes in the surface tension of the water.

EXPERIMENTAL METHODS

The present experiment of measuring surface tension is divided into two steps: making water sample and measuring the surface tension of the sample water. Figure 1 shows the schematic diagram of the present test facility for water sampling, which consists of a reservoir tank, a pump, a flow meter, a control valve, a PWT using a permanent magnet (PMDU) or a solenoid coil (SCED).

Figure 2 shows the arrangement and dimensions of a PWT system using a PMDU. Total four permanent magnets were positioned in the present experiment, an arrangement that is known to maximize the magnetic treatment on water. The maximum strength of the magnetic field was measured to be 0.16 T (or 1,600 gauss) by using an Alphalab DC Magnetometer. The cross-sectional dimension of the flow channel in the PMDU was 0.68 mm $\times$ 9.27 mm $\times$ 100 mm (H $\times$ W $\times$ L). This arrangement of the PMDU was fixed through the entire experiment.

Figure 3 shows a sketch of a PWT system using a solenoid coil (SCED). The solenoid coil was wrapped over a plastic tube with an outside diameter (O.D.) of 50.8

mm. 14-gage wire was wound with 80 turns. Two ends of the solenoid coil were connected to a SCED-control unit.

The SCED-control unit produced a pulsing current at a frequency of 600 Hz. Subsequently, an induced pulsating electric field was generated inside the pipe by Faraday's law [12]:

$$\int E \cdot ds = -\frac{\partial}{\partial t}\int B \cdot dA$$

where E [V] is an induced electric field vector, s is a line vector along the circumferential direction, B [Wb/m^2] is a magnetic field strength vector, and A is the cross sectional area of the solenoid coil. Excess mineral ions such as calcium and magnesium precipitate into mineral salts. Details of the operating principle of the SCED treatment including the precipitation mechanism by the induced pulsating electric field can be found elsewhere [5,7]. Copper tube carrying test water was located at a off-centered position relative to the solenoid coil since the strength of the induced electric field had a maximum value at the surface of the coil and a minimum value at the center of the coil.

First, the repeated treatment effect of the PWT on the surface tension of water was studied with the Philadelphia City tap water and natural hard water that was made through evaporation in a cooling-tower system. Table 1 gives the result of water analysis that was performed with standard titration methods. Tap water in the reservoir tank was pumped up and passed through a flow meter and a PMDU or SCED system and finally collected in another tank at the ground level. The treatment number of the PWT was changed from 0 to 30, i.e., 0 means no-treatment, and 30 means the water sample passed the PWT device 30 times. The flow velocities through the PMDU and SCED devices

were 6.3 and 1.0 m/s, respectively. Note that the flow velocity of 6.3 m/s for the PMDU was the optimum velocity for the PMDU used in the study.

To investigate the relationship between the surface tension and the present experimental system itself, tests were repeated under identical conditions without the PWT for baseline data.

The second set of experiments was conducted to investigate the relationship between flow velocity through the PMDU and the surface tension of hard water by changing the flow velocity over a range (i.e., V = 0, 2, 4, 6.3, and 8.5 m/s).

The third set of experiments was conducted with five different frequencies in the square-wave current signal in the SCED system (i.e., f = 0, 0.3, 0.5, 2.0, and 3.5 kHz) using a fixed flow velocity of 1.0 m/s.

After finishing each test run, the surface tension of the sample water was measured with precision glass capillary tubes, Corning Inc. Figure 4a shows the schematic diagram of the capillary-tube system. A glass capillary tube was attached beside a ruler, and then a 100-ml beaker was placed on an adjustable jack so that the capillary tube was positioned at the center of the sample water in the beaker. The capillary tube was first wetted with the sample water by raising the beaker, and then the beaker was lowered slowly. When the water level reached near the bottom of the capillary tube, a point exactly 5 mm from the bottom, the height of the water level inside the capillary tube was read. This step was repeated ten times in each water sample for the reliability of the measured value. The dimension of capillary tube was 1.15 mm $\times$ 100 mm (I.D. $\times$ Length). Through the whole experiment, the temperature of the sample water

was controlled at 25°C. The maximum reading error on the height of the water was estimated to be ± 1%.

Figure 4b shows the schematic diagram of a dye-injection experiment system that is composed of a micro-syringe pump, a needle with a vinyl tube, and a camera system. The dye injection test was performed to investigate the surface tension effect on the motion of dye. Eriochrome Black T (SG = 1.109, Aldrich Inc.) was used for the test. A micro syringe pump (kd Scientific Co.) was used to deliver an exact amount of dye, 0.005 ± 0.0003 g, without manual interventions. The needle tip used for dye injection (21G1.5, Precision Glide) was always positioned at 3 mm above the surface of the sample water.

RESULTS AND DISCUSSION

Table 1 shows the results of water analysis for tap water and natural hard water that were made from a cooling-tower system. Two different water samples in the present experiment were tested to check the efficiency of the PWT on hard water. The natural hard water had 5 to 8 times higher total hardness than that of the tap water.

Before starting with a PWT device, the relationship between the effect of the surface tension and the experimental system itself was established as the baseline data. Table 2 and Figure 5 show the results of the surface tension of the sample water without the PWT device. The difference between (a) and (b) is water quality (i.e., tap water and natural hard water, respectively). After 30 passes, the surface tension dropped max. by 2% comparing to that of the initial state. This result may be attributed to the fact that pump agitation itself might have reduced the surface tension through bulk precipitation although the amount is small.

Table 3 and Figure 6 shows the results of the surface tension of the sample water treated by the PWT (using PMDU). In the case of the tap water which is given in Table 3(a) and Fig. 6(a), the maximum reduction of the surface tension was 7.7 %, and for the natural hard water case it was 8.2 % (see Table 3(b) and Fig. 6(b)). This suggests that water hardness doesn't affect the reduction of the surface tension much. A possible explanation could be as follows: when the hard water passes through the PMDU, the mineral ions dissolved in the cooling-tower water collide with anionic ions such as bicarbonate and make big colloidal particles in the bulk water. Therefore, as the number of passes through the PWT device increases, the number and/or the size of the colloidal particles increase, thus reducing the surface tension of the water.

Surface tension can be described as the surface energy per unit area. The surface energy of a liquid-liquid state is less than that of a solid-liquid state in water [13-15]. Hence, the surface energy at the interface of water molecule and glass tube is much bigger than that between two water molecules. But as the number of the colloidal particles increases in the water, the surface energy at the interface of water molecule and colloidal particle increases. In other words, the surface energy at the interface between water molecule and glass tube decreases relatively. Therefore, the surface tension of the water will decrease as the number of colloidal particles increases in the water.

Figure 7 shows the photographs of the dye-injection experiment with three water samples (i.e., no treatment, 2 passes, and 10 passes through the PMDU). As can be seen, the dye drop in the no-treatment case rapidly spread out to the radial direction, in other words, dye did not fall through the water but stayed on the top surface of the water indefinitely. But when the dye was introduced to the water sample that passed 10 times

through the PMDU, the dye drop quickly fell through the water as it was released from the needle and reached the bottom of the beaker in approximately ten seconds. This result can be attributed to the reduction of the surface tension caused by the PWT.

Table 4 shows the results of the surface tension of the sample water as the water repeatedly treated by the PWT using a solenoid coil (SCED). As the number of passes through the PWT with the SCED increased the surface tension of the water sample reduced by 5.9 and 7.8 % from those of the tap water and natural hard water, respectively. The reduction amount of the surface tension in the natural hard water was slightly larger than that for the case of the tap water. This means the efficiency of SCED is somehow proportional to the water hardness, in other word; the fraction of the collisions of ions that led to bulk precipitation might have increased in the hard water. These results are consistent with those presented in Figure 8.

Figure 9 shows photographs from the dye-injection experiment with three different water samples (i.e., no treatment, 2 passes, and 10 passes through the SCED). As the PWT is repeated, the dye drop fell faster and faster. Similar results were observed for the case with the PWT using permanent magnets (PMDU).

Table 5 and Figure 10 represent the surface tension of the sample water that was treated at various flow velocities with the PMDU and compare with fouling resistance values taken from a separate fouling test. When the flow velocity through the PMDU increased to 4.0 m/s, there was no big change in the surface tension form the value measured for the untreated water sample. But when the flow velocity increased by 6.3 m/s, the surface tension reduced by about 8% compared to that of the no-treatment case.

In a higher flow velocity (i.e., 8.5 m/s), the surface tension did not decrease anymore but rather increased slightly.

This phenomenon gave good agreement with the fouling resistance data obtained from a separate heat-transfer test. To get the fouling resistance value, a heat transfer experiment was conducted in a heat exchanger and a cooling-tower system with the PMDU. The minimum value of the fouling resistance was obtained at a flow velocity of 6.3 m/s, and the overall trend of the fouling resistance with various flow velocities was almost similar to that of the surface tension. This result suggests that there is a certain flow velocity for the maximum efficiency of the PMDU. In other words, when the flow velocity reaches a certain value, the magnetic field in the PMDU effectively forces the mineral ions into colloidal seed particles, thus producing the maximum efficiency.

Table 6 and Figure 11 show the effect of the surface tension of the water when the different frequency in the square-wave current signal in the SCED was applied to the natural hard water. As the frequency of in the signal in the SCED increased, the surface tension of the water reduced by 8% compared to that for the no-treatment case. This result consistent with those obtained from the fouling experiment as depicted in Figure 11(b). Since the ion-ion collision depends on the frequency of the SCED signal, one can speculate that the higher the frequency is, the better the SCED is.

CONCLUSIONS

In the present study, the surface tension was measured with precision glass capillary tubes. A dye-injection experiment was performed to examine whether or not the PWT using a permanent magnetic (PMDU) or solenoid coil (SCED) changes the

diffusion characteristics of the dye in treated water, so that one can investigate the relationship between the surface tension of hard water and the PWT. As experimental variables, the number of passes through the PWT, water quality, flow velocity through the magnetic device, and the frequency of the current signal in the SCED were used.

As the PWT with PMDU or SCED was repeated, the surface tension of the treated water reduced by 8 % compared to that of the no-treatment case. When the flow velocity through the PMDU was 6.3 m/s, the surface tension value reduced to its minimum value, indicating the effect of the flow velocity on the effectiveness of the PMDU. The surface tension of the water treated by the SCED varied with the frequency of the current signal in the SCED. Generally, the surface tension results gave a good agreement with the results of fouling-resistance experiment. The study suggests that the simple measurement of the surface tension appears to be promising to evaluate the efficiency of a physical water treatment method although further investigations are needed.

REFERENCE

[1] T. Vermeiren, Magnetic treatment of liquids for scale and corrosion prevention, Corrosion Technology, (1958) 215-219

[2] R.E. Herzog, Q. Shi, J. N. Patil, and J. L. Katz, Magnetic water treatment: The effect of iron on calcium carbonate nucleation and growth, Langmuir, 5 (1989) 861-867

[3] K. J. Kronenberg, Experimental evidence for effects of magnetic fields on moving water, IEEE Transcations on magnetics, MAG-21 (1985) 2059-2061

[4] K. W. Busch, M. A. Busch, D. H. Parker, An investigation of the role of magnetic water treatment devices in calcium carbonate scale formation, Baylor University, Waco, TX 1985

[5] C. Fan and Y.I. Cho, A New Electronic Anti-fouling Technology to Control precipitation Fouling, HTD-Vol. 350, National Heat Transfer Conference, Vol. 12, ASME 1997, pp. 183-188

[6] Y. I. Cho and Byung-Gap Choi, Validation of an Electronic Anti-Fouling Technology in a Single-Tube Heat Exchanger, International Journal of Heat and Mass Transfer, Vol.42, pp.1491-1499, 1999.

[7] Y.I. Cho, C. Fan and Byung-Gap Choi, Theory of Electronic Descaling Technology of Control Precipitation Fouling in Heat Exchangers, Int. Comm. Heat Mass Transfer, Vol.24, 747-756, 1997.

[8] C. Fan and Y.I. Cho, Microscopic observation of calcium carbonate crystallization induced by an electronic descaling technology, Int. Comm. Heat Mass Transfer, Vol.24, 757-770, 1997.
[9] K. Higashitani, et al., Effects of a magnetic field on the formation of $CaCO_3$ particles, Journal of Colloid and interface science, 156 (1993) 90-95
[10] K. W. Busch, M. A. Busch, Laboratory studies on magnetic water treatment and their relationship to a possible mechanism for scale reduction, Desalination, 109 (1997) 131-148
[11] J. D. Donaldson and S. Grimes, Lifting the scales from our pipes, The City University, London, UK, Newscientist, 1990
[12] R. A. Serway, Physics for Scientists and Engineers (3^{rd} Edition), Saunders College Publishing, Philadelphia, PA (1990) 874-891
[13] S. K. Lower, Solids in contact with natural waters, A Chem1 reference text, Simon Fraser University, pp.21-24, 1997.
[14] K. J. Mysels, Introduction to Colloid Chemistry, Interscience Publishers, Inc. NY, pp. 184-187, 1976.
[15] R. D. Vold and M. J. Vold, Colloid and Interface Chemistry, Addison-Wesley Publishing Company, Inc., pp. 116-148, 223-259, 1983

	Tap Water	Tap Water	Hard Water
Conductivity (µS/cm)	450	570	2990
pH	7.1	7.4	8.3
Total hardness (mg/L)	140	204	1190
Ca^{+} hardness (mg/L)	120	142	780
Total alkalinity (mg/L)	65	75	320
Chloride (mg/L)	75	95	640

Table 1. Water quality data of tap water and natural hard water

No. of pass	h,ave (m)	γ (N/m^3)	R (m)	θ (deg.)	σ (N/m)	Reduction rate (%)
0	0.0255	9777	0.00057	0	0.07105	0.0
1	0.0252	9777	0.00057	0	0.07022	1.2
2	0.025	9777	0.00057	0	0.06966	2.0
5	0.025	9777	0.00057	0	0.06966	2.0
10	0.025	9777	0.00057	0	0.06966	2.0
30	0.025	9777	0.00057	0	0.06966	2.0

(a)

No. of pass	h,ave (m)	γ (N/m^3)	R (m)	θ (deg.)	σ (N/m)	Reduction rate (%)
0	0.0245	9777	0.00057	0	0.06827	0.0
1	0.0242	9777	0.00057	0	0.06743	1.2
2	0.0242	9777	0.00057	0	0.06743	1.2
5	0.0242	9777	0.00057	0	0.06743	1.2
10	0.0242	9777	0.00057	0	0.06743	1.2
30	0.0242	9777	0.00057	0	0.06743	1.2

(b)

Table 2.(a) Results of the surface tension of tap water with changing of number of treatment without electro-magnetic device (b) for the natural hard water

No. of pass	h,ave (m)	γ (N/m^3)	R (m)	θ (deg.)	σ (N/m)	Reduction rate (%)
0	0.026	9777	0.00057	0	0.07245	0.0
1	0.025	9777	0.00057	0	0.06966	3.8
2	0.0245	9777	0.00057	0	0.06827	5.8
5	0.024	9777	0.00057	0	0.06687	7.7
10	0.024	9777	0.00057	0	0.06687	7.7
30	0.024	9777	0.00057	0	0.06687	7.7

(a)

No. of pass	h,ave (m)	γ (N/m^3)	R (m)	θ (deg.)	σ (N/m)	Reduction rate (%)
0	0.0245	9777	0.00057	0	0.06827	0.0
1	0.0235	9777	0.00057	0	0.06548	4.1
2	0.023	9777	0.00057	0	0.06409	6.1
5	0.023	9777	0.00057	0	0.06409	6.1
10	0.0225	9777	0.00057	0	0.0627	8.2
30	0.0225	9777	0.00057	0	0.0627	8.2

(b)

Table 3.(a) Results of the surface tension of tap water with changing of the number of PMDU treatment (b) for natural hard water

No. of pass	h,ave (m)	γ (N/m^3)	R (m)	θ (deg.)	σ (N/m)	Reduction rate (%)
0	0.0255	9777	0.00057	0	0.07105	0.0
1	0.025	9777	0.00057	0	0.06966	2.0
2	0.0247	9777	0.00057	0	0.06883	3.1
5	0.0242	9777	0.00057	0	0.06743	5.1
10	0.024	9777	0.00057	0	0.06687	5.9
30	0.024	9777	0.00057	0	0.06687	5.9

(a)

No. of pass	h,ave (m)	γ (N/m^3)	R (m)	θ (deg.)	σ (N/m)	Reduction rate (%)
0	0.0245	9777	0.00057	0	0.06827	0.0
1	0.0234	9777	0.00057	0	0.0652	4.5
2	0.0227	9777	0.00057	0	0.06325	7.3
5	0.0227	9777	0.00057	0	0.06325	7.3
10	0.0227	9777	0.00057	0	0.06325	7.3
30	0.0226	9777	0.00057	0	0.06297	7.8

(b)

Table 4.(a) Results of the surface tension of tap water with changing of the number of SCED treatment (b) for natural hard water

Flow velocity	h,ave (m)	γ (N/m^3)	R (m)	θ (deg.)	σ (N/m)	R_f (m^2K/W)
0 m/s	0.0245	9777	0.00057	0	0.06827	0.00015
2.0 m/s	0.025	9777	0.00057	0	0.06966	0.0001
4.0 m/s	0.0245	9777	0.00057	0	0.06827	0.00009
6.3 m/s	0.0225	9777	0.00057	0	0.0627	0.000065
8.5 m/s	0.024	9777	0.00057	0	0.06687	0.000115

Table 5 Results of the surface tension of sample water that performed with various flow velocities through PMDU

Frequency (kHz)	h,ave (m)	γ (N/m^3)	R (m)	θ (deg.)	σ (N/m)	R_f (m^{2}K/W)
0	0.0245	9777	0.00057	0	0.06827	0.00041
0.3	0.0235	9777	0.00057	0	0.06548	
0.5	0.0226	9777	0.00057	0	0.06297	0.00036
2	0.0227	9777	0.00057	0	0.06325	
3.5	0.0227	9777	0.00057	0	0.06325	0.0003

Table 6 Results of the surface tension of sample water that performed with various frequencies of SCED

Figure 1. Schematic diagram of the present test facility for water sampling

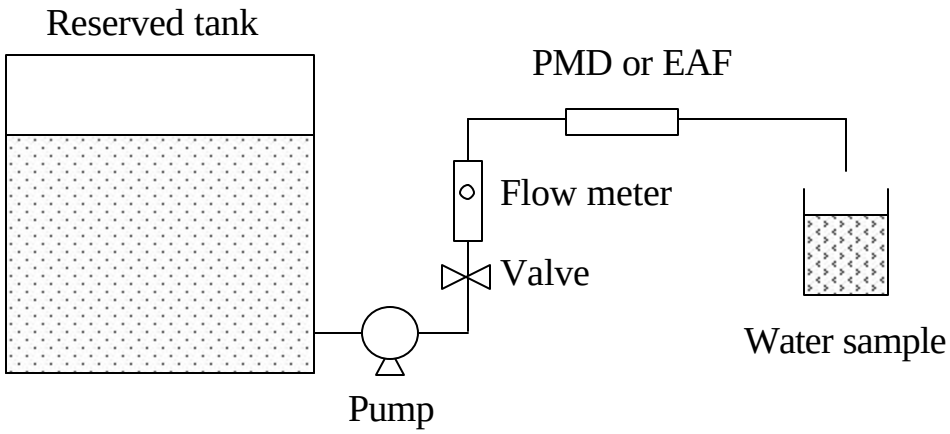

Figure 2. Arrangement of permanent magnets and cross-sectional dimension

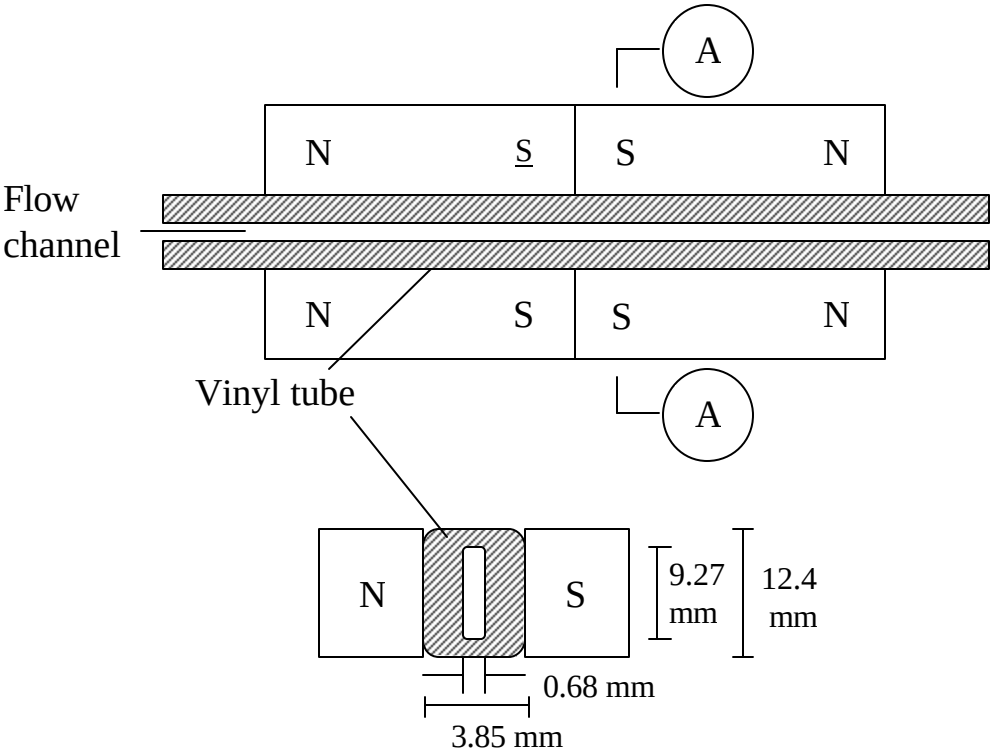

Section view

Figure 3. Sketch of a SCED unit and a solenoid coil

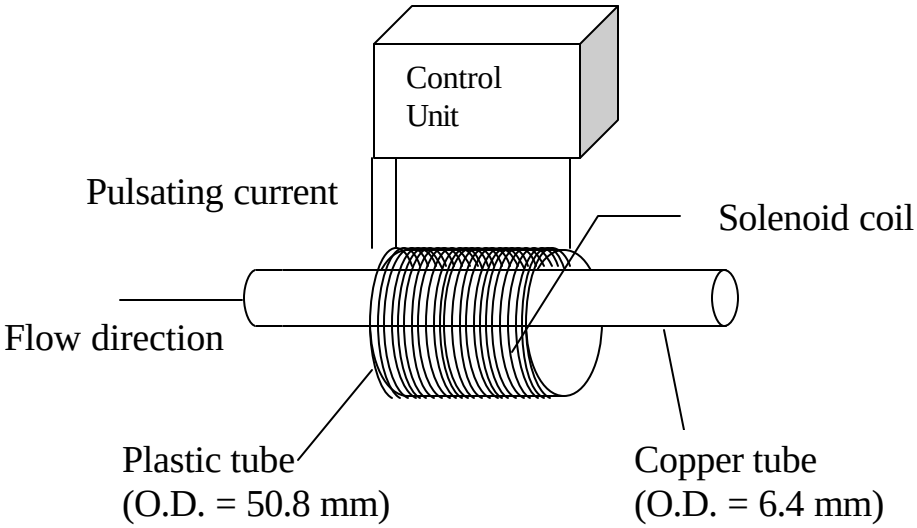

Figure 4. (a) Schematic diagram of capillary tube system

(b) Schematic diagram of dye injection experiment system

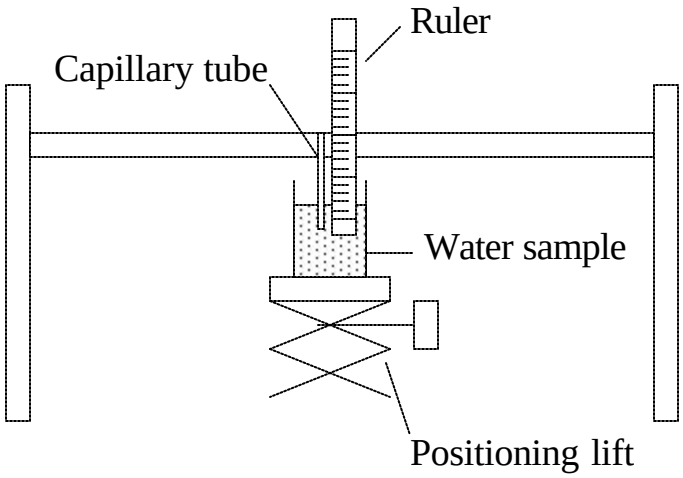

(a)

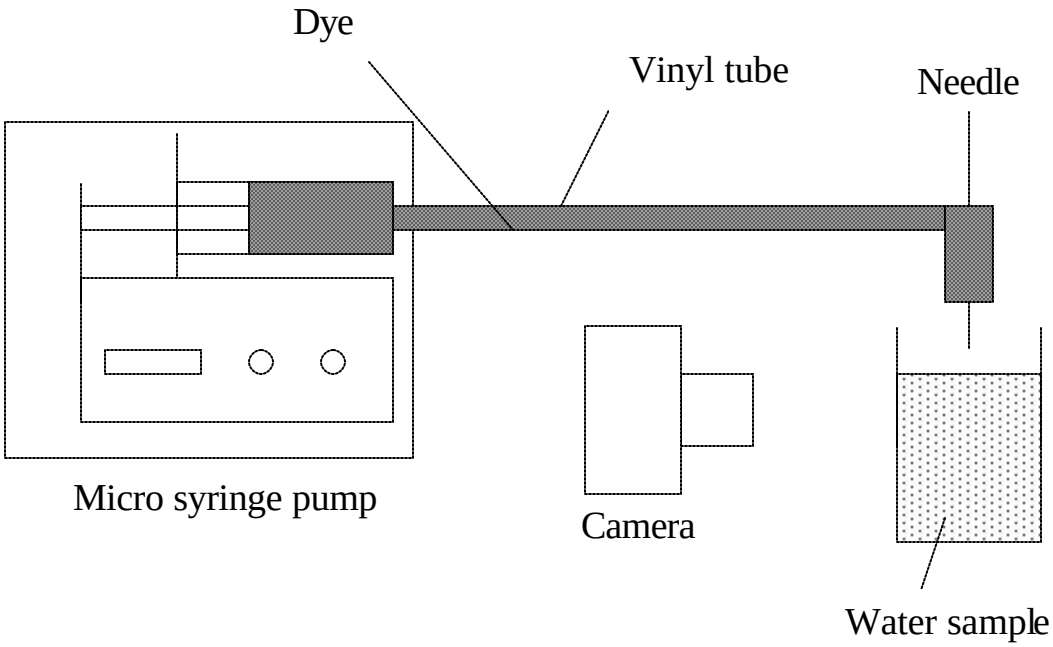

(b)

Figure 5. (a) Results of the surface tension of tap water with changing of the number of treatment without the PWT (baseline date) (b) for natural hard water

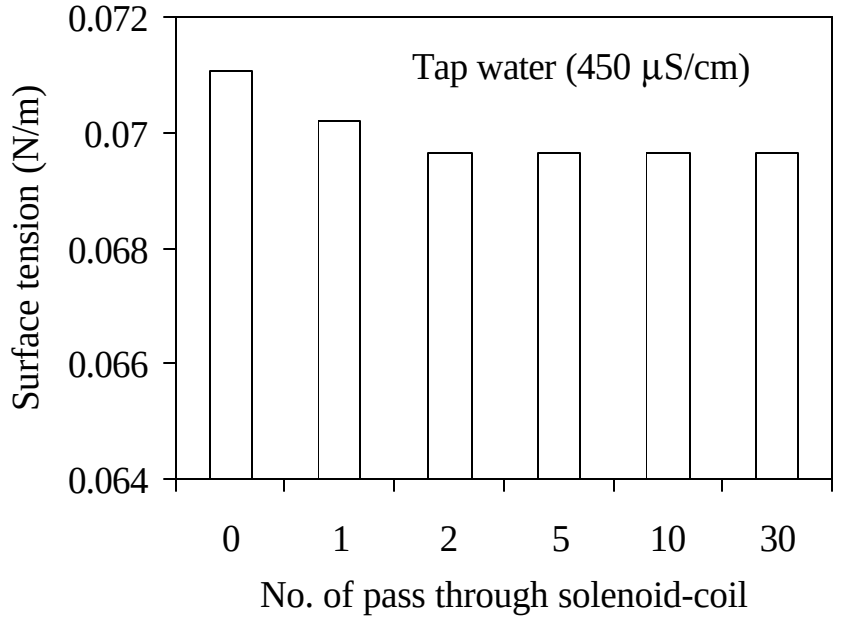

(a)

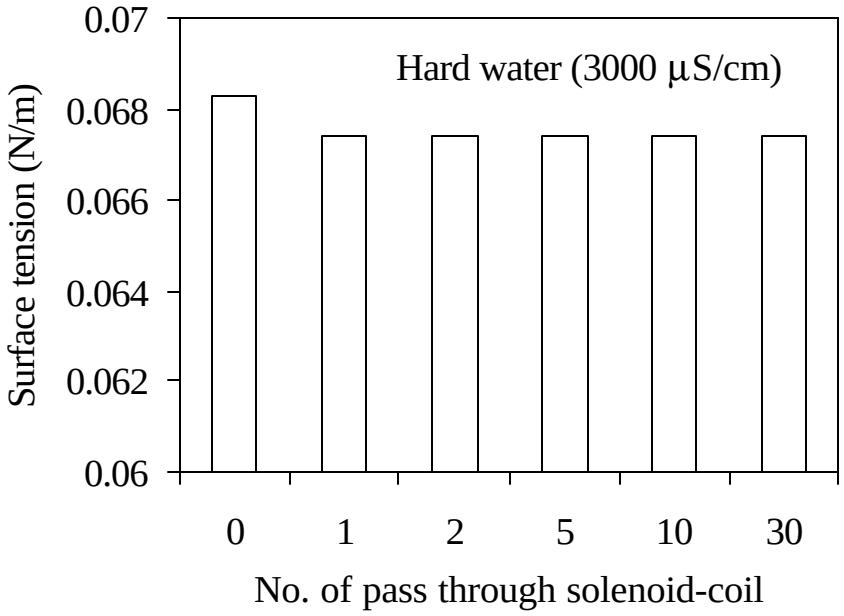

(b)

Figure 6. (a) Results of the surface tension of tap water with changing of the number of PMDU treatment (b) for natural hard water

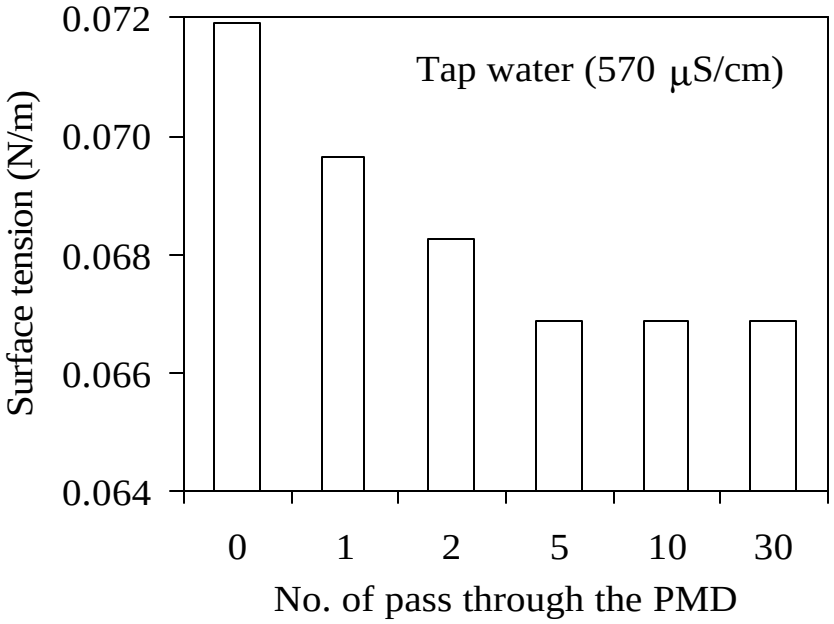

(a)

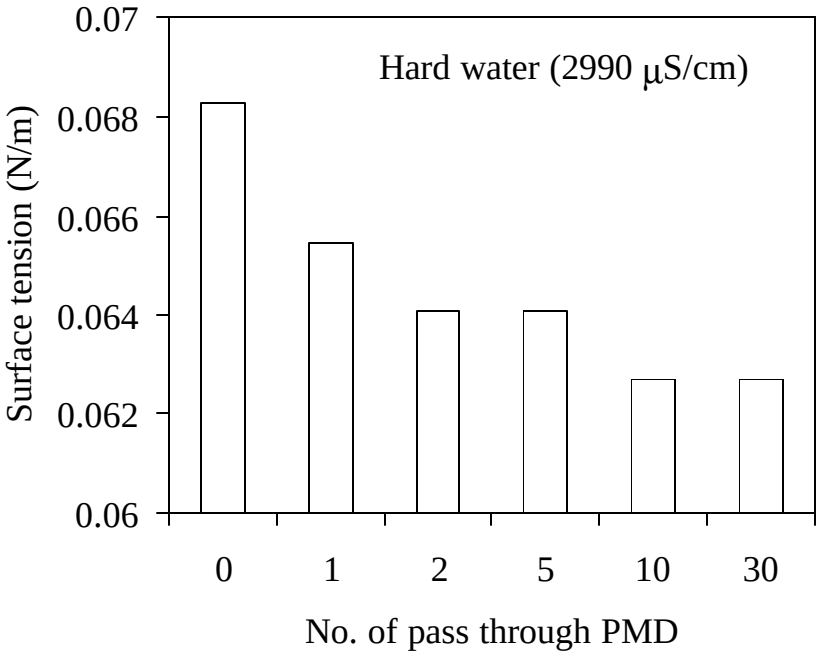

(b)

Figure 7. Photographs of dye injection experiment with water samples treated by PMDU

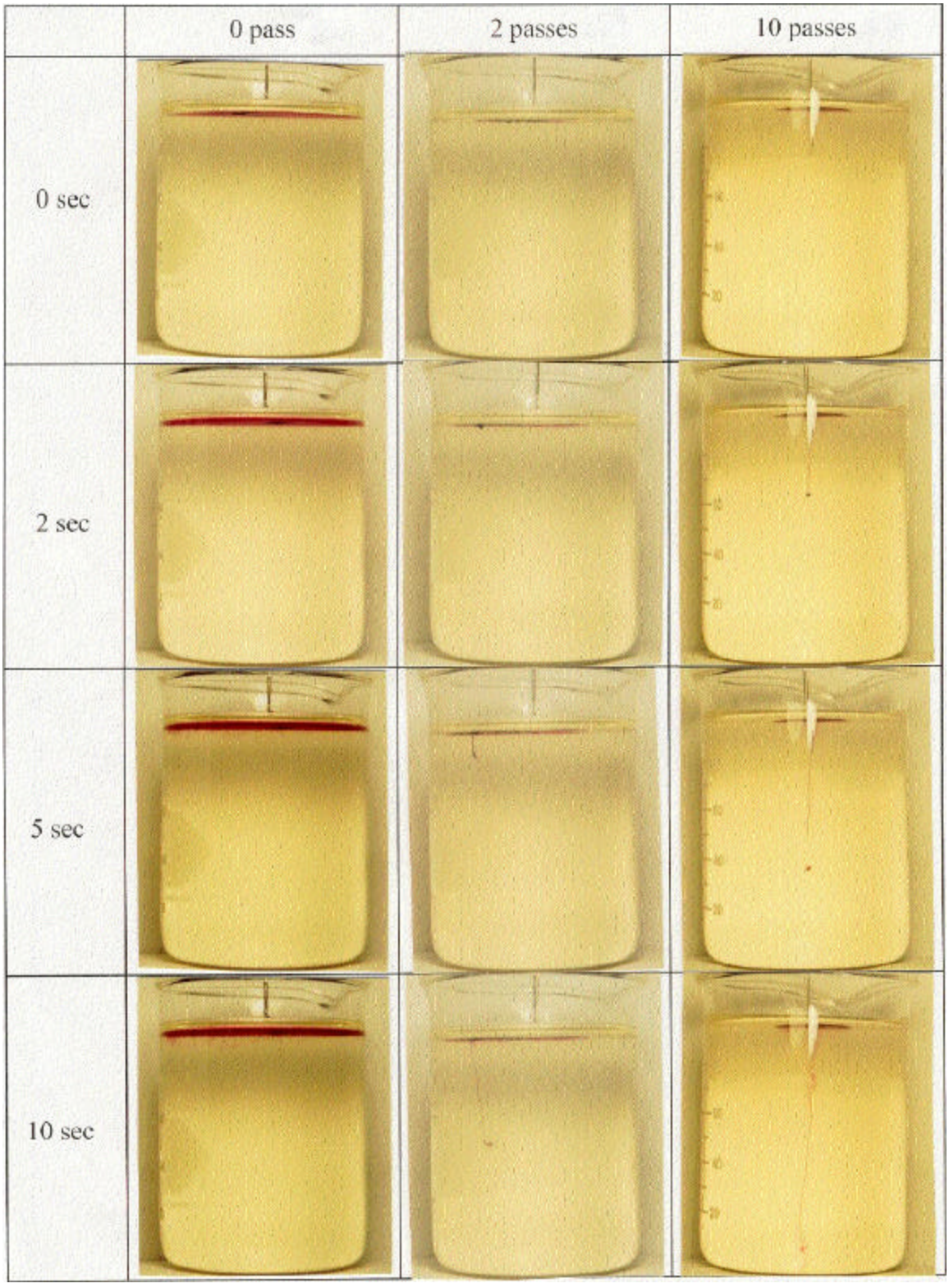

Figure 8. (a) Results of the surface tension of tap water with changing of the number of SCED treatment (b) for natural hard water

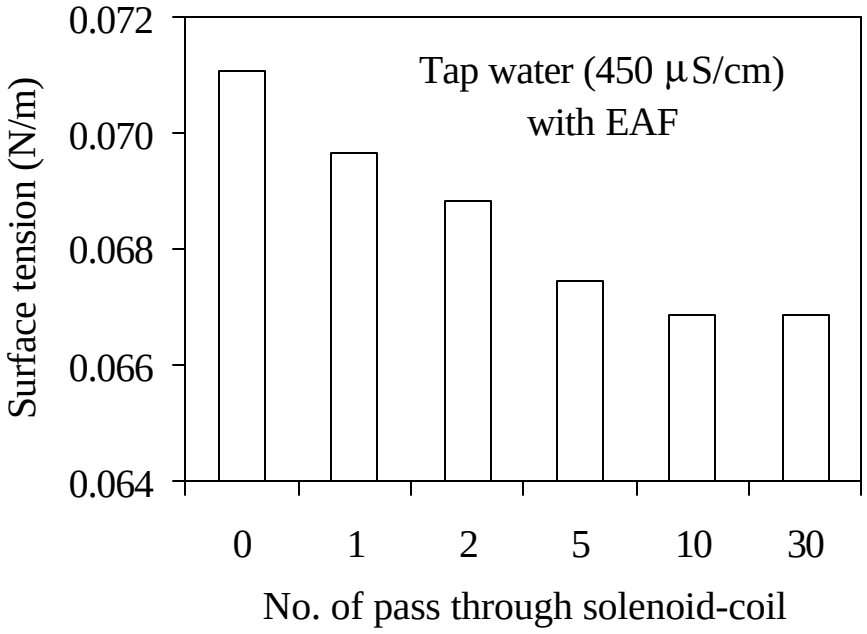

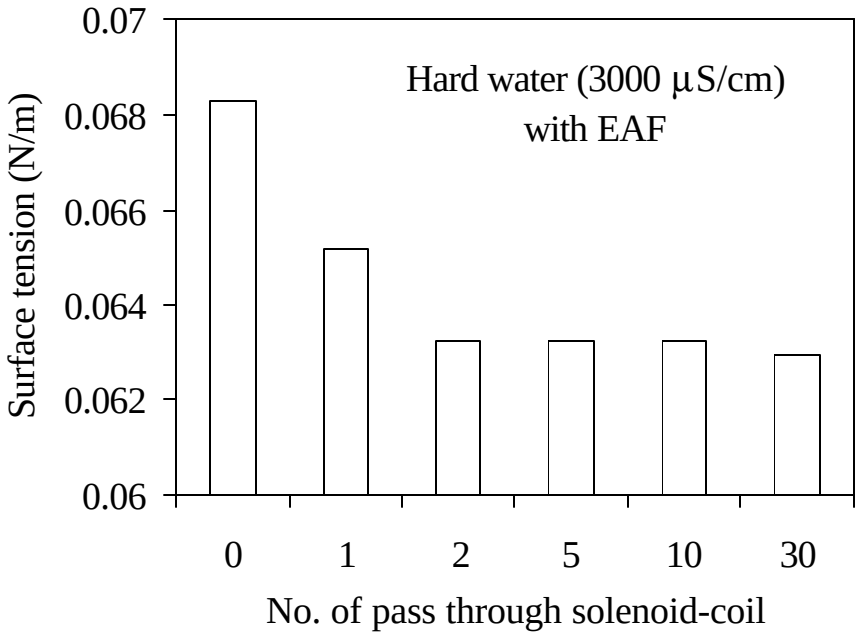

(b)

Figure 9. Photographs of dye injection experiment with water samples treated by SCED

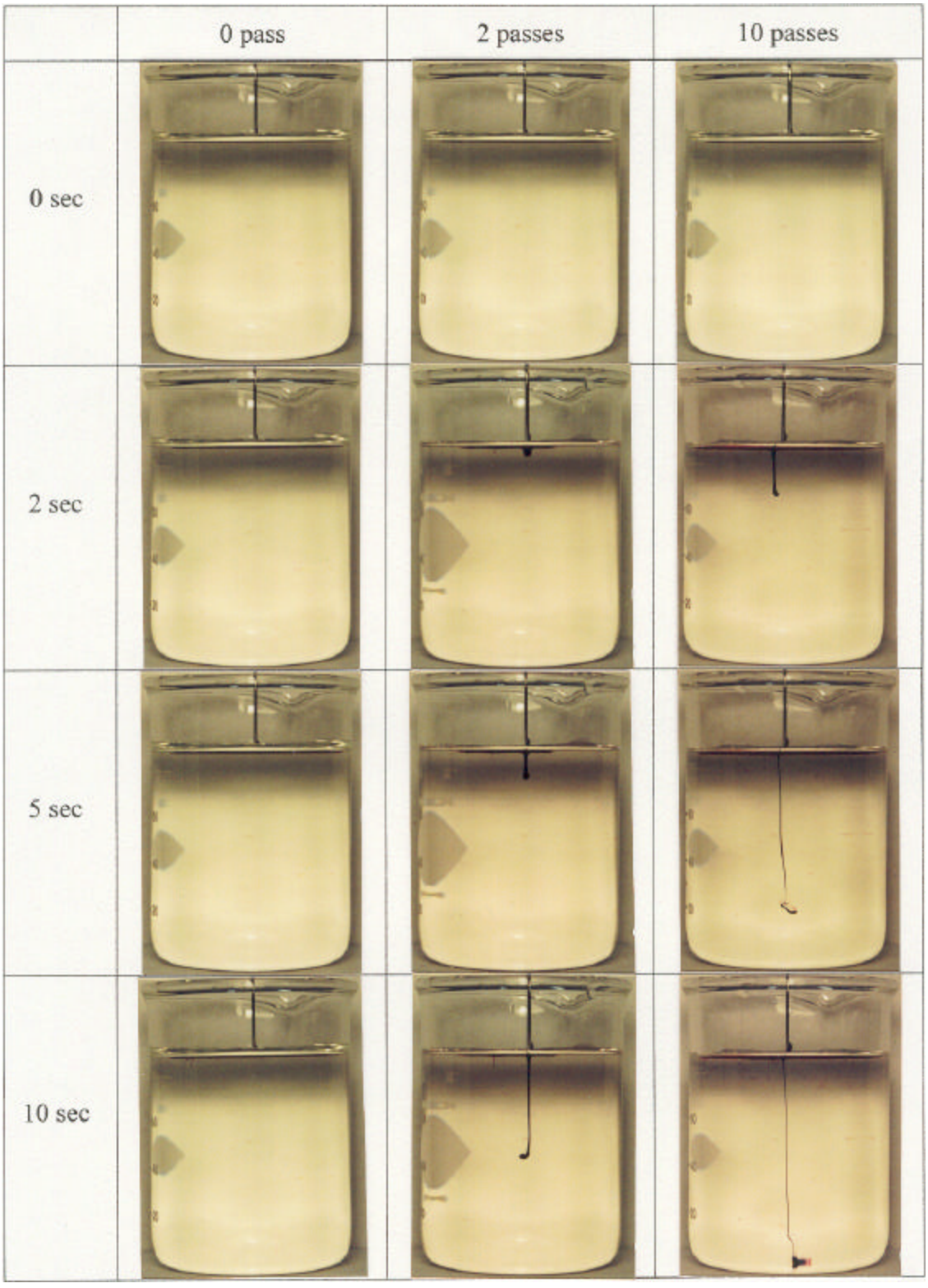

Figure 10. (a) Results of the surface tension of sample water that performed with various flow velocities through PMDU
(b) Results of fouling resistance from a previous heat exchanger experiment

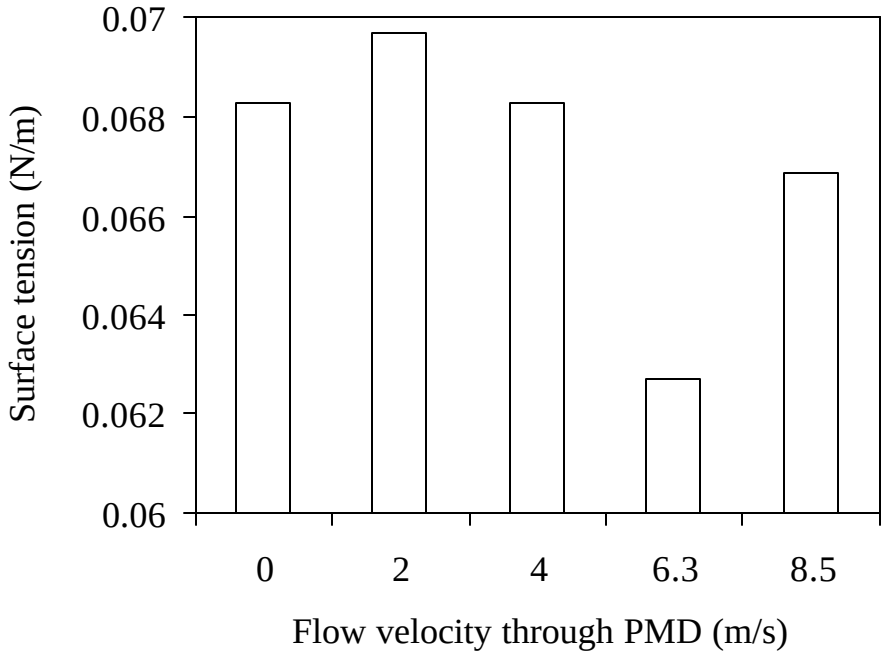

(a)

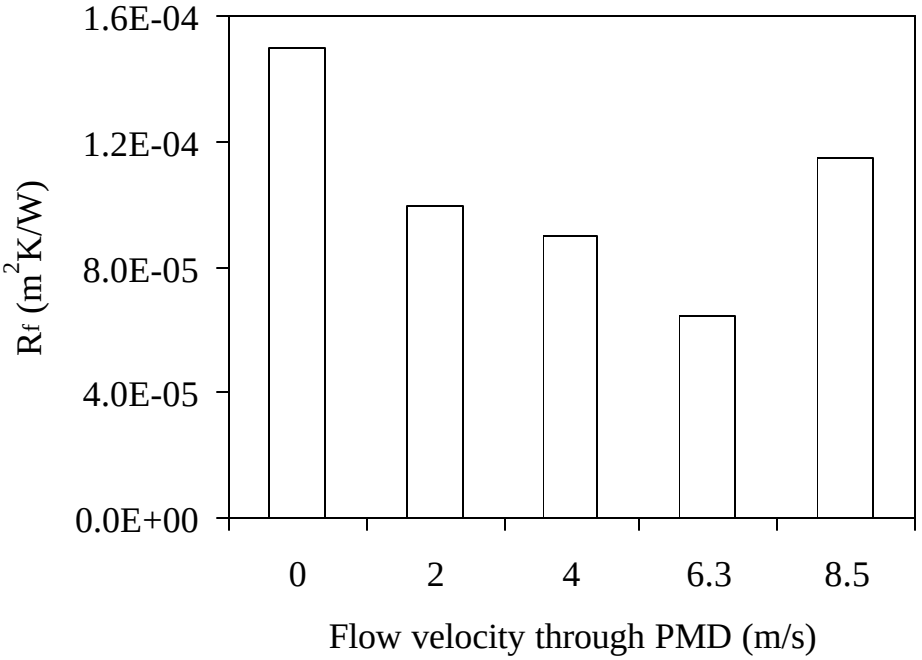

(b)

Figure 11. (a) Results of the surface tension of sample water that performed with various frequencies of SCED
(b) Results of fouling resistance from a previous heat exchanger experiment

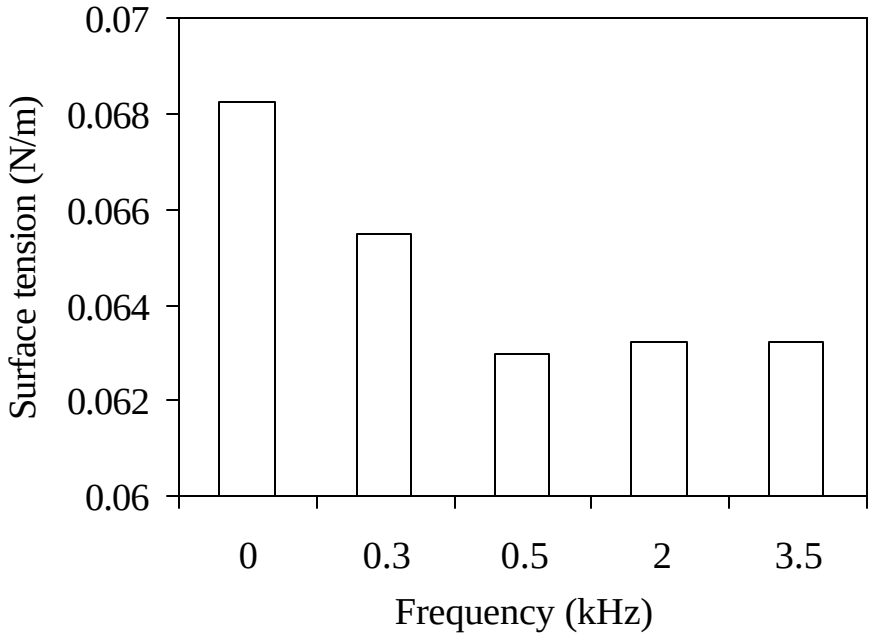

(a)

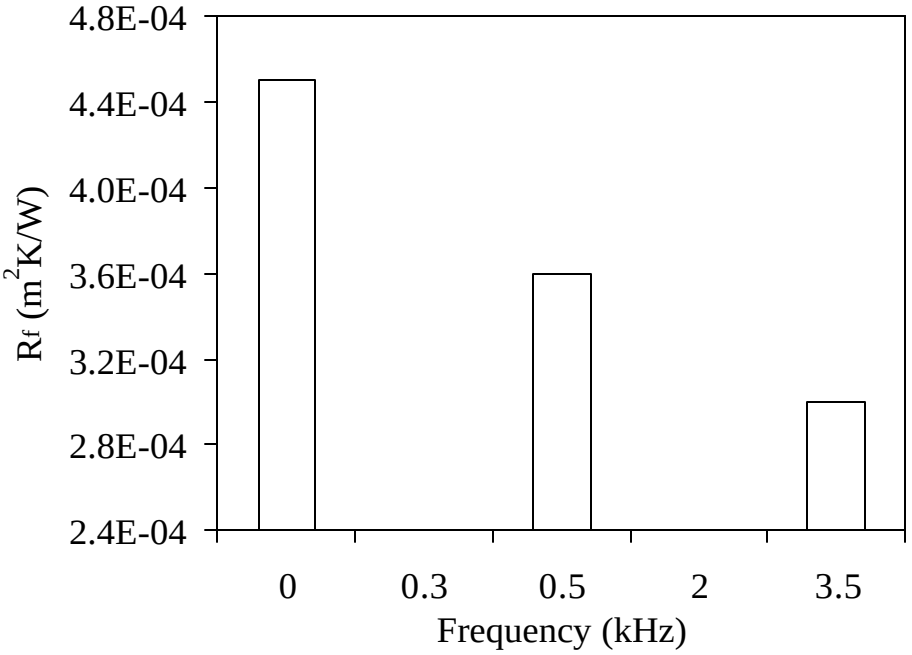

(b)

Appendix

Review of Magnetic Water Treatment

ASHRAE Research Project 1155-TRP

Title: Efficiency of physical water treatments in controlling calcium scale accumulation in recirculating open cooling water system

prepared by

Professor Young I. Cho
Department of Mechanical Eng. & Mechanics
Drexel University
Philadelphia, PA 19104
Phone: 215-895-2425
Fax: 215-895-1478
e-mail: choyi@drexel.edu

March 31, 2002

References	Theory/Hypothesis	Observation	Discussion
Vermeiren 1958	Magnetism changes a behavior of electrons; it increases their kinetic energy.	Increase of pH $\rightarrow$ formation of matter in solution	The treatment gives a physical sensation of softness to the water, as the roughening action on the skin due to hardness disappears, resulting in the colloidal state.
Joshi 1966	Changes in physical properties of water - surface tension - pH - dielectric constant	Neutral water is seen to become more alkaline by the treatment.	A possible reason for this may be the change in the ionization constant of water under the influence of magnetic field resulting in decrease in the concentration of H_3O^+ ions.
Batrakov 1969		After the magnetic treatment, the excess calcium carbonate separated out in the form of very fine crystallites and their number and dimension varied in a regular fashion with the variation in the magnetic field' s intensity.	
	Many compounds even in conventional distilled water have ferromagnetic properties (many hydrated forms of iron oxide) and their colloidal particles must move intensely during passage through a magnetic field. As a result, just as in the case of simple mechanical mixing, the supersaturated solution must be crystallized.		A multitude of microscopic crystallites was formed in the conventional distilled water, while there were no such crystallites in the water that contained practically no iron.
	* Reproducibility : The treatment with a magnetic field does not always give the same result.		
Klassen 1969	The magnetic treatment yields measurable results only if the water, figuratively speaking, is first somehow "perturbed": for example, it flows with a definite velocity, is supersaturated with various substances, is subjected to a sharp temperature change, or, an electric current is passed through the water along with the application of the magnetic field.		Verified in practice and confirmed in laboratories: - reduction of scale formation in steam boilers - effective removal of finely dispersed particles from water ; in the purification of waste and recycled water
Diamant 1970	Crystallization takes place on multiple nuclei in the solution, producing sludge.		The water is passed through the magnetic field at a specially chosen speed and this changes the precipitator properties of the dissolved salts.

Belova 1972	The magnetic field reduces the freedom of movement of charged particles. An effective magnetic treatment of water is achieved only if the liquid flows in a field with a sufficiently steep gradient or even in the field of several magnets with alternate poles. The limitation of the motion of particles in the field leads to an increase in the number of collisions and the formation of centers of crystallization.		To understand the interactions of the velocity field and the magnetic field, it will be necessary to carry out experiments strictly thought out so as to reduce to a minimum the number of variable parameters.
Duffy 1977	Magnetic anti-scale devices could indirectly retard $CaCO_3$ scale formation. The function of the magnetic device is to increase the concentration of iron ions in solution by increasing the rate of corrosion of the attached iron pipe by either magnetic and/or galvanic effects.		Adverse effect of the magnetic devices on the corrosion rate of the iron pipe
Sandulyak 1982	Effect of Heat flux (2.6-13 kW/m^2)	With increasing specific heat load the achieved anti-scale effect is due to "secondary" scale formation – adherence of suspensions to the heat exchanger surfaces. > more effective with a relatively low heat load	
	Hydrodynamic criterion	The hydrodynamic criterion for magnetic treatment is not the velocity, but the Reynolds number.	
Grutch 1984	Conclusions - Carefully selected magnetic water treating devices, designed and installed to operate to yield magnetohydrodynamic (MHD) energy, were highly successful controlling scaling when operating in an industrial environment under conditions of $CaCO_3$ and $CaSO_4$ scaling. - A magnetic device having two focused magnetic fields of about 1,700 gauss with the water flowing through the magnetic field at a rate of at least 6 m/s (20 fps) resulted in adequate treatment for scale control. - MHD energy may play a role in determining the effectiveness of the magnetic water treatment unit as evidenced by the experience that low flow rates through the magnetic fields resulted in scaling whereas at 6 m/s no scaling was observed.		
Raisen 1984	The magnetic field induces the scale forming species to either remain soluble and be discharged with the bleed or blowdown in the system, or form small particles which settle in low velocity portions of the system where they can be easily removed.		The magnetic unit was very effective in controlling scale and corrosion in water systems, in such diverse applications as, a large air conditioner, syrup evaporators in a sugar mill, cooling exchangers in a large chemical processing plant, in a boiler and a steam generator.
API 1985	Alteration of the solubility product constant: - through a change in the association of ions with each other or with the water molecules that hydrate them, or - through a change in the structure of the water surrounding the ions The passage of conducting solutions through the MTD generates voltages and currents, which result in an electrolysis reaction involving the corrosion of iron.		Need to study - possible role of the iron-containing colloidal - alteration in the electric double layer surrounding colloidal material - changes in the water of hydration of dissolved species - interactions of the magnetic field with charged colloidal dispersions

Szostak 1985	The multi-intersect design of the magnetic fluid conditioner (MFC) causes the precipitating agents to combine to form nucleating centers – colloids having excessive surface charge or Zeta potential. The positively charged colloidal particles repel one another and remain in suspension due to Brownian forces.	The internal design of the MFC reduces the cross-sectional area to accelerate the fluid flow through the magnetic fields – from the nominal 7 ft/sec to over 20 ft/sec (flow rate is restored to 7 ft/sec at the end of the spool). The high velocity causes calcium carbonate, calcium sulfate and other salts to nucleate.	Test conditions - Cooling tower - above50 COC (10,000 µS/cm) - hardness (above 4,000 ppm) - pH = 8 to 9
Hasson 1985	The accurate rate data showed that magnetic exposure had no effect on deposit growth.		Test conditions Recycle runs [Ca] = 125-170; [CO_3] = 160-260; [Na_2SO_3] = 200-275 pH=9.5 flow velocity = 2 m/s
Kronenberg 1985	Resonance between the time sequence of the magnetic fields and the internal vibratory frequency of the water complexes results in the fracture of some of the complexes.	• Effective magnetic treatment results in a separation of formerly dissolved minerals from the liquid water by forming micro-crystals, which move with the water in suspension. • The internal seeding effect of the magnetic water treatment lasts for up to two days. • The following changes last only for a few minutes. - Reduction of surface tension - Reduction of viscosity by up to 2% - Changes of the electro-optical values of the water	The dependency of the magnetic effects on a specific velocity of the water leads to the conclusion that the weak interaction between the magnetic fields and the hydrogen bonds is amplified to the breaking point by resonance.
Kronenberg 1986	Experiences in the Russian papers 1. The water to be treated has to move across magnetic fields not stronger than 1000 to 2000 Oersted. 2. For a certain flow-velocity the effect is a maximum. 3. It usually works better for water of a lower temperature. 4. Some small changes of the physical constants of the water last only for a few minutes. 5. The capability of the water to prevent formation of hard lime scale may last for up to 2 days. 6. Instead of forming hard lime scale (“Slake”) clinging to the walls of the container, the calcium carbonate of magnetically treated water forms a soft sludge, flowing with the water. 7. Reliable observations of the effects of the magnetic treatment require several weeks. Many attempts of faster results have not always been conclusive. 8. The magnetically treated water is able to dissolve formerly deposited lime scale.		

Parker 1985	<u>Postulation</u> It is postulated that the MTD tested may operate via the electrolysis reaction by producing nucleation centers, which favor precipitation of scaling salts in the bulk of the solution rather than on the walls of the plumbing.		Magnetic treatment parameters - magnet types - flow velocity - strength of magnetic field
Busch 1986	The magnitude of the voltage is found to vary with the solution flow rate in accordance with well-known laws of physics governing the motion of charged particles under the influence of a magnetic field. A minimum flow velocity that created sufficient induced current was in the range of 5 to 6 m/s.		A minimum flow rate is required for the effective operation of MTD in scale control.
Reimers 1986	<u>Overall review</u> Marked reduction of scale formation in steam boilers has been verified in practice and confirmed in laboratories. But, in the various studies of and experiments with magnetic treatment of water, many arguments have been raised because the magnetic treatment does not always produce the same result and one of the fundamental requirements imposed on any experiment is complete reproducibility of the results.		
	U.S. Testing Company, Inc.	The dominant crystal species in the untreated sample is calcium sulfate and calcium silicate, while in the treated sample the dominant species are a calcium carbonate and calcium sulfate. The samples are physically different.	
	Advanced Research Projects Agency	Reduction of freedom of movement of charged particles > increase in the number of collisions > formation of crystallization centers * Magnetic treatment is effective only if the liquid is passed between the poles of a magnet having a sufficiently strong field and magnetic gradient, providing that the temperature of the liquid is not too high.	
	NASA	50 mils per year using chemical inhibitors 0.0 mils per year for the magnetic treatment	
	USSR Academy of Sciences	Marked reduction of scale formation in steam boilers	
	Ohio State University	Results did support the crystal growth inhibition mechanism.	

	Water Reuse Symposium	<u>Basic phenomenon behind the treatment</u> 1. Matter is composed of atoms containing outer valence electrons. 2. Minerals generally form ionic bonds which are specifically arranged into a definite structure of ionic lattice. 3. These ions within the crystalline lattice are held in place by the balance of both attractive and repulsive electrostatic forces. Generally, ionic salts will dissolve in aqueous solutions due to the highly polar structure of the water molecules. 4. Immediately prior to precipitation of any inorganic substance such as calcium sulfate, these ions will form a quasi-ionic lattice similar to its solid crystalline structure (commonly called liquid crystals). 5. A magnetic field resulting from an electrode will exert a force on an electron moving perpendicular to it. Therefore, an electrode will tend to dislocate the ionic lattice by displacing the electrons from their normal state and inhibit the formation of solid crystals.	
Donaldson & Grimes 1988	<u>Lorentz effect</u>: The combined effects of an applied magnetic field, a charged species, the induced magnetic field on the charged species and rate of flow the fluid, could together produce energy that, by normal collision processes between molecules, could act downstream in the system, removing and preventing scale. This explanation may have a weak point because the amount of energy produced in this process in typical scale-forming systems is likely to be small. Thus, this energy might be important in modifying the way in which crystals form around a nucleus. <u>Modification in ionic interactions</u>: The magnetic field acts at the surface of the crystallites, modifying the nature of the charges at the surface. The change in solubility explains why scale starts to dissolve.		
Grimes 1988	Two major factors - solubility - nucleation process	The nucleation centers of crystal growth will be very small and have highly charged surfaces. The Lorentz energy will be dissipated by the normal collision of the ions. It could be a significant factor in the crystal nucleation process when the ions collide with, and grow on, the surface of the growing crystal.	
Herzog 1989	• A magnetic field somehow alters the properties of water. • A magnetic field directly affects precipitation of scale-forming salts.	None of the ferric hydroxide minerals was particularly effective at inducing nucleation of $CaCO_3$ from supersaturated solution. Magnetic water treatment devices could induce the liberation of iron into the water, and scale growth thus could be inhibited.	

Kronenberg 1990	Issue Whenever the calcium carbonate becomes over concentrated, it starts to solidify wherever it finds available starting points. In ordinary water, all starting points are ineffective because they are hidden in the water molecule clusters. Therefore, only the walls of the container offer a starting point for the crystallization. All we have to do is open up a number of these clusters to expose the enclosed foreign particles. Then, the calcium carbonate does not have to settle on the walls of the container because there are sufficient starting points nearby in the entire volume of the water.		Function of the permanent magnets There is a requirement that the water travels passed a number of magnetic fields of alternating polarity. The flow velocity is critical for the conditioning effect. As the flow passes through alternating poles, a vibration is generated. Note that a static magnetic field would need to be a million times stronger to have a direct effect on the bonds in the water complexes (water clusters) but resonance may make amplifications in the billions possible. There will be a number of complexes in the water the internal vibratory motion happens to have the same frequency as the sequence of the magnetic fields encountered. Those complexes are fractured and their internal, foreign particle is made available to the over concentrated calcium carbonate. The complexes are so numerous that only a very small portion of them needs to break open to provide enough nucleation centers to the over concentrated calcium carbonate.
Bernardin 1991	Issue How may magnetic fields indirectly reduce scale buildup by introducing higher amounts of iron by increased corrosion?	• Transmission test (effect on molecular structure) The sample was placed in a 1200 G magnetic field. It was found 0% change in the structure of water. • Polymerization test (effect on polymerization rates of various brines supersaturated with silica) No difference in polymerization rates between the control and test solutions was detected.	It is reasonable to assume that magnetic water treatment devices indirectly prevent scale buildup by accelerating the corrosion of the iron piping. The iron in turn retards crystal growth both on heat exchanger and plumbing surfaces as well as in the bulk of the supersaturated solutions. Therefore, the supersaturation level of the solution is retained and more nucleation sites are activated. This results in a relatively greater number of smaller crystals forming in solution.
Hu & Jacobi 1991	Literature review To conclusively prove the potential applicability of magnetic water treatment in heat transfer applications, repeatable experiments must be reported in the literature, which indisputably demonstrate an alteration in the thermophysical or scaling behavior of water. If repeatable observations are produced in the laboratory, then the burden will shift to the theoreticians, who must then explain the observations within the current theoretical framework, or expand this framework such that the observations are consistent.		
Higashitani 1993	• The nucleation frequency of $CaCO_3$ particles is suppressed but the growth of particles is accelerated, if the exposed magnetic flux density is greater than about 0.3 T and the exposure time is greater than 10 min; • The magnetic effect is attributable mainly to the magnetic exposure on Na_2CO_3 solutions but not to that on $CaCl_2$ solutions; • The magnetic effect was observed even if $CaCl_2$ and Na_2CO_3 solutions were mixed at 120h after the magnetic exposure (so called a magnetic memory effect); • The formation of aragonite structure of $CaCO_3$ crystals is accelerated by the magnetic exposure.		

<table>
<tr><td rowspan="3">Lipus
1994</td><td>The magnetic effect is due to structural change in water.</td><td>But, the energy of interaction between a water molecule and the magnetic field is in the order of 10^{-6} of the hydrogen bonds, i.e. negligible. Also, there is no reason to expect relaxation times (memory effect) longer than 10^{-6} second.</td><td rowspan="2">We believe that the effect of magnetic treatment in reducing scale formation is due to the magnetic force (Lorenze force). This force tends to displace positive and negative ions in opposite directions, which can activate dislocations on the surfaces of seed crystals.
We postulate further that these crystallization centers would allow $CaCO_3$ to precipitate in the solution rather than on the surface of heating apparatus, resulting in an increase in amount of non-adhering precipitate and a decrease in amount of adhering scale.</td></tr>
<tr><td>The effect is caused by physical or chemical changes in the impurities contained in the water as a result of magnetic exposure.</td><td></td></tr>
<tr><td colspan="3">[Consideration of flow velocity]
• Higher velocity gives too short retention time in the magnetic field, while lower velocity causes at given water flow rate too large exposure cross-section with weaker magnetic field at given electric input.
• At very high flow rates, the system is no more economic in the hydraulic sense, because pressure drops are quadratic proportional to flow rate.</td></tr>
<tr><td>Gehr
1995</td><td>Tests in the magnetic field of a nuclear magnetic resonance spectrometer</td><td>The magnetic treatment had an effect on the precipitation of $CaSO_4$ crystals. Conductivity, soluble Ca, and zeta potential all decreased, whereas total suspended solids increased.</td><td>The reason for the drop in zeta potential is not clear, but it does point indirectly to the effect of magnetic treatment increasing the coagulating tendency of the suspension.</td></tr>
<tr><td rowspan="2">Al-Qahtani
1996</td><td colspan="2">According to Faraday' s law, charged particles moving through a magnetic field with a velocity perpendicular to the field, create a localized electrical field perpendicular to both particle velocity and the magnetic field. If the ion concentration, velocity, and magnetic strength are sufficiently large, the Lorentz effect can be observed. Therefore, whenever a conductive fluid is passed through a magnetic field under the right conditions, an induced electrical current is generated and effectively oriented the charged particles suspended in the solution.</td><td>[Ca] = 950 ppm;
[Mg] = 6,300
7,000 gauss
5 ft/s</td></tr>
<tr><td colspan="3"><u>Conclusion</u>
Passing seawater solutions through a permanent magnetic device increased the conductivity and the pH of the solutions. Separation of salt from water by reverse osmosis was enhanced when the solutions circulated through the magnet device. Therefore, it is believed that the magnetic device might cause certain physical or/and chemical changes to the nature of the ions, which might have a lower possibility of passing through the membrane.</td></tr>
</table>

Baker 1996 *Review paper*	<u>Difficulties of demonstration of MTD effect</u> - Irreproducibility by subsequent research - Inadequate or unspecified control of solution chemistry, in particular the solution pH and the level of contamination by scale-adjusting ions - Unspecified physical conditions, for example the magnetic field orientation and treatment time <u>Physicochemical mechanisms</u> - Intra-atomic effects (e.g. changes in electron configuration) - Contamination effects (due to magnetically-enhanced dissolution) - Inter-molecular/ionic effects (e.g. changes in coordination of water with ions) - Interfacial effects (e.g. distortion of the double layer; change in the charge and potential) <u>The majority of the reported evidence</u> - orthogonal fluid flow respect to the magnetic field orientation - recirculated solution and/or prolonged magnetic exposure <u>Conclusions</u> - The efficacy of MTD with respect to specific applications, operating under particular physicochemical conditions, remains unclear. - Since no universally agreed mechanism for the process exists, optimum operating conditions with respect to field strength, field orientation, treatment time and fluid flow velocity cannot be defined from first principles. - Strict control of critical controlling parameters such as temperature and pH must be maintained for result to be unambiguous. <u>Further works</u> - Experimental correlations of field strength, field orientation, flow velocity and exposure time with surface charge/electrokinetic parameters on crystallizing and noncrystallizing particles - Calculation of energy demanded to change the potential at the shear plane by redistribution of ions in the electrical double layer for various oxide-ion systems	
Wang 1996	Performed laboratory experiments concerning the formation of calcium carbonate from super-saturated solution with a light-scattering method.	Under certain conditions in the presence of an external magnetic field, the nucleation rate can be greatly increased. This was observed as a rapid onset or burst of crystallization within the bulk solution, and can be quantitatively described as the scattering of incident light (Tyndall effect). As a consequence of the faster precipitation in the presence of the magnetic field, the resultant crystals are greater in number, with smaller sizes and irregular shapes.

Busch 1997 *Review paper*	Prediction of successful operation of MTD - The MTD will require a sufficiently fast, continuous flow of fluid. If magneto-hydrodynamic forces are responsible for the action of the device, continuous fluid flow is required to generate these forces. - The magnetic field must be of sufficient strength and oriented 90^{o} relative to the direction of fluid flow. Only when the conducting fluid cuts the magnetic lines of force will magneto-hydrodynamic forces of the type described here be generated. - By Ohm' s Law, the magnitude of the current produced by fluid flow through the field is proportional to the solution conductivity. Thus, the treated solution must have sufficient conductivity to produce a current. Conclusions - We cannot yet prove that these effects are directly linked to the claims of scale reduction. - Even if magnetic treatment can be shown to reduce scaling conditions when used properly, the question remains as to whether the technology is robust enough in comparison with chemical means of scale prevention. If magnetic treatment devices are effective, and we are finally able to understand how they operate, the best strategy could be a combination of magnetic and chemical treatment.
Marth 1997	The Magnetic treatment of water process is defined as: the coherent orientation of the water' s molecules to a direction that is dependent on the directions of the applied magnetic induction field and water' s velocity. The rate of orientation of the water molecules is dependent on the magnitudes of the applied magnetic induction field, the water' s velocity, the magnitude of the water' s electric dipole moment, and on the angles between the field, velocity, and dipole moment.
Baker 1997	No reproducible change was found in the nature or the quantity of scale adhered to the wire loops for any of the magnetic treatment regimes used. However, gross physical differences were evident in the nature of this deposit when a highly supersaturated solution was passed through the magnetic field with a sufficient contact velocity.
Parsons 1997 IChem	Test conditions - Orthogonal fluid flow with respect to the magnetic field orientation - Recirculated solution - Accumulative exposure to the magnetic fields of strength >3000 Gauss Results and discussion - No velocity dependency of the magnetically-induced changes on scaling rate was apparent between flow rates of 1-2 m/s. - Magnetic treatment can reduce calcium carbonate scale formation by up to 80%. - The degree of the magnetically-induced change is dependent on solution chemistry. - Magnetic amelioration of scaling is removed when the system' s pH is controlled. - Surface charge (zeta potential) is reduced by an average 16% in the reported experiments. - Nucleation and crystal growth rates are reduced, leading to the formation of irregularly shaped crystal forms. - Magnetic treatment is an interfacial effect.

Barrett 1998 Wat. Res.	Test conditions - Artificial hard water (distilled water + $CaCl_2$, $CaSO_4$, and Na_2CO_3) - Static magnetic field was generated by an electromagnet, average magnetic field strength=4500 gauss - Measurement of absorbance and SEM photographs Results and discussion - Absorbance for the magnetized was always less than that of non-magnetized solution - After filtration with 0.45 micron, absorbance reduced. - Magnetic effect on the formation of $CaCO_3$ crystals can be mainly attributed to the magnetic exposure of Na2CO3 soution. - SEM photographic evidence of crystal morphology was considered too subjective to be of value in qualitative analysis of magnetic effect. Conclusion - Application of a magnetic field to a quiescent solution influences $CaCO_3$ particle formation and is reproducible.	
Bogatin 1999	Magnetic field results in: - the total or partial destruction of hydrate layers, - an increase in the amount of active crystallization centers, and - the enhancement of the probability of coagulation. Centers of phase formation can be ions, molecules, or micro-particles with disturbed hydrate shells. A rapid change of the magnetic field in a magnetic apparatus of appropriate design loosens and distracts hydrate layers and films in a moving liquid, thus facilitating coagulation and coalescence.	The test results showed that the important components for effective magnetic treatment were flow rate (velocity) through the apparatus and certain chemical parameters of water, namely, carbonate water hardness of more than 50 mg/L and concentration of hydrogenous ions in water at pH>7.2.
Parsons 1999 MAG3	In the work for the effect of MTD over the past four year, Parsons concluded that: - Magnetic treatment can reduce scaling under the correct conditions of temperature, pH, hardness and flow. There is no reproducible evidence that once-through magnetic treatment can consistently reduce scaling. - The type of scale formed during magnetic treatment is changed when compared to a reference. - Results seen during static treatment require further evaluation. - Electronic water conditioners cannot soften water under the conditions tested here. - Magnetic treatment increasing the coagulating tendency of the suspension by decreasing double-layer repulsion. This then keeps the crystals in solution rather than allowing them to crystallize on the pipe walls.	
Coey 2000	Test conditions - Water sample : Well water, mineral water - Static magnetic field was generated by an electromagnet, range of magnetic field strength - 1000 gauss - Measurement of X-ray diffraction and electron microscopy Results and discussion - By applying magnetic field, the aragonite/calcite ratio in the deposit was increased. - By applying magnetic field, memory of magnetic treatment extended beyond 200 hours.	

Kobe 2001	Test conditions - Artificial hard water (distilled water + $CaCl_2$, $CaSO_4$, and Na_2CO_3) - Static magnetic field was generated by an electromagnet, range of magnetic field strength - 5000 to 15000 gauss - Measurement of X-ray analysis and TEM Results and discussion - Separate aragonite crystals were formed in the treated water and clusters of calcite in the untreated water.
Gabrielli 2001 Wat. Res.	Test conditions - Carbonically pure water containing 200 mg dm^{-3} Ca^{2+} was prepared by dissolving 500 mg dm^{-3} $CaCO_3$ in deionized water through bubbling of carbon dioxide. - Used permanent magnetic device, one wass alternated poles the other was not, magnetic field strength - 1600 gauss - Measurement of ionic calcium content and amount of dissolved oxygen (oxygen reduction > pH increase > increase precipitation of calcium carbonate) Results and discussion - By using alternating arrangement, the efficiency of the magnetic treatment seemed to be better. - The efficiency of the magnetic treatment seemed to be independent of the water hardness. - When the flow velocity through the magnetic device was increased from 0 to 3.6 m/s, the amount of dissolved calcium ions was reduced.
Vedavyasan 2001 Desalination	Practical study of biofouling of seawater/brackish water and the pre-treatment methods Experimental system is composed of - Reverse Osmosis system + turbulence generating flow distributors + EMF device Results - Energy saving as much as 18% and significant reduction in downtime

References

[Vermeiren,1958] T. Vermeiren, Magnetic treatment of liquids for scale and corrosion prevention, Corrosion Technology, (1958) 215-219

[Joshi,1966] K.M. Joshi and P.V. Kamat, Effect of magnetic field on the physical properties of water, Jour. Indian Chem. Soc., 43, 9 (1966) 620-622

[Batrakov,1969] V. Batrakov, It is magnetic but not water, Khimiya I Zhizn, Russian, No. 9 (1969) 28-29

[Klassen,1969] V.I. Klassen, Magnetic water: between Scylla and charybdis, Khimiya I Zhizn, Russian, No 9 (1969) 24-27

[Diamant,1970] R.M.E. Diamant, Magnetic treatment of water, Hospital Engineering (1970)

[Belova,1972] V. Belova, Magnetic treatment of water, Soviet Science Review (May 1972) 150-156

[Duffy,1977] E.A. Duffy, Investigation of Magnetic Water Treatment Devices, Ph.D. Thesis, School of Clemson University (August 1977)

[Sandulyak,1982] A.V. Sandulyak and V.V. Krivtsov, Heat and hydrodynamic conditions of magnetic treatment of water against scale formation, Soviet Power Engineering, 5 (1982) 362-367

[Grutsch,1984] J.F. Grutsch and J.W. McClintock, Corrosion and deposit control in alkaline cooling water using magnetic water treatment at AMOCO' s largest refinery, Corrosion 84, 330 (1984) 1-26

[Raisen,1984] E. Raisen, The control of scale and corrosion in water systems using magnetic fields, Corrosion 84, Paper No. 117 (1984)

[API,1985] Evaluation of the principles of magnetic water treatment, Refining Department, American Petroleum Institute, API Publication 960 (1985)

[Szostak,1985] R.J. Szostak, Magnetic fluid conditioning system allows 3000 ppm hardness without cooling tower scale buildup, Chemical Processing (1985) 44-45

[Hasson,1985] D. Hasson and D. Bramson, Effectiveness of magnetic water treatment in suppressing $CaCO_3$ scale deposition, Ind. Eng. Chem. Process Des. Dev., 24 (1985) 588-592

[Kronenberg,1985] K.J. Kronenberg, Experimental evidence for effects of magnetic fields on moving water, IEEE Transactions on magnetics, (1985) 2059-2061

[Kronenberg,1986] K.J. Kronenberg, Magnetic water treatment de-mystified, Magnets (1986) 6-15

[Parker,1985] D.H. Parker, An investigation of the role of magnetic water treatment devices in calcium carbonate scale formation, MS thesis, Baylor University, Texas (1985)

[Busch,1986] K. W. Busch, M. A. Busch, D. H. Parker, An investigation of the role of magnetic water treatment devices in calcium carbonate scale formation, Baylor University, Waco, TX 1985. also, Laboratory studies involving magnetic water treatment devices, Corrosion 85, Paper no. 251, 1985., also, Corrion-NACE, Vol.42, (1986) 211-221

[Reimers,1986] R. S. Reimers, S. F. Bock, L. E. White, Applied fields for energy conservation, water treatment and industrial applications, US DOE/CE/40568-T1, (1986)

[Donaldson,1988] J. D. Donaldson and S. Grimes, Lifting the scales from our pipes, The City University, London, UK, Newscientist, 1990. also, Tube International, (1988) 111-118

[Grimes,1988] S.M. Grimes, Magnetic field effect on crystals, Tube International (March 1988) 111-113

[Herzog,1989] R. E. Herzog, Q. Shi, J. N. Patil and J. L. Katz, Magnetic water treatment: The effect of iron on calcium carbonate nucleation and growth, Langmuir, Vol.5, no.3, (1989) 861-867

[Kronenberg,1990] K.J. Kronenberg, The glory and the riddle of water, Science of Softron (summer 1990)

[Bernardin,1991] J.D. Bernardin and S.H. Chan, Magnetic effects on simulated brine properties pertaining to magnetic water treatment, 28th National Heat Transfer Conference, HTD, 164 (1991) 109-117

[Hu,1991] X. Hu and A.M. Jacobi, A review of the literature: magnetic water treatment in heat transfer applications, Johns Hopkins University Technical Report No. HMT-9101 (1991)

[Higashitani,1993] K. Higashitani, et al., Effects of a magnetic field on the formation of CaCO3 particles, Journal of Colloid and interface science, 156 (1993) 90-95

[Lipus,1994] L. Lipus, J. Krope and L. Garbai, Magnetic water treatment for scale prevention, Hungarian Journal of Industrial Chemistry, 22 (1994) 239-242

[Gehr,1995] R. Gehr, et al., Reduction of soluble mineral concentrations in CaSO4 saturated water using a magnetic field, Wat. Res., 29, 3 (1995) 933-940

[Al-Qahtani] H. Al-Qahtani, Effect of magnetic treatment on Gulf seawater, Desalination, 107 (1996) 75-81

[Baker,1996] J.S. Baker and S.J. Judd, Magnetic amelioration of scale formation, Wat. Res., 30, 2 (1996) 247-260

[Wang,1997] Y. Wang, et al., Rapid onset of calcium carbonate crystallization under the influence of a magnetic field, Wat. Res., 31, 2 (1997) 346-350

[Busch,1997] K.W. Busch and M.A. Busch, Laboratory studies on magnetic water treatment and their relationship to a possible mechanism for scale reduction, Desalination, 109 (1997) 131-148

[Marth,1997] R.A. Marth, A scientific definition of the magnetic treatment of water: It' s subsequent use in preventing scale formation and removing scale, MTW intro v6.1 (July 1997)

[Baker,1997] J.S. Baker, S.J. Judd and S.A. Parsons, Antiscale magnetic pretreatment of reverse osmosis feedwater, Desalination, 110 (1997) 151-166

[Parsons, Ichem,1997] S.A. Parsons, S.J. Judd, T. Stephenson, S. Udol and B-L. Wang, Magnetically augmented water treatment, Institution of Chemical Engineers, 75, B2 (1997) 98-104

[Barrett, Wat. Res., 1998] R.A. Barrett and S.A. Parsons, The influence of magnetic fields on calcium carbonate precipitation, Water Research, Vol. 32, No. 3, pp. 609-612, (1998)

[Parsons,MAG3,1999] S.A. Parsons, Overall of recent magnetic treatment research at Cranfield University, 3rd Symposium, Cranfield University, UK (April 1999)

[Bogatin,1999] J. Bogatin, “ Magnetic Treatment of Irrigation Water: Experimental Results and Application Conditions” , Environmental Science & Technology, 33, 8 (1999) 1280-1285

[Coey, 2000] J.M.D. Coey and Stephen Cass, Magnetic water treatment, J. Mag. And Magnetic Matrials, Vol. 209 (2000) pp. 71-74

[Kobe, 2001] S. Kobe, G. Drazic, P.J. McGuiness, J. Strazisar, The influence of the magnetic field on the crystallization form of calcium carbonate and the testing of a magnetic water treatment device, J. Mag. And Magnetic Materials, Vol. 236 (2001) pp. 71-76

[Gabrielli, Wat. Res., 2001] C. Gabrielli, R. Jaouhari, G. Maurin and M. Keddam, Magnetic water treatment for scale prevention, Wat. Res. Vol. 35, No. 13, pp. 3249-3259, (2001)

[Vedavyasan, Desalination, 2001] C.V. Vedavyasan, Potential use of magnetic fields – a perspective, Desalination, Vol. 134 (2001) pp. 105-108